

REVIEW

[View Article Online](#)
[View Journal](#) | [View Issue](#)Cite this: *RSC Adv.*, 2019, **9**, 16606Received 11th April 2019
Accepted 7th May 2019DOI: 10.1039/c9ra02749a
rsc.li/rsc-advances

An overview on synthetic strategies for the construction of star-shaped molecules

Hadeer M. Diab, Amr M. Abdelmoniem, Mohamed R. Shaaban, Ismail A. Abdelhamid * and Ahmed H. M. Elwahy *

Strategies for the synthesis of star-shaped molecules have been in high demand in the last decades due to the importance of those compounds in various fields. The distinctly different properties of these compounds compared to their linear analogues make them versatile building blocks for the formation of mesophases of interesting mesomorphic and photophysical properties. Moreover, the applications of star-shaped molecules as building units for dendrimers as well as in supramolecular host–guest chemistry have also been recently studied. The star-shaped molecules mentioned in this review are classified according to the central core as well as the type of side arms. The properties and applications of these compounds are described in the appropriate contexts. This report summarizes the recent advances in this area.

1. Introduction

Star-shaped molecules (SSMs) are a class of branched compounds with a general structure consisting of several (three or more) linear chains connected to a central core. Star-shaped molecules began to draw the interest of chemists and physicists in the last decades due to distinctly different properties as compared to their linear analogues. Over the years, interesting names have been given to these molecules in an attempt to describe these complex structures like tripodal, tetrapodal, octopus, hexahost or multi-armed molecules. In 1948, Schaefgen and Flory reported

the synthesis of the first star-shaped polyamides.¹ In 1962, Morton *et al.* reported the synthesis of tetra-liked branched polystyrene through anionic polymerization. Due to its shape, this polymer was named for the first time as a star molecule.² The name star-shaped molecules (SSMs) was then given to all structures, even small molecules, in which more than two arms are attached symmetrically to a single multifunctional core. Compared to polymer materials, small molecules offer potential advantages in terms of defined molecular structure, definite molecular weight, easy purification, and good batch-to-batch reproducibility.^{3–5}

Some derivatives of these compounds were synthesized as promising molecules for application in optoelectronics and electrochromic devices.^{6–17} The structure of such molecules makes them versatile building blocks for the

Chemistry Department, Faculty of Science, Cairo University, Giza, Egypt. E-mail: ismail_shafy@yahoo.com; aelwahy@hotmail.com



Hadeer M. Diab was born in 1992 in Giza, Egypt. She graduated from Cairo University, Faculty of Science, Egypt in 2013 then she was awarded her M.Sc. degree in 2018.



Amr M. Abdelmoniem was born in Egypt in November 1984. He graduated from Cairo University, Egypt in 2005 then he obtained his M.Sc. and Ph.D. degrees in 2009 and 2014, respectively, at Cairo University in the field of organic synthesis. His M.Sc. dissertation was awarded the best thesis from Cairo University in 2009. He was awarded the Alexander von Humboldt research fellowship in 2019–2021 with Prof. Holger Butenschön, at Hannover University, Germany. In 2018 he received a Cairo University Incentive Award.



formation of mesophases of interesting mesomorphic and photophysical properties.^{18–31} The applications of star-shaped molecules as building units for dendrimers^{32,33} as well as in supramolecular host–guest chemistry have been also reported.^{34,35} Moreover, the interesting biological activities of some diverse multivalent scaffolds adamantane have been recently investigated.³⁶ Some of these compounds were designed to study their promising photovoltaic application in organic solar cells OSCs.^{37–55}

The present review casts light on the main strategies for the synthesis of star-shaped molecules especially those containing heterocyclic core and/or heterocyclic arms. The star-shaped molecules mentioned in this review are classified according to the central core as well as the type of side arms.

The properties and applications of these compounds are described in the appropriate contexts.



Mohamed R. Shaaban was born in 1971 in Cairo, Egypt. He graduated from Cairo University, Egypt in 1992 then he joined Professor Ahmad M. Farag's research group. He received his Ph.D. in 2001 at Tokyo, Institute of Technology, Japan. In 2001 he was promoted to a Lecturer of Organic Chemistry at Cairo University and continued his research work on organic synthesis as well as on palladium

catalyzed C–C cross-couplings. In 2009 he was promoted to Associate Professor of Organic Chemistry, and in 2014 he was promoted to Professor of Organic Chemistry at the Faculty of Science, Cairo University.



Ismail A. Abdelhamid was born in Egypt in December 1978. He graduated from Cairo University, Egypt in 2001 then he obtained his M.Sc. and Ph.D. degrees in 2005 and 2007, respectively, at Cairo University in the field of organic synthesis. In 2017 he was appointed as a full Professor of Organic Chemistry at Cairo University. He was awarded the Alexander von Humboldt research fellowship in 2008–2011 and in 2014, 2017, and 2019 with Prof. Holger Butenschön, at Hannover University, Germany. He received several research prizes; Cairo University Incentive Award (2012), Cairo University Scientific Excellence Award (2016) and State Incentive Award (2019).

To the best of our knowledge, a number of other reviews^{24,56–67} that have appeared, concerning the chemistry of star-shaped molecules, did not pay special attention to the synthesis of such systems in an organized manner with respect to central core as well as the type of side arms. The review will cover the literature in this area over the last decades. Star-shaped molecules based on triphenylamine, truxene or other polycyclic aromatic cores have been recently reviewed and will not be mentioned in this review.^{56,61,66}

The reported yields of the target molecules in this review are those given in the last step reaction except when an overall yield was given.

2. Classification of star-shaped molecules

A schematic illustration of the classification of star-shaped molecules (SSMs) is depicted in Fig. 1. The cores and the side arms are the main factors in this classification. The cores are usually an atoms (C, Si, Ge and N), acyclic aliphatic (asparatic, glutamic, pentaerythritol and tris(2-aminoethyl)amine), cyclic aliphatic (cyclohexatrione and polyhedral oligomeric silsesquioxane (POSS)), aromatic (benzene, truxene, isotruxene, hexa-*peri*-hexabenzocoronene, hexakisfluorenylbenzene, oligofluorene and hexatriphenylene), heteroaromatic (1,3,5-triazine, pyrimidine, phenylquinoxaline, phenylcarbazole, oligothiophene, triindole, benzodifuran, benzodithiophene, benzotriithiophene, thieno[3,2-*b*]thiophene, dithienyl naphthothiophene, tetrathienoanthracene, naphthalimide-fused pyrazinacenes, triazatrinaphthylene, pyrrole-fused TTF and triazatruxene). It is worthy to mention that that benzene and 1,3,5-triazine are considered as the most popular aromatic and heterocyclic cores, respectively. Side arms may also contain aliphatic, aromatic or heterocyclic moieties. The incorporation of heterocyclic systems into the structure of the star-shaped molecules is highly useful for optical and electronic applications.



Ahmed H. M. Elwahy was born in 1963 in Giza, Egypt. He graduated from Cairo University, Egypt in 1984 then he obtained his M.Sc. and Ph.D. degrees in 1988 and 1991, respectively, at Cairo University in the field of organic synthesis. He was awarded the Alexander von Humboldt research fellowship in 1998–2000 and in 2003, 2005, 2009, 2010 and 2012 with Prof. Klaus Hafner, at TU Darmstadt, Germany. In 2002 he was appointed as a full Professor of Organic Chemistry at Cairo University. In 2001 he received the State-Award in Chemistry. He has published around 120 scientific papers in distinguished international journals.



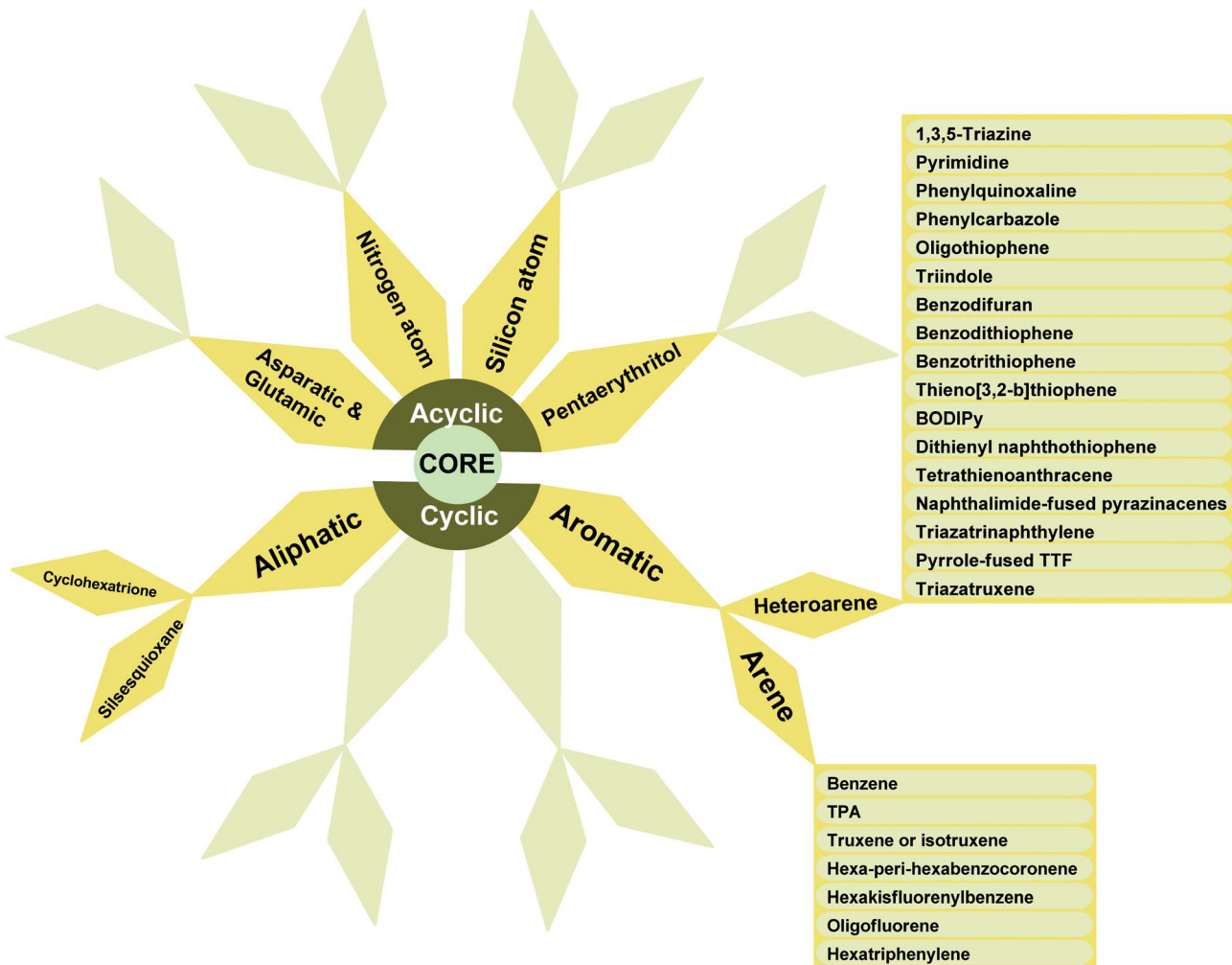
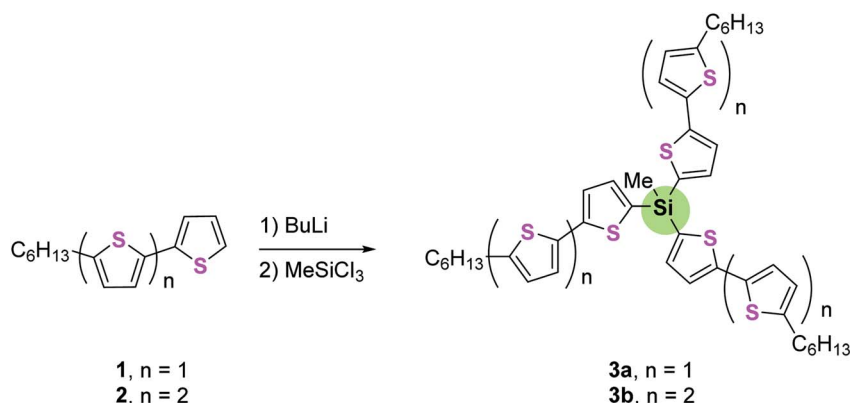


Fig. 1 Core-based classification of star-shaped molecules.

3. General synthetic approaches for star-shaped molecules

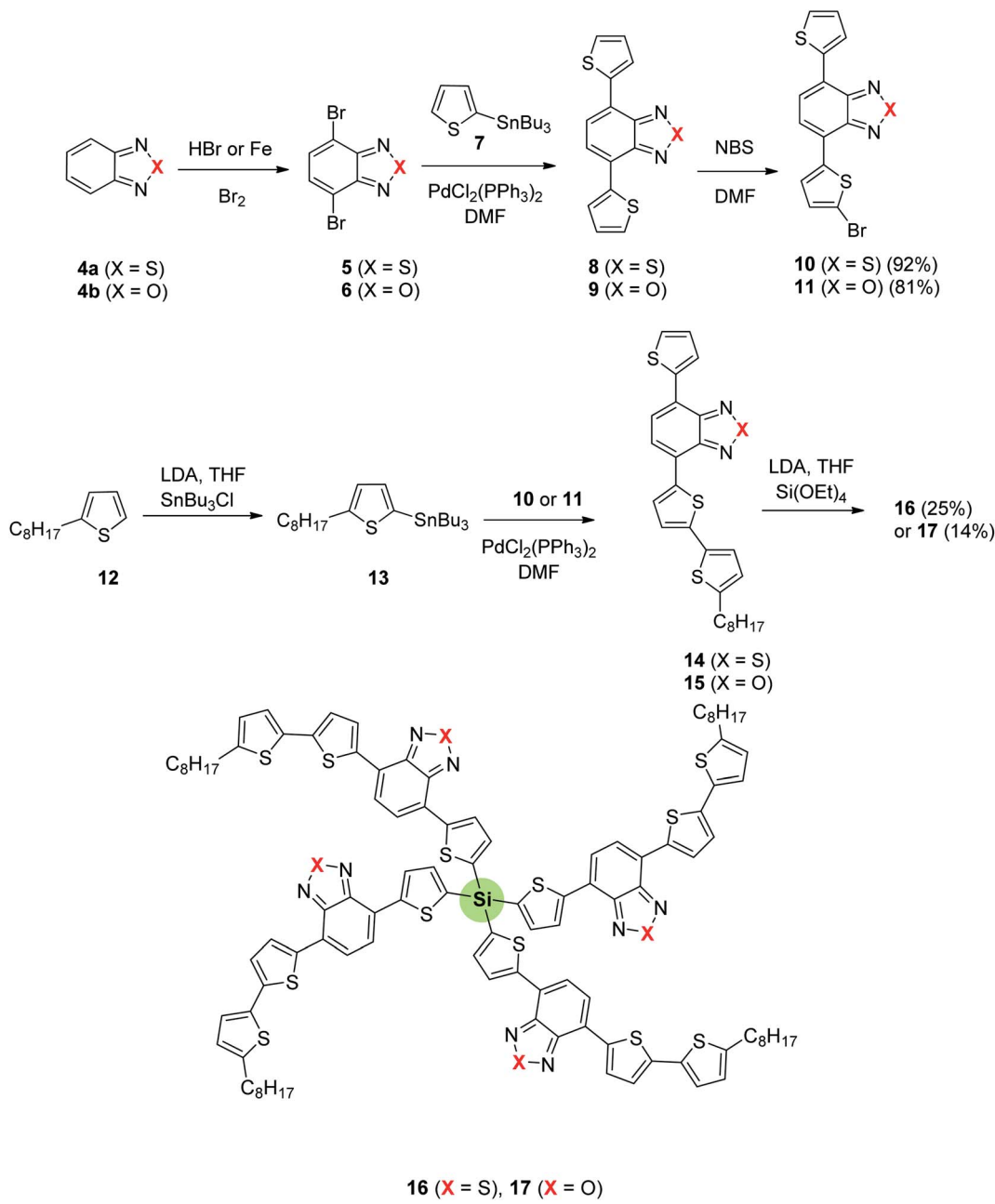
This section summarizes the synthetic approaches that have been developed for the synthesis of star-shaped molecules

mentioned in this review. Generally, SSMs were synthesized from poly-functionalized building blocks which are then manipulated to generate the target compounds using mainly the following reactions:



Scheme 1 Synthesis of star-shaped oligothiophenesilanes 3.





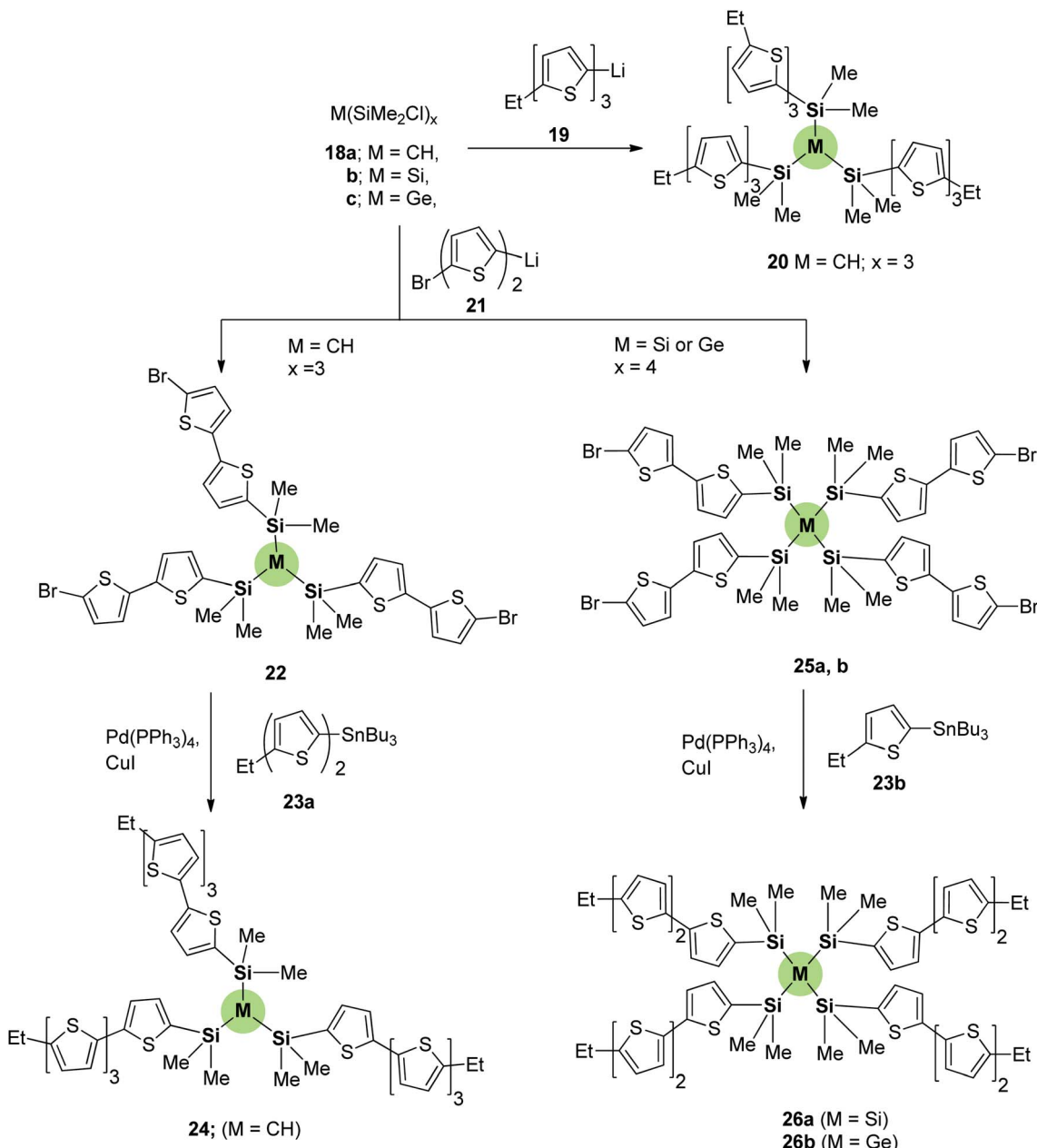
Scheme 2 Synthesis of four-armed SSMs with silicon atom-core 16 and 17.

3.1. O-, S- and N-Alkylation reactions

The star shaped molecules were prepared in this case by polyalkylation of the appropriate alcohol, phenols, heterocyclic thiol, aromatic or heteraromatic amines with a variety of alkyl or aryl halides. The reactions are fast, operationally simple, and allows rapid access to a variety of poly(heterocyclic) derivatives. Achieving selectivity in these reactions or prediction of the site of the alkylation remains a challenging point for substrates with more nucleophilic centers.

3.2. Cyclocondensation reactions

SSMs prepared using this strategy depends mainly on the formation of polychalcones and subsequent reaction with hydrazine derivatives to give the corresponding polydihydropyrazoles. Polythiazoles can also be prepared by cyclocondensation of polythiosemicarbazones with the appropriate α -haloketones. Moreover, cyclization of polybenzoylhydrazides with POCl_3 was reported to give polyoxadiazole derivatives. Furthermore, cyclocondensation of 3-aminobut-2-enenitrile with polyaldehydes represent one of the most interesting



Scheme 3 Synthesis of silicon-cored SSMs 20, 24, 26a and 26b.

approaches which led to the formation of polydihydropyridines. Although the overall yields of these reactions are moderate, only a small library of poly(heterocycles) prepared by this strategy are available.

3.3. Cyclotrimerization reactions

This reaction was used to prepare tris(thiophenyl)benzenes *via* cyclotrimerization of 2-acetylthiophene derivatives upon treatment with SiCl_4 . Tris(4-(thiophenyl)phenyl)-1,3,5-triazines can also be obtained *via* cyclotrimerization of (thiophenyl)benzonitriles in the presence of $\text{CF}_3\text{SO}_3\text{H}$. Hexaheteroarylbenzene derivatives were prepared by cobalt-catalyzed cyclotrimerization reaction of different alkyne

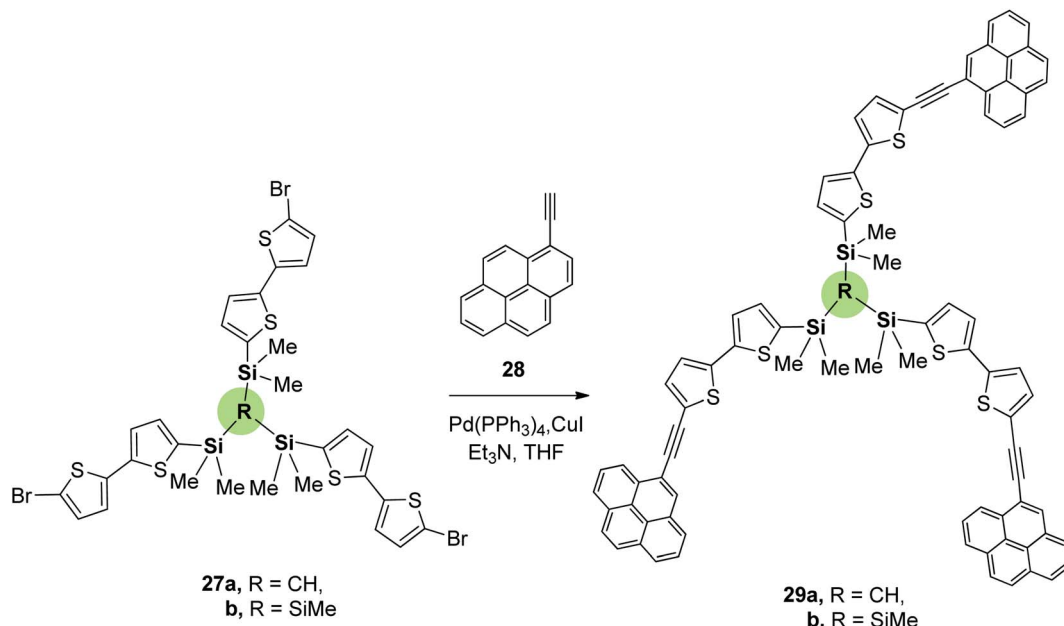
precursors. The scope of this reaction in this area is limited and the overall yields of the products are moderate.

3.4. 1,3-Dipolar cycloaddition reactions

This strategy was mainly used to synthesize star-shaped molecules with pyrrolidine side arms *via* the reaction of chalcones with sarcosine and paraformaldehyde.

3.5. Imidization *via* cleavage–cyclization reactions

Star-shaped molecules with cyclic imide structure were synthesized by imidization reaction of 1,3,5-triamino benzene with cyclic carboxylic anhydride in the presence of $\text{Zn}(\text{OAc})_2$.



Scheme 4 Synthesis of silicon-cored SSMs 29a,b.

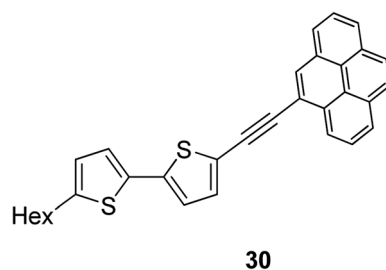


Fig. 2 Structure of linear (hexylbithiophenyl)pyrenylacetylene 30.

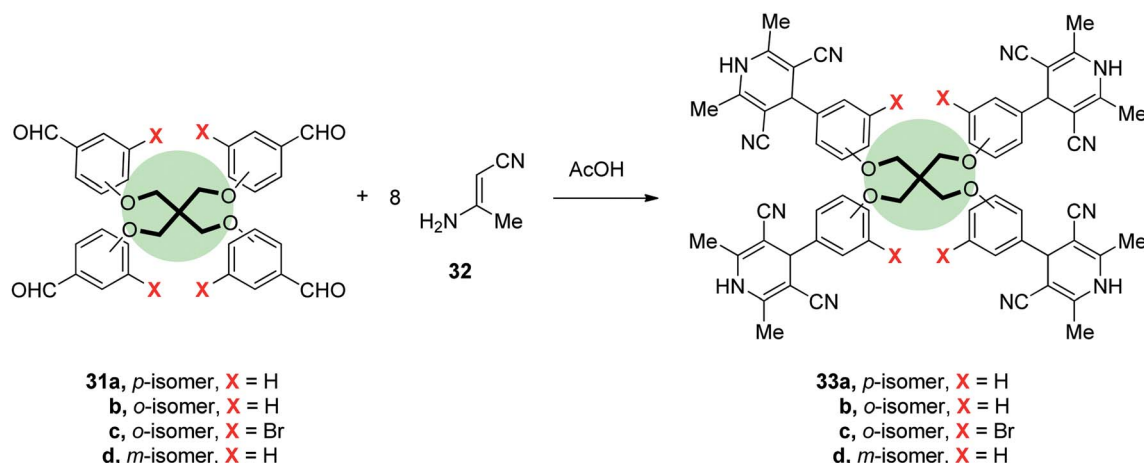
3.6. Palladium-catalyzed C-C and C-N bond formation *via* Heck, Negishi, Sonogashira, Stille and Suzuki cross-coupling reactions

A variety of metal-catalyzed reactions, such as Suzuki, Stille, Sonogashira, Heck, and Negishi cross-coupling reactions have

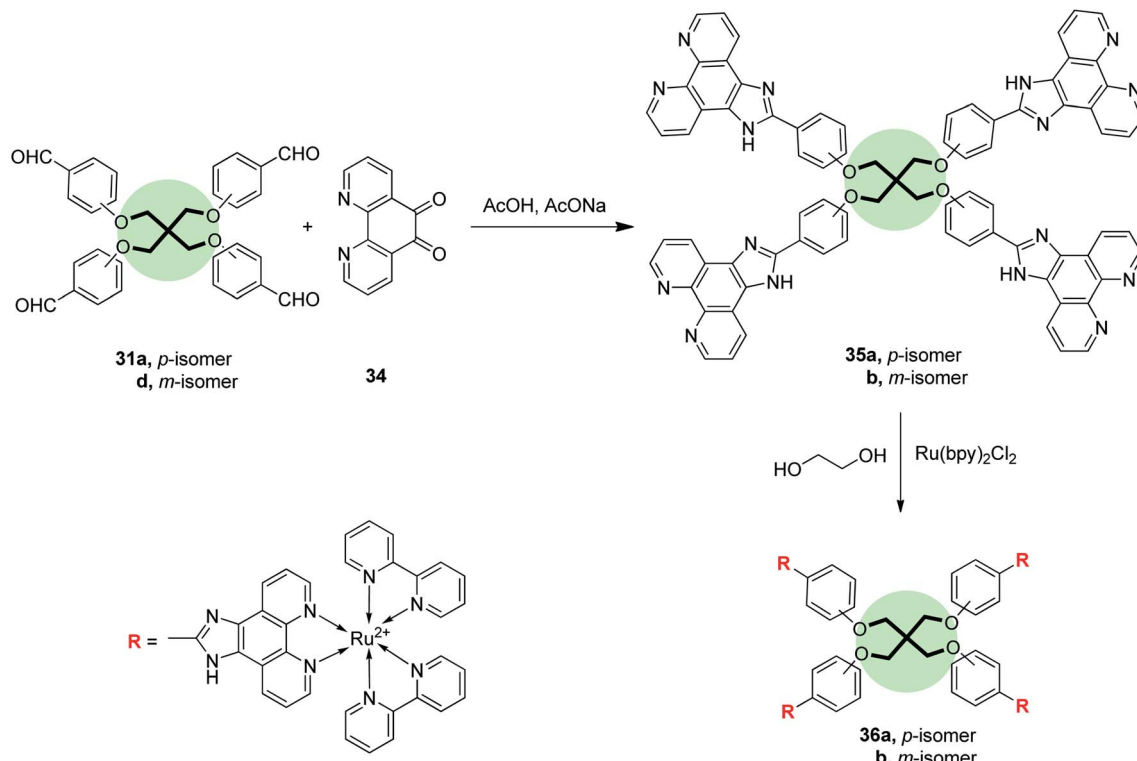
been employed to functionalize a range of star-shaped molecules.

3.6.1. Suzuki-Miyaura reaction. This reaction led to the formation of SSMs with biphenyl, thiophene, bithiophene, tri-thiophene, pyrrolo[3,4-*c*]pyrrole, quinolone carbazole or fluorene arms by cross-coupling reaction of boronic acid derivatives with the appropriate polyhalo compounds in the presence of palladium catalyst. Aryl-alkylboronic acids or boronate esters, used in this reaction, very often suffer from a few limitations associated with their preparation, purification, and handling.

3.6.2. Sonogashira reaction. Sonogashira cross-coupling between the appropriate halo compounds with the corresponding alkyne derivatives in the presence Pd catalyst furnished star-shaped molecules with thiophene, pyrene, carbazole or fluorene side arms attached to the core *via* ethylenic linkages.



Scheme 5 Synthesis of tetrakis(2,6-dimethyl-4-phenyl-1,4-dihydropyridinyl)methanes 33a-d.



Scheme 6 Synthesis of tetrapodal ligands **35a,b** and their ruthenium complexes **36a,b**.

3.6.3. Stille cross-coupling reactions. A Stille cross-coupling reaction between halo compounds and tributylstannyli derivatives in the presence of Pd catalyst afforded mainly thiophene-containing SSMs liked to benzothiadiazole, benzoxadiazole, pyrrolopyrrole or thiadiazolo[3,4-*c*]pyridine arms. One of the disadvantage of this reaction is the possible development of organotin by-products in reaction products.

3.6.4. Negishi cross-coupling reaction. This approach was used to prepare thiophene, thieno[3,2-*b*]thiophene, arylethynyl containing triphenylamine, fluorene, and/or carbazole-based SSMs by Pd-catalysed cross-coupling reaction of the appropriate halides with the corresponding organozinc compounds. The scope of the reactions could be significantly extended to the synthesis of a variety of SSMs using electron deficient heteroaromatic aryl bromides or chloride and acyclic zinc reagents as coupling partners.

3.6.5. Heck coupling reaction. Heck coupling reaction was utilized for the synthesis of vinylbithiophene-based SSMs *via* coupling of haloarenes with vinylbithiophene in the presence of $\text{Pd}(\text{OAc})_2$.

3.7. van Leusen oxazoles synthesis

This reaction was used to prepare oxazole-containing star-shaped molecules by the reaction of tris-aldehydes with *p*-toluenesulfonylmethyl isocyanide (TosMIC).

The scope of this method is rather low and applied only for the synthesis of very few systems of tris((oxazolyl)thiophenyl)benzene.

3.8. Ullmann reactions

Benzimidazole-based SSMs were synthesized using this carbon–nitrogen bond-forming reaction through coupling of benzimidazole with tribromobenzene using CuSO_4 in the presence of a base catalyst. The applications of Ullmann reaction in this area are limited due to some limitations like harsh reaction conditions, high copper catalyst loading, poor functional group tolerance and generally the low yield of the products.

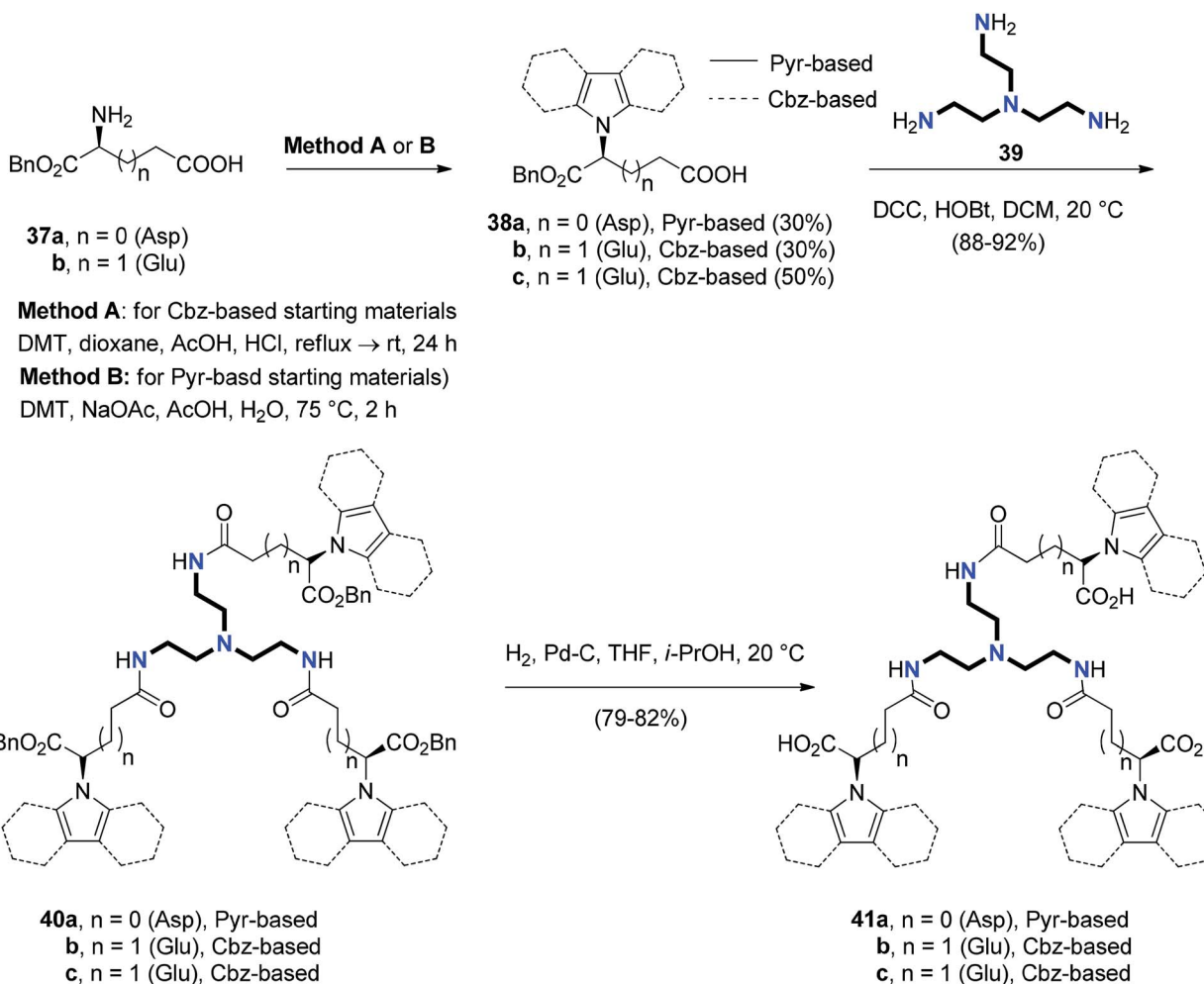
3.9. Click reaction

This reaction was used mainly to synthesize 1,2,3-triazole-based SSMs by the classic copper-catalyzed click reaction of the appropriate azide with the corresponding alkyne. Some important limitations of Click reaction are the stability of some azides in addition to the use of copper catalyst and the possible of alkyne homocoupling under the reaction conditions.

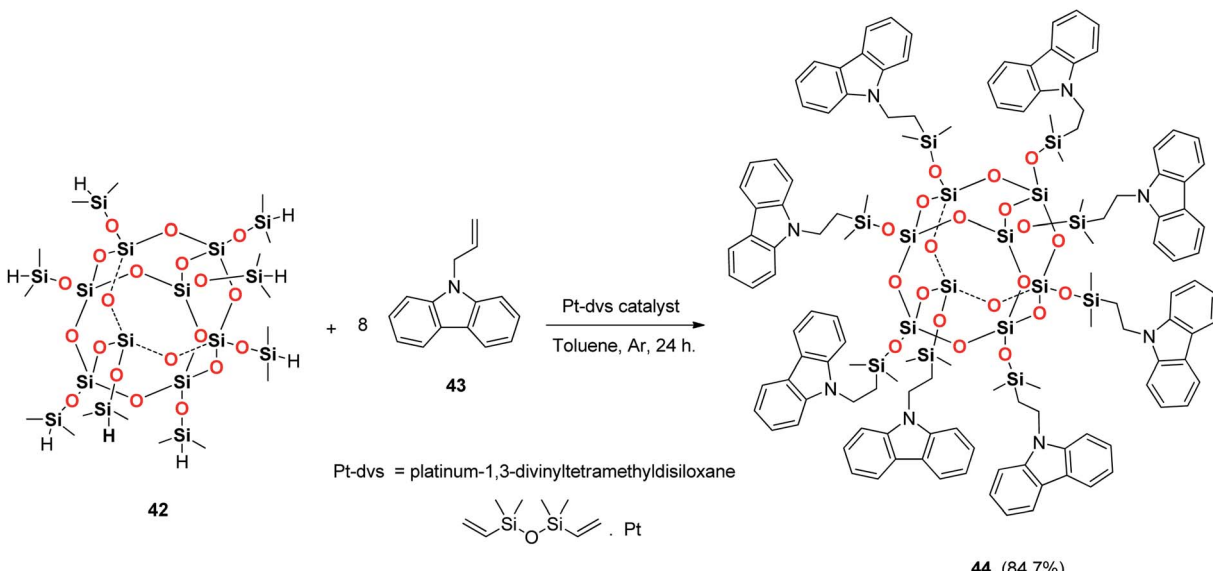
3.10. Diels–Alder reactions

Diels–Alder reaction was used to prepare star-shaped molecules with hexakis(fluoren-2-yl)benzene by heating of cyclopentadienone with the appropriate acetylene derivatives. A significant limitation of this reaction is the poor reactivity associated with *cis*-dienes as well as prolonged reaction time.

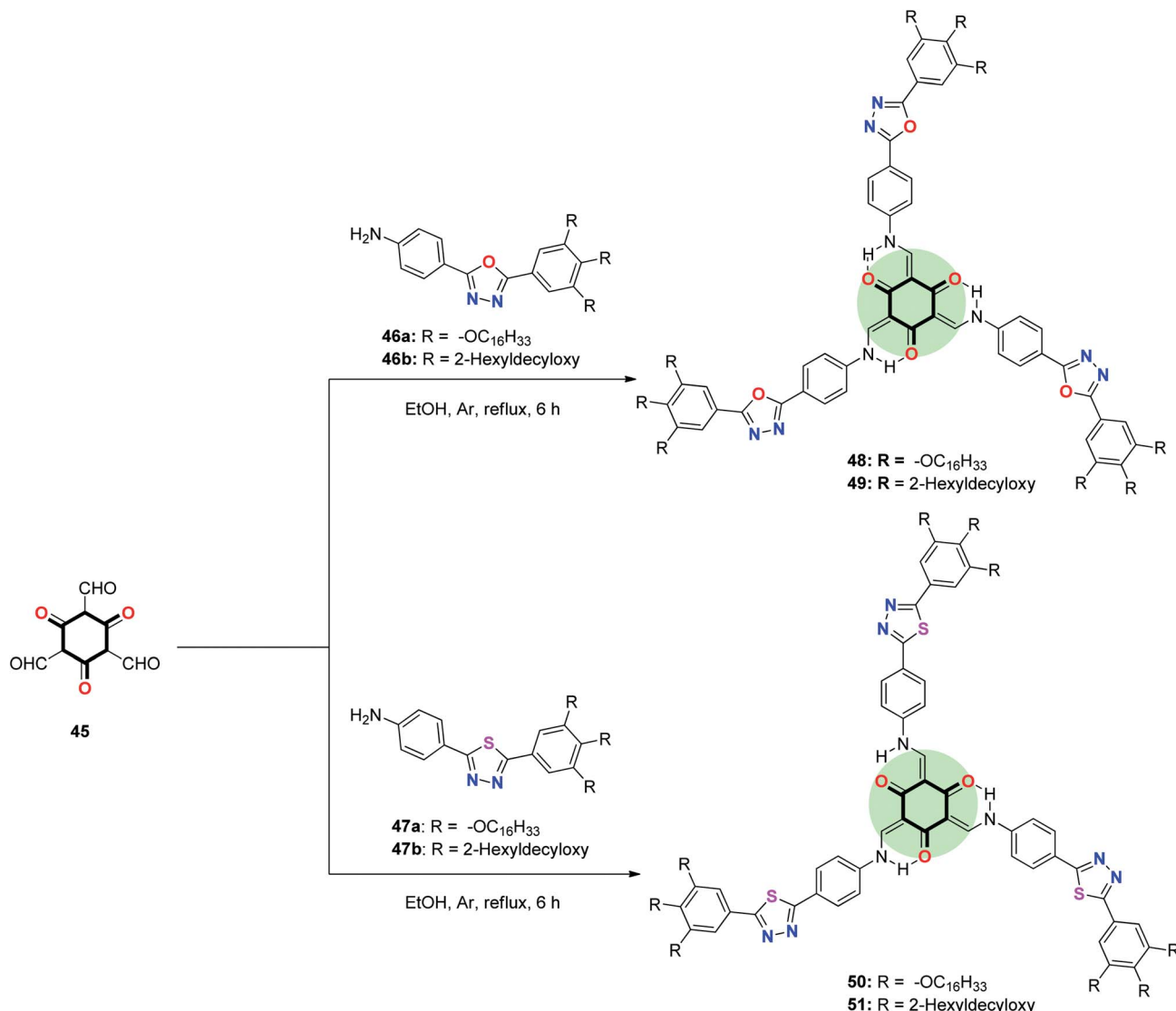




Scheme 7 Synthesis of homochiral C3-symmetrical dendritic carboxylic acids 41a–c.



Scheme 8 Synthesis of POSS-cored SSMs 44.



Scheme 9 Synthesis of star-shaped tris(*N*-salicylideneanilines incorporated azoles) **48–51**.

3.11. Wittig reaction

Using this strategy tris- and tetrakis(2-(benzofuran-2-yl)vinyl)benzene as well as tris- and tetrakis[2-(benzo[*b*]thien-2-yl)vinyl]benzene were prepared by the reaction of the appropriate carbaldehyde with benzene-cored phosphonates. The reaction may be slow and give low yields in addition to the labile nature of aldehydes which can oxidize, polymerize or decompose.

4. Specific synthesis of star-shaped molecules

4.1. SSMs with acyclic cores

This class of star-shaped molecules comprises compounds with Si, Ge or carbon atoms as cores.

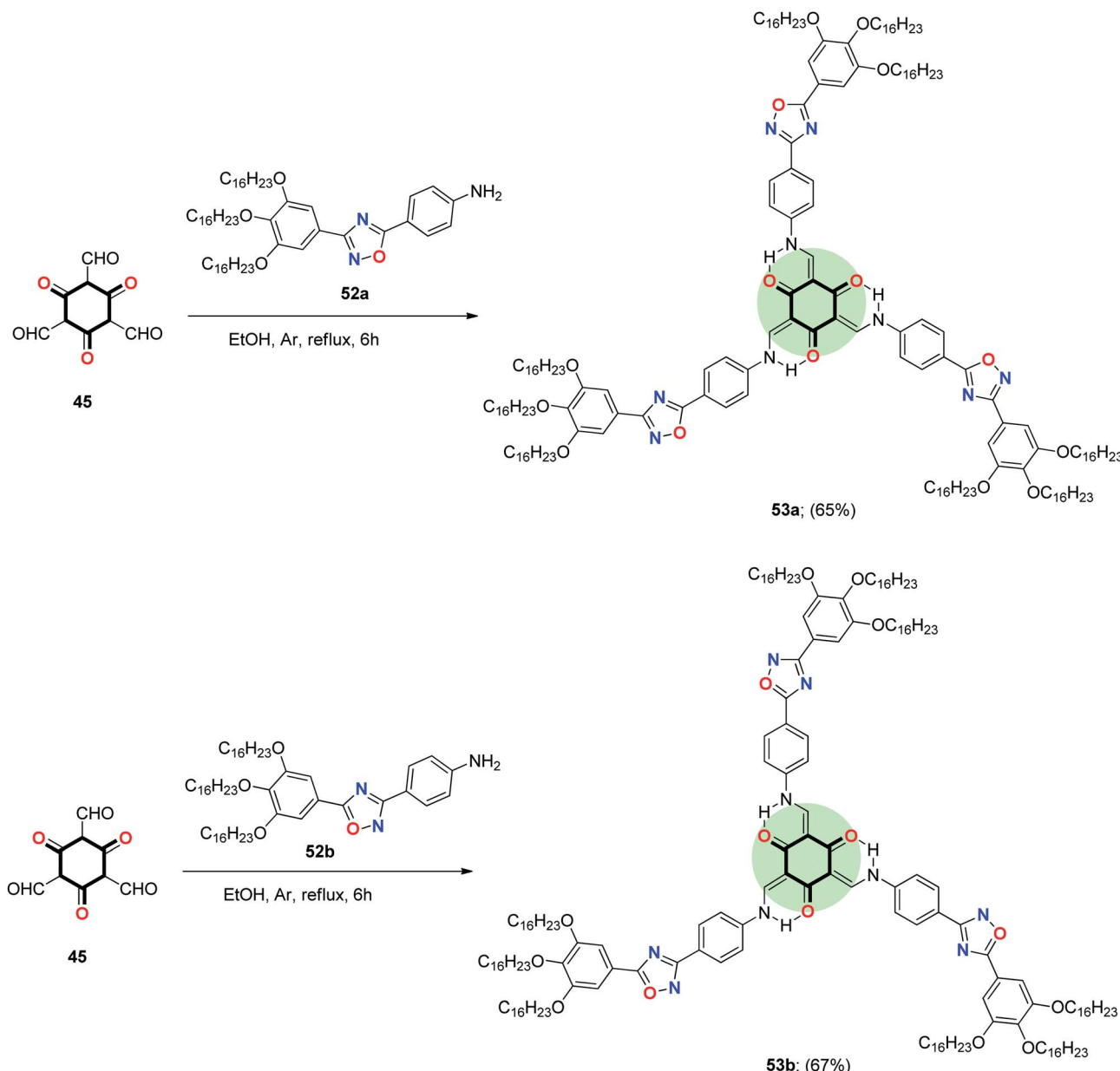
4.1.1. Silicon, germanium or carbon atom cores. Star-thiophene derivatives with one central silicon atom linked to three oligothiophene units has attracted a considerable interest

since a discovery of strong fluorescence of the star-like molecules that have a regular arrangement of Si–Si bonds and bithiophene units.⁶⁸

Luponosov *et al.*⁶⁹ synthesized star-shaped oligothiophene-silanes **3a,b** by firstly lithiation of 5-hexyl-2,2'-bithiophene **1** or 5-hexyl-2,2':5',2"-terthiophene **2**, respectively, followed by reaction with methyltrichlorosilane (Scheme 1). This work was extended to the synthesis of some different dentritic oligothiophenes, *via* Suzuki coupling reaction.^{70–72}

These compounds showed very effective energy transfer from the outer bithiophene to the internal terthiophenesilane units. Some of these compounds show efficient photoluminescence in the violet-blue region, the quantum yield of which is 5–15 times higher than that for the parent bithiophene or bithiophenesilanes.

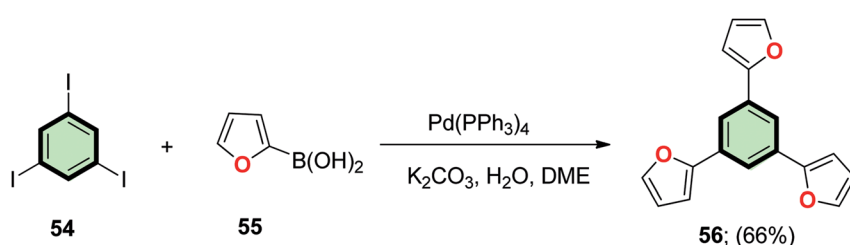
The synthesis of four-armed SSMs with silicon atom-core **16** and **17** starting from benzothiadiazole or benzooxadiazole is outlined in Scheme 2. Bromination of **4a** and **4b**



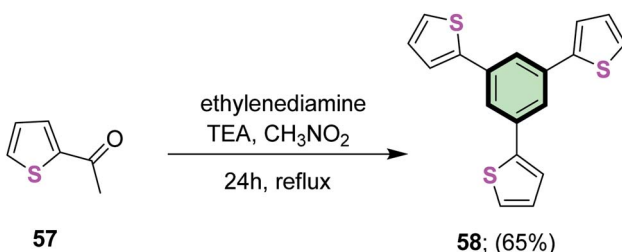
Scheme 10 Synthesis of star-shaped tris(*N*-salicylideneanilines incorporated 1,2,4-oxadiazole) **53a,b**.

afforded the 4,7-dibromo derivatives **5** and **6**, respectively. Stille coupling of **5** or **6** with 2-tributylstannylthiophene **7** resulted in the formation of 4,7-bis(2-thienyl) derivative **8** or

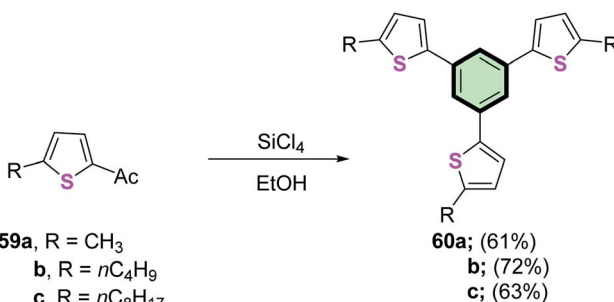
9 which underwent a single bromination to yield **10** or **11**, respectively. Another Stille coupling of **10** or **11** with 2-tributylstannyl-5-octylthiophene **13** (obtained from 2-



Scheme 11 Synthesis of 1,3,5-tris(2-furyl)benzene **56**.



Scheme 12 Synthesis of 1,3,5-tri(thiophen-2-yl)benzene 58.



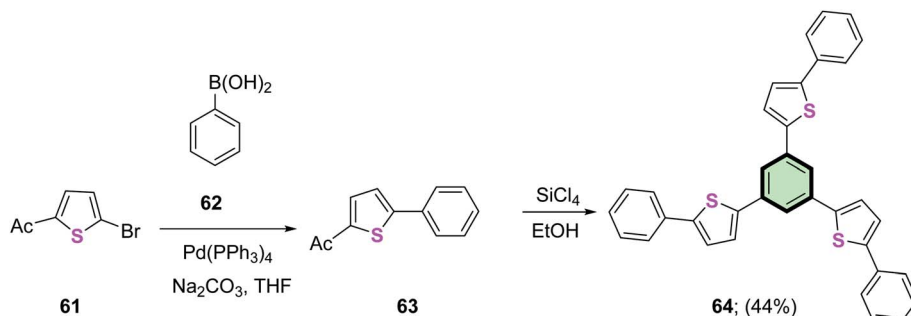
Scheme 13 Synthesis of 1,3,5-tris(5-alkylthiophen-2-yl)benzenes 60a-c.

octylthiophene **12** upon treatment with tributylstannyl chloride) affords the arm **14** or **15** in 92% and 81%, respectively. Lithiation of compounds **14** and **15** followed by

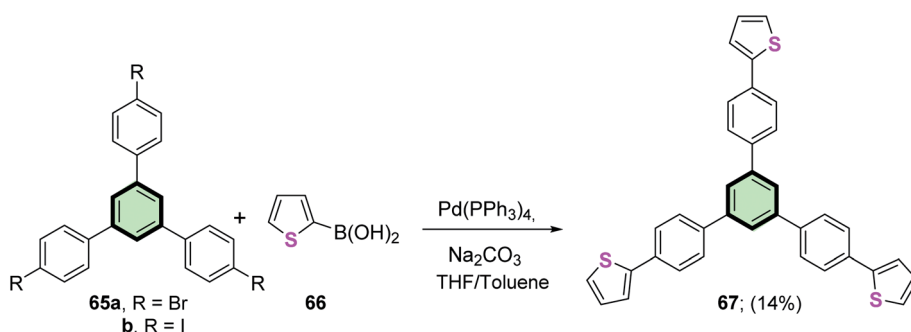
reaction with tetraethoxysilane led to SSMs **16** and **17** in low isolated yields of 25% and 14%, respectively, presumably due to aggregation and solubility issues. SSMs **16** and **17** were synthesized as low band gap compounds for applications in organic photovoltaic devices. Generally, benzothiazidazole SSM **16** showed a better photovoltaic performance than benzoxadiazole SSM **17**. The energy band gaps, E_g of **16** (1.83 eV) and **17** (2.05 eV) were found to be higher than 1.5 eV (ideal organic photovoltaics). The energy gap values reflect that the electron-attracting ability of benzoxadiazole is higher than that of benzothiazidazole moiety.⁷³

Silicon-cored SSMs **20**, **24**, **26a** and **26b** were synthesized as shown in Scheme 3.⁷⁴ The three-armed thiophene-containing SSM **20** was prepared by nucleophilic substitution of tris(chlorodimethylsilyl)methane **18a** by ethylthienyllithium **19**. SSM **24** is prepared in two steps: the first is nucleophilic substitution of **18a** with bromobithienyllithium **21** and the second is a Stille coupling with tributyl(ethyl)stannylbithiophene **23a**. Similarly, the four-armed silicon- or germanium-centered SSMs **26a** and **26b** were synthesized starting from **18b** and **18c**, respectively, by firstly reaction with **21** to give tetrabromoderivative **25** and subsequent Stille coupling reaction with **23b**. These compounds have been studied as hole-transporting materials for the sake of use as thin film transistor and TFT-active materials.

Pyrene-containing SSMs **29a,b** with high potential as photovoltaic materials were synthesized in 41 and 39%

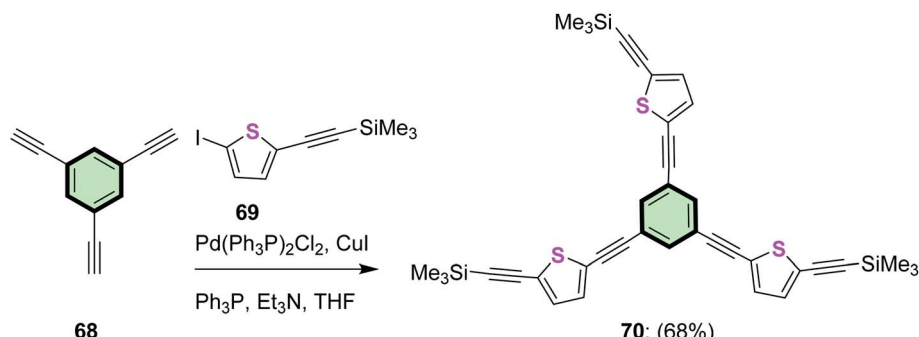


Scheme 14 Synthesis of 1,3,5-tris(5-phenylthiophen-2-yl)benzene 64.



Scheme 15 Synthesis of 1,3,5-tris[4-(2'-thienyl)phenyl]benzene 67.

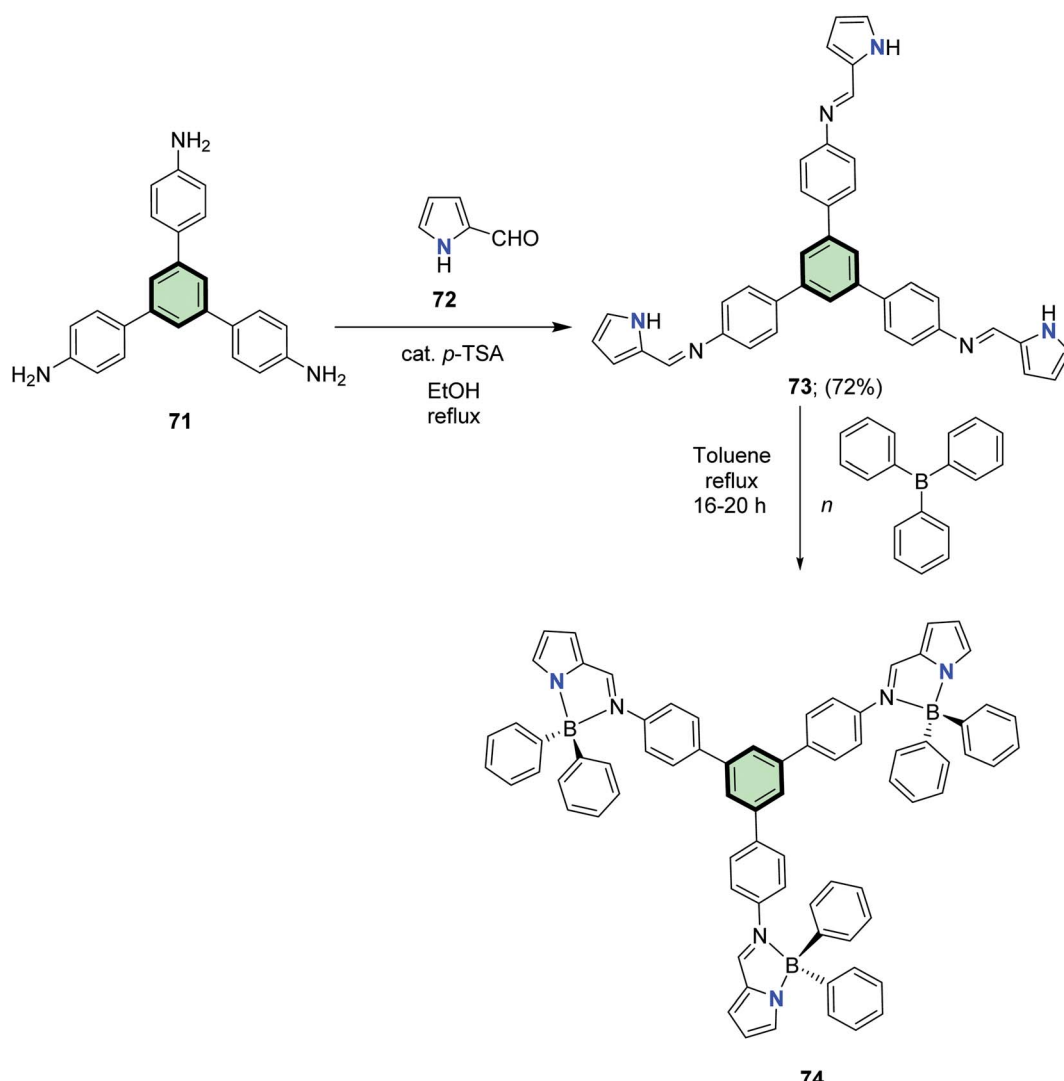




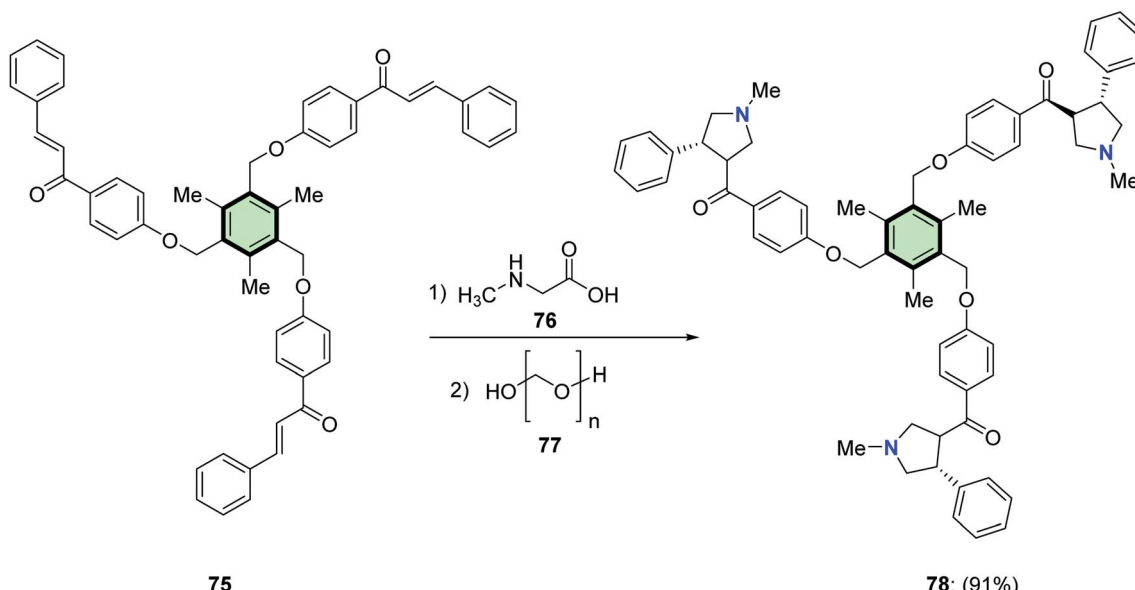
Scheme 16 Synthesis of 1,3,5-tris((5-((trimethylsilyl)ethynyl)thiophen-2-yl)ethynyl)benzene 70.

yields by Sonogashira coupling of tris[(bromobithiophenyl)dimethylsilyl]methylsilane **27a** or tris[(bromobithiophenyl)dimethylsilyl]methane **27b**, respectively, with ethynylpyrene **28** (Scheme 4).⁷⁵ These compounds showed good solubility

in common organic solvents; presumably due to the flexible organosilicon core that reduces the intermolecular π -stacking. Comparison of the UV spectra of compounds **29a** ($\lambda_{\text{max}} = 404$ nm), **29b** ($\lambda_{\text{max}} = 407$ nm) and **30** (linear



Scheme 17 Synthesis of star-shaped molecule with benzene core and pyrrole side arms **73** and its boron complex **74**.

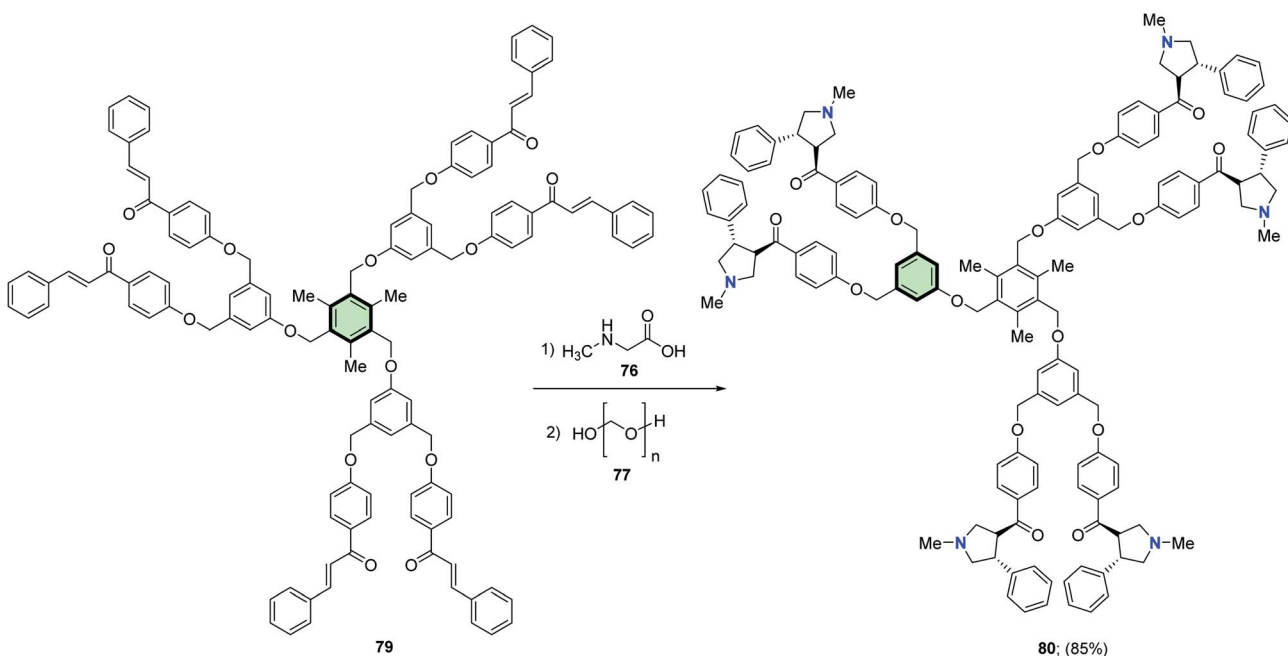
Scheme 18 Synthesis of star-shaped molecule with pyrrolidine side arms **78**.

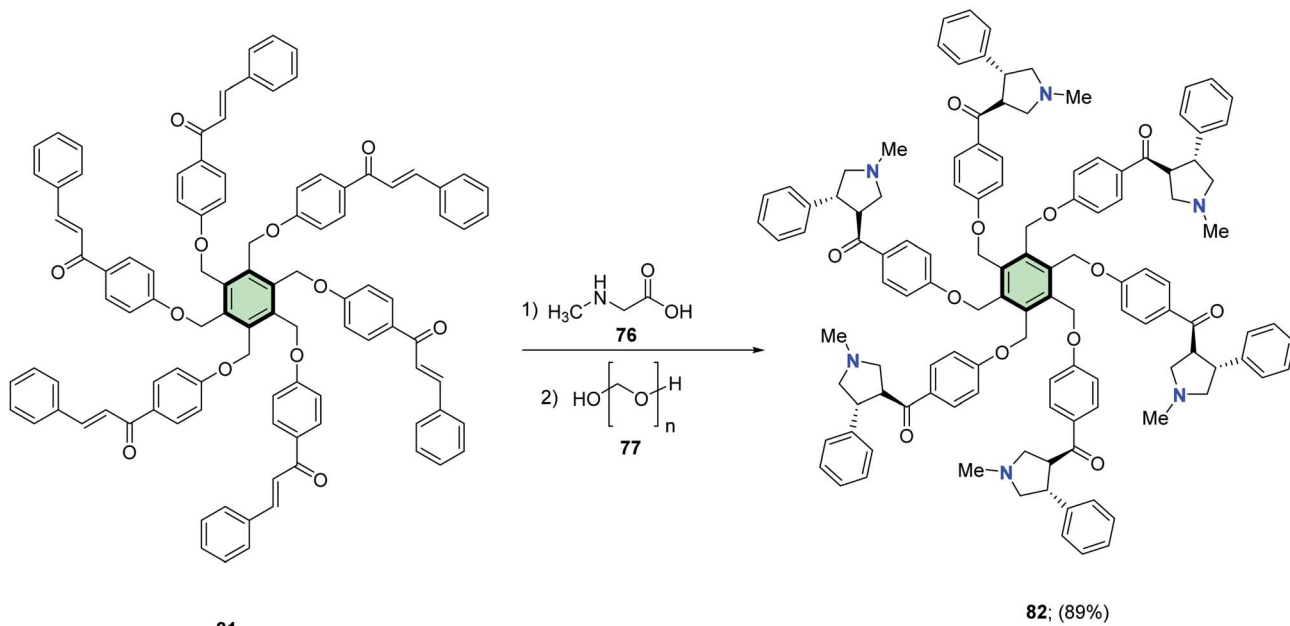
(hexylbithiophenyl)pyrenylacetylene, $\lambda_{\max} = 404$ nm which is depicted in Fig. 2) showed a negligible effect of the bridging core. However, UV spectra of spin-coated films of **29a,b** showed a red shift ($\lambda_{\max} = 440$ nm) apparently due to π -stacking in the solid state.

4.1.2. Pentaerythritol core. Mohamed *et al.*⁷⁶ reported the synthesis of tetrakis(2,6-dimethyl-4-phenyl-1,4-dihydropyridinyl)methanes **33a-d** by acid-catalyzed

condensation of tetrakis-aldehydes **31a-d** with eight equivalents of 3-aminobut-2-enenitrile **32** in acetic acid. These tetrapodal 1,4-dihydropyridines, especially **33**, revealed high anti-proliferative effect *in vitro* studies against human tumor cell lines (A549, HCT116, and MCF7) (Scheme 5).

Cheng *et al.*⁷⁷ reported the synthesis of tetrapodal ligands with imidazo[4,5-f][1,10]phenanthroline units **35a,b** in good yields by the reaction of 1,10-phenanthroline-5,6-dione **34**

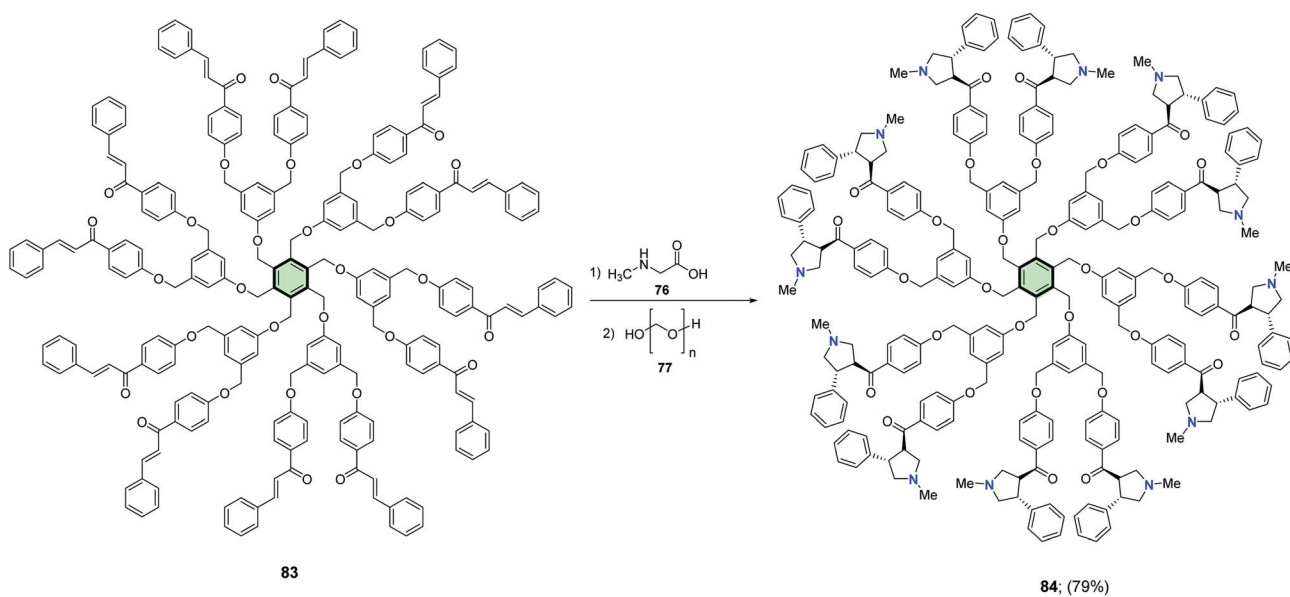
Scheme 19 Synthesis of star-shaped molecule with pyrrolidine side arms **80**.



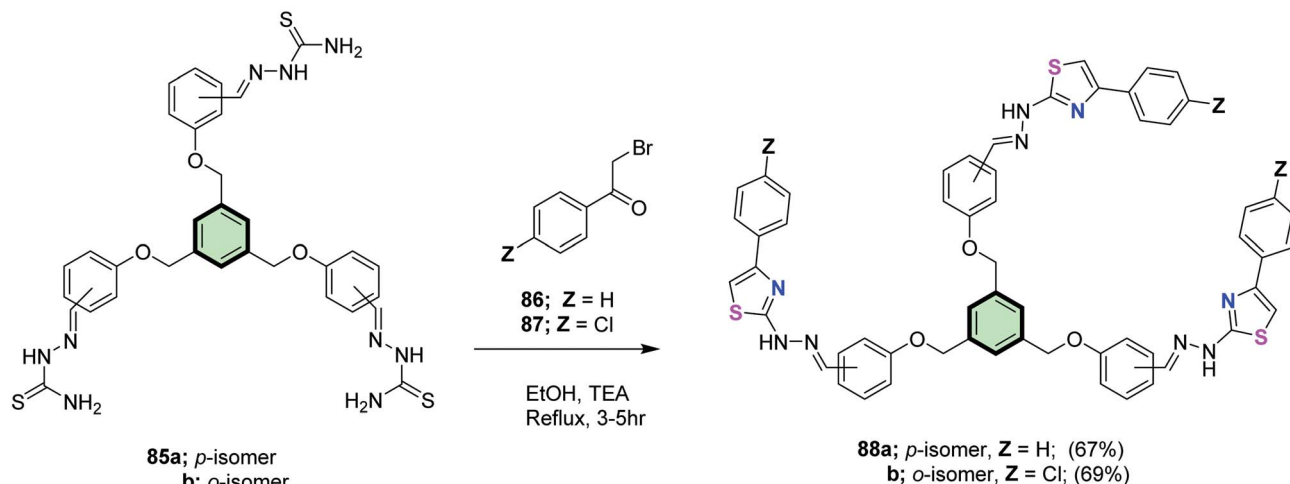
Scheme 20 Synthesis of star-shaped molecule with pyrrolidine side arms 82

with each of tetrakis[(4-formylphenoxy)methyl]methane **31a**, and tetrakis[(3-formylphenoxy)methyl]methane **31d**, respectively, in acetic acid at reflux. The corresponding Ru(II) complexes **36a,b** were prepared by heating **35a,b** with Ru(bpy)₂Cl₂·2H₂O in ethylene glycol solution at reflux (Scheme 6). It is worth-mentioning that these complexes are possible pH indicators because of their pH-dependent photophysical properties. For instance, the UV-vis spectra

of Ru(II) complex **36a** showed three distinct bands at 458, 318, 286 nm corresponding to metal-to-ligand charge transfer, centered ligand $\pi \rightarrow \pi^*$, and bipyridyl $\pi \rightarrow \pi^*$, respectively. On the other hand, fluorescence emission spectrum of **36a** showed a characteristic peak at 592 nm for metal-to-ligand charge transfer, Ru(II) dn \rightarrow d π^* . The pH alteration 1.82 \rightarrow 6.22 caused a blue shift to 598 nm with a 25% increase in the intensity while pH change 6.22 \rightarrow



Scheme 21 Synthesis of star-shaped molecule with pyrrolidine side arms 84.



Scheme 22 Synthesis of multi-armed thiazole derivatives 88a and 88b.

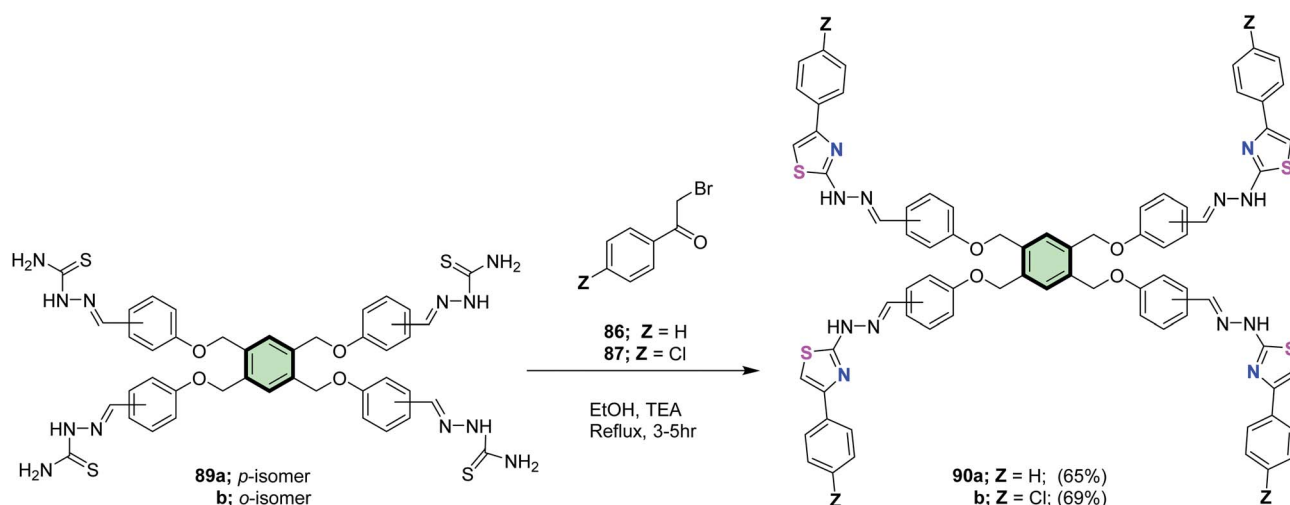
12.04 resulted in a red-shift to 606 nm with a remarkable quenching to 78%. Thus, complex **36a** acts as off-on-off fluorescence pH switch.

4.1.3. Tris(2-aminoethyl)amine core. Homochiral C3-symmetrical dendritic compounds **41a-c** were synthesized as shown in Scheme 7. The protected (*S*)-L-aspartic acid (Asp) **37a** and (*S*)-L-glutamic acid (Glu) **37b** underwent modified Clauson-Kaas ring closure reaction with 2,5-dimethoxytetrahydrofuran (DMT) under acidic condition to form pyrrolyl and carbazolyl derivatives **38a-c**. The amidation reactions of these compounds with tris(2-aminoethyl)amine **39** in presence of a mixture of dicyclohexylcarbodiimide (DCC) and 1-hydroxybenzotriazole (HOBT) afforded the protected dendritic compound **40a-c**. Palladium-deprotection of the latter compound gave the

dendritic carboxylic acids **41a-c**.⁷⁸ It should be noted that SSMs **41b** and **41c** with peripheral carbazole groups underwent an oxidative electropolymerization to form a stable electroactive polymer films which might find application for stereoselective recognition of biomolecules.

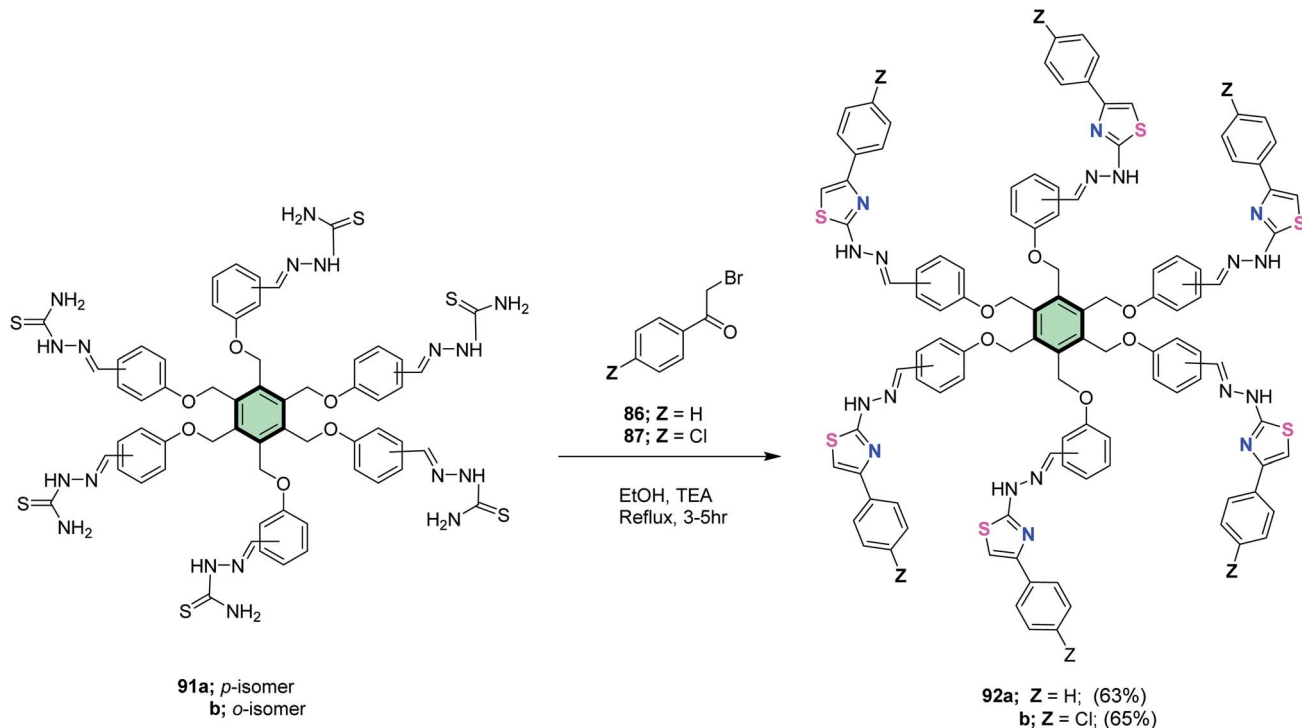
4.2. SSMs with alicyclic cores

4.2.1. Polyhedral oligomeric silsesquioxane core. Polyhedral oligomeric silsesquioxane, POSS-cored SSMs are examples of organic-inorganic hybrid materials which have interesting optoelectronic properties. Incorporating POSS core in place of traditional hole transport materials in organic light emitting devices (OLEDs) could improve both their brightness and efficiencies. Xu *et al.*⁷⁹ reported the synthesis of POSS-cored SSM **44** with incorporated carbazole moiety in excellent yield



Scheme 23 Synthesis of tetrakis(thiazoles) 90a and 90b.





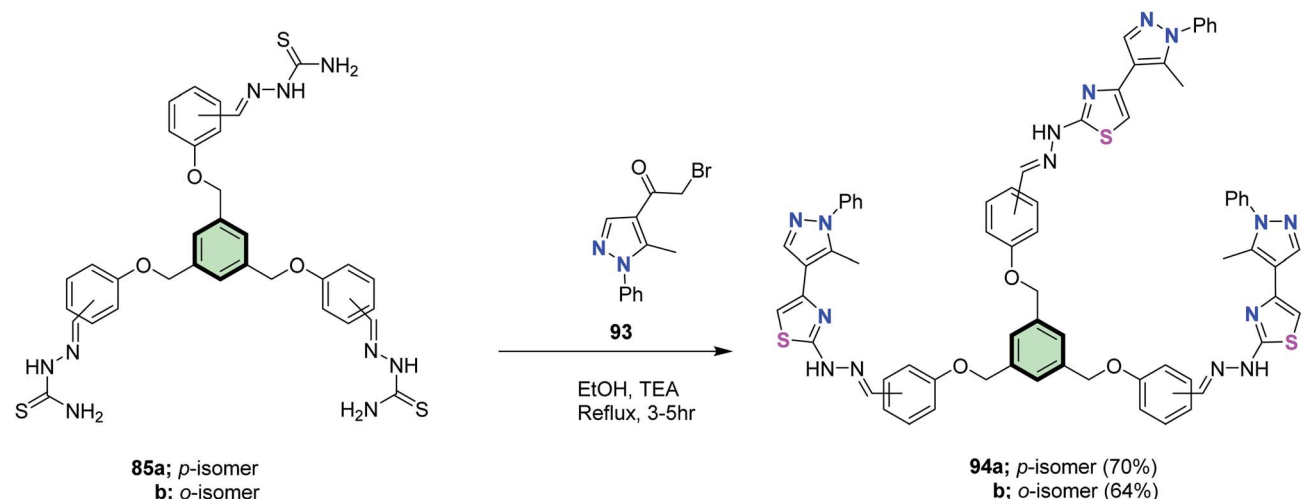
Scheme 24 Synthesis of hexakis(thiazoles) 92a and 92b.

(85%) *via* the hydrosilylation reaction of 9-allylcarbazole **43** by the action of POSS **42** in the presence of platinum(0)-1,3-divinyl-1,1,3,3-tetramethyldisiloxane (Pt-dvs) catalyst (Scheme 8). POSS-cored SSM **44** showed thermal stability with no aggregation in either solution or solid film probably due to the short POSS spacer. The UV and photoluminescence spectra showed a blue emission in both cases.

4.2.2. Cyclohexatrinone core. Pathak *et al.*¹⁹ reported the synthesis of star-shaped tris(*N*-salicylideneanilines) (TSANs) containing 1,3,4-oxadiazole **48** and **49**, as well as 1,3,4-

thiadiazole based arms **50** and **51** in 65–80% yields by the reaction of 1,3,5-triformylphloroglucinol **45** with the appropriate amine derivatives **46a,b** and **47a,b**, respectively, in EtOH at reflux (Scheme 9).

A similar approach was used to synthesize a star-shaped molecule **53a,b** with 1,3,5-cyclohexatrinone as a core and 1,2,4-oxadiazole as arms in good yield by the reaction of **45** with the respective 4-(3-aryl-1,2,4-oxadiazol-5-yl)aniline **52a** and 4-(5-aryl-1,2,4-oxadiazol-3-yl)aniline **52b** in ethanol at reflux (Scheme 10).³⁰

Scheme 25 Synthesis of star-shaped molecules with benzene core and (pyrazolyl)thiazole side arm **94a** and **94b**.

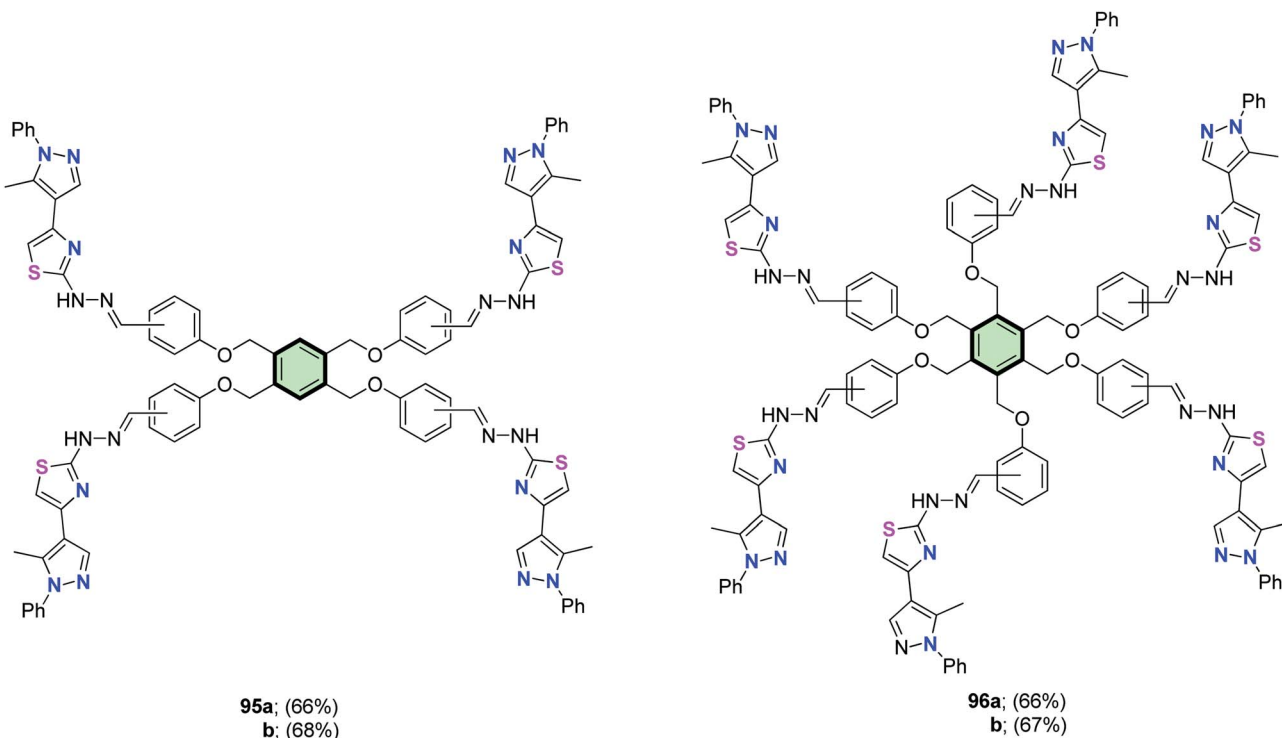
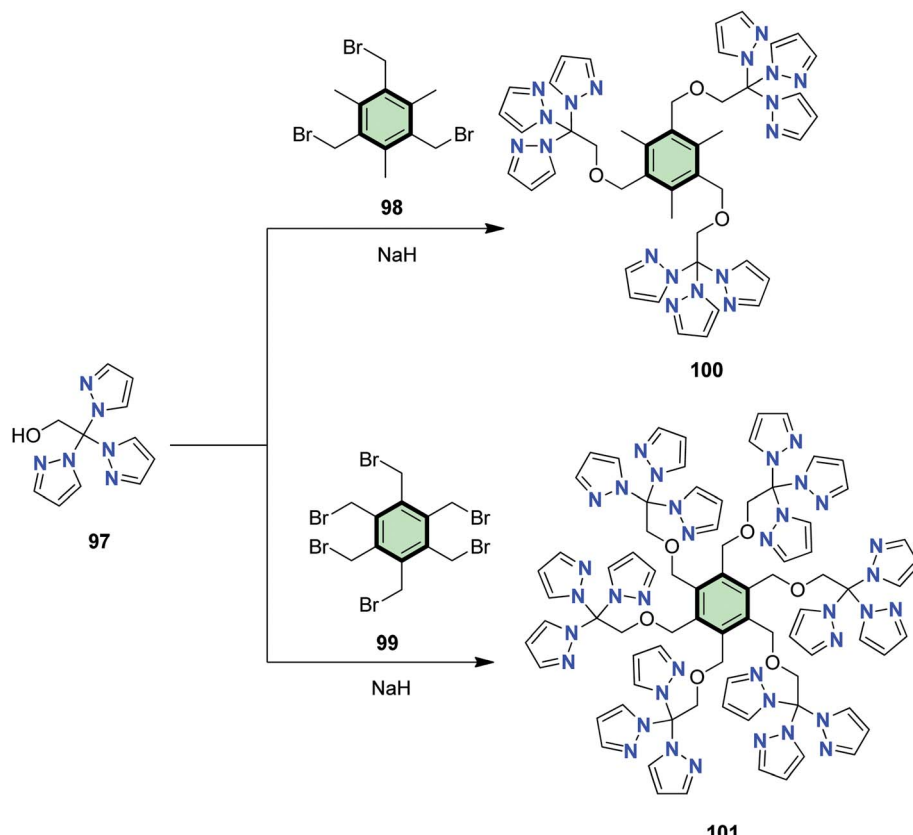
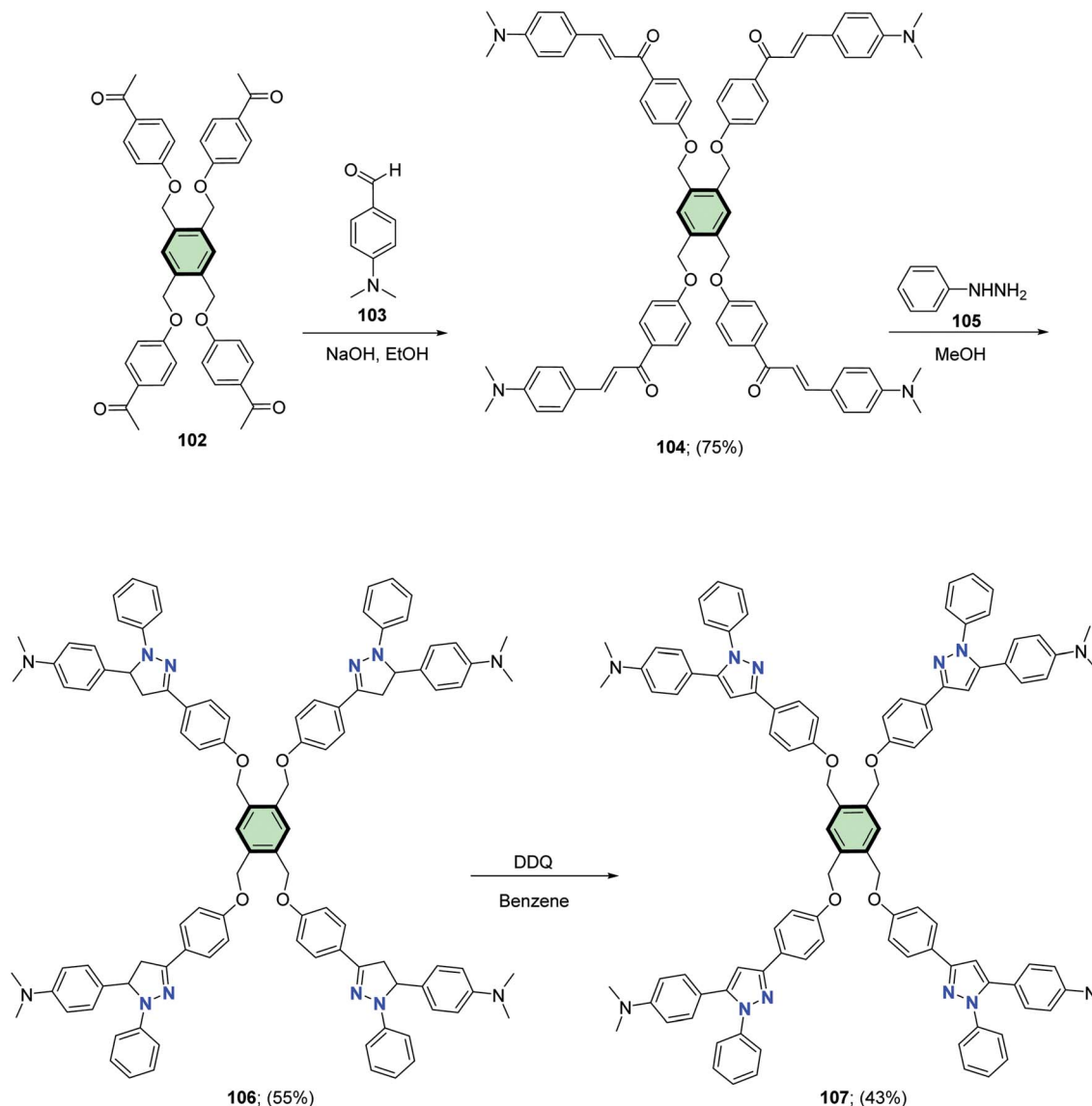


Fig. 3 Structures of tetrakis(pyrazolyl)thiazoles 95a and 95b and hexakis(pyrazolyl)thiazoles 96a and 96b.

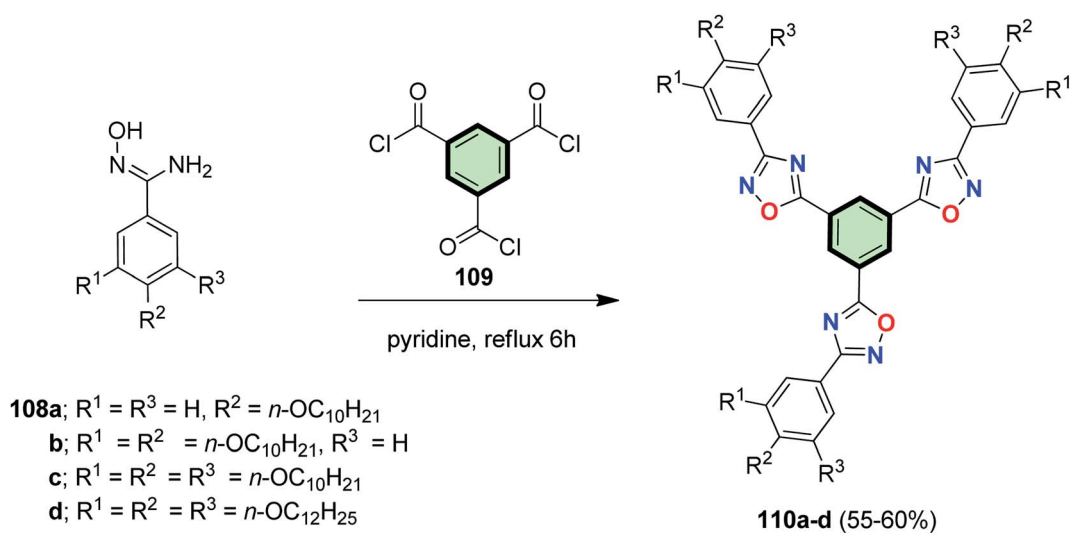


Scheme 26 Synthesis of SSMs 100 and 101.

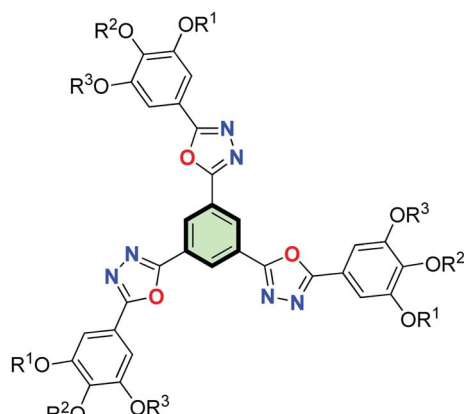




Scheme 27 Synthesis of SSMs containing four pendant pyrazole rings 107.



Scheme 28 Synthesis of 1,2,4-oxadiazole-based benzene-cored SSMs 110a-d.

**117-120 (31-36%)**

117: $R^1 = R^3 = H$, $R^2 = n\text{-C}_{10}\text{H}_{21}$
118: $R^1 = R^2 = n\text{-C}_{10}\text{H}_{21}$, $R^3 = H$
119: $R^1 = R^2 = R^3 = n\text{-C}_{10}\text{H}_{21}$
120: $R^1 = R^2 = R^3 = 2\text{-Ethyl hexyl}$

Fig. 4 SSMs with three pendant 1,3,4-oxadiazole moieties 117–120.

It should be mentioned that replacing oxygen in the five-membered ring (in star-shaped TSANs **48** and **49**) by a more voluminous and more basic sulfur atom (in star-shaped TSANs **50** and **51**) has a pronounced effect on bent angle and electron distribution. It caused a larger longitudinal/lateral dipole moment and attractive $S\cdots S$ interactions in the condensed state as well. Tuning the peripheral groups from straight to branched chains affected the transition temperature, self-assembly and photophysical behavior in the solid state. The 1,3,4-oxadiazole based TSANs with branched tails **49** stabilized a columnar rectangular Col_r phase at room temperature, while the straight chain analogue **48** showed a columnar hexagonal Col_h phase at a high temperature. In contrast to **48** and **49**, 1,3,4-thiadiazole

TSAN with straight peripheral tail **50** showed a Col_r phase (presumably because of intermolecular attraction of 1,3,4-thiadiazole rings) while that with the bulkier branched tail **51** became a non-crystalline viscous liquid.¹⁹ 1,2,4-Oxadiazole-based TSANs **53a,b**, on the other hand, showed lower melting, clearing points and wider mesophase range than 1,3,4-oxadiazole-based TSANs **50** and **51**. The position of trialkoxyphenyl group at the heterocycle has a prominent effect on the self-assembly properties; **53a** with a trialkoxyphenyl group at 5-position showed Col_r phase while **53b** with a trialkoxyphenyl group at 3-position exhibited Col_h phase. Both compounds **53a** and **53b** emitted green light in solution with quantum yield (0.27–0.31) and red-shifted compared to 1,3,4-oxadiazole derivatives in thin film.³⁰

4.3. SSMs with aromatic or heterocyclic cores

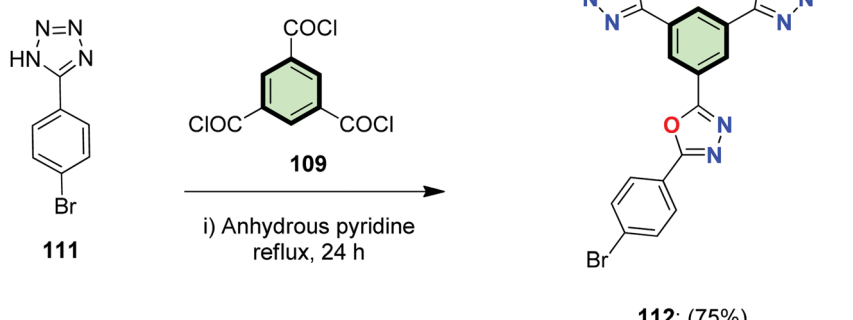
4.3.1. Benzene-cored SSMs. This class of SSMs are characterized by the presence of a central benzene core connected to different arms.

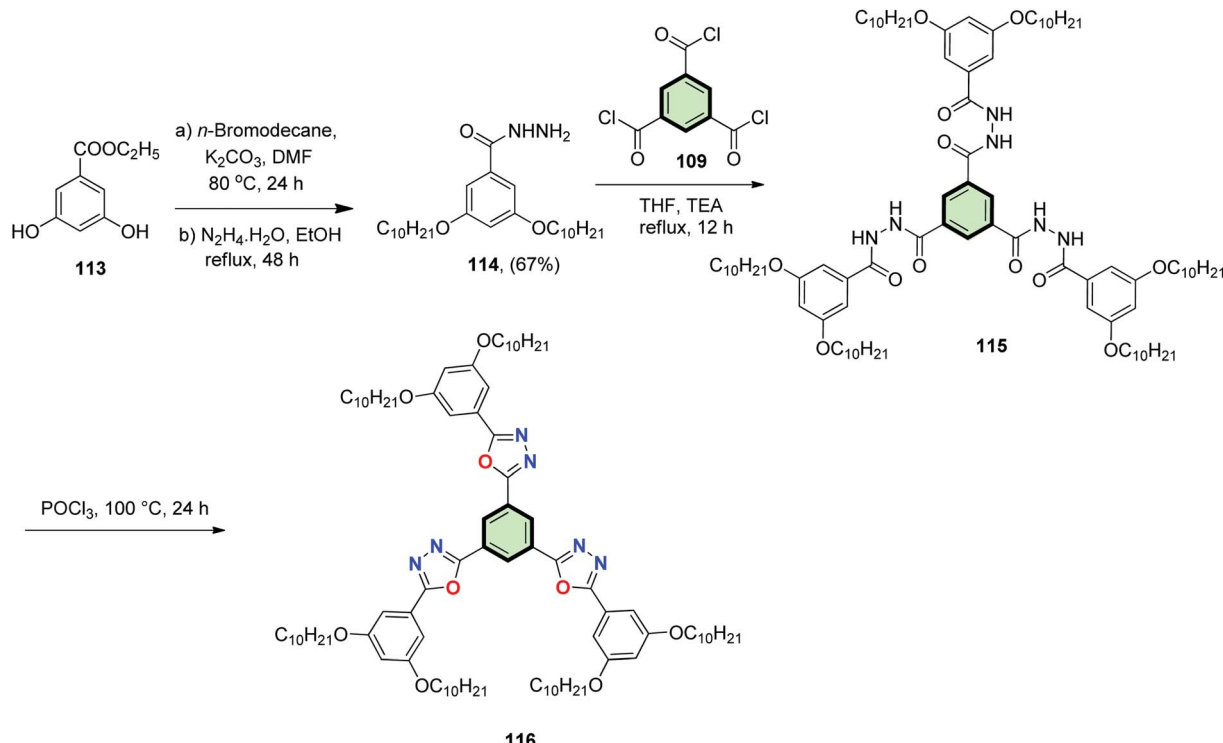
4.3.1.1. Benzene-cored SSMs with five-membered heterocyclic arms

4.3.1.1.1. Five-membered heterocyclic arms containing one heteroatom. **4.3.1.1.1.1. Furan.** Kotha *et al.*⁸⁰ reported the synthesis of 1,3,5-tris(2-furyl)benzene **56** in 66% yield by heating a mixture of 1,3,5-triiodobenzene **54** and furan-2-boronic acid **55** in THF/toluene mixture in the presence of $\text{Pd}(\text{PPh}_3)_4$ (Scheme 11).

4.3.1.1.1.2. Thiophene. A star-shaped molecule 1,3,5-tri(thiophen-2-yl)benzene **58** was synthesized in 65% yield, *via* trimerization of 2-acetyl thiophene **57** in the presence of TEA (Scheme 12).⁸¹

2-Acetyl-5-alkylthiophenes **59a–c** underwent cyclo-trimerization reaction upon treatment with SiCl_4 to give 1,3,5-tris(5-alkylthiophenyl)benzenes **60a–c** in 61, 72 and 63% yields, respectively (Scheme 13).⁸⁰

Scheme 29 Synthesis of 1,3,5-tris((4-bromophenyl)-1,3,4-oxadiazol-2-yl)benzene **112**.

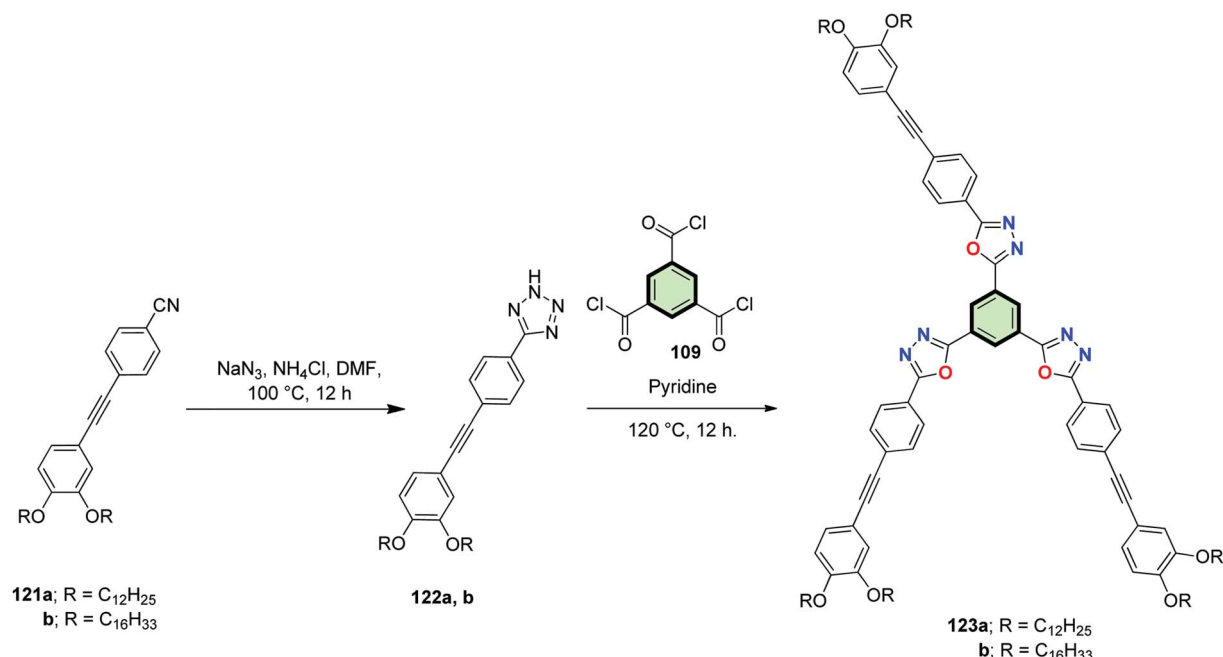


Scheme 30 Synthesis of SSMs with three pendant 1,3,4-oxadiazole moieties 116

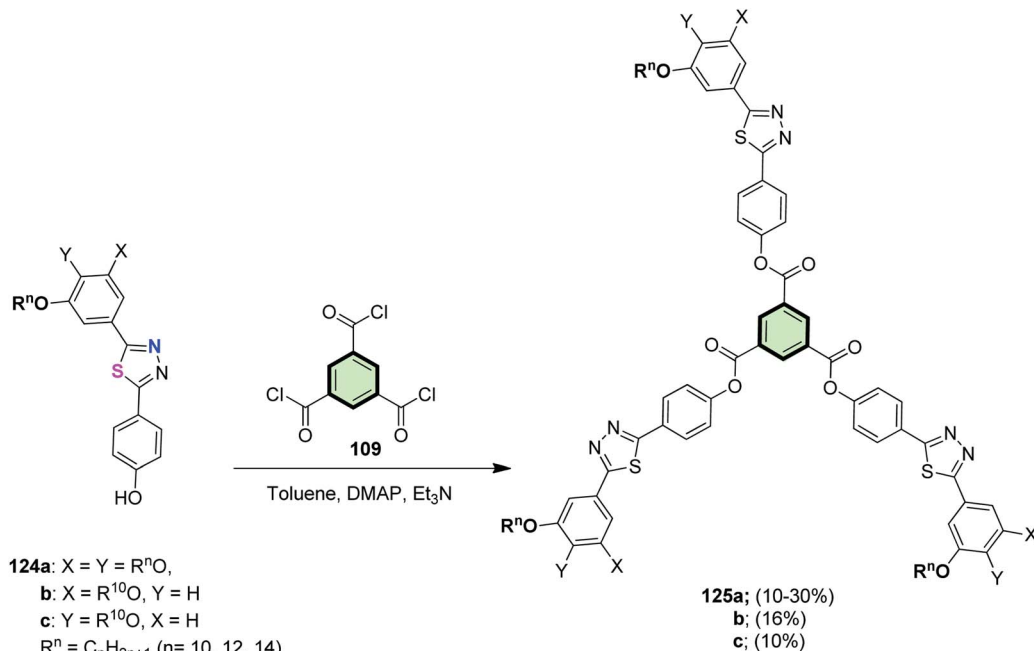
1,3,5-Tris(5-phenylthiophen-2-yl)benzene **64** was synthesized in 44% yield *via* the reaction of 2-acetyl-5-phenylthiophene **63** with SiCl_4 in ethanol. Compound **63** was synthesized from the reaction of 2-acetyl-5-

bromothiophene **61** with phenylboronic acid **62** in the presence of $\text{Pd}(\text{PPh}_3)_4$ (Scheme 14).⁸⁰

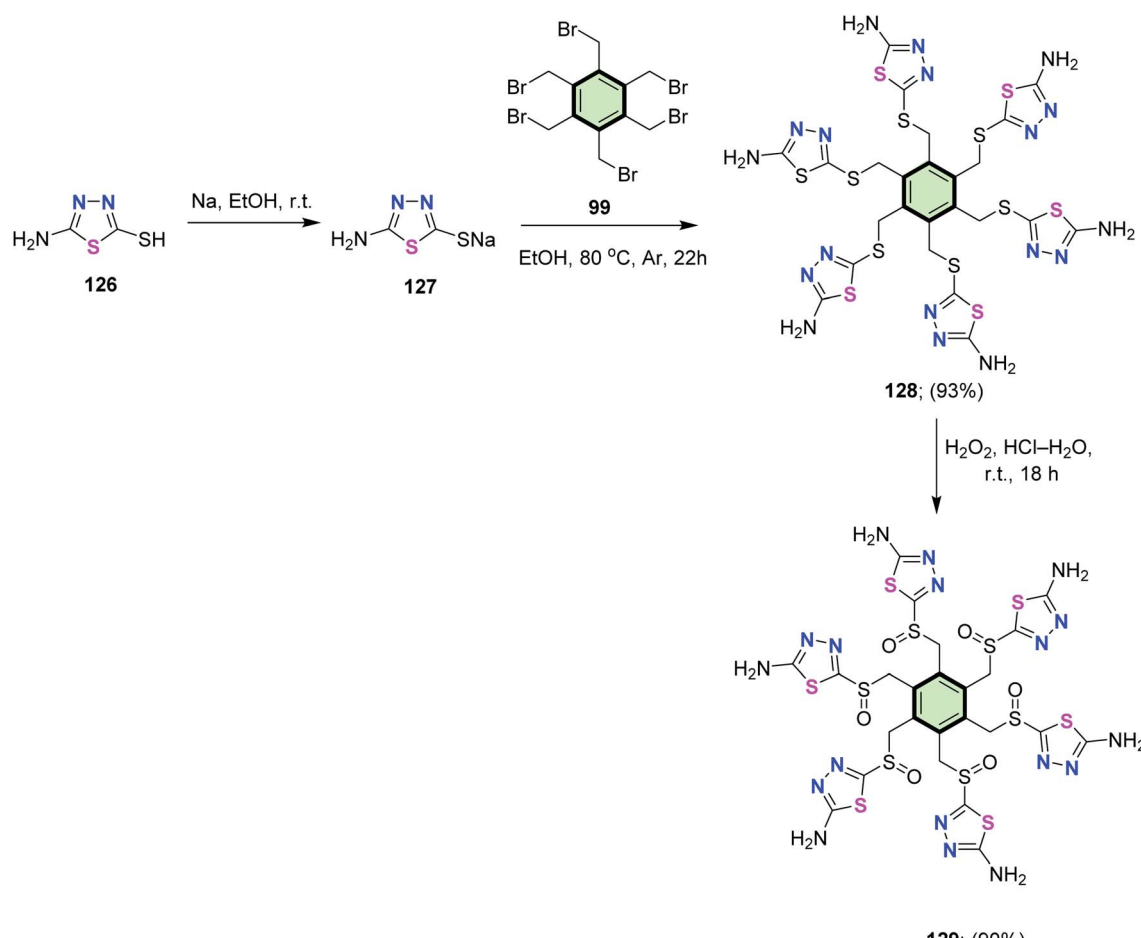
1,3,5-Tris[4-(2'-thienyl)phenyl]benzene **67** was obtained in 14% yield by the reaction of 1,3,5-tris(4-halophenyl)benzenes



Scheme 31 Synthesis of 1,3,4-oxadiazole-based SSM **123a** and **123b**

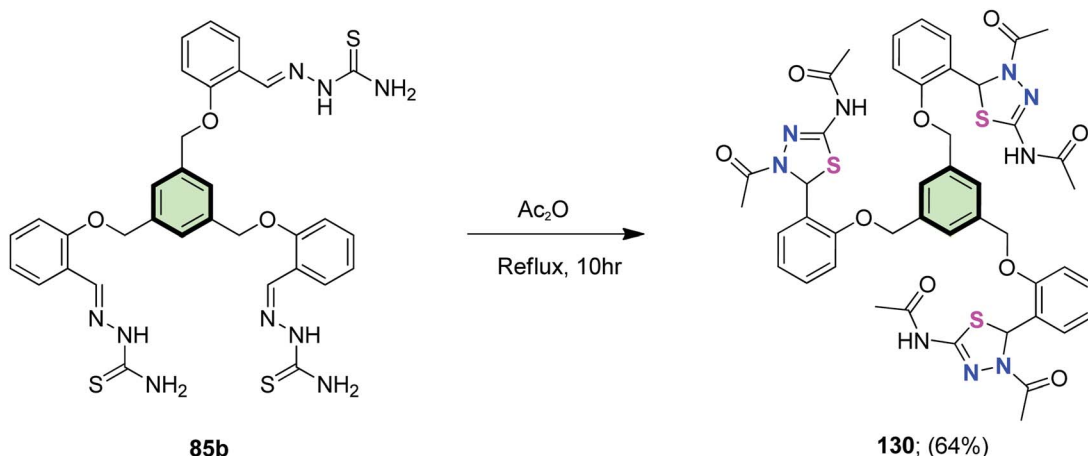


Scheme 32 Synthesis of SSMs with pendant 1,3,4-thiadiazole rings 125a-c.



Scheme 33 Synthesis of hexakis(1,3,4-thiadiazol-2-amines) 128 and 129.





Scheme 34 Synthesis of SMM with benzene core and 1,3,4-thiadiazole side arm 130.

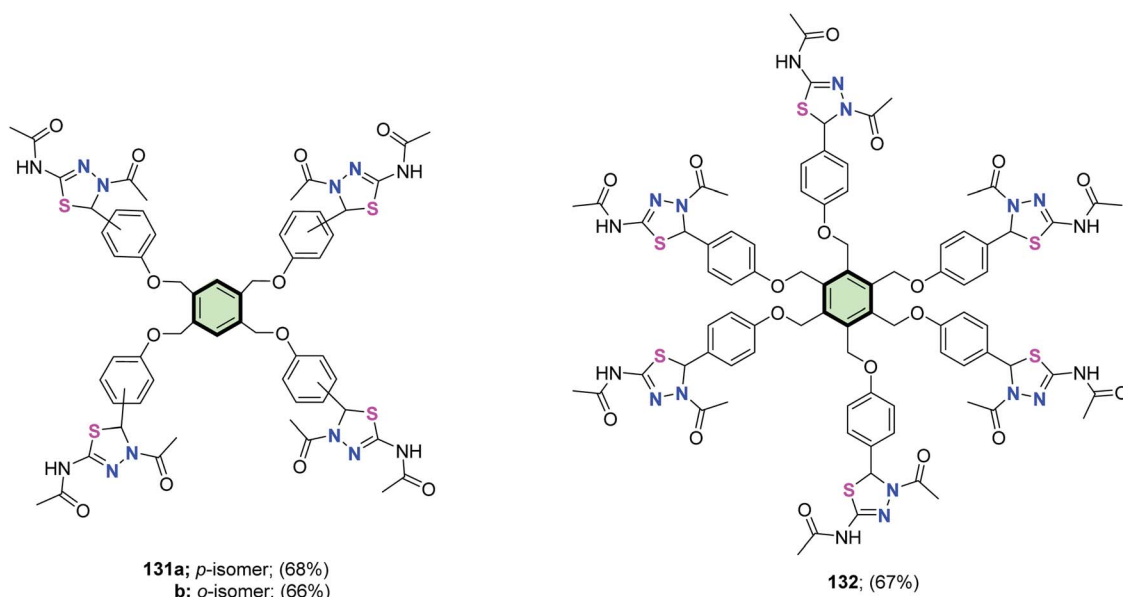
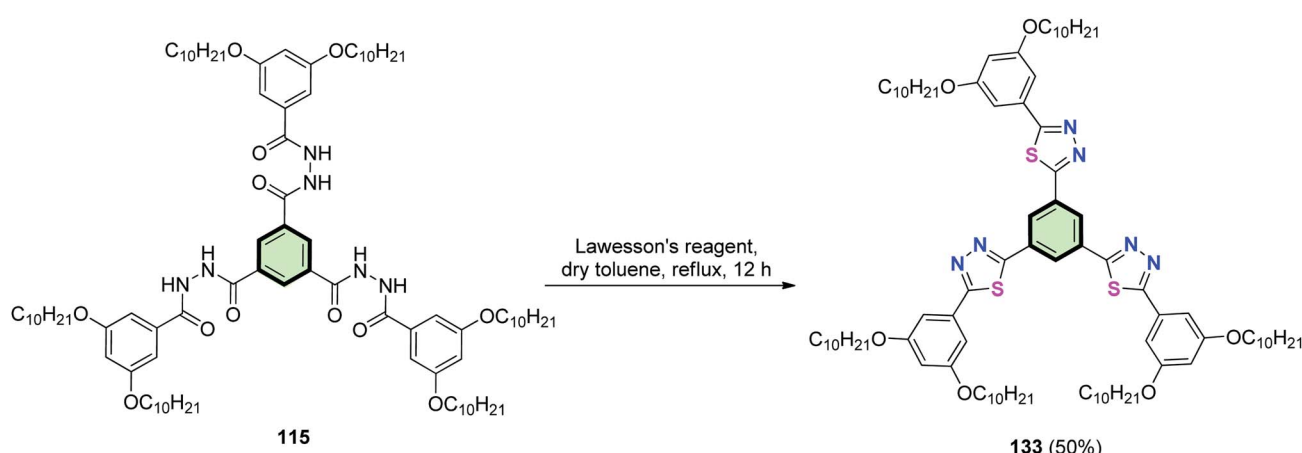
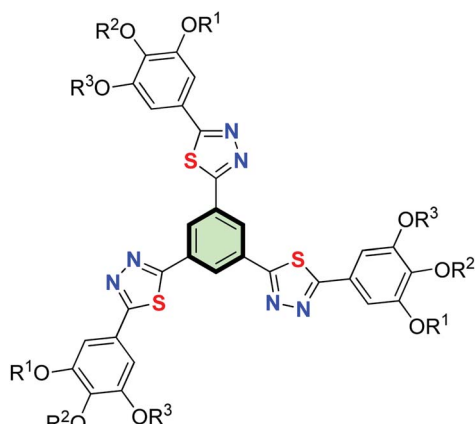


Fig. 5 Tetra- and hexakis(4,5-dihydro-1,3,4-thiadiazolyl) derivatives 131a, 131b and 132.



Scheme 35 Synthesis of SSM 133 with three pendant 1,3,4-thiadiazole moieties.



134a-d (31-36%)

134a: R¹ = R³ = H, R² = n-C₁₀H₂₁
 134b: R¹ = R² = n-C₁₀H₂₁, R³ = H
 134c: R¹ = R² = R³ = n-C₁₀H₂₁
 134d: R¹ = R² = R³ = 2-Ethyl hexyl

Fig. 6 SSMs 134a-d with three pendant 1,3,4-thiadiazole moieties.

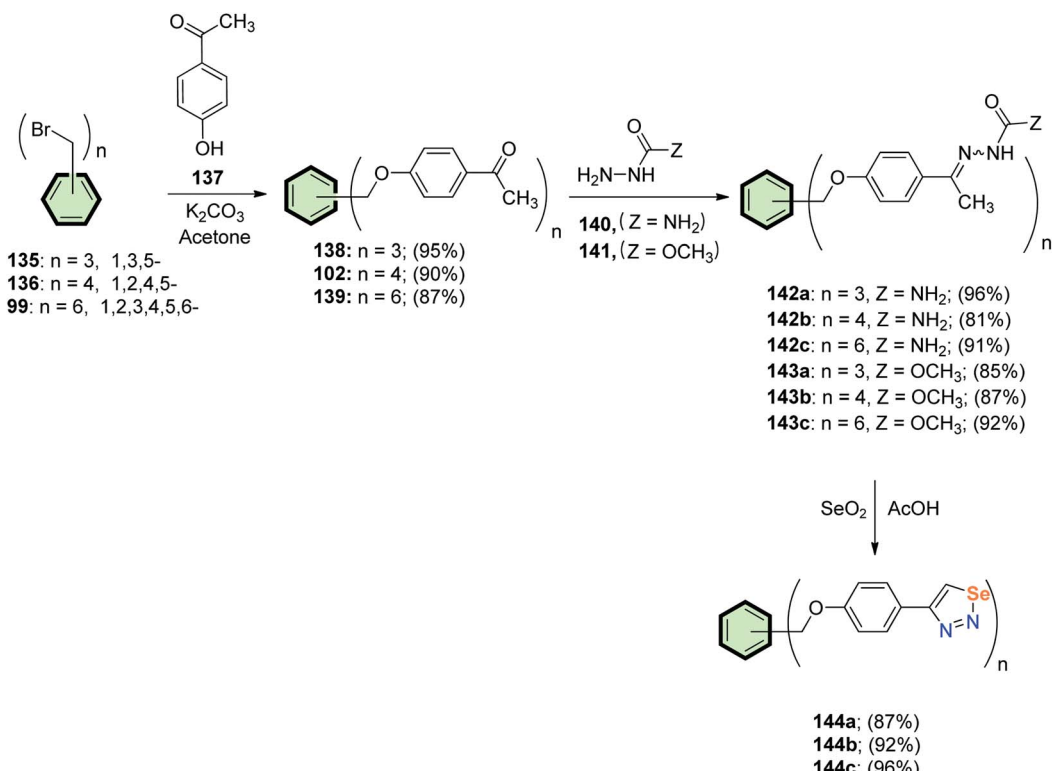
65a or 65b with thiophene-2-boronic acid 66 in the presence of Pd(PPh₃)₄ in refluxing THF/toluene mixture (Scheme 15).⁸⁰

Sonogashira coupling of ((5-iodothiophen-2-yl)ethynyl) trimethylsilane 69 and 1,3,5-triethynylbenzene 68 afforded 1,3,5-tris((5-((trimethylsilyl)ethynyl)thiophen-2-yl)ethynyl)

benzene 70 in good yield (68%) (Scheme 16). Star-shaped molecule 70 showed excellent luminescent properties. The fluorescence emission spectrum of 70 indicated four peaks at 375, 390, 418 and 446 nm, respectively, and the emission maximum peak at 375 nm. The fluorescence intensities of 70 showed a dramatic change in chloroform relative to concentration; it increased (from 1235 to 6714 a.u.) with the concentration (from 5.0 × 10⁻⁴ to 5.0 × 10⁻⁶ M), while it decreased (from 5364 to 2042 a.u.) with the concentration (from 1.0 × 10⁻⁶ to 1.0 × 10⁻⁷ M). This behavior was attributed to the concentration aggregate-enhanced emission (AEE) effect⁸² and aggregation-caused quenching (ACQ) effect. Increasing the polarity of solvent from toluene to acetonitrile resulted in a blue shift of the peaks.⁸³

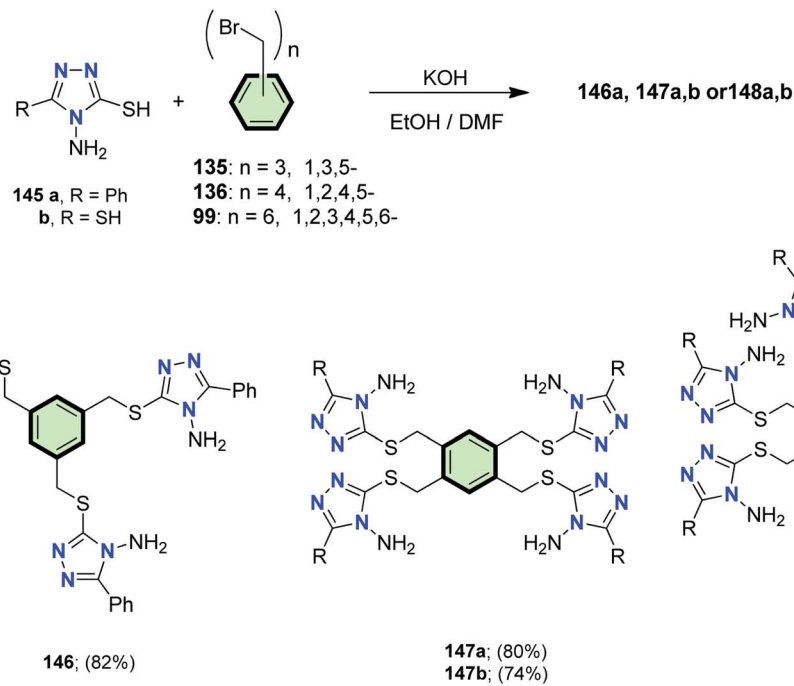
4.3.1.1.3. Pyrrole. Suresh *et al.*⁸⁴ reported the synthesis of star-shaped molecule with benzene core and pyrrole side arms 73 in 72% yield, through the reaction of 4',4'',4'''-triamino-1,3,5-triphenyl-benzene 71 with three equivalents of 1*H*-pyrrole-2-carbaldehyde 72 in the presence of (*p*-TSA) in EtOH at reflux (Scheme 17). The ligand molecule 73 itself is non-emissive; however, its boron complex 74 acted as a blue emitter (510 nm) with a fluorescence quantum yield of 0.46. DFT calculations explained that in the singlet excited state, only one iminopyrrolyl group remains planar while the two others remain at their original geometries.

4.3.1.1.4. Pyrrolidine. Rajakumar *et al.*⁸⁵ reported the synthesis of some novel star-shaped molecules with pyrrolidine side arms 78, 80, 82 and 84 in high yields through 1,3-dipolar



Scheme 36 Synthesis of SSMs 144a-c with 1,2,3-selenadiazole side arms.





Scheme 37 Synthesis of SSMs with benzene core and 1,2,4-triazole side arms.

cycloaddition reaction of the respective chalcones **75**, **79**, **81** and **83** with sarcosine **76** and paraformaldehyde **77** in toluene at reflux (Schemes 18–21).

4.3.1.1.2. Five-membered heterocyclic arms containing two heteroatoms. **4.3.1.1.2.1. Thiazole and its derivatives.** Salem *et al.*⁸⁶ reported the synthesis of multi-armed thiazole derivatives **88a** and **88b** in 67 and 69% yields, respectively, by the reaction of tris(aldehyde thiosemicarbazones) **85a** and **85b** with each of 2-bromo-1-phenyl ethanone **86** and 2-bromo-1-(4-chlorophenyl)ethanone **87** in ethanol at reflux in the presence of TEA (Scheme 22). The same methodology was extended to the preparation of tetrakis- and hexakis(thiazoles) **90a**, **90b**, **92a** and **92b** in good yields from the corresponding poly(aldehyde thiosemicarbazones) **89a**, **89b**, **91a** and **91b** (Schemes 23 and 24).

Star-shaped molecules with benzene core and (pyrazolyl)thiazole side arm **94a** and **94b** were synthesized in 70 and 64% yields, upon reaction each of tris(aldehyde thiosemicarbazones) **85a** and **85b** with 2-bromo-1-(5-methyl-1-phenyl-1*H*-pyrazol-4-yl)ethanone **93** in ethanol at reflux in the presence of TEA (Scheme 25).⁸⁶

In analogy, tetrakis(pyrazolyl)thiazoles **95a** and **95b** and hexakis(pyrazolyl)thiazoles **96a** and **96b** were synthesized by the reaction of the appropriate poly(thiosemicarbazones) **89a, b** and **91a, b** with 4-bromoacetylpyrazole **93** under the same condition (Fig. 3).⁸⁶

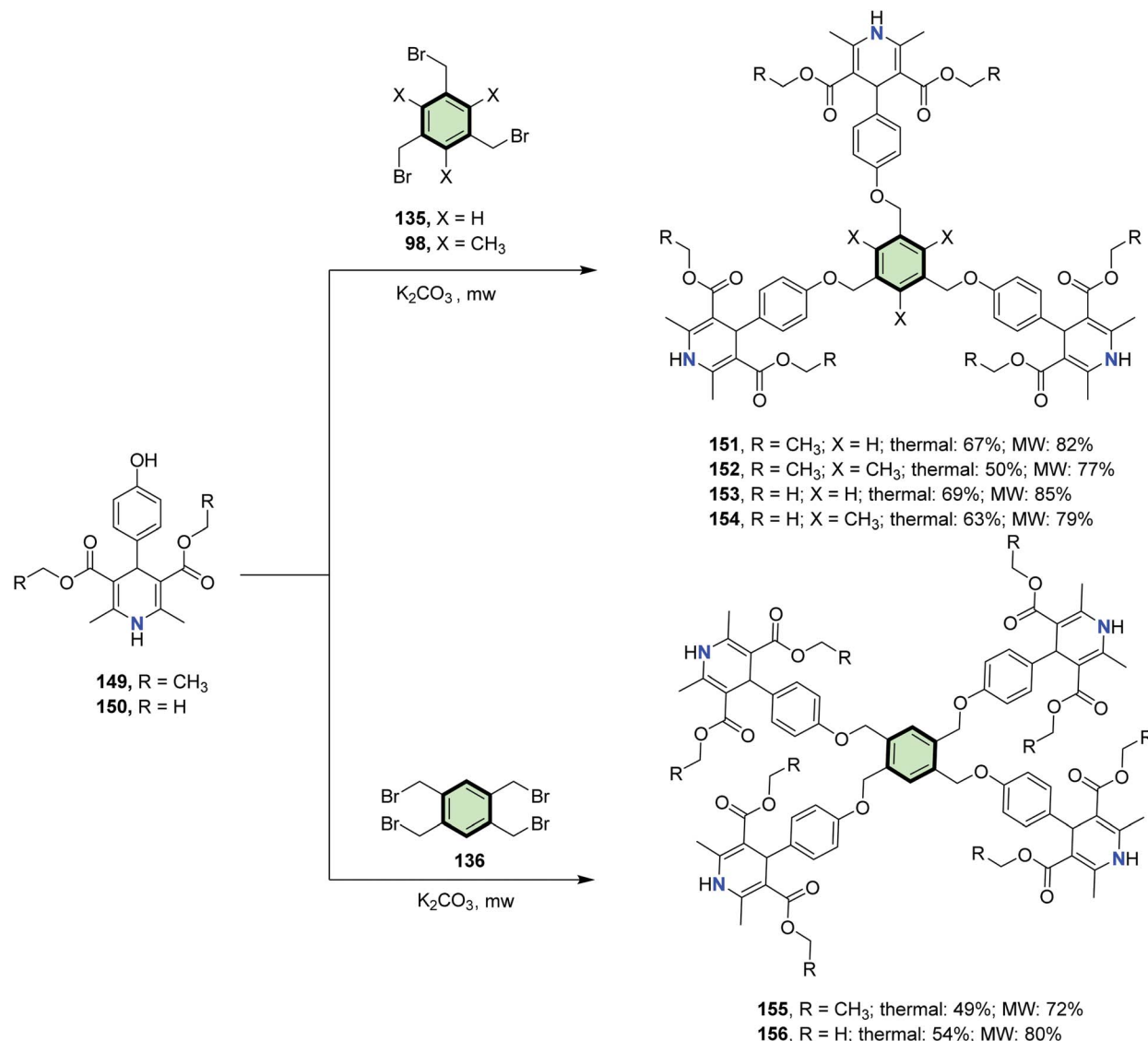
4.3.1.1.2.2. Pyrazole. Reger *et al.*³⁴ reported the synthesis of ligands with tris(pyrazolyl)methane units **100** and hexakis(pyrazolyl)methane units **101** in good yields by the reaction of tris-2,2,2-(1-pyrazolyl)ethanol **97** with each of 2,4,6-tris(bromomethyl)mesitylene **98** and 1,2,3,4,5,6-

hexakis(bromomethyl)benzene **99**, respectively, in the presence of NaH (Scheme 26). These star-shaped ligands have been used to synthesize interesting metallacage complexes *via* symmetry-interaction approach. The ligands showed a semi-flexible coordination behavior depending on the central metal mode of bonding, *i.e.* closed metallacage of high thermal stability at 200 °C was formed in case of Ag(I) while in case of Cd(II) open cage was produced.

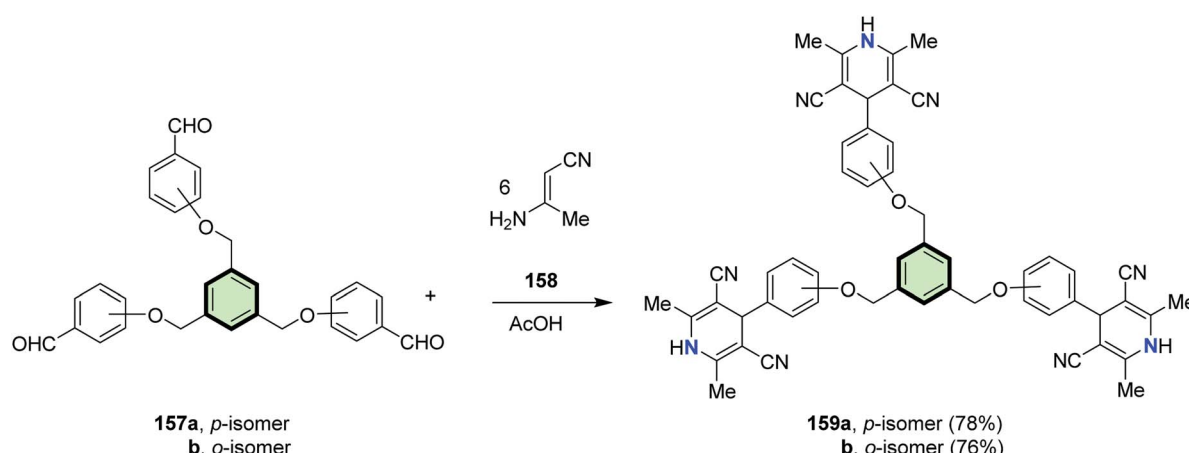
Al-Smadi *et al.*⁸⁷ reported the synthesis of multi-armed aromatic chalcone **104** in 75% yield through cross-aldo condensation reaction between multi-armed aromatic ketone **102** and 4-(dimethylamino)benzaldehyde **103** in basic medium. The multi-armed aromatic chalcone **104** underwent cyclization reactions upon treatment with phenyl hydrazine **105** to yield the corresponding multi-armed pyrazoline derivatives **106** in 55% yield. Aromatization of the pyrazoline rings of the latter compound with 2,3-dichloro-5,6-dicyano-1,4-benzoquinone (DDQ) in benzene gave the corresponding multi-armed compound **107** in 43% yield (Scheme 27).

4.3.1.1.3. Five-membered heterocyclic arms containing three heteroatoms. **4.3.1.1.3.1. 1,2,4-Oxadiazole.** Heating benzamidoxime derivatives **108** (prepared from ethyl gallate *via* a multistep procedure) with trimesic acid chloride **109** (prepared by heating benzene-1,3,5-tricarboxylic acid **4** with thionyl chloride in DMF) in pyridine at reflux afforded 1,2,4-oxadiazole-based benzene-cored SSMs **110** in moderate yields (55–60%) (Scheme 28). The number and length of the peripheral tails altered greatly the mesophase stability and the thermal range. Single crystal XRD analysis indicated that **110a** (with

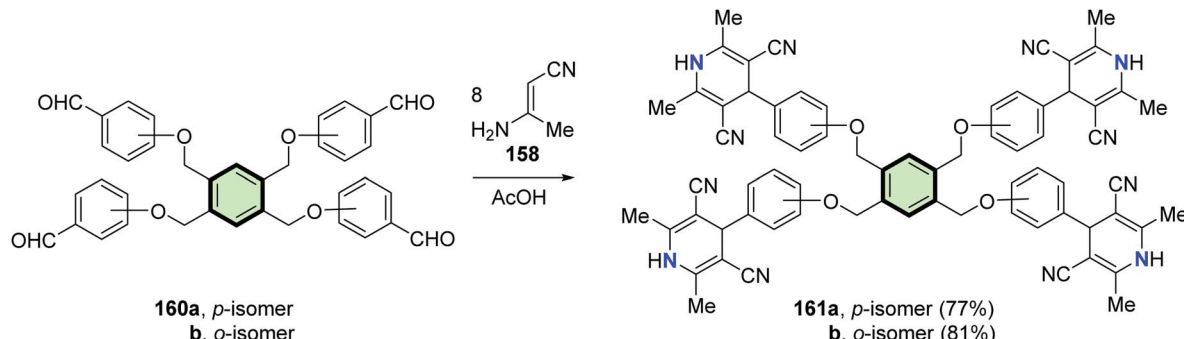




Scheme 38 Synthesis of tripodal and tetrapodal(1,4-dihydropyridines) 151–156.



Scheme 39 Synthesis of tris(1,4-dihydropyridines) 159a and 159b.



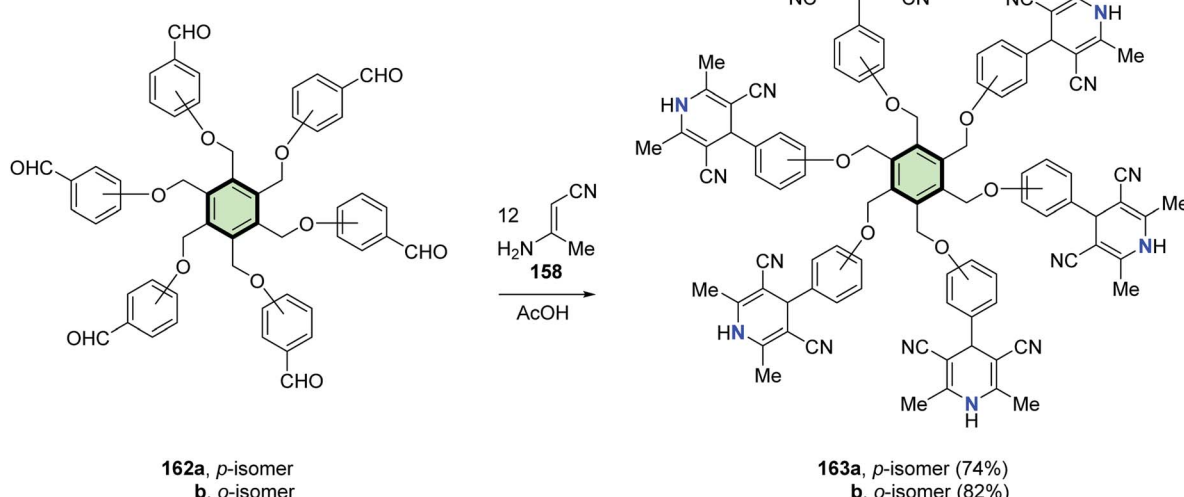
Scheme 40 Synthesis of tetrakis(1,4-dihydropyridines) 161a and 161b.

three peripheral chains) was crystalline and lamellar. The star-shaped compound has to contain at least six peripheral alkyl groups to attain a Col_h phase. The thermal range is direct proportional to the number of peripheral alkyl tails. Furthermore, increasing the length of alkyl chain led to a reduction of Col_h phase. Although all hekates **110a–d** exhibited weak fluorescence in solution, they have a strong emission in solid state and exhibited a red shift upon increasing the number of alkyl tails. The energy gap ΔE_g^{opt} values of **110a–d** are 4.21–4.23 eV which is higher than that of 1,3,4-oxadiazole analogues 117–120 (3.35–3.48 eV,³¹ cf. Fig. 4). The emission spectra of **110a–d** displayed maxima centered at 299–314 nm which were red-shifted on increasing the number of peripheral groups. In particular, Hekate **110b** acted as a supergelator forming gel in non-polar solvent (which is so rare). At higher concentration, it formed a stable gel which could be molded. Compound **110b** exhibited aggregation-induced blue light emission twelve times higher than that of the monomer. Photophysical studies showed that

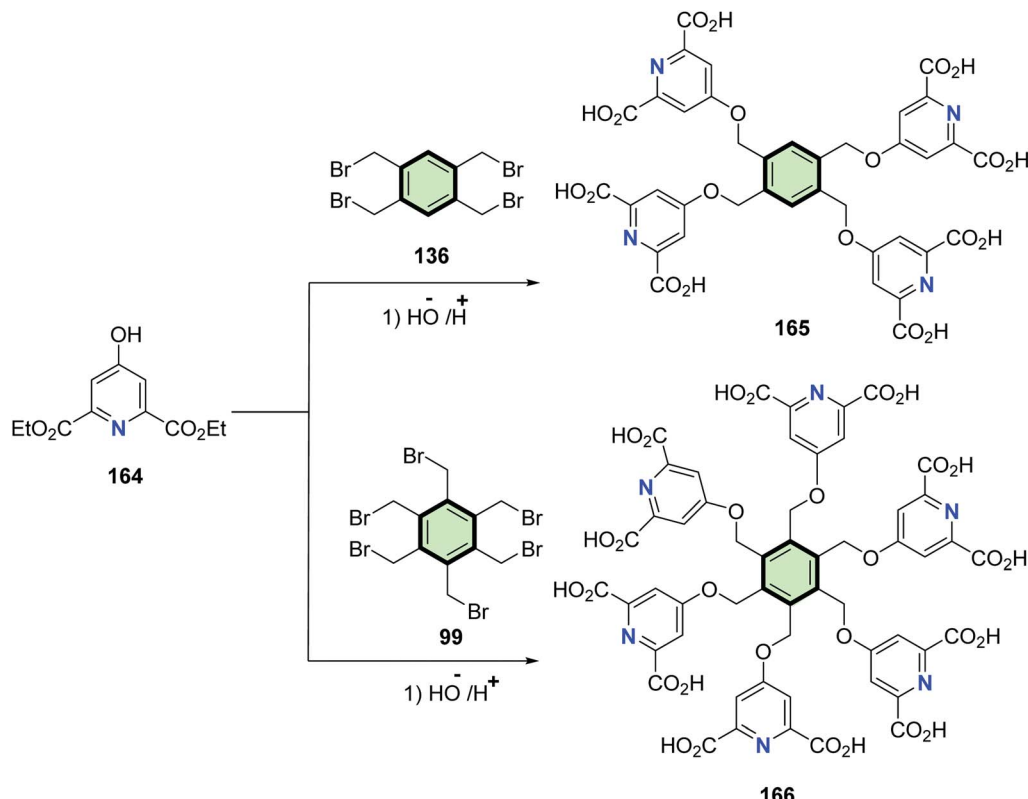
110b forms J-aggregate in thin film while H-aggregate in gel. XRD of **110b** clarified a Col_h assembly in the xerogel state.²⁵

4.3.1.1.3.2. 1,3,4-Oxadiazole. 5-(4-Bromophenyl)-1*H*-tetrazole **111** underwent cleavage–cyclization reaction upon treatment with benzene-1,3,5-tricarbonyl trichloride **109** in anhydrous pyridine to give 1,3,5-tris(5-(4-bromophenyl)-1,3,4-oxadiazol-2-yl)benzene **112** in 75% yield (Scheme 29).⁸⁸

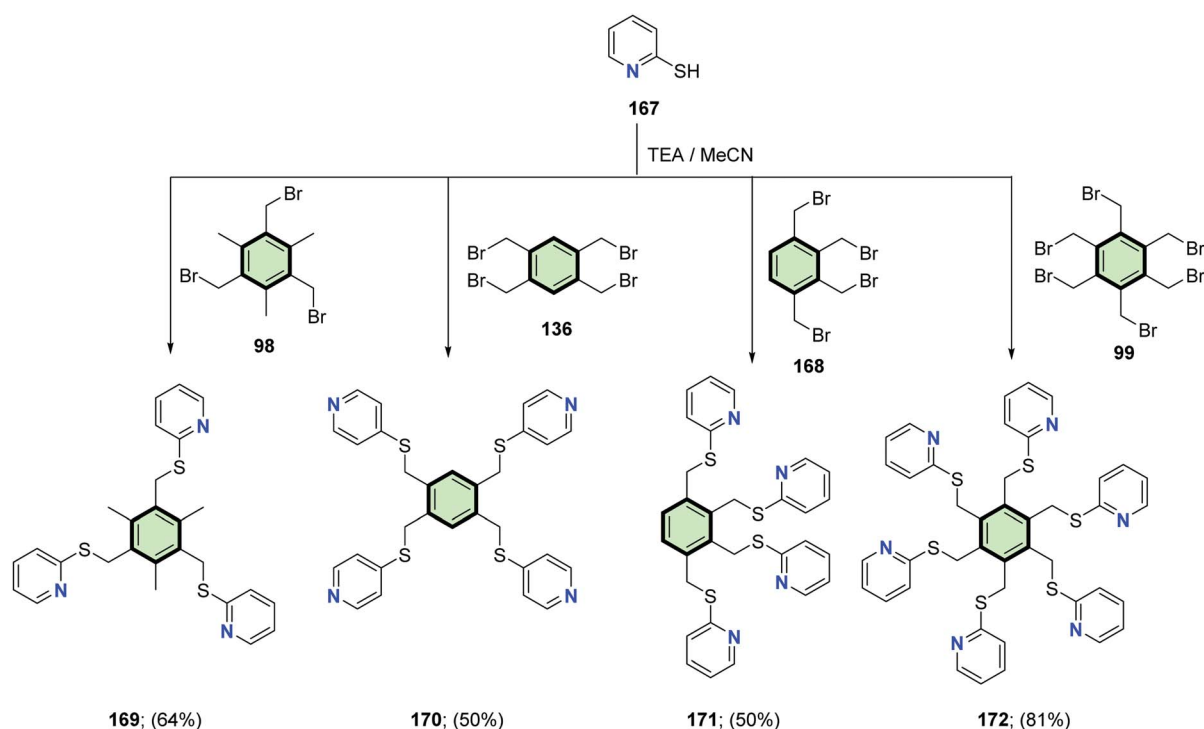
Williamson's *O*-alkylation of ethyl 3,5-dihydroxybenzoate **113** with *n*-bromodecane followed by reaction with hydrazine hydrate gave 3,5-bis(decyloxy)benzohydrazide **114** in moderate yield (67%). The acylation of **114** with benzene-1,3,5-tricarbonyl trichloride **109** in THF in the presence of triethylamine at reflux resulted in the formation of tris(aroyl)benzene-1,3,5-tricarbohydrazide **115**. Cyclization of **115** was affected by treatment with phosphorus oxychloride to form SSMs with three pendant 1,3,4-oxadiazole moieties **116** (Scheme 30). Compound **116** stabilized a Col_h phase and showed supergelation property due to π – π interactions. It also showed many fold hyperchromic increase in photoluminescence.⁸⁹



Scheme 41 Synthesis of hexakis(1,4-dihydropyridines) 163a and 163b.

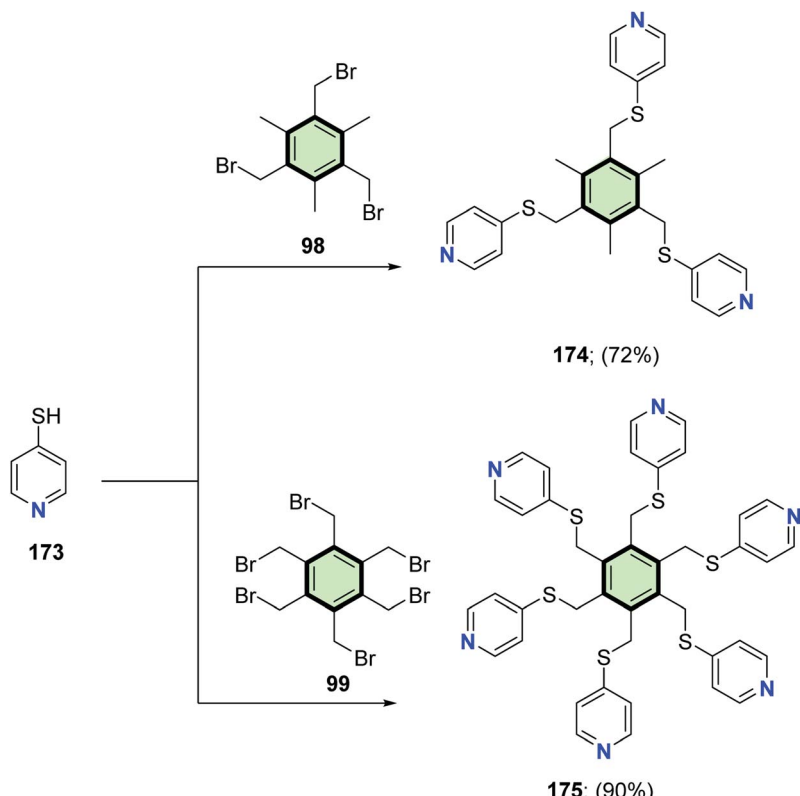


Scheme 42 Synthesis of SMM 165 and 166 with benzene core and pyridine-2,6-dicarboxylic acid side arm.



Scheme 43 Synthesis of poly(pyridylsulfanyl methyl)arenes 169–172.





Scheme 44 Synthesis of poly(pyridylsulfanyl)methyl)arenes 174 and 175.

In a similar reaction sequence, SSMs 117–120 were synthesized in 31–36% yields starting from ethyl gallate (Fig. 4).³¹

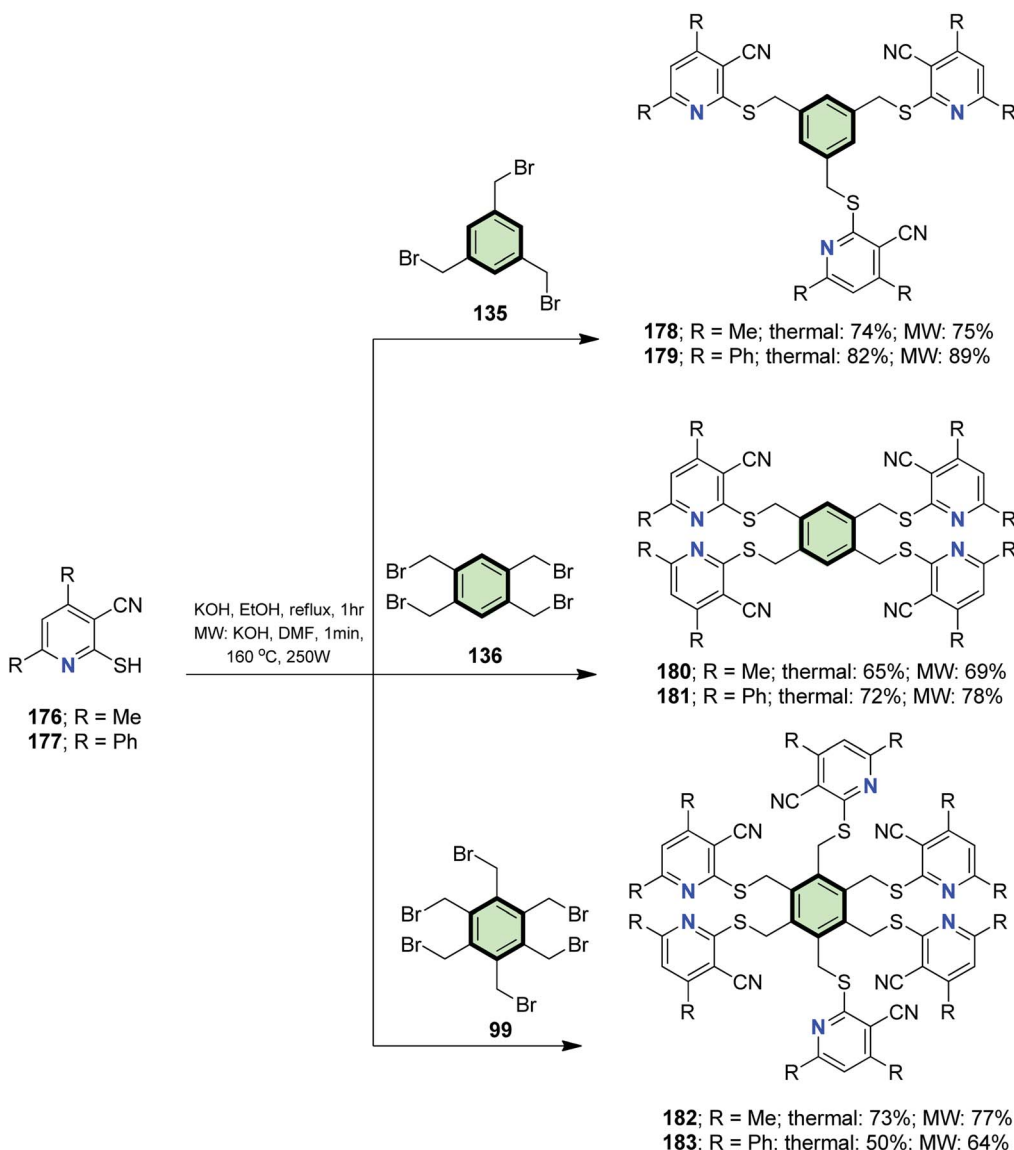
1,3,4-Oxadiazole-based SSMs 123a,b were synthesized as outlined in Scheme 31 *via* firstly reaction of 4-((3,4-bis(alkoxy)phenyl)ethynyl)benzonitrile 121a or 121b with sodium azide to afford tetrazole derivatives 122a and 122b, respectively, in excellent yields (85–90%). Synthesis of 123a and 123b was then achieved *via* treating 122a and 122b, respectively, with trimesic acid chloride 109 by a typical Huisgen reaction mechanism. 1,3,4-Oxadiazole-SSMs 123a and 123b exhibited enantiotropic columnar mesophases over a wide temperature range, with the liquid crystalline phases exhibiting strong blue fluorescence. On cooling, 123a transformed into a transparent glass at room temperature wherein the liquid crystalline texture was retained. The glassy film remained stable over a period of one year and exhibited blue luminescence with an absolute quantum yield of 26%.

The length of the alkyl substituent was observed to have a significant effect on the absorption and fluorescence properties of the gels, which was attributable to the role of the alkyl substituents in controlling the nature of the molecular packing within the self-assembled fibers of the gels. The optical properties of these derivatives in gel state were found to be alkyl chain dependent. The gel derived from 123a exhibited blue emission whereas 123b exhibited bluish-green emission in decane.

The extent of aggregation was found to be higher in 123b which is evident from their large red shift observed in absorption and emission spectra compared to the other derivative. These observations clearly demonstrate that perturbation of molecular structure has remarkable influence on their bulk macroscopic properties.⁸⁵

4.3.1.1.3.3. 1,3,4-Thiadiazole. A series of star-shaped molecules based on benzene as the central core and three pendant 2-phenyl-5-(di-, and/or tri-*n*-alkoxyphenyl)-1,3,4-thiadiazole arms 125a–c were synthesized by the reaction of 1,3,5-benzene-tricarbonyl trichloride 109 with the corresponding phenolic 1,3,4-thiadiazole precursors 124a–c, respectively, in the presence of dimethylaminopyridine (DMAP) and triethylamine in dry toluene (Scheme 32).¹⁸ The position and number of alkoxy substituents was found to affect the photophysical and liquid crystalline properties of SSMs 125. Of the synthesized SSMs, 125a and 125b showed enantiotropic liquid crystalline properties adopting hexagonal columnar phase on cooling the isotropic liquid to room temperature. These mesogens were luminescent at room temperature either in solid or in film. The cyclic voltammetry data of 125b indicated that it can act as hole-blockers.

Yang *et al.*⁹⁰ reported that heating hexakis(bromomethyl) benzene 99 with the sodium salt of 2-amino-5-sulfanyl-1,3,4-thiadiazole 127 (obtained upon treatment of 126 with sodium ethoxide) in ethanol at reflux gave hexakis(1,3,4-thiadiazol-2-amine) 128 bonded to benzene core *via* methylenesulfinyl



Scheme 45 Synthesis of SMM with benzene core and nicotinonitrile side arm 178–183.

(CH₂–S) linkages in 93% yield. The latter compound underwent oxidation upon treatment with hydrogen peroxide to give hexakis(methylenesulfinyl)hexakis(1,3,4-thiadiazol-2-amine) 129 in 90% yield (Scheme 33). Three arms of compound 129 could successfully encapsulate one or two copper(II) ions.

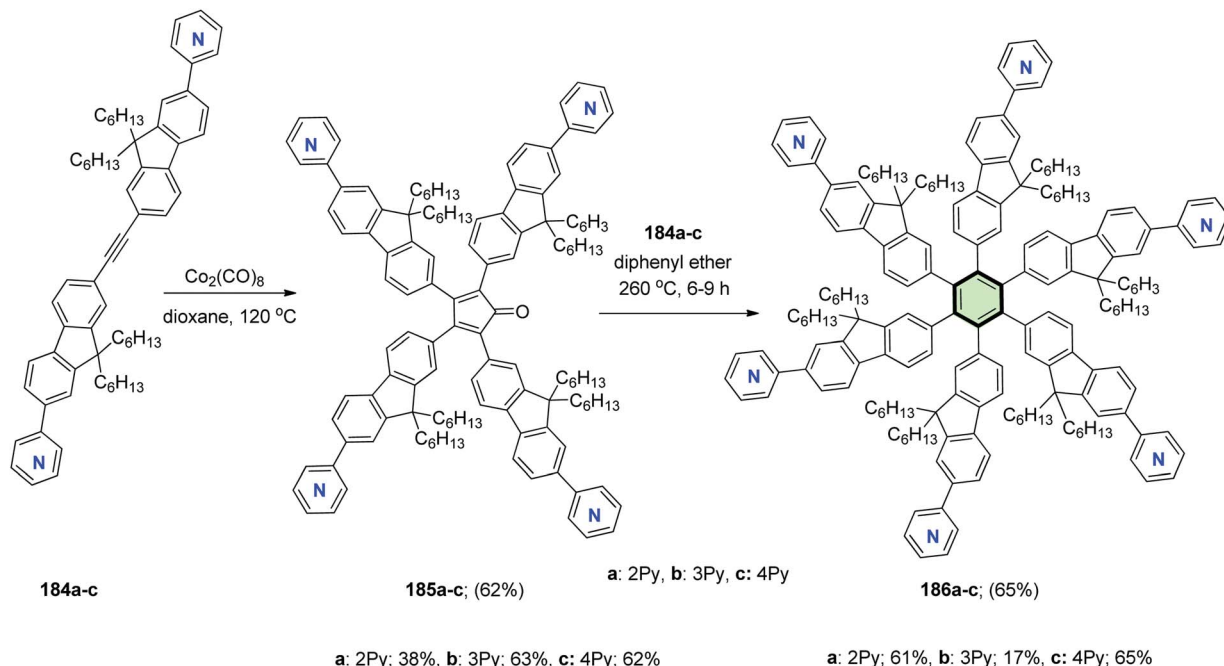
A star-shaped molecule with benzene core and 1,3,4-thiadiazole side arm 130 was synthesized in 64% yield by refluxing tris(aldehyde thiosemicarbazone) 85b in acetic anhydride (Scheme 34).⁸⁶

Similarly, tetrakis(4,5-dihydro-1,3,4-thiadiazolyl) derivatives 131a and 131b as well as hexakis(4,5-dihydro-1,3,4-thiadiazolyl) 132 have been synthesized in good yields from the corresponding tetra- and hexa(aldehyde thiosemicarbazone) (Fig. 5).⁸⁶

Heating of tris(aryl)benzene-1,3,5-tricarbohydrazide 115 with Lawesson's reagent in dry toluene furnished SSM 133 with three pendant 1,3,4-thiadiazole moieties (Scheme 35).⁸⁹

In a similar reaction sequence, SSMs 134a–d were synthesized in 30–49% yields starting from ethyl gallate (Fig. 6).³¹

4.3.1.1.3.4. 1,2,3-Selenadiazole. Al-Smadi and Ratnout⁹¹ reported a multi-step procedure for the synthesis of multi-armed benzene derivatives 144a–c containing two, three, four and six 1,2,3-selenadiazole side arms as outlined in Scheme 36. The poly ketones 138, 102 and 139 were prepared by reacting bromomethyl benzene derivatives 135, 136 and 99, respectively, with 4-hydroxyacetophenone 137 in acetone in the presence of K₂CO₃. Condensation of 138, 102 and 139 with semicarbazide 140 or methyl hydrazine carboxylate 141 afforded the corresponding semicarbazones 142a–c or the ethoxycarbonyl

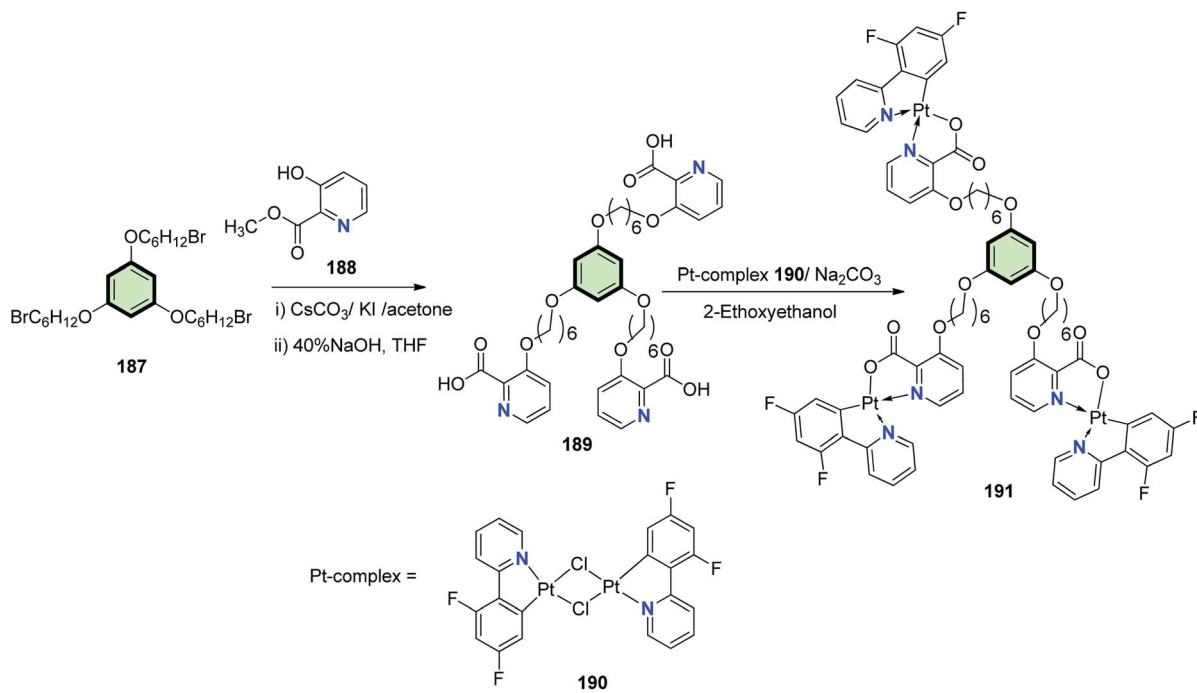


Scheme 46 Synthesis of hexakis(9,9-dihexyl-7-(pyridin-4-yl)-9H-fluoren-2-yl)benzene 186a–c.

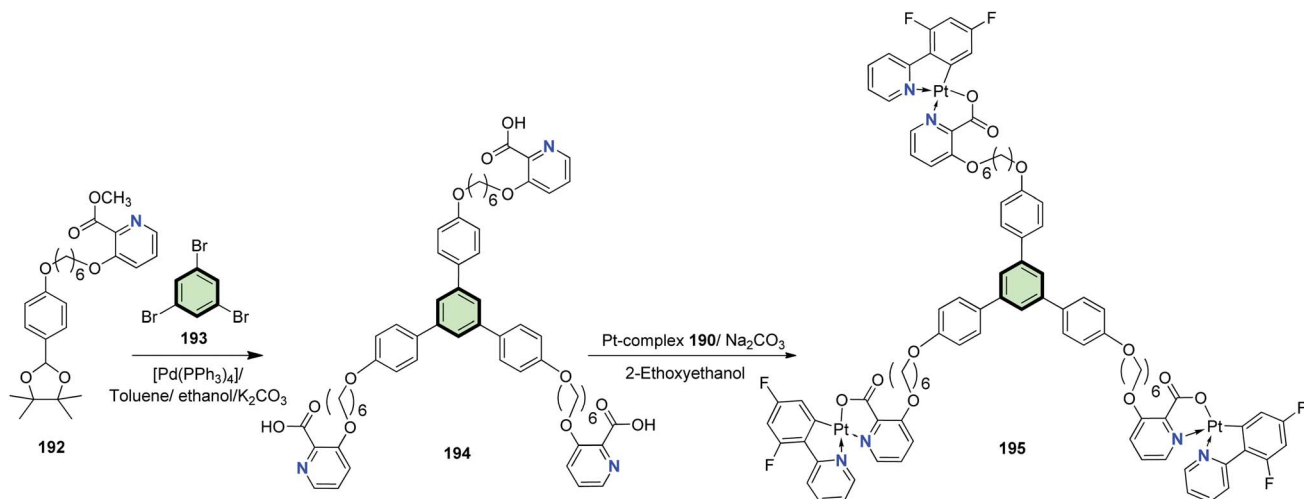
hydrazones **143a-c**, respectively. Subsequent treatment of the latter compounds with selenium dioxide in acetic acid gave compounds **144a-c** in good yields (Scheme 36).

4.3.1.1.3.5. 1,2,4-Triazole. Elwahy *et al.*⁹² reported the synthesis of 1,3,5-tris(4-amino-5-phenyl-4H-3-sulfanyl methyl)

benzene **146** in 82% yield by the reaction of tris(bromomethyl)benzene **135** with 4-amino-5-phenyl-4*H*-1,2,4-triazole-3-thiol **145a** in refluxing EtOH/DMF mixture containing KOH. Under similar conditions, tetrakis- and hexakis(4-amino-5-phenyl-4*H*-3-sulfanyl methyl)benzenes **147a,b** and **148a,b** were prepared in 74–80% yields, respectively, upon treatment of the



Scheme 47 Synthesis of cyclometalated platinum(II) complexes 191.



Scheme 48 Synthesis of cyclometalated platinum(II) complexes 195.

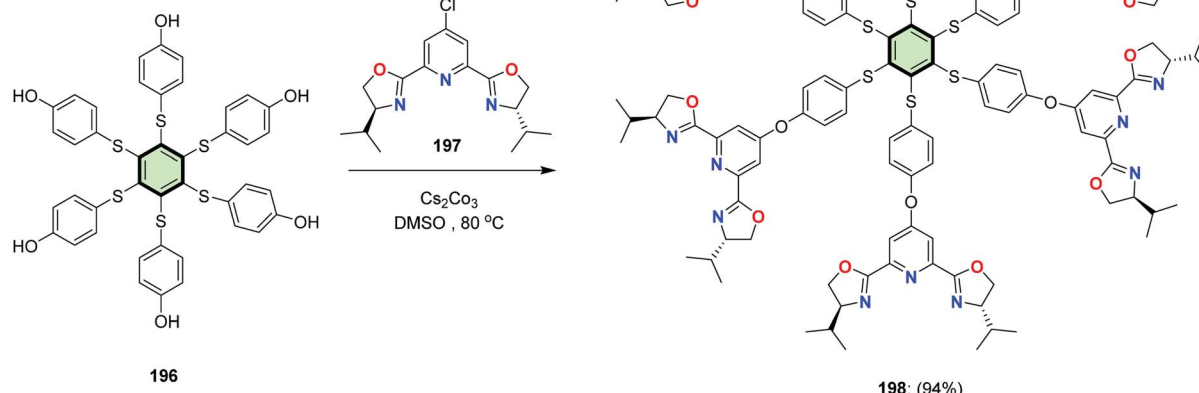
aminotriazoles **145a,b** with the corresponding tetrakis(-bromomethyl)benzene **136** and hexakis (bromomethyl)benzene **99** in refluxing EtOH/DMF mixture containing KOH (Scheme 37).

4.3.1.2. Benzene-cored SSMs with six-membered heterocyclic arms

4.3.1.2.1. Six-membered heterocyclic arms containing one heteroatom. 4.3.1.2.1.1. 1,4-Dihydropyridine. Rajesh *et al.*⁹³ reported the synthesis of tripodal and tetrapodal 1,4-dihydropyridines (DHP) **151–156** by the reaction of monofunctional 1,4-DHP **149** and **150** with the appropriate tri-bromomethylbenzenes **135** and **98** or tetra-bromomethyl

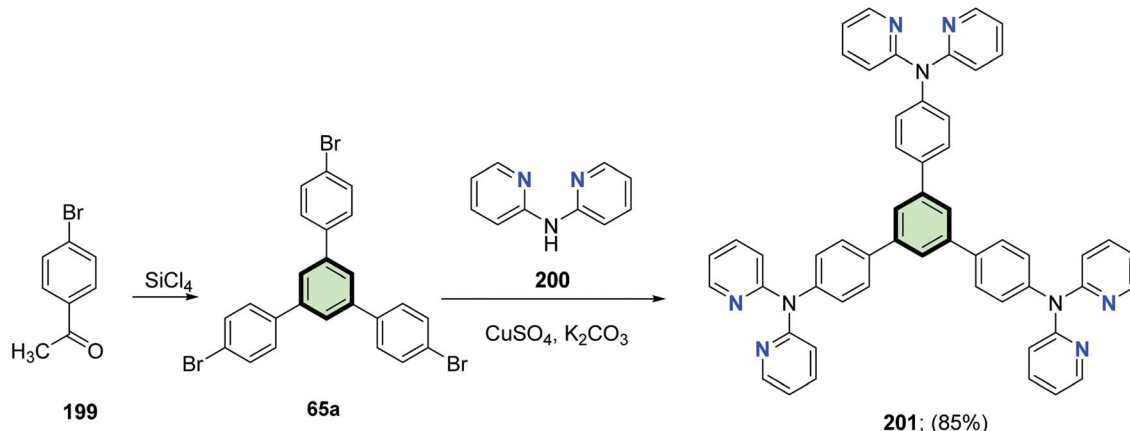
benzene **136**, respectively, in the presence of K_2CO_3 as a base. The reactions were performed under conventional heating (49–69% yields) as well as under microwave irradiation (72–85% yields) (Scheme 38).

Abdelhamid *et al.*⁹⁴ reported the synthesis of poly(2,6-dimethyl-4-phenyl-1,4-dihydropyridinyl)arenes **159a**, **159b**, **161a**, **161b**, **163a** and **163b** in good yields through reaction of tris-, tetrakis-, and hexakis(formylphenoxy methyl)benzenes **157a**, **157b**, **160a**, **160b**, **162a** and **162b**, respectively, with 3-aminobut-2-enenitrile **158** in acetic acid at reflux (Schemes 39–41).



Scheme 49 Synthesis of SSMs with (phenylthio)benzene core and 2,6-bis(4,5-dihydrooxazol-2-yl)pyridine side arms 198.



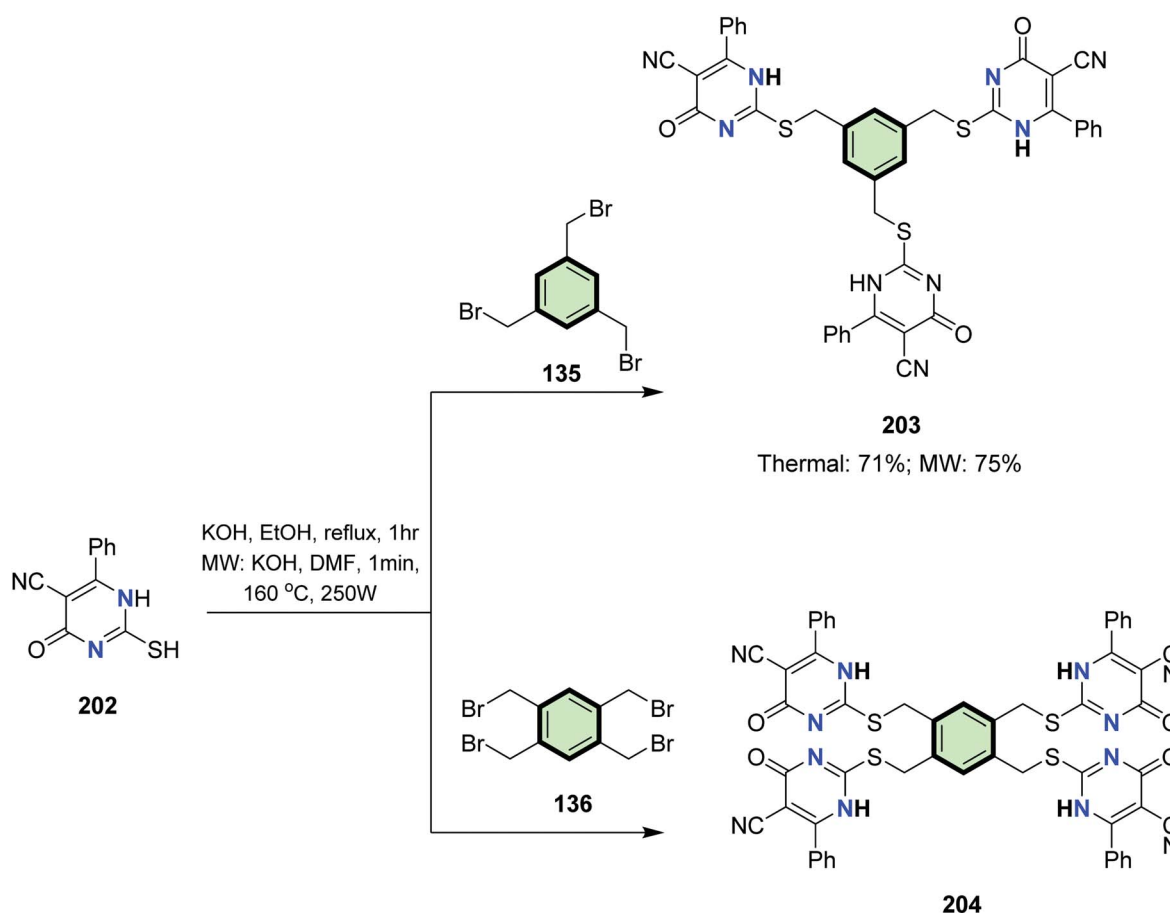


Scheme 50 Synthesis of 1,3,5-tris(*p*-(2,2'-dipyridylamino)phenyl)benzene 201

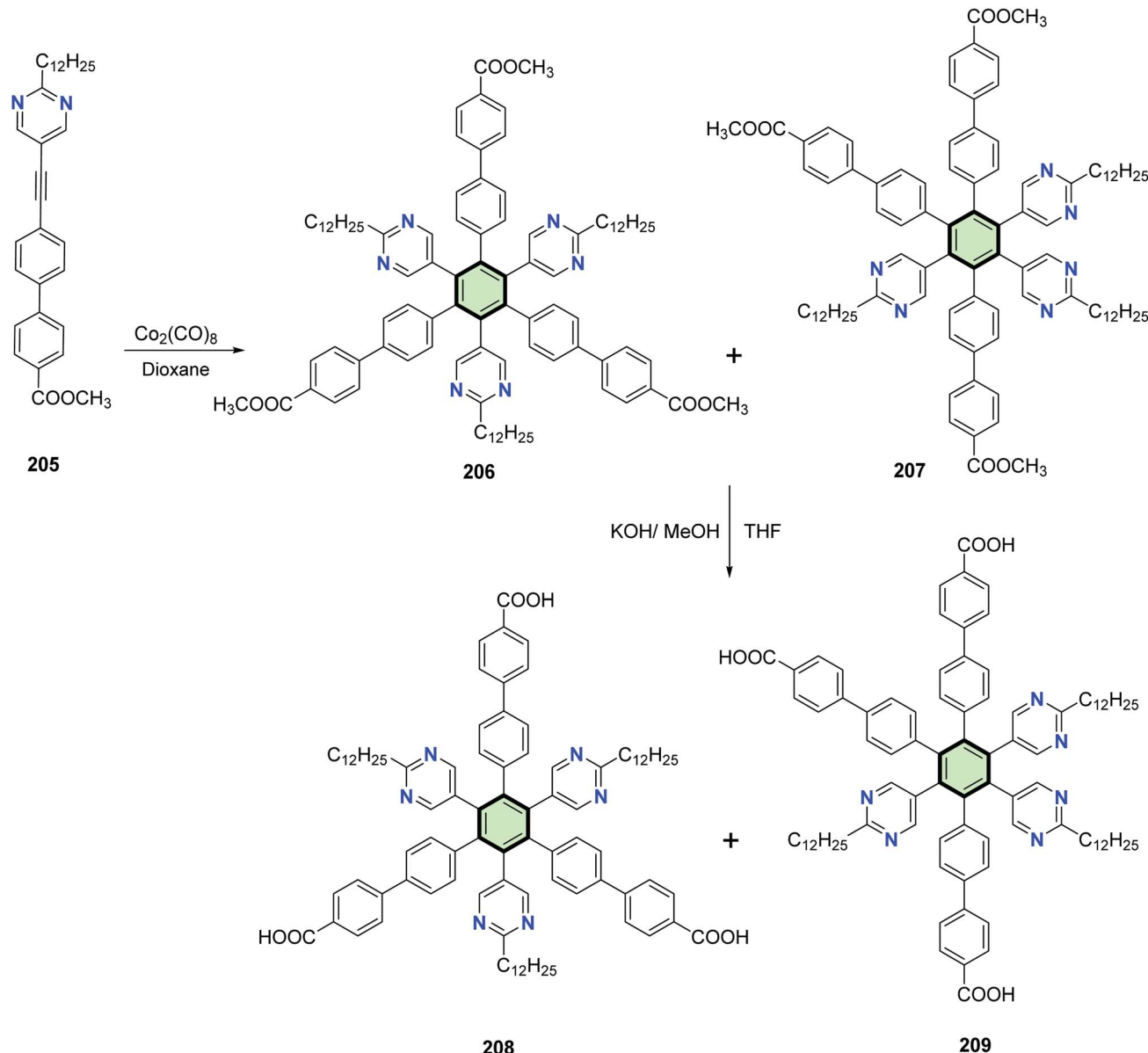
4.3.1.2.1.2. Pyridine and its derivatives. Yin and Tan⁹⁵ reported the synthesis of multifunctional pyridine-2,6-dicarboxylic acid derivatives **165** and **166** by coupling of diethyl 4-hydroxypyridine-2,6-dicarboxylate **164** with

tetrakis(bromomethyl)benzene **136** and hexakis(-bromomethyl)benzene **99**, respectively, in basic medium (Scheme 42).

McMorran and Steel⁹⁶ reported the synthesis of a series of poly(pyridylsulfanyl methyl)arenes **169–172**, **174** and **175** in



Scheme 51 Synthesis of tris- and tetrakispyrimidine derivatives **203** and **204**.



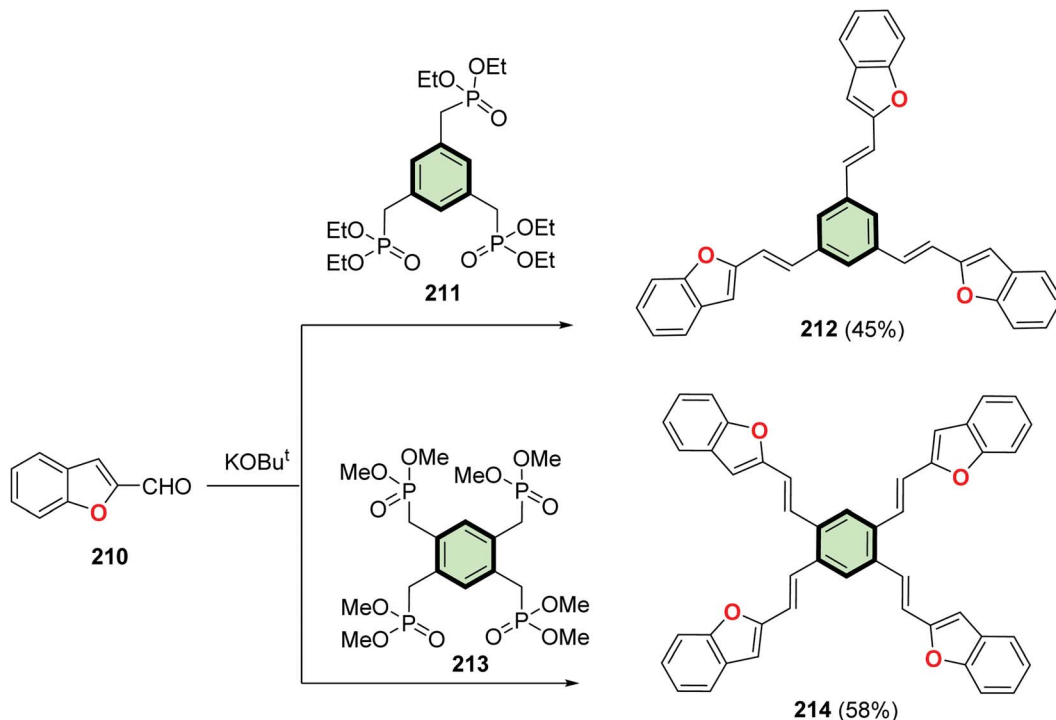
Scheme 52 Synthesis of hexaheteroaryl benzene derivatives 206–209 containing three pyrimidylbenzene side arms.

good yields from the reaction of either 2- or 4-mercaptopypyridine **167** and **173** with the corresponding poly(bromomethyl)arene **98**, **136**, **168** and **99** in the presence of triethylamine (Schemes 43 and 44).

Reaction of 2-mercaptopicotinonitriles **176** and **177** with poly(bromomethyl) benzenes **135**, **136** and **99** in ethanolic KOH under conventional heating as well as under microwave irradiation, afforded the corresponding polypyridines **178–183** in good yields (Scheme 45).⁹⁷

Yin *et al.*⁹⁸ reported the synthesis of star-shaped macromolecules **186a–c** with hexakis(fluoren-2-yl)benzene as the core and pyridine as the periphery. The synthetic strategy includes octacarbonyldicobalt-catalyzed cycloaddition reaction for different alkyne precursors **184a–c**. The coordination interaction between the pyridine ring of alkyne precursor and the

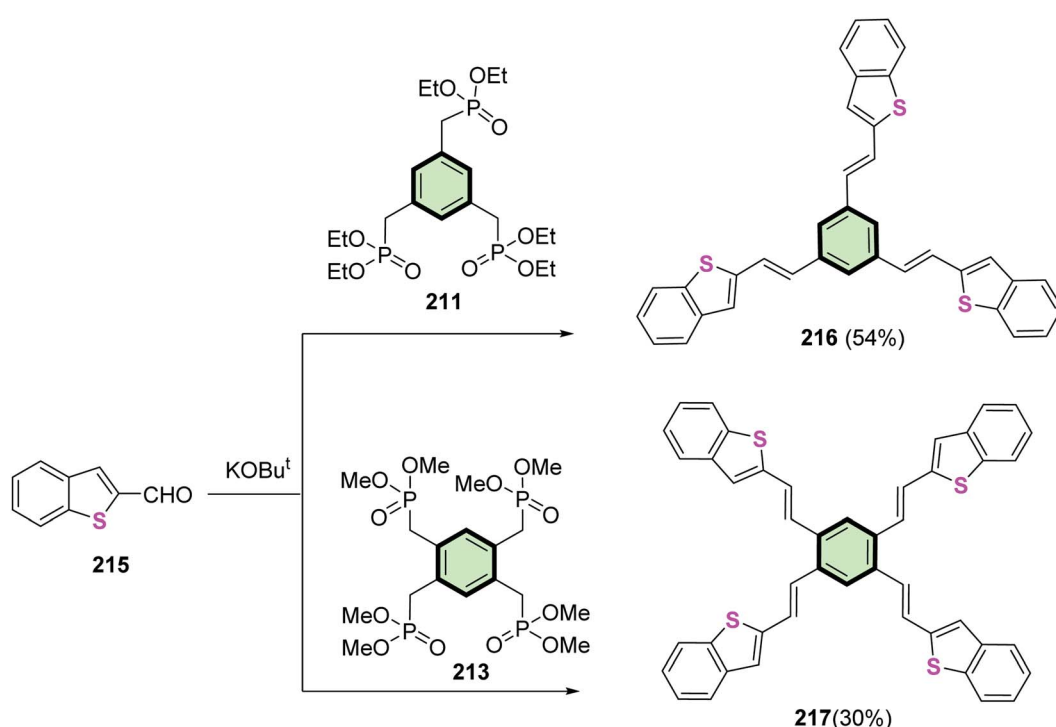
cobalt catalyst may result in very low yield of the cyclo-trimerization product. However, with the increase of the catalyst loading, the yields of the intermediates cyclopentadienone **185a–c** are more likely to generate *via* cycloaddition reactions presumably due to the electron-deficient property of the alkyne precursors. The desired cyclotrimerization products can be obtained by the Diels–Alder reactions of cyclopentadienone **185a–c** with acetylene **184a–c** in good yield (Scheme 46). Under the initial catalyst loading 10%, the desired cyclotrimerization product **186a** was exceptionally obtained from the precursor of **184a** with a good yield of 61%. These compounds exhibit good thermal stability and favorable electron affinity. By using these compounds as electron-transporting materials, all-solution-processed phosphorescent organic light-emitting devices (OLEDs) show good performance with a maximum current

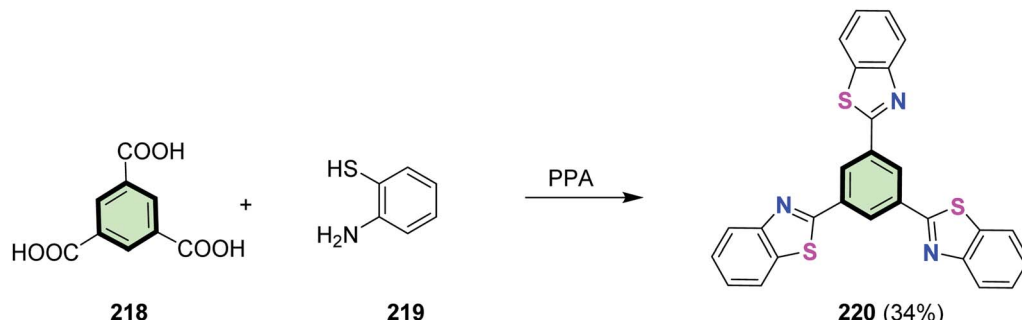
Scheme 53 Synthesis of tris- and tetrakis(2-(benzofuran-2-yl)vinyl)benzene **212** and **214**.

efficiency of 5.6 cd A^{-1} and maximum external quantum efficiency of 4.68%.

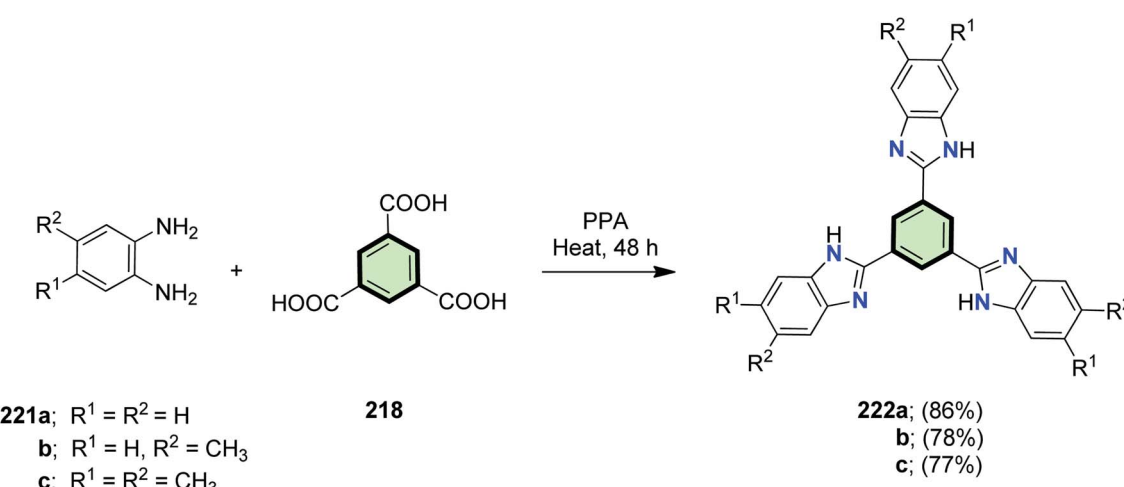
The synthesis of cyclometalated platinum(II) complexes **191** and **195** for the application as single emitters in polymeric white

emitting diodes (WPLED) is described in Schemes 47 and 48. The starting SSMs containing picolinic acid residues **189** and **194** were prepared by either of the following procedures: (a) tris(bromohexyl)phloroglucinol **187** reacts with methyl 3-

Scheme 54 Synthesis of tris and tetra[2-(benzo[b]thien-2-yl)vinyl]benzene **216** and **217**.



Scheme 55 Synthesis of tris(benzo[d]thiazol-2-yl)benzene 220.



Scheme 56 Synthesis of SSMs with benzene core and benzimidazole side arms 222a-c.

hydroxypicolinate **188** in the presence of cesium carbonate as a base followed by basic hydrolysis by sodium hydroxide in THF to yield **189**, or (b) the Suzuki coupling reaction of boronic acid bearing methyl picolinate residue **192** with 1,3,5-tri-bromobenzene **193** followed by basic hydrolysis to give **194**. The cyclometalated complexes **191** and **195** was then synthesized by the reaction of SSMs **189** with dimer **194** in 2-ethoxyethanol in the presence of sodium carbonate as a base.⁹⁹

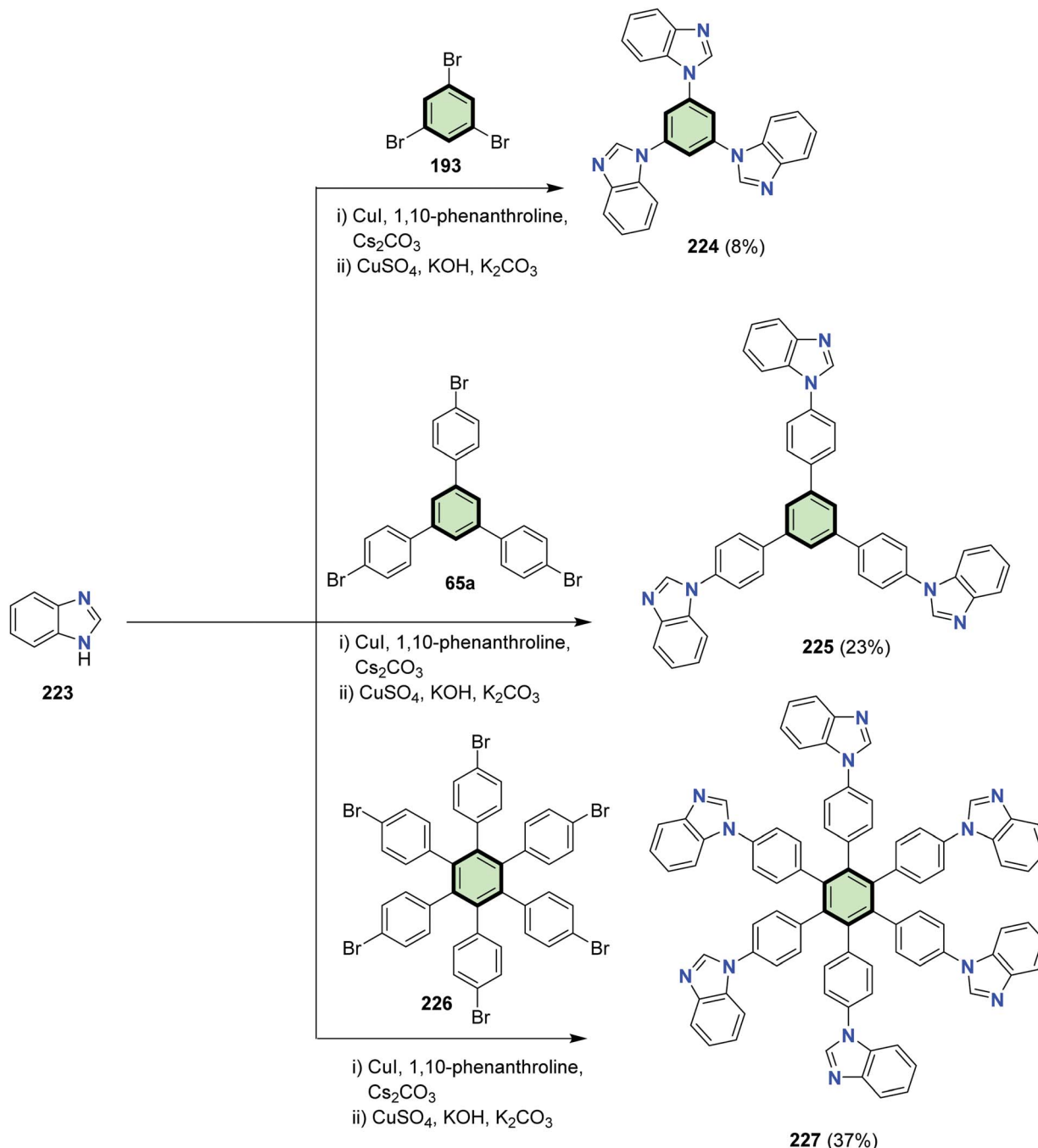
The UV/Vis absorption data of **191** showed an intense high-lying absorption band (around 240 nm) for ligand-centered $\pi-\pi^*$ electron transition and two moderate low-lying absorption peaks (about 324 nm and 352 nm) for spin-allowed and spin-forbidden metal-to-ligand charge transfer transitions. Considering **195**, a fourth intense absorption band at 266 nm owing to the effect of the 1,3,5-(4-oxytriphenyl)benzene core. Thus, modifying the aryl core has small effect on the electron transition. The photoluminescence spectra of **191** and **195** showed a clear similarity. Increasing the concentration led to gradual red-shifted emissions. In thin film, significant difference in photoluminescence: two intense high-lying bands (425–485 nm) and a moderately intense, low-lying band (600 nm) are

exhibited by **191**. Complex **195** showed a much weaker low-lying emission. In general, the Pt(II) complexes **195** displayed lower aggregation with a controllable excimer emission.

Aubert *et al.*¹⁰⁰ described the synthesis of star shaped compound with (phenylthio)benzene core **198** in 94% overall yield, *via* coupling of (4S,4'S)-2,2'-(4-chloropyridine-2,6-diyl)bis(4-isopropyl-4,5-dihydrooxazole) **197** with hexakis(4-hydroxyphenylthio)benzene **196** in the presence of Cs_2CO_3 as a base (Scheme 49). Star compound **198** acted as a catalyst for Rh-catalyzed hydrosilylation of acetophenone.

4.3.1.2.1.3. Dipyridylamine. Pang *et al.*¹⁰¹ reported the synthesis of 1,3,5-tris(*p*-(2,2'-dipyridylamino)phenyl)benzene **201** in 85% yield, by the reaction of 1,3,5-tris(*p*-bromo phenyl)benzene **65a** [obtained from trimerization of 1-(4-bromophenyl)ethanone **199** with SiCl_4] with 2,2'-dipyridylamine **200** in the presence of K_2CO_3 and CuSO_4 (Scheme 50). Zinc(II) complex of **201** was synthesized and its application as fluorescent sensor for detection of benzene vapors was investigated.





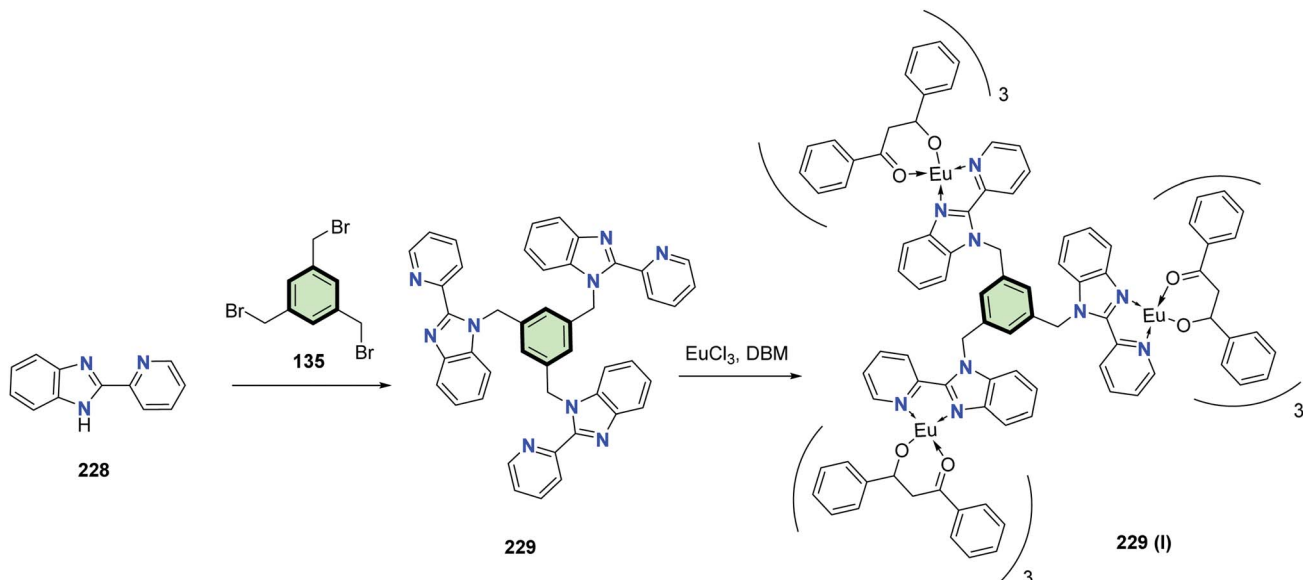
Scheme 57 Synthesis of SSMs with benzene core and benzimidazole side arms 224, 225 and 227.

4.3.1.2.2. Six-membered heterocyclic arms containing two heteroatoms. **4.3.1.2.2.1. Pyrimidine.** Tris- and tetrakispyrimidine derivatives **203** and **204** were synthesized in good yields via alkylation of 2-mercaptop-4-oxo-6-phenyl-1,4-dihydropyrimidine-5-carbonitrile **202** with **135** and **136**, respectively (Scheme 51).⁹⁷

Xiang *et al.*¹⁰² reported the synthesis of electron-deficient hexaheteroarylbenzene derivatives containing three pyrimidine rings **208** and **209** through multi-step reactions

including the cobalt-catalyzed cyclotrimerization reaction of methyl 4'-(2-dodecylpyrimidin-5-yl)ethynyl-[1,1'-biphenyl]-4-carboxylate **205** to yield isomeric carboxylated hexaheteroarylbenzene derivatives **206** and **207** which were then hydrolyzed to the corresponding acids **208** and **209**, respectively, upon treatment with methanolic KOH (Scheme 52).

4.3.1.3. Benzene-cored SSMs with benzofused arms



Scheme 58 Synthesis of (1,3,5-tris((2-(pyridin-2-yl)-1H-benzo[d]imidazol-1-yl)methyl)benzene) 229 and its Eu³⁺-complex 229 (I).

4.3.1.3.1. Benzofused five-membered heterocyclic ring arms.

4.3.1.3.1.1. Benzo[b]furan. The Wittig reaction of benzo[b]furan-2-carbaldehyde 210 with benzene-cored tris- and tetrakis(phosphonate) 211 or 213 afforded the corresponding tris- and tetrakis(2-(benzofuran-2-yl)vinyl)benzene 212 and 214 in moderate yields of (Scheme 53). Compound 212 is sensitive to the crystallization condition involving two phases (α , β) in solution and one phase in thin film. (β -phase) Molecule of 212 pack into a three-dimensional cofacial herringbone structure (H-aggregate). It has moderate emission efficiency with quantum yield of 34% (solution), 16% (α -phase) and 22% (β -phase). On the other hand, compound 214 decomposed before melting. It adopts an inter-inserted two-dimensional hexagonal packing structure and can be considered as 2D-semiconductor. It has quantum yield of 53% (solution) and 16% (solid). Compound 212 exhibited hole-mobility and its amorphous film performance is similar to its crystalline film, which should simplify device fabrication.¹⁰³

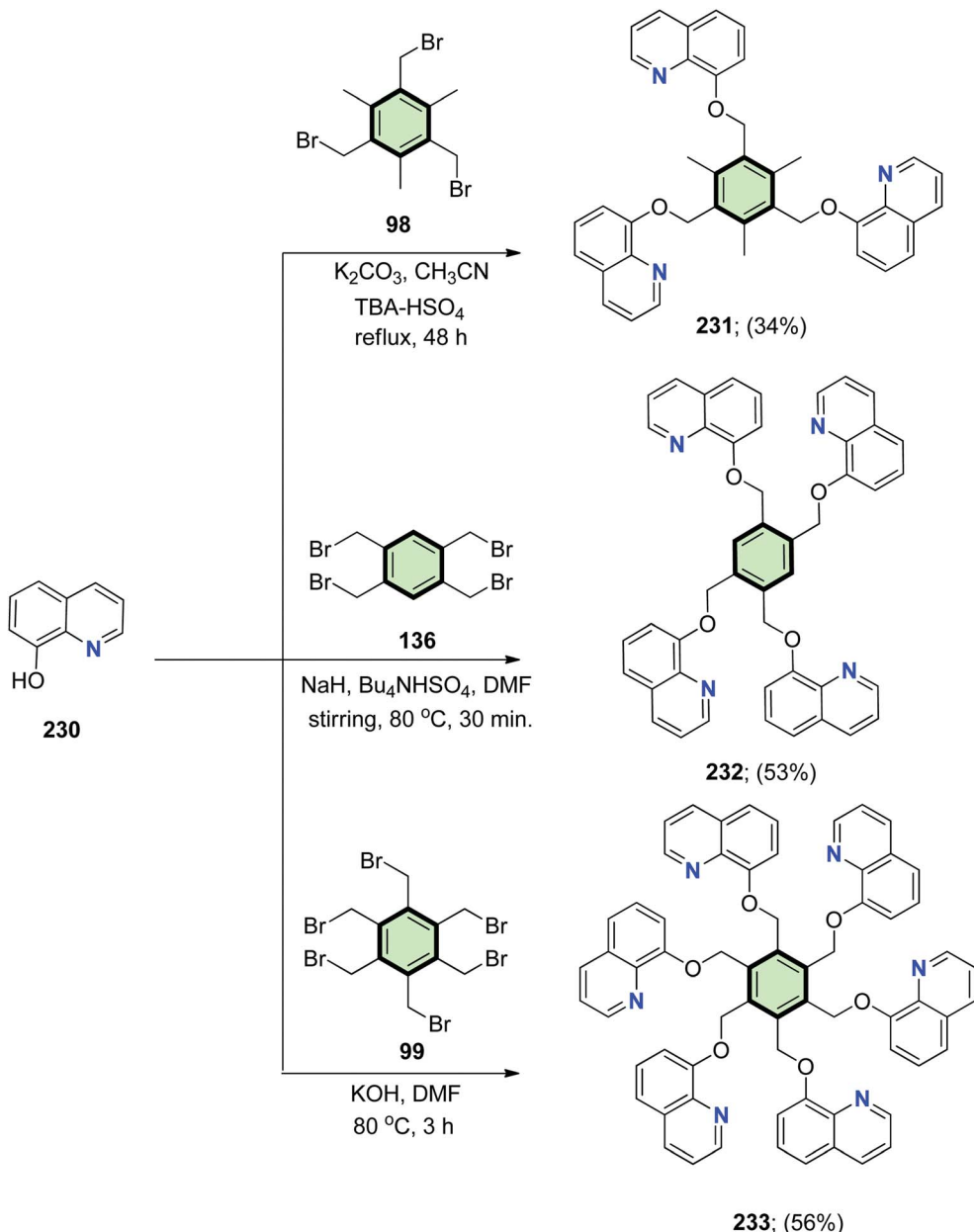
4.3.1.3.1.2. Benzo[b]thiophene. Reaction of benzo[b]thiophene-2-carbaldehyde 215 with 1,3,5-tris(diethoxy phosphorylmethyl)benzene 211 and 1,2,4,5-tetra(dimethoxyphosphoryl methyl)benzene 213 in THF in the presence of *t*-BuOK afforded the corresponding 1,3,5-tris[2-(benzo[b]thien-2-yl)vinyl]benzene 216 and 1,2,4,5-tetra[2-(benzo[b]thien-2-yl)vinyl]benzene 217, respectively, in good yields (Scheme 54).¹⁰⁴ Similar to SSMs with benzo[b]furan arms 212 and 214, compound 216 showed 3D-cofacial herringbone structure. Absorption and emission spectra of 216 showed a more efficient hypsochromic shift than 217, due to discontinued π -conjugation of *meta*-substitution.

4.3.1.3.1.3. Benzo[d]thiazole. The polyphosphoric acid PPA-catalyzed cyclocondensation of trimesic acid (benzene-1,3,5-

tricarboxylic acid) 218 with 2-aminothiophenol 219 affords tris(benzo[d]thiazol-2-yl)benzene 220 in low yield (34%) (Scheme 55). Compound 220 is an efficient iron(III) fluorescent probe with fast response of 50 s. The dynamic quenching mechanism was proven by time-correlated single photon counting (TCSPC) experiment. The probe 220 can be used to detect rapidly iron(III) ions in aqueous solutions at pH range (3–12). It can be efficiently employed for detection of iron(III) ions in real water.¹⁰⁵

4.3.1.3.1.4. Benzo[b]imidazole. Star-shaped molecules with benzene core and benzimidazole side arms 222a–c were synthesized in 86, 78 and 77% yields, by the simple condensation of *o*-phenylenediamine derivatives 221a–c with trimesic acid 218 in the presence of polyphosphoric acid as a catalyst (Scheme 56). Compounds 221a–c could be successfully utilized as chemosensors for fluoride ions with good selectivity, high sensitivity, and fast response. The effect of addition of fluoride ion to the chemosensors 222a–c led to a distinct color change from blue to light cyan in either solution or solid state (with TLC or solution-coated strips) under UV irradiation. Compounds 222a–c were efficiently applied to the detection of fluoride ion from inorganic origin and commercial toothpaste samples.¹⁰⁶

Different benzimidazole-based SSMs 224, 225 and 227 were synthesized *via* a modified Ullmann aromatic C–N coupling of benzimidazole 223 with tribromobenzene 193, 1,3,5-tris(4-bromophenyl)benzene 65a, and hexakis(4-bromophenyl)benzene 226, respectively (Scheme 57). These SSMs 224, 225 and 227 showed all deep LUMO and HOMO–LUMO energy gap of 3.45–3.95 eV. They are fluorescent ion the UV regions and possess highly stable thermal and morphological features. They have an obvious fluorescent response to silver(I) and zinc(II) ions in solution.¹⁰⁷



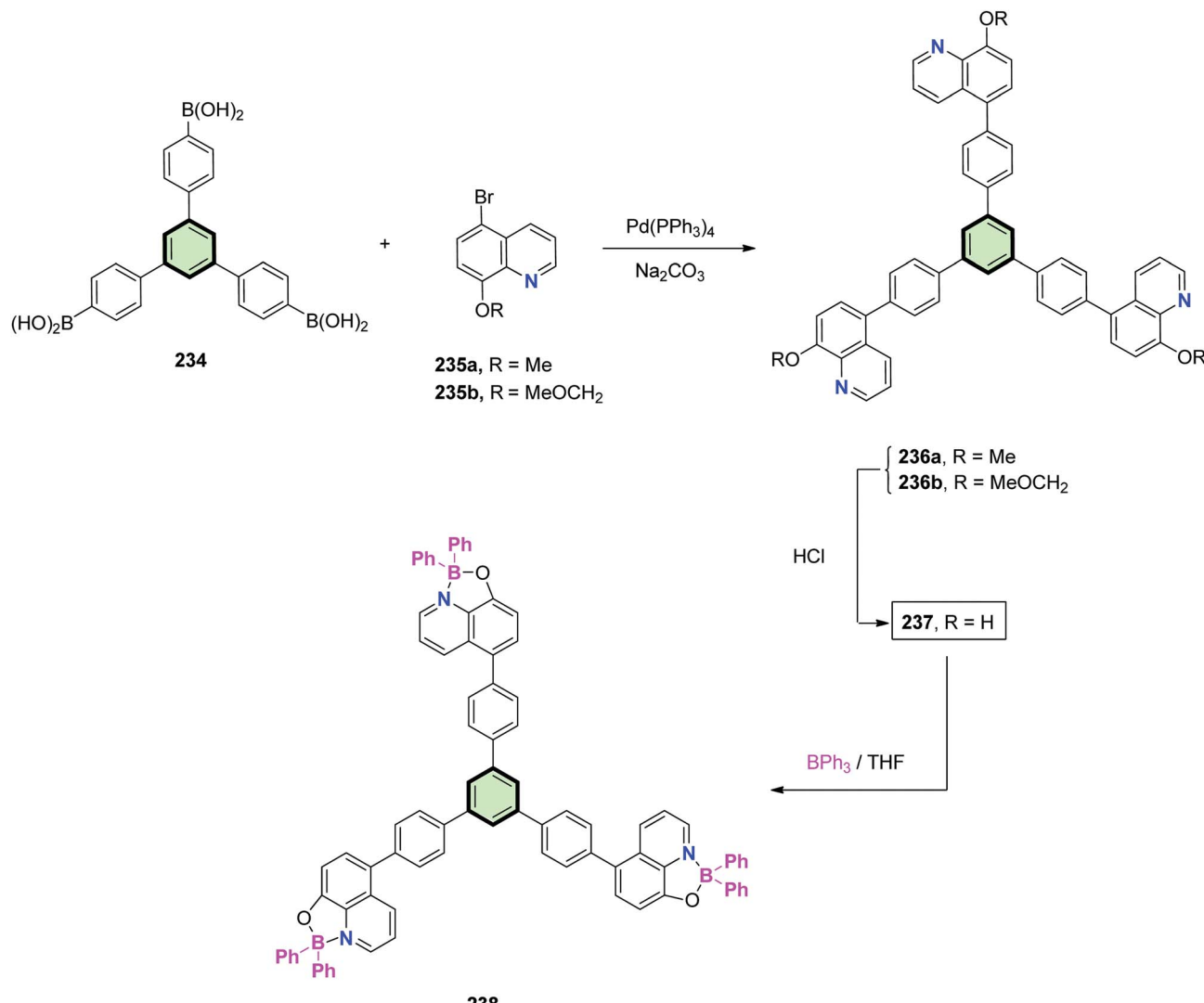
Scheme 59 Synthesis of SSMs with benzene core and quinoline side arms **231–233**.

The reaction of 1,3,5-tris(bromomethyl)benzene **135** with 2-pyridylbenzimidazole **228** in DMF in the presence of sodium hydroxide at reflux afforded hexadentate ligand (1,3,5-tris((2-(pyridin-2-yl)-1*H*-benzo[*d*]imidazol-1-yl)methyl)benzene) **229** in good yield (62%). Heating **229** with europium chloride/dibenzoylmethane (DBM) in ethanol at reflux in the presence of sodium hydroxide yielded the Eu³⁺-complex **229 (I)** (Scheme 58). Europium(III) complex **229 (I)** was found to be promising red emitter in view of its structural and photophysical properties. It showed high photoluminescence yield (0.64) with a short lifetime of excited state (120 μ s). It is thermally stable to high temperature (315 °C). The HOMO-LUMO energy gap (2.5 eV) of **229 (I)** is suitable for organic functional devices.

Electroluminescence and photovoltaic devices of **229 (I)** led to a white emission (maximum luminance of 168 cd m⁻²) and a maximum power conversion efficiency of 1.05%, respectively.¹⁰⁸

4.3.1.3.2. Benzofused six-membered heterocyclic ring arms.

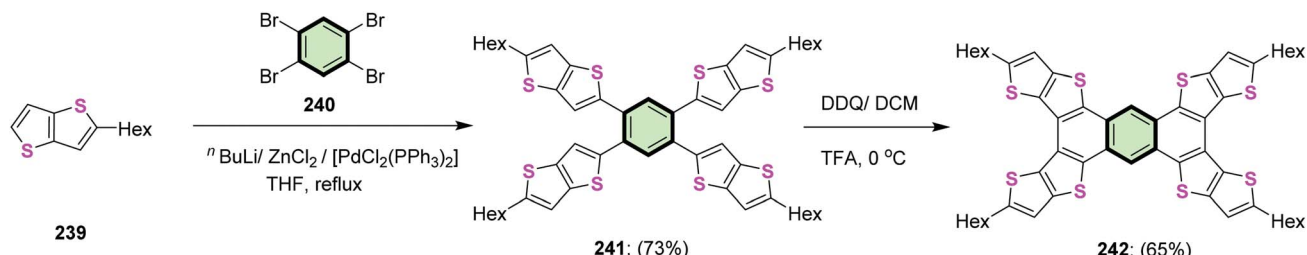
4.3.1.3.2.1. Quinoline. Reaction of 8-hydroxyquinoline **230** with the appropriate bromomethyl benzenes **98**, **136** and **99** afforded tris-, tetrakis-, and hexakis(8-quinolinoxyethyl)benzene derivatives **231**, **232** and **233**, respectively, in good yields (Scheme 59). SSM **231** exhibited selective fluorescence quenching with copper(II) and could be used for estimation of copper(II) (1–6 ppm) even in the presence of nickel(II),



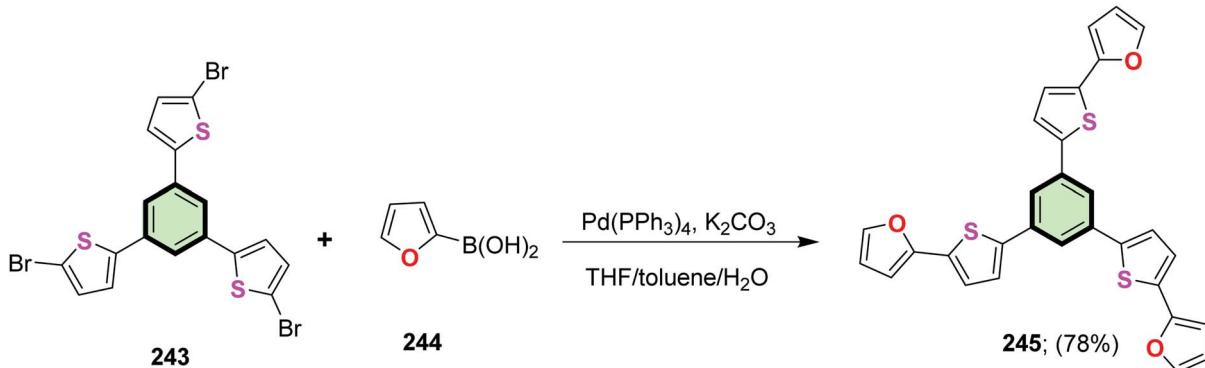
Scheme 60 Synthesis of 5,5'-(5'-(4-(8-hydroxyquinolin-5-yl)phenyl)-[1,1':3',1"-terphenyl]-4,4"-diyl)bis(quinolin-8-ol) **237** and its boron complex **238** 5,5'-(5'-(4-(8-hydroxyquinolin-5-yl)phenyl)-[1,1':3',1"-terphenyl]-4,4"-diyl)bis(quinolin-8-ol).

cadmium(II), zinc(II) (1000 ppm), or silver(II) (100 ppm). Different coordination modes of **232** (with silver(I) and copper(I)) and **233** (with cobalt(II) and palladium(II)) were studied. SSMs **231** and **232** displayed different fluorescence perturbation

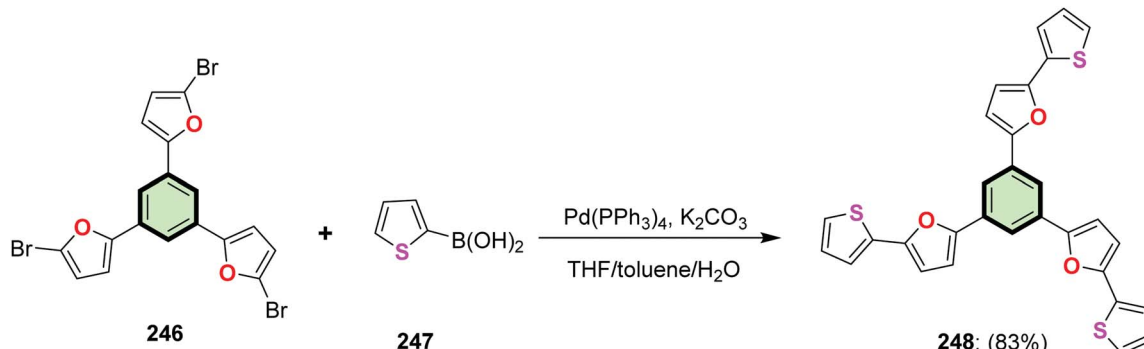
with change in the concentration of silver(I). Compound **231** showed a simultaneous fluorescence quenching with addition of silver(I). Compound **232**, on the other hand, introduced “ON-OFF-ON switching” involving two fluorescence perturbations



Scheme 61 Synthesis of tetra(5-hexyl)thieno([3,2-b]thieno)anthracene **242**.



Scheme 62 Synthesis of 1,3,5-tris(5-(furan-2-yl)thiophen-2-yl)benzene 245.



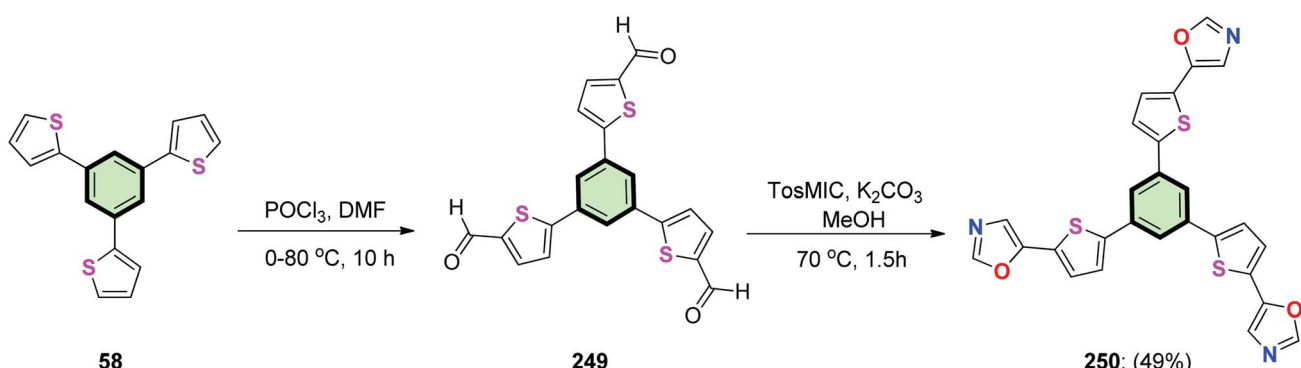
Scheme 63 Synthesis of 1,3,5-tris(5-(thiophen-2-yl)furan-2-yl)benzene 248.

with incremental increase of silver(I) concentration: the first fluorescence quenching (with <1.0 equiv. of Ag^+ , at $\lambda_{\text{max}} = 395$ nm) and the second is fluorescence enhancement (at $\lambda_{\text{max}} = 500$ nm, with >3 equiv. of Ag^+).^{109–111}

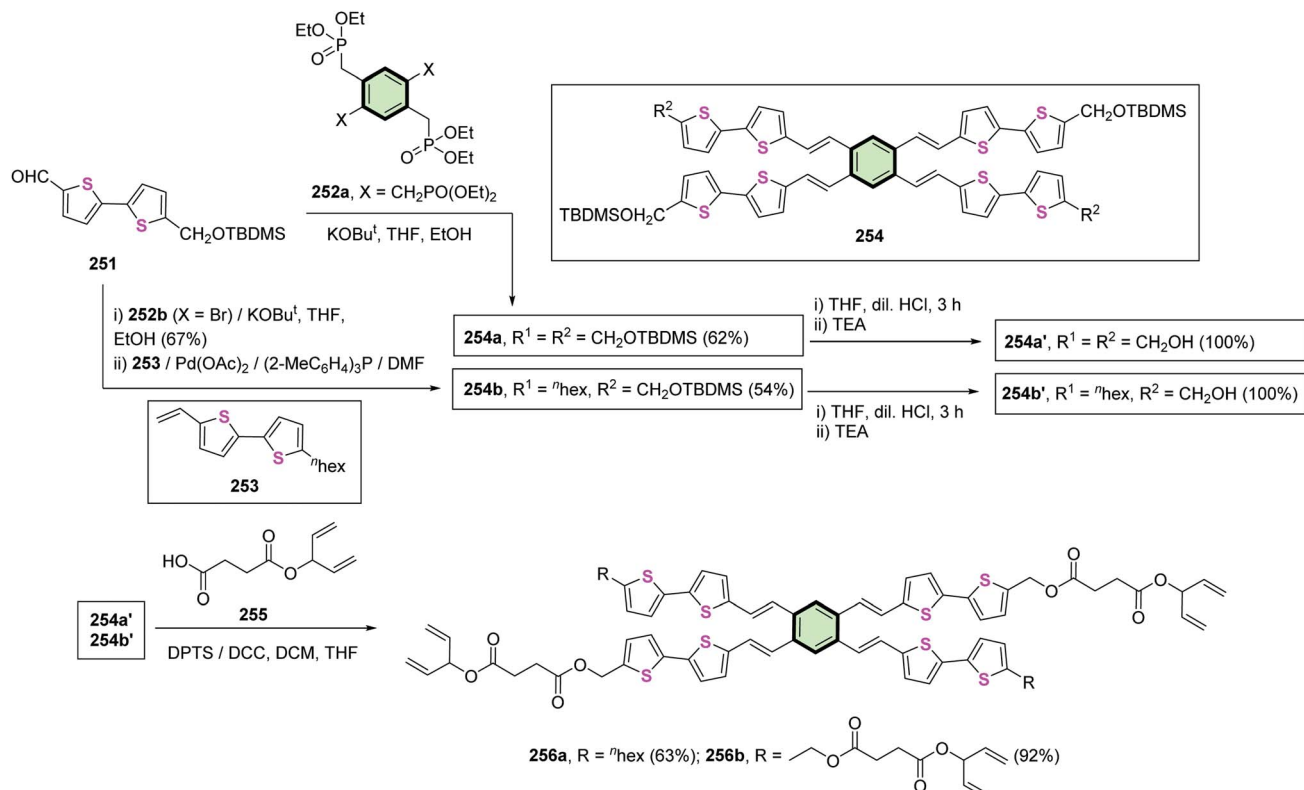
Cui and Wang¹¹² reported the synthesis of star-shaped conjugated molecules 236a and 236b in good yields using Suzuki–Miyaura coupling reaction of boronic acid derivatives 234 with 5-bromo-8-methoxyquinoline 235a and 5-bromo-8-methoxy-2-methylquinoline 235b, respectively, in the presence

of Na_2CO_3 and $\text{Pd}(\text{PPh}_3)_4$ (Scheme 60). The starburst compounds 236a,b were found to act as blue emitters with excellent thermal stabilities (~ 300 °C) and layered arrangements in solid state. Treatment of SSMs 236a,b with HCl gave the 8-hydroxyquinoline derivative 237. Chelation of the latter compound with triphenylborane in THF at reflux afforded the boron complex 238 which exhibited green emissions.

4.3.1.4. Miscellaneous arms



Scheme 64 Synthesis of 1,3,5-tris(5-(oxazol-5-yl)thiophen-2-yl)benzene 250.



Scheme 65 Synthesis of bithiophene SSMs side arms 254 and 256.

4.3.1.4.1. Thieno[3,2-*b*]thiophene. Magnan *et al.*¹¹³ reported the synthesis of star-shaped compounds **241** in 73% yields by four-fold Negishi coupling between 1,2,4,5-tetrabromobenzene **240** with 2-hexylthieno[3,2-*b*]thiophene **239** in the presence of *n*BuLi and anhydrous ZnCl₂. Subsequent oxidative cyclo-dehydrogenation of the latter compound in chlorobenzene using anhydrous ferric chloride gave tetra(5-hexyl)thieno([3,2-*b*]thieno)anthracene **242** in 65% yield (Scheme 61). It was found that cyclization of **241** to **242** led a red shift of the absorption due to decrease of HOMO-LUMO energy gap affected by an efficient π -conjugation.

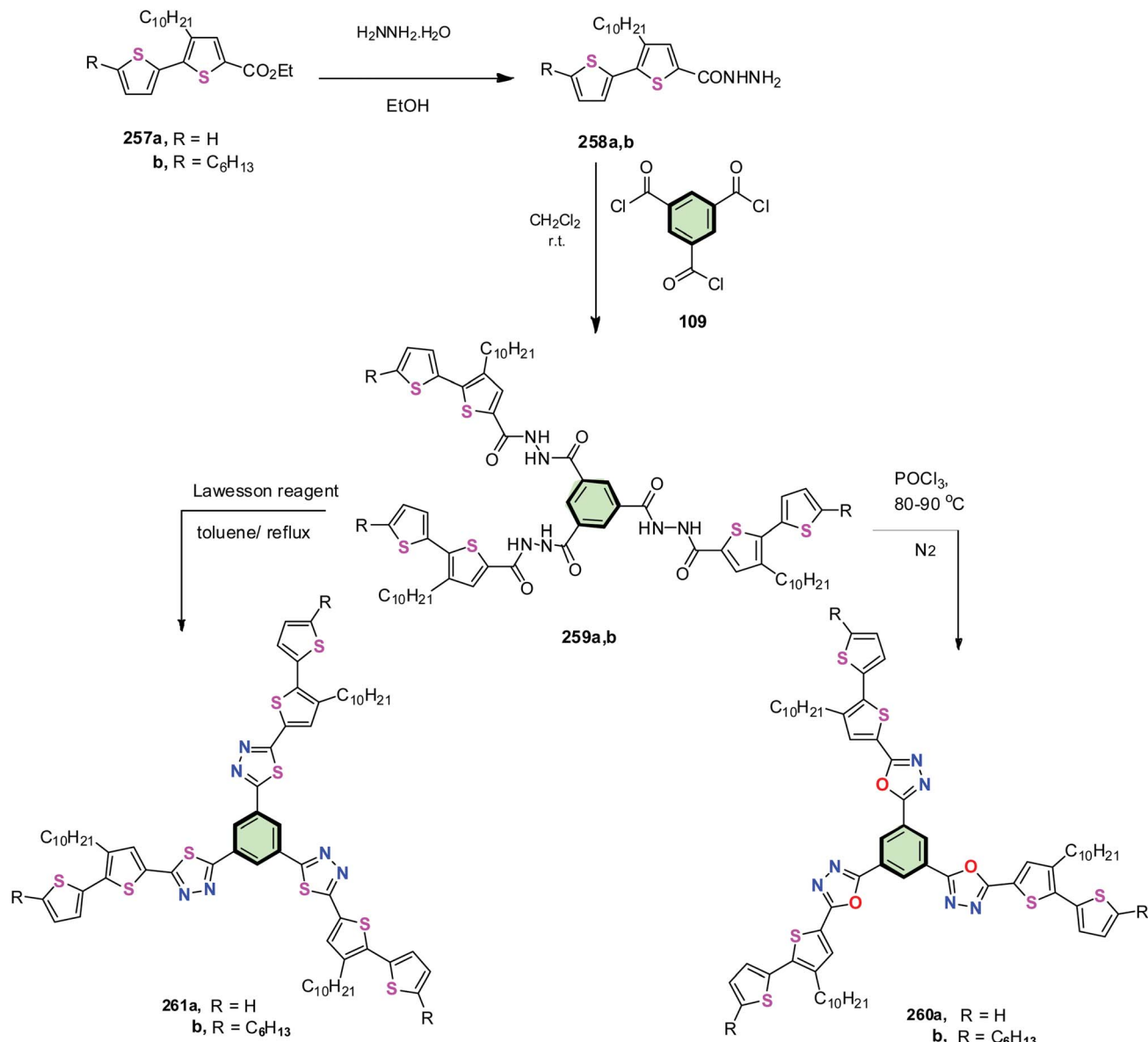
4.3.1.4.2. 2-(Thiophen-2-yl)furan. 1,3,5-Tris(5-(furan-2-yl)thiophen-2-yl)benzene **245** was synthesized in 78% yield by the reaction of 1,3,5-tris(5-bromothiophen-2-yl)benzene **243** with 2-furanyl boronic acid **244** in the presence of Pd(PPh₃)₄. Similarly, 1,3,5-tris(5-(thiophen-2-yl)furan-2-yl)benzene **248** was synthesized in 83% yield by the reaction of 1,3,5-tris(5-bromofuran-2-yl)benzene **246** with 2-thiophenylboronic acid **247** (Schemes 62 and 63).⁸¹ SSM **248** (containing peripheral thiophene moieties) was found to be better fluorophore than **245** (containing peripheral furan) as evident from the fluorescence quantum yield values of 0.15 and 0.06, respectively.

4.3.1.4.3. 2-(Thiophen-2-yl)oxazole. Kotha *et al.*⁸¹ reported the synthesis of a star-shaped molecule with benzene core and (thiophen-2-yl)oxazole as arms **250** by firstly treatment of 1,3,5-

tri(thiophen-2-yl)benzene **58** with POCl₃ in DMF to give 5,5',5"- (benzene-1,3,5-triyl)tris(thiophene-2-carbaldehyde) **249**. The latter compound underwent van Leusen reaction upon treatment with toluene sulfonylmethyl isocyanide (TosMIC)/K₂CO₃ in methanol under reflux to afford 1,3,5-tris(5-(oxazol-5-yl)thiophen-2-yl)benzene **250** in 49% yield (Scheme 64).

4.3.1.4.4. 2,2'-Bithiophene and 2-([2'-bithiophen]-5-yl)-1,3,4-oxa(thia)diazole. The synthesis of SSMs **256a,b** is represented in Scheme 65. Star-shaped tetrapod **256a** was synthesized *via* the Horner-Emmons coupling of 5'-(((*tert*-butyldimethylsilyl)oxy)methyl)-[2,2'-bithiophene]-5-carbaldehyde **251** and octaethyl (benzene-1,2,4,5-tetrayltetrakis(methylene))tetrakis(phosphonate) **252a**. Deprotection of TBDSMS proceeded to form **254a'** in a quantitative yield, followed by esterification with 4-oxo-4-(penta-1,4-dien-3-yloxy)butanoic acid **255** furnished SSMs **256a** with four pentadiene tails in good yield (63%). Other SSM **256b** (with two pentadiene tails) was synthesized similarly but with a slight modification. It employed the Horner-Emmons coupling of **251** with tetraethyl (2,5-dibromo-1,4-phenylenebis(methylene))bis(phosphonate) **252b** followed by Heck coupling of the resulting dibromo product with 5-hexyl-5'-vinyl-2,2'-bithiophene **253** to yield **254b** in moderate yield (54%). Deprotection of **254b** to **254b'** followed by reaction of **254b** with **255** afforded SSM **256b** in excellent yield (92%). The SSMs **256a** and **256b** acted as photopatternable organic semiconductors due to their ability to photopolymerize enabled by



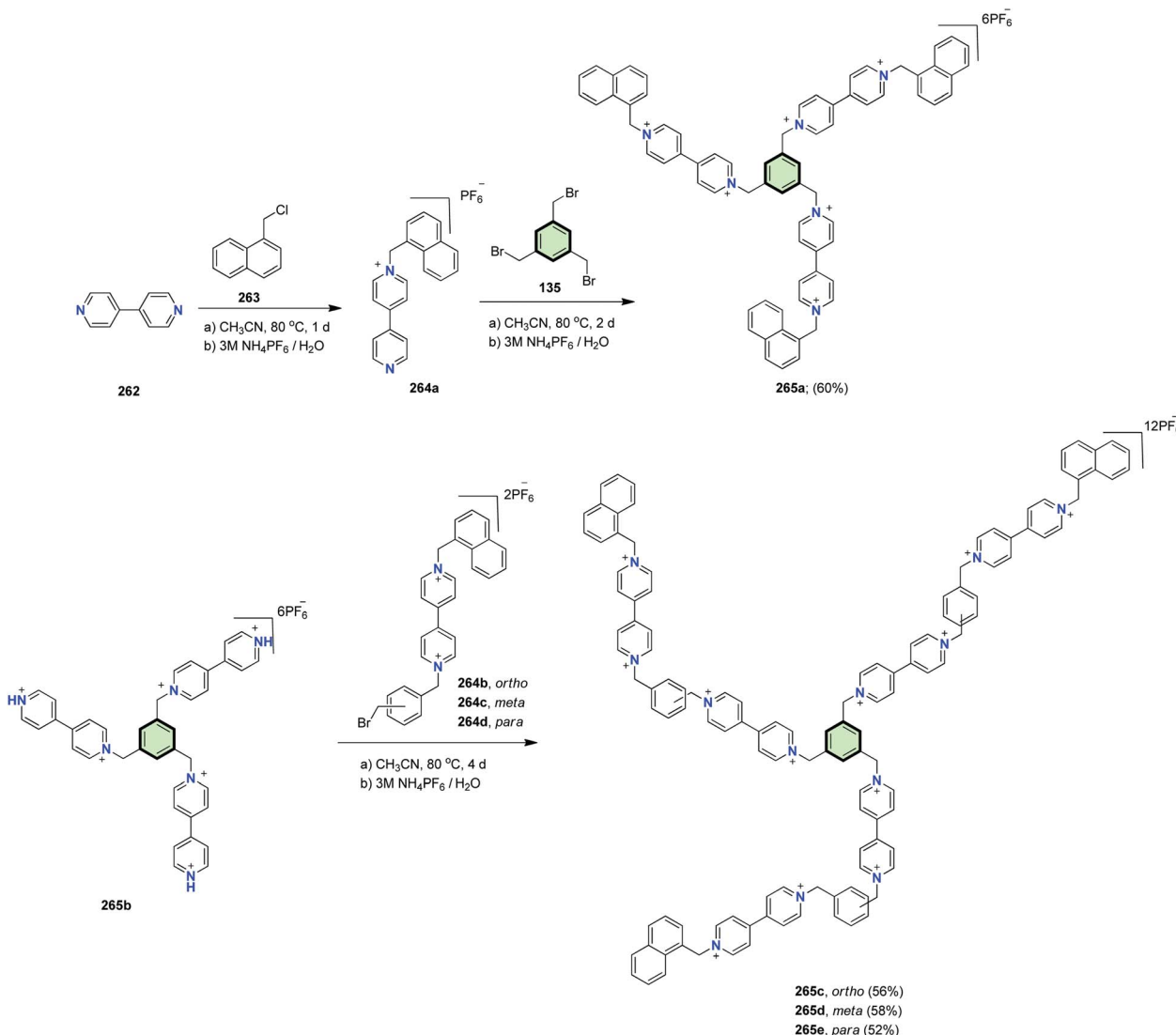


Scheme 66 Synthesis of SSMs containing either oxadiazole or thiadiazole side arms 260 and 261.

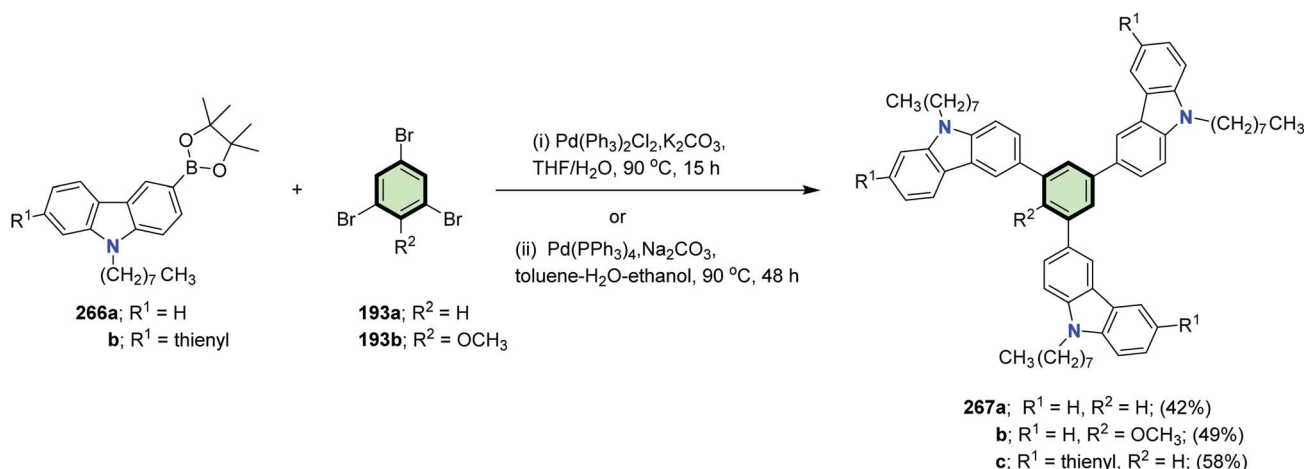
the reactive pentadiene tails. The transistor devices based on **256a** and **256b** exhibited a field-effect mobility of $1.3 (\pm 0.2) \times 10^{-3}$ to $3.7 (\pm 0.5) \times 10^{-3} \text{ cm}^2 \text{ V}^{-1} \text{ s}^{-1}$, $I_{\text{on/off}}$ value ($>10^3$), and a small threshold voltage (-16 V). The field-effect mobility of SSM **256b** persisted even after being cross-linked during photopolymerization. This was explained on the basis of the strong intermolecular interaction of conjugated structure which may freeze the molecular axis under push-pull force during the cross-linking and is accompanied by a highly lamella-ordered in two directions.¹¹⁴

Kotwica *et al.*¹¹⁵ reported the synthesis of star-shaped molecules containing either oxadiazole or thiadiazole side arms each connected by bithiophene moiety **260a**, **260b**, **261a** and **261b**. Thus, the esters **257a** and **257b** were converted into the corresponding hydrazide derivatives **258a** and **258b**, respectively, by

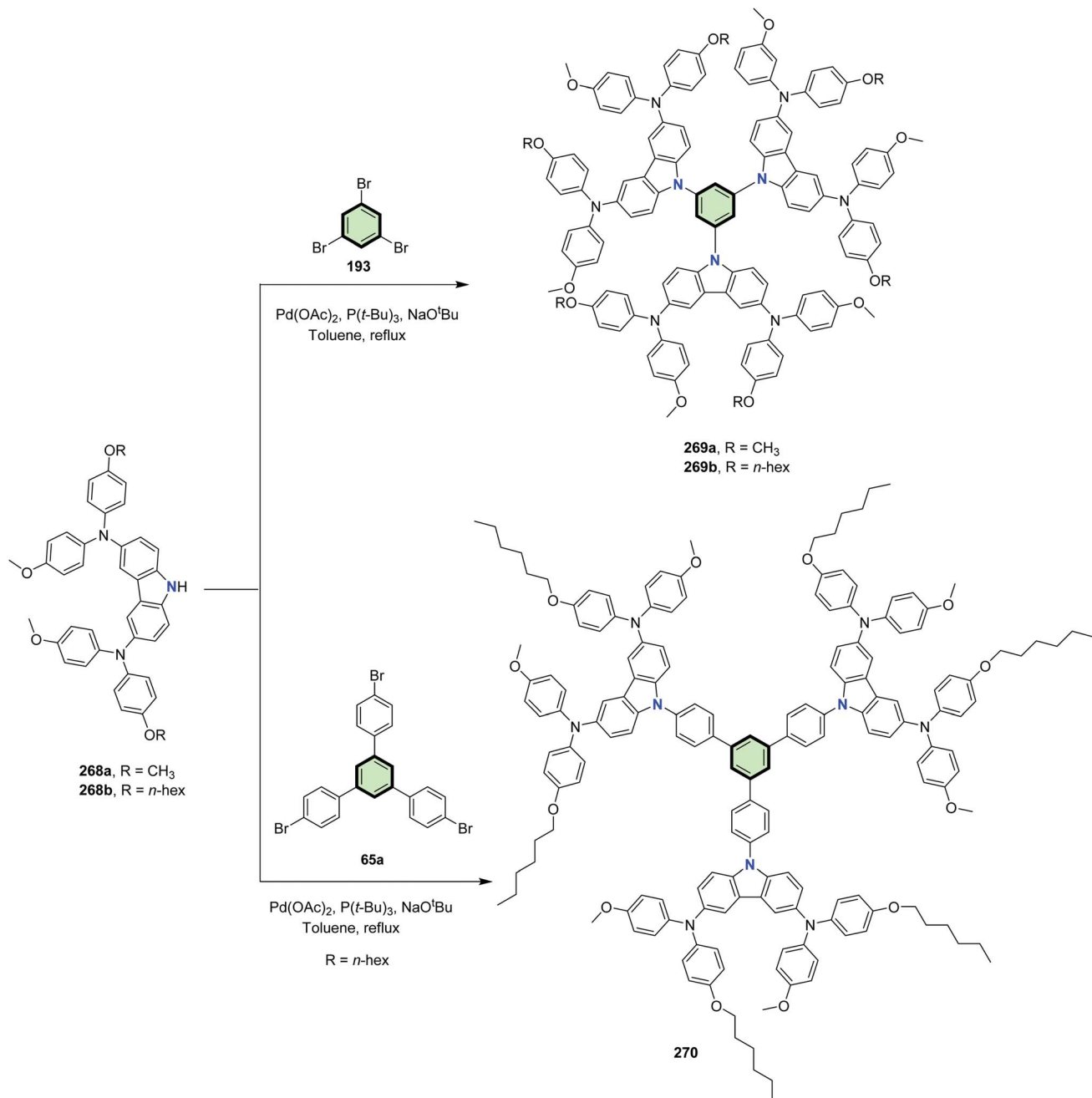
heating with hydrazine hydrate. Treatment of **258a** and **258b** with benzene-1,3,5-tricarbonyl trichloride **109** gave alkyl-substituted $N'1,N'3,N'5$ -tris[(3-decyl-2,2'-bithien-5-yl)carbonyl]benzene-1,3,5-tricarbohydrazides **259a** and **259b**, respectively. The latter compounds were converted into the oxadiazole bithiophene series **260a** and **260b** upon treatment with phosphorus oxychloride. On the other hand, treatment of **259a** and **259b** with Lawesson's reagent led to the formation of the corresponding thiadiazole bithiophene series **261a** and **261b**, respectively, in good yields (Scheme 66). The HOMO-LUMO energy gap of oxadiazole SSMs **260a,b** were found to be just below 3 eV and higher than that of thiadiazole SSMs **261a,b** by 0.2 eV. Substitutions were shown to affect further reduction of energy gap. SSMs **260** and **261** displayed an excellent electroluminescence in guest/host LEDs. Unsubstituted SSMs **260** and



Scheme 67 Synthesis of SSMs containing 4,4'-bipyridyl naphthalene side arms 265.



Scheme 68 Synthesis of SSMs 267a-c with 1,3,5-tris(9-octyl-9H-carbazol-3-yl)benzene side arms.

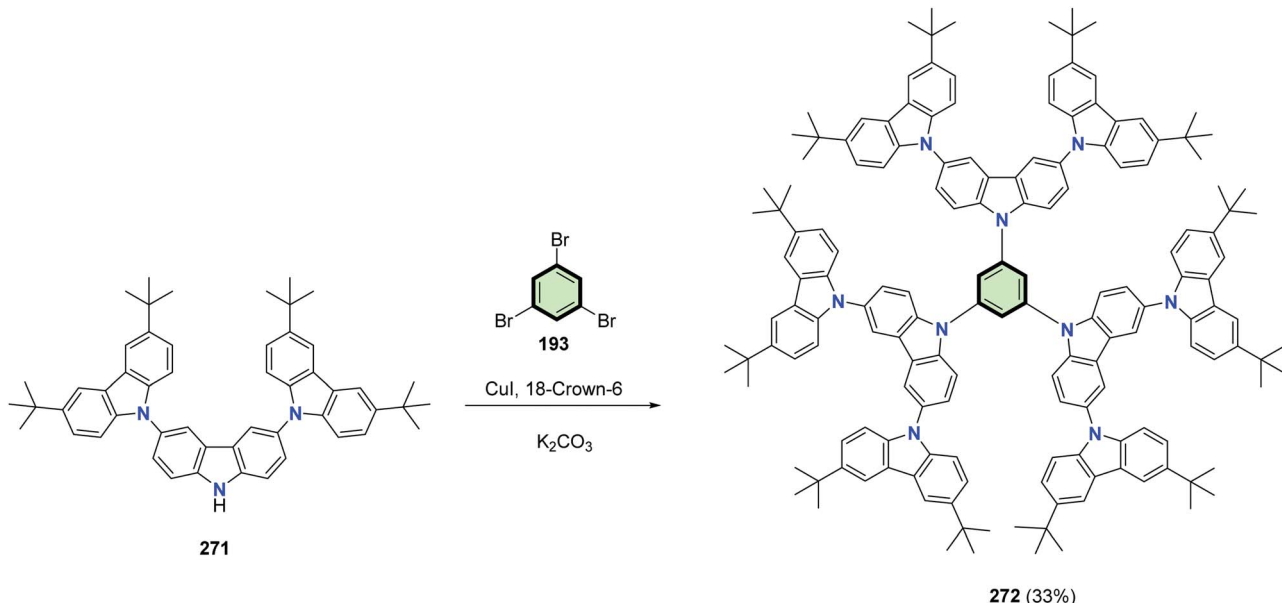


Scheme 69 Synthesis of SSMs 269a,b and 270.

261 ($R = H$) were electropolymerizable. The macromolecules based on SSMs 260 and 261 retained a reversible electrochromism on the oxidation and reduction modes.

4.3.1.4.5. 4,4'-Bipyridine. Madasamy *et al.*¹¹⁶ reported the synthesis of viologen (4,4'-bipyridinium) star shaped molecule with benzene core and naphthalene tails 265a in 60% yields upon reaction of 1,3,5-tris(bromomethyl)benzene 135 with the key intermediate 264a. The latter compound was obtained from alkylation of 4,4'-bipyridine 262 with 1-chloromethylnaphthalene 263 (Scheme 67). In addition, several dendritic viologin

molecules 265c–e were synthesized *via* a similar strategy incorporating the dealkylated star-shaped derivative 265b and bromoxyl viologins 264b–d. Cyclic voltammetry showed that among the different viologen SSMs 265a–e, only 265c (*ortho*) exhibited the most positive reduction potential due to both intermolecular and intramolecular charge transfer. The absorption spectra of 265c as well indicated absorption of radical monocation and pimer while 265a,e (*meta* and *para*) revealed absorption for radical monocation only. This suggested that the intramolecular charge transfer is evident only in

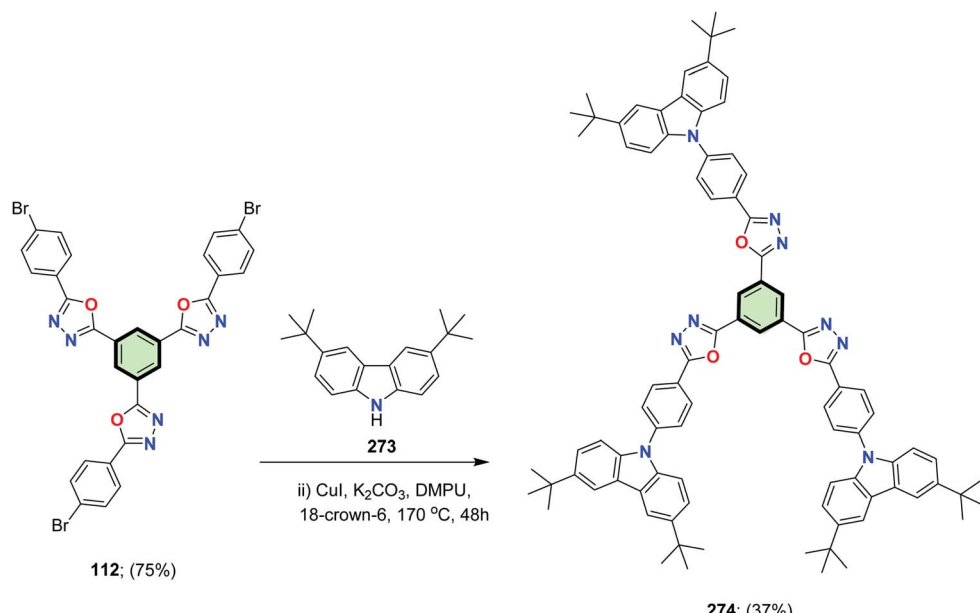


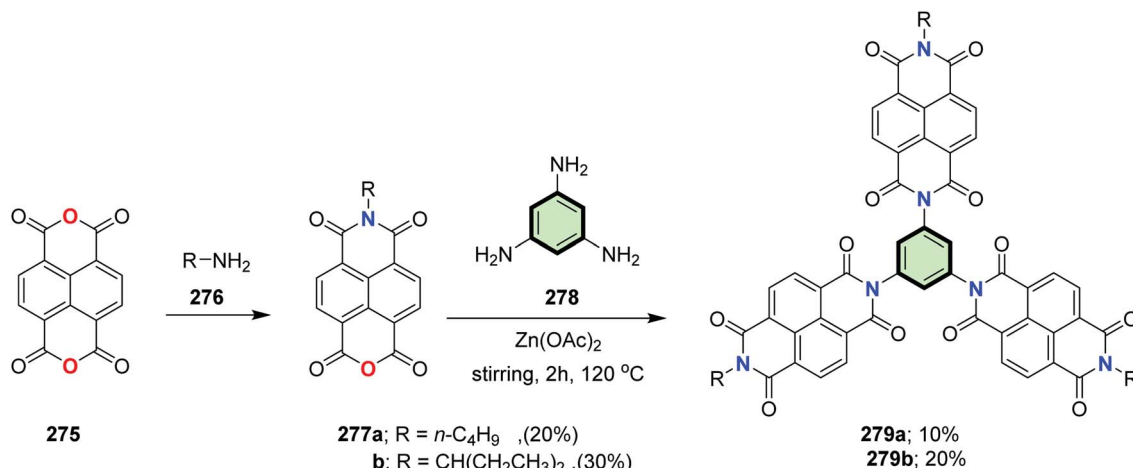
Scheme 70 Synthesis of dendritic tercarbazole-based SSM 272.

the *ortho* derivative **265c**. It should be mentioned that the viologen SSMs could form (1 : 1) inclusion complexes with β -cyclodextrin. In these complexes, β -cyclodextrin capped the hydrophobic part of **265c–e** as detected from NMR measurements. This capping was solvent-dependent. In polar aprotic solvents, no capping was observed as the solvent molecules were capped more efficiently to β -cyclodextrin. In aqueous media, a partial capping of naphthalene tails of **265c–e** to β -cyclodextrin was noticed.

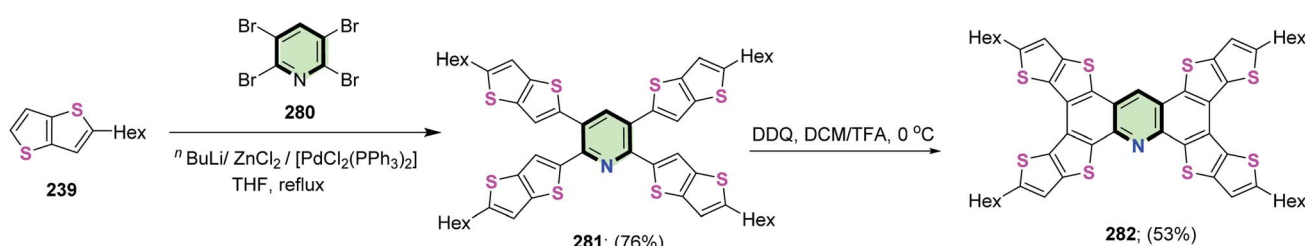
Madasamy *et al.*¹¹⁶ reported the synthesis of viologen (4,4'-bipyridinium) star shaped molecule with benzene core and naphthalene tails **265** in 60% yield upon reaction of 1,3,5-tris(-bromomethyl)benzene **135** with the key intermediate **264**. The latter compound was obtained from alkylation of 4,4'-bipyridine **262** with 1-chloro methylnaphthalene **263** (Scheme 67).

4.3.1.4.6. Carbazole and its derivatives. Brzczek *et al.*¹¹⁷ reported the synthesis of star-shaped molecules 1,3,5-tris(9-octyl-

Scheme 71 Synthesis of 1,3,5-tris(5-(4-(3,6-di-tert-butylcarbazol-9-yl)phenyl)-1,3,4-oxadiazol-2-yl)benzene **274**.



Scheme 72 Synthesis of SSMs with benzene core and three naphthalene diimide side arms 279

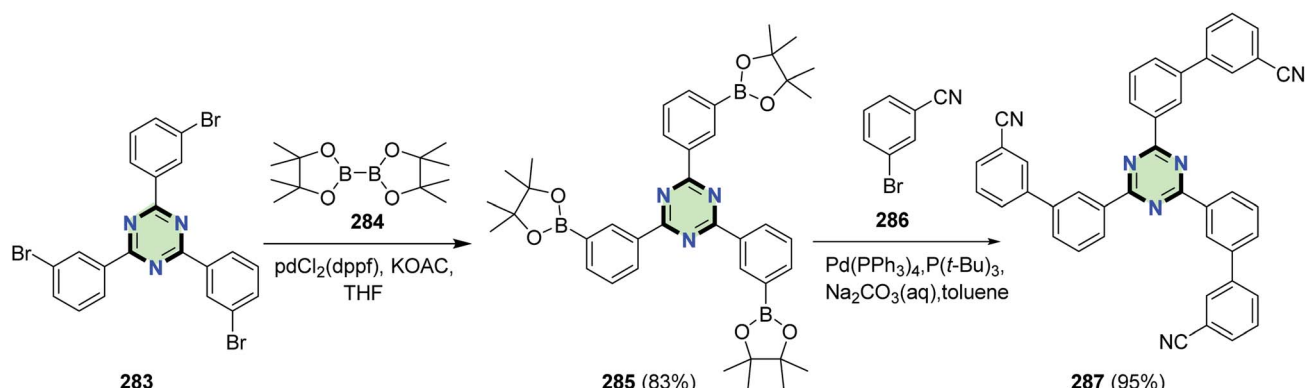


Scheme 73 Synthesis of star-shaped compound with pyrimidine core **281** and tetra(5-hexylthieno[3,2-*b*]thieno)acridine **282**

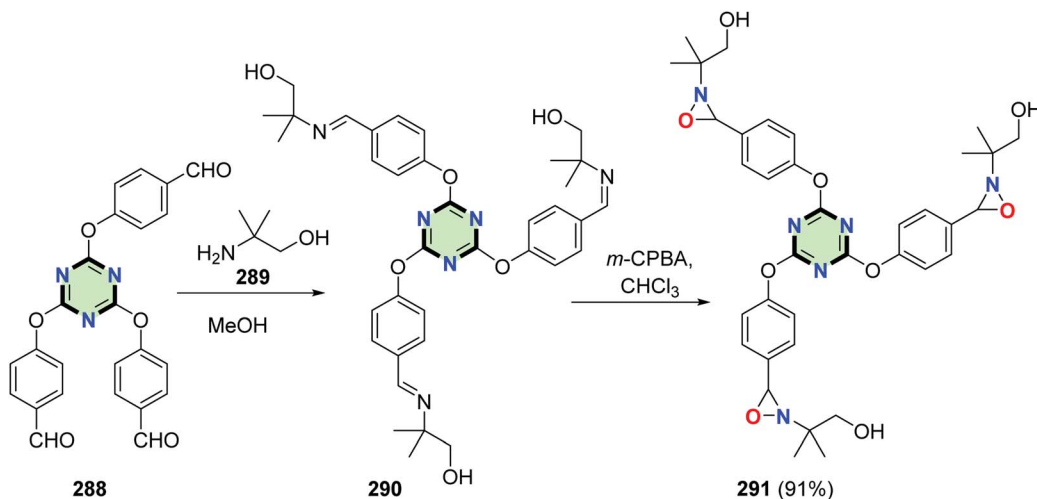
9H-carbazol-3-yl)benzene **267a**, 2-methoxy-1,3,5-tris(*9*-octyl-*9H*-carbazol-3-yl)benzene **267b** and 1,3,5-tris(*9*-octyl-6-(thiophen-2-yl)-*9H*-carbazol-3-yl)benzene **267c** in 42, 49 and 58% yields, respectively, *via* Suzuki–Miyaura coupling reaction between the appropriate carbazolyl boronic acid pinacol esters **266a** and **266b** with the corresponding 1,3,5-tribromobenzene derivatives **193a** and **193b** (Scheme 68). The star-shaped compounds **267a**–**c** were shown to be promising p-types semiconducting materials for application in OLEDs and OFETs in view of their HOMO

energies (−5.5 to −5.3 eV), energy gaps (E_g 3.20 to 3.38 eV), and IP values (5.5 eV). Presence of thiophene ring caused a red shift of both the UV and fluorescence spectra due to extra conjugation.

Star-shaped molecules **269a,b** and **270** were synthesized in good yields, *via* C–N palladium catalyzed coupling of 1,3,5-tribromobenzene **193** or 4,4"-dibromo-5'-(4-bromo-phenyl)-1,1':3',1"-terphenyl **65a** with *N*3, *N*6-bis(4-(alkyloxy)-phenyl)-*N*3, *N*6-bis(4-methoxyphenyl)-9H-carbazole-3,6-



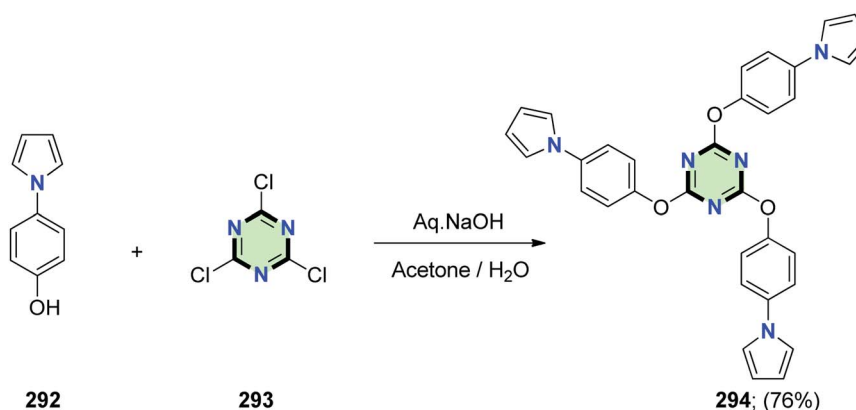
Scheme 74 Synthesis of SSM containing 1,3,5-triazine core and biphenyl arms 287



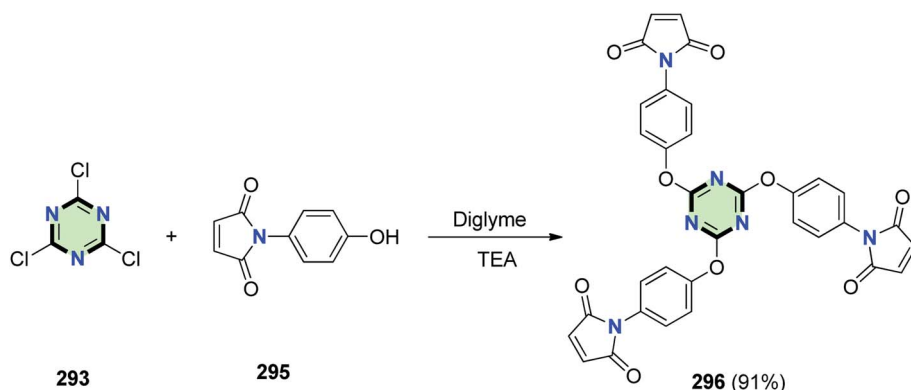
Scheme 75 Synthesis of a star-shaped molecule with triazine core and oxaziridine side arm 291.

diamine **268a,b** in toluene at reflux in the presence of $\text{Pd}(\text{OAc})_2$ (Scheme 69).⁴⁰ Among the synthesized starburst molecules, **269a** possessed the best hole-transporting properties. Mesoporous perovskite solar cells

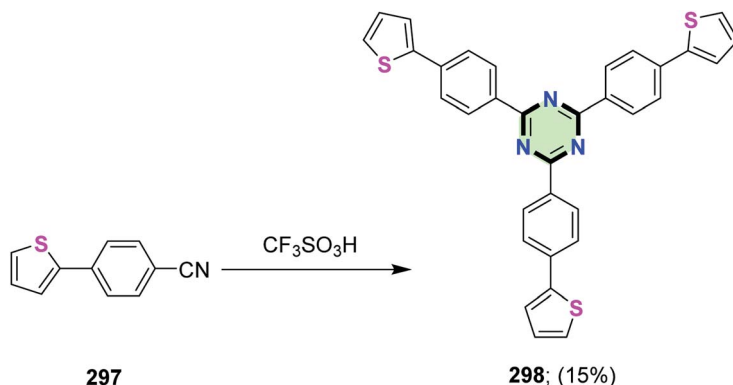
incorporating **269a** showed excellent power conversion efficiency PCE 18.87% which even higher than that of the common photovoltaic devices based on spiro-OMeTAD as a hole-transporting material with PCE 17.71%.



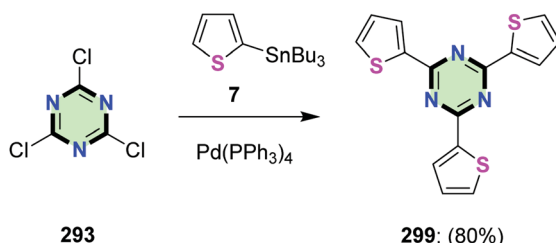
Scheme 76 Synthesis of 2,4,6-tris(4-(1H-pyrrol-1-yl)phenoxy)-1,3,5-triazine **294**.



Scheme 77 Synthesis of triazine-cored compound **296**.

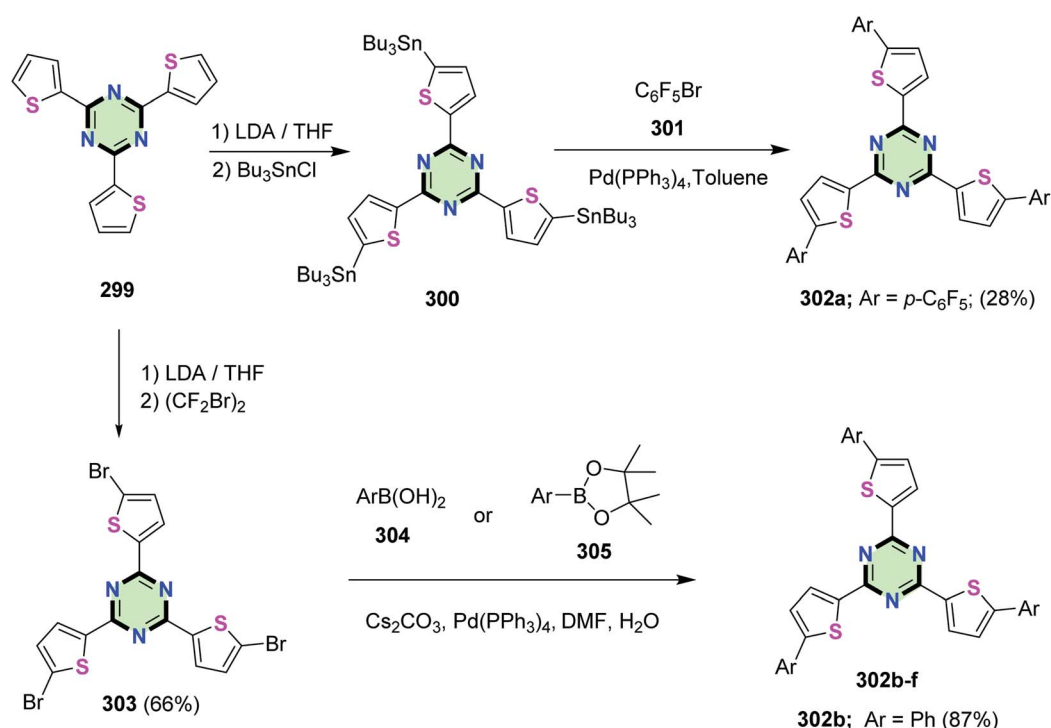


Scheme 78 Synthesis of 2,4,6-tris(4-(thiophen-2-yl)phenyl)-1,3,5-triazine 298.

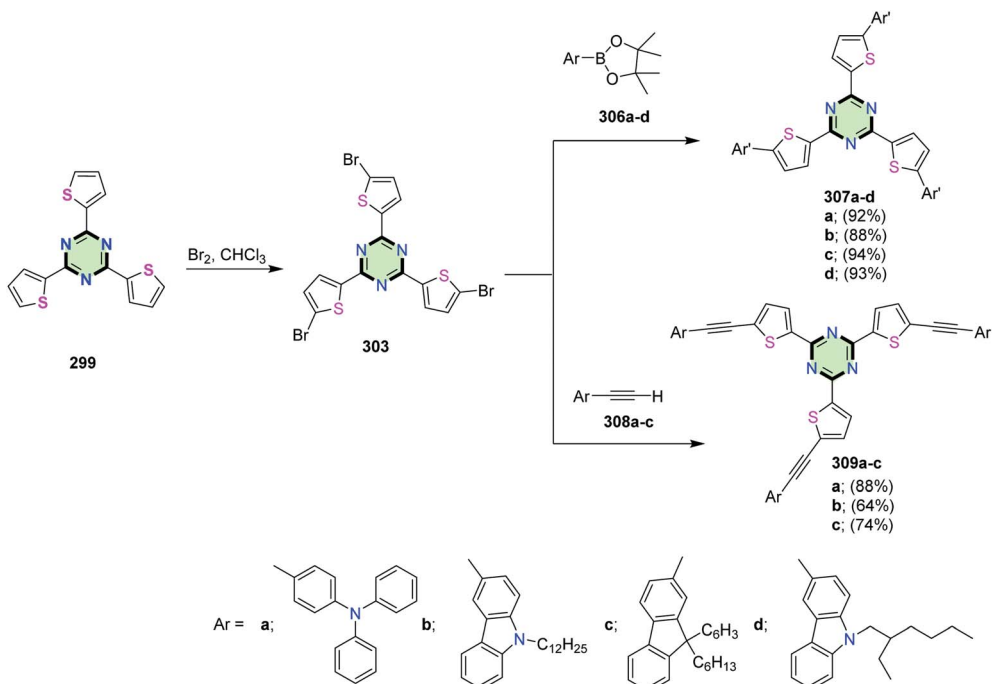


Scheme 79 Synthesis of 2,4,6-tri(thiophen-2-yl)-1,3,5-triazine 299.

The aromatic C–N coupling of 1,3,5-tribromobenzene 193 with 3,3'',6,6''-tetra-*tert*-butyl-9,3':6',9''-tercarbazole 271 in 18-crown-6 ether in the presence of copper(I) iodide and potassium carbonate resulted in the formation of dendritic tercarbazole-based SSM 272 in acceptable yield (33%) (Scheme 70). The non-planar twisted starburst configuration of 272 resulted in excellent thermal stability and morphological stabilities. It retain the triplet state energy high at 2.86 eV (compared to 1,3,5-tri(*N*-carbazolyl)benzene (TCB), 3.01 eV) showing the inefficient conjugation of the additional carbazole



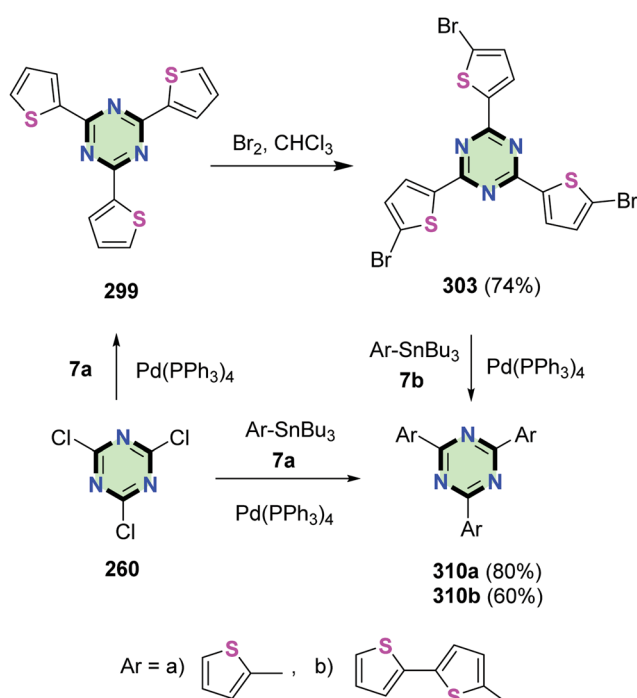
Scheme 80 Synthesis of 2,4,6-tri(5-aryl-thiophen-2-yl)-1,3,5-triazines 302a-f.



Scheme 81 Synthesis of SSMs with 1,3,5-triazine core and thiophene side arms 307 and 309

moieties due to lack of planarity. The application of **272** as a dendritic host material in solution-processed phosphorescent blue OLEDs was investigated and found to be far better than TCB.¹¹⁸

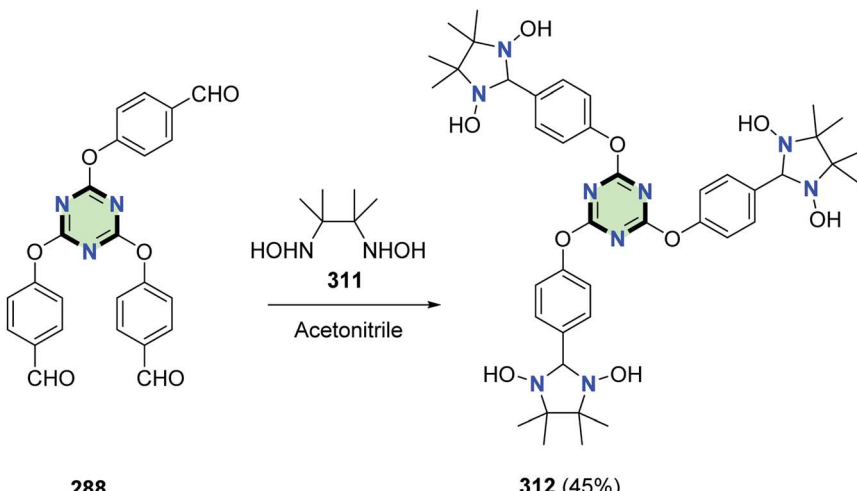
He *et al.*⁸⁸ reported the synthesis of 1,3,5-tris(5-(4-(3,6-di-*tert*-butylcarbazol-9-yl)phenyl)-1,3,4-oxadiazol-2-yl)benzene **274** in 37% yield, upon reaction of 1,3,5-tris(5-(4-bromophenyl)-1,3,4-oxadiazol-2-yl)benzene **112** with 3,6-di-*tert*-butyl-9H-carbazole **273** in the presence of CuI and K₂CO₃ (Scheme 71). The donor- π -acceptor (D- π -A) structured SSM **274** emitted a blue color at 424 nm with an excellent quantum efficiency $\Phi_f = 93\%$ in dilute toluene and $\Phi_f = 72\%$ in thin film. The photoluminescence spectrum of **274** persisted even at elevated temperature 150 °C for 220 hours in air which permits an ease of applicability. Non-doped electroluminescent blue-emitting device based on **274** displayed a turn-on voltage of 3.7 V because of its bipolar structure. Excellent current efficiency (CE) and external quantum efficiency (EQE) were 4.22 cd A⁻¹ and 3.37%, respectively.



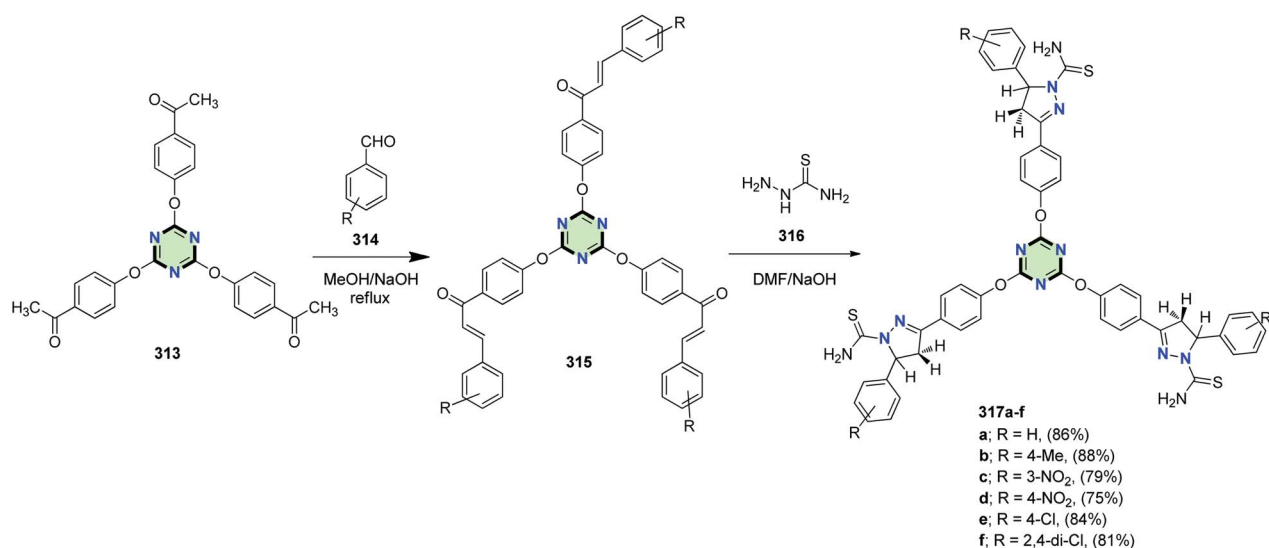
Scheme 82 Synthesis of star-shaped 1,3,5-triazines **310a,b** with thiophene or bithiophene end groups.

4.3.1.4.7. Naphthalene diimide. Two star-shaped molecules with benzene core and three naphthalene diimide side arms **279a** and **279b** were synthesized by imidization reaction of 1,3,5-triamino benzene **278** with naphthalene derivatives **277a** and **277b**. The latter compounds were obtained by treatment of 1,4,5,8-naphthalenetetracarboxylic dianhydride **275** with amine derivatives **276** in the presence of $Zn(OAc)_2$ (Scheme 72).¹¹⁹ These star-shaped compounds **279a** and **279b** showed a bathochromic shift in the film state compared to solution which reflects the aggregation in the solid state. Also, these compounds were characterized by low-lying LUMO levels at -3.83 and -3.87 eV, respectively, which indicates the applicability of these compounds as n-type semi-conductors.

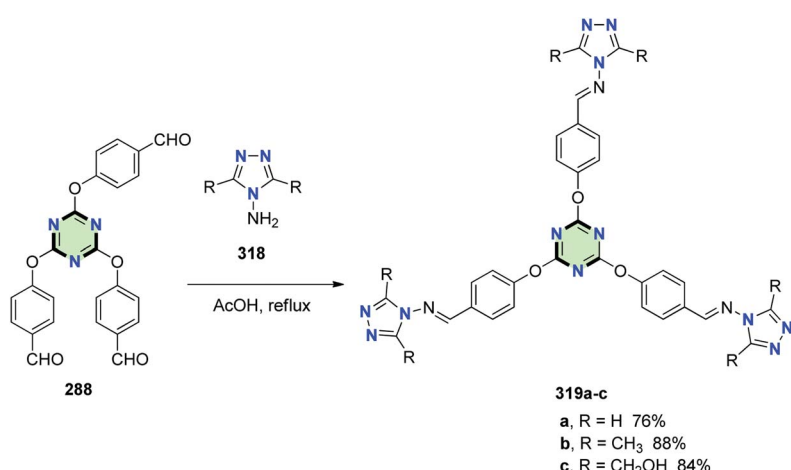
4.3.2. Pyridine-cored SSMs. Magnan *et al.*¹¹³ reported the synthesis of star-shaped compound with pyrimidine core **281** in



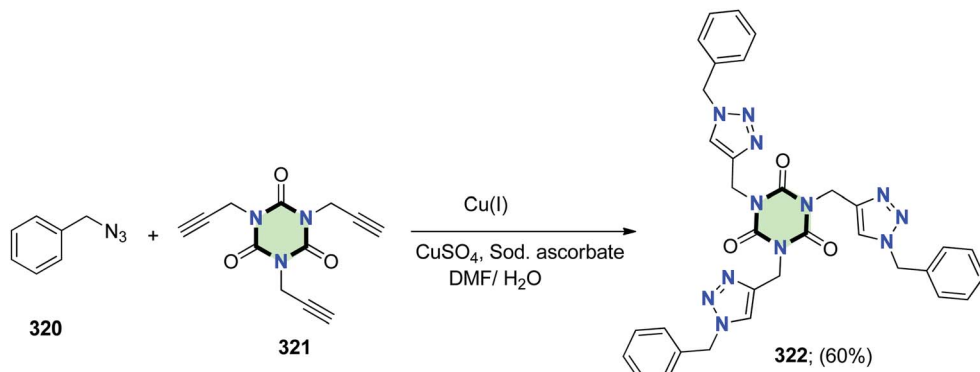
Scheme 83 Synthesis of star-shaped molecule with triazine core and imidazolidine side arms 312.



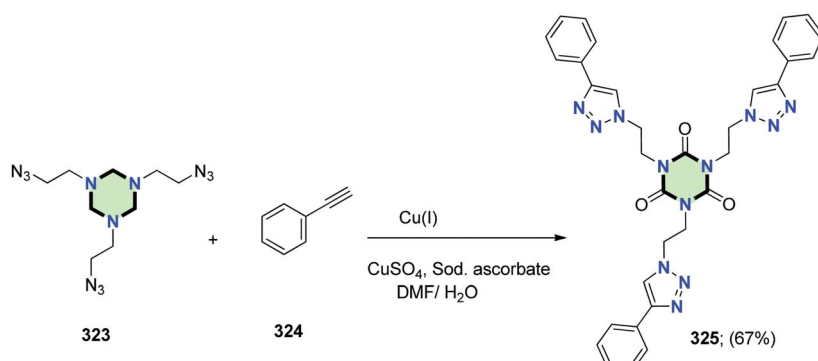
Scheme 84 Synthesis of tris-pyrazoline 317a-f.



Scheme 85 Synthesis of star-shaped Schiff bases 319a-c.



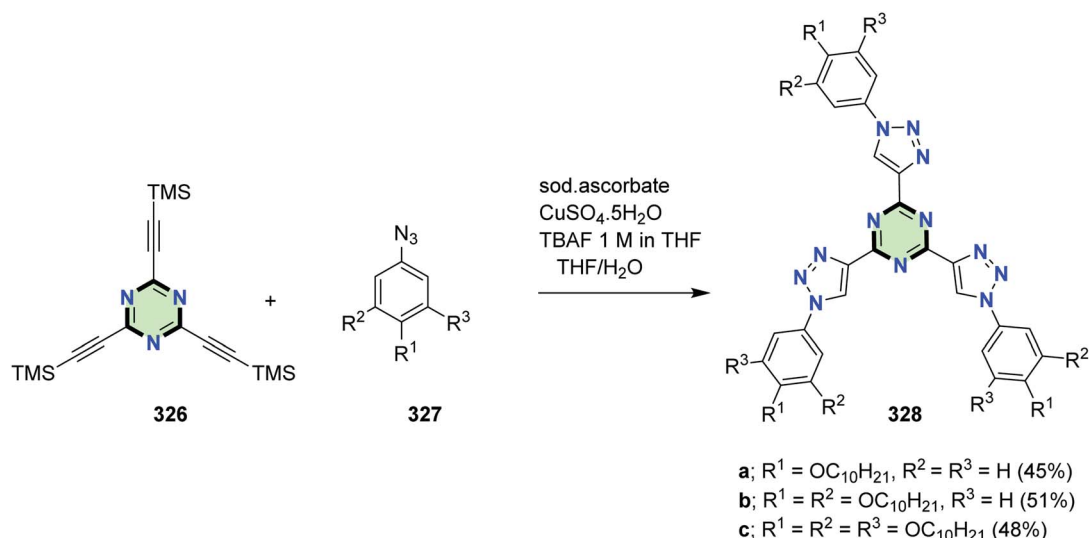
Scheme 86 Synthesis of tris(triazole) derivative 322.



Scheme 87 Synthesis of tris(triazole) derivative 325.

76% yield by four-fold Negishi coupling between 2,3,5,6-tetra-bromopyridine **280** with 2-hexylthieno[3,2-*b*]thiophene **239** in the presence of *n*BuLi and anhydrous ZnCl₂. Subsequent oxidative cyclodehydrogenation of the latter compound in chlorobenzene

using anhydrous ferric chloride gave tetra(5-hexylthieno[3,2-*b*]thieno)acridine **282** in 53% yield (Scheme 73). Changing the benzene core in compound **242** (*cf.* Scheme 61) with the electron-deficient pyridine ring in **282** resulted in a red shift from 468 to

Scheme 88 Synthesis of SSMs with triazine core and phenyltriazole side arms **328**.

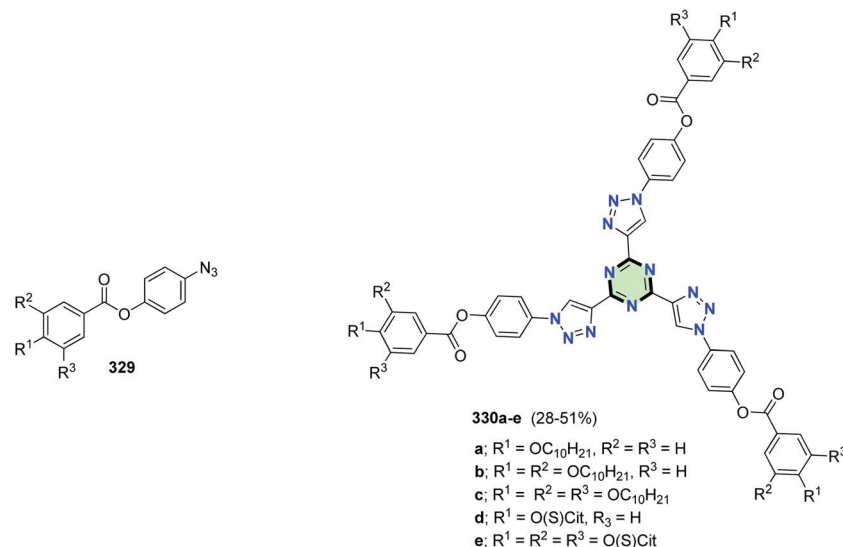


Fig. 7 Structures of 4-azidophenyl benzoate 329 and SSMs 330a–e.

494 nm, respectively. This may be attributed to the presence of the electronegative nitrogen atom which lowers the energy of the LUMO of 282 and thus, decreases the energy gap.

4.3.3. *s*-Triazine-cored SSMs with different arms

4.3.3.1. Biphenyl. SSM containing 1,3,5-triazine core and biphenyl arms 287 was synthesized in an excellent yield (95%) *via* Suzuki cross-coupling of 2,4,6-tris(3-(4,4,5,5-tetramethyl-1,3,2-dioxaborolan-2-yl)phenyl)-1,3,5-triazine 285 with 3-bromobenzonitrile 286 in the presence of $Pd(PPh_3)_4$ catalyst and $P(t-Bu)_3$ as co-catalyst. Compound 285 was obtained in 83% yield by the reaction of 1,3,5-tris(bromophenyl)triazine 283 with octamethyl-2,2'-bi(1,3,2-dioxaborolane) 284 in the presence of Pd catalyst (Scheme 74).¹²⁰

4.3.3.2. Oxaziridine. Peng *et al.*¹²¹ reported the synthesis of a star-shaped molecule with triazine core and oxaziridine side arm 291 in 91% yield by reaction of 2,4,6-tris(*p*-formylphenoxy)-1,3,5-triazine 288 with 2-amino-2-methyl-1-propanol 289 to give tris(imine) 290 followed by oxidation using *m*-CPBA in chloroform (Scheme 75).

4.3.3.3. Pyrrole. 2,4,6-Tris(4-(1*H*-pyrrol-1-yl)phenoxy)-1,3,5-triazine 294 was synthesized in 76% yield upon treatment of 4-(1*H*-pyrrol-1-yl)phenol 292 with 2,4,6-trichloro-1,3,5-triazine 293 under basic condition (Scheme 76). Electropolymerization of the star-shaped molecule 294 was then conducted and the resulting polymer was studied spectroelectrochemically. Three bands were shown at 346, 508 and 665 for $\pi-\pi^*$ transition, polaron and bipolaron formation, respectively. The switching ability of this polymer was examined by means of chronoabsorptometry and the optical contrast was 20% with a switching time of 1.1 s. A dual complementary-colored electrochromic device was designed for both of the latter polymer and poly(3,4-ethylenedioxythiophene) (PEDOT) in a sandwich configuration. It switched between dark blue and red colors within 2.2 s and with an optical contrast of 25%.¹²²

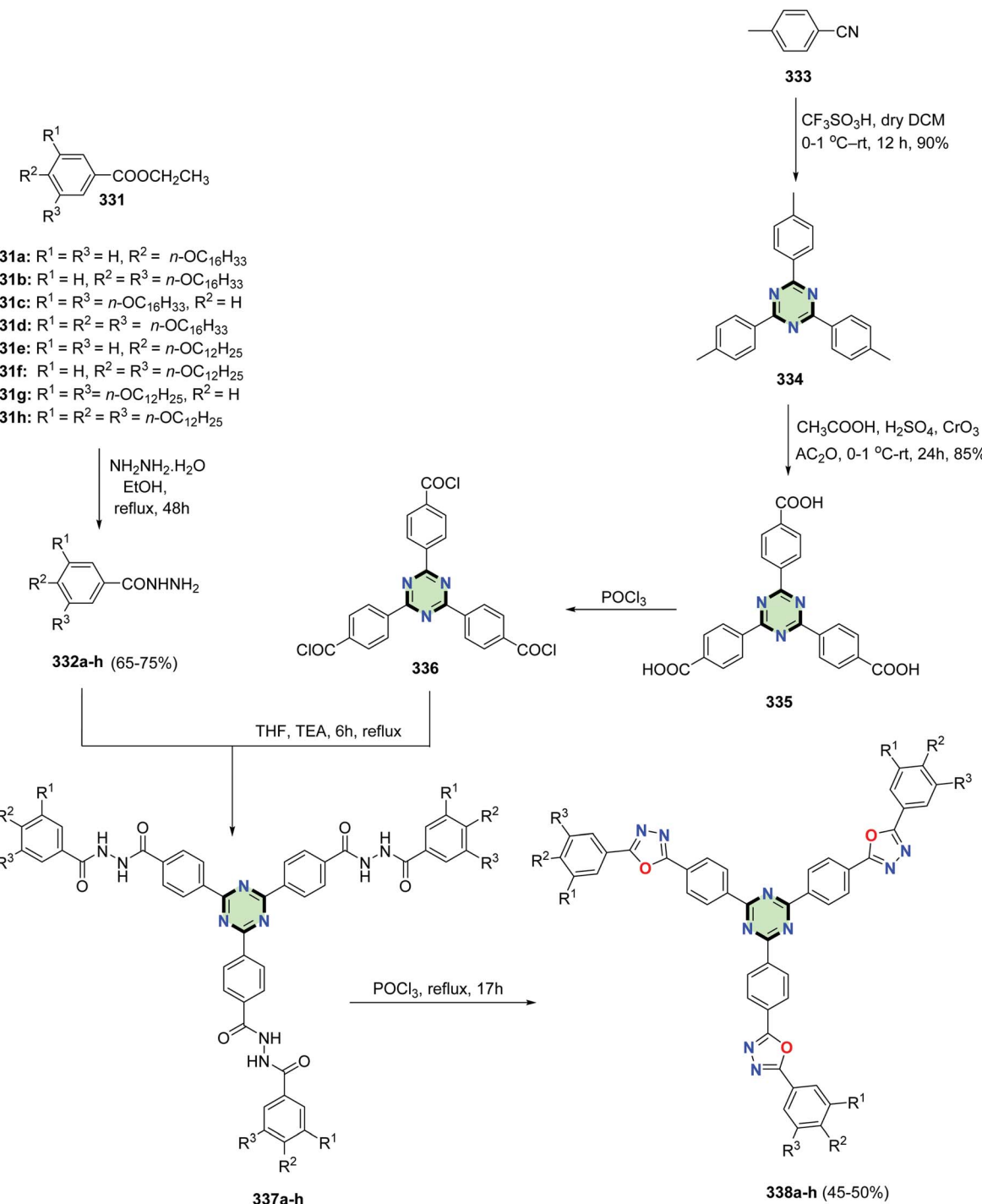
Triazine-cored compound 296 was synthesized in 91% yield through reaction of cyanuric chloride 293 with 1-(4-

hydroxyphenyl)-1*H*-pyrrole-2,5-dione 295 in the presence of TEA (Scheme 77).

4.3.3.4. Thiophene and bithiophene. Li *et al.*¹⁵ reported the synthesis of 2,4,6-tris(4-(thiophen-2-yl)phenyl)-1,3,5-triazine 298 in 15% yield through cyclotrimerization of 4-(thiophen-2-yl)benzonitrile 297 in the presence of CF_3SO_3H (Scheme 78). Electropolymerization of 298 resulted in the formation of a polymer of insignificant electrochromic properties. However, the copolymerization of this polymer with (a polymer of low ionization potential) PEDOT improved greatly the electrochromic properties.

2,4,6-Tri(thiophen-2-yl)-1,3,5-triazine 299 was synthesized in 80% yield by the reaction of 2-tributylstannylthiophene 7 with cyanuric chloride 293 in the presence of $Pd(PPh_3)_4$ (Scheme 79).^{6,123}

A selective lithiation of 299 and subsequent stannylation gave 2,4,6-tris(5-tributylstannyl-2-thienyl)-1,3,5-triazine 300. The latter compound underwent Stille coupling reaction with pentafluorophenylbromide 301 in the presence of $Pd(PPh_3)_4$ to give 2,4,6-tris(5-pentafluorophenyl-2-thienyl)-1,3,5-triazine 302a in 28% yield. On the other hand, 2,4,6-tri(5-aryl-thiophen-2-yl)-1,3,5-triazines 302b-f were synthesized *via* Suzuki–Miura cross-coupling reactions of 2,4,6-tri(5-bromo-2-thienyl)-1,3,5-triazine 303 with arylboronic acids 304 or tetramethyl-2-aryl-1,3,2-dioxaborolane 305 in the presence of cesium carbonate and Pd catalyst (Scheme 80).⁶ The effect of tuning the electronic nature of aryl groups connected to thiophene peripheral of SSMs 302 was found to be consistent with the electron-accepting or electron-attracting capabilities of these molecules as deduced from their UV absorption and fluorescence emission spectra. Moreover, compound 302e having Bu_2N^- group showed both absorption and emission solvatochromism (due to internal charge transfer), as well as colorimetric and luminescence proton-sensing properties in view of the visually observed changes in the color of the solution and emission related to the two-step protonation of the Bu_2N^- groups and the nitrogen



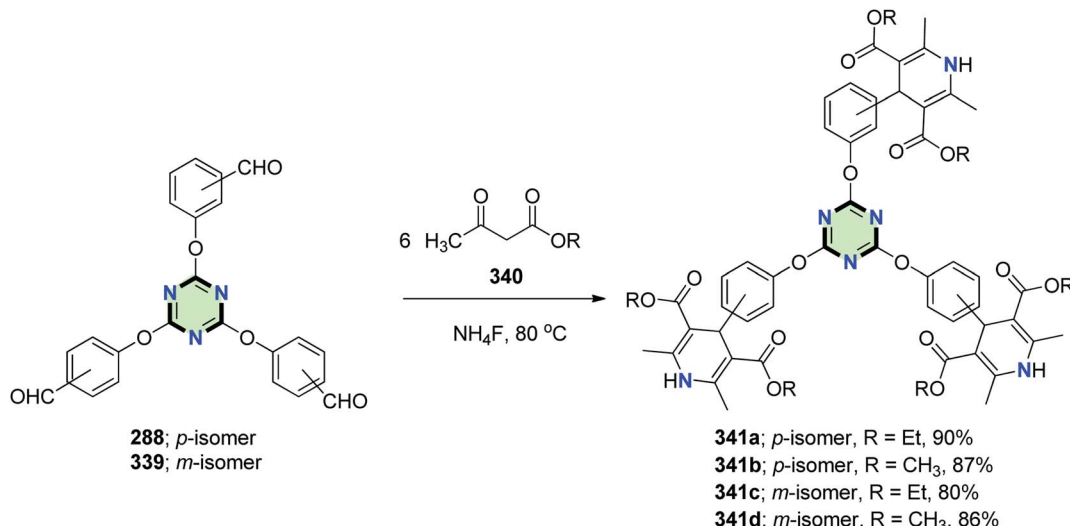
Scheme 89 Synthesis of SSMs with a central triazine core appended with three 1,3,4-oxadiazole arms 338a–h.

atoms on the 1,3,5-triazine moiety. This makes compound 302e to be a promising polarity or pH sensors.

A series of SSMs with 1,3,5-triazine core and thiophene attached directly or *via* ethylenic linkages to triphenylamine, carbazole or fluorene moieties as side arms 307 and 309 could be synthesized starting from the 2,4,6-tri(5-bromo-2-thienyl)-1,3,5-triazine 303 through Suzuki–Miyaura and Sonogashira

cross-coupling reactions involving arylboronates 306a–d or ethynylarenes 308a–c, respectively, in moderate-to-excellent yields (64–93%). Compound 303 was obtained by bromination of tris-2,4,6-thienyl-1,3,5-triazine 299 in the presence of bromine in chloroform at reflux (Scheme 81). The UV-vis spectra of compounds 307 and 309 showed that the absorption maximum was affected not only by the electron-donating

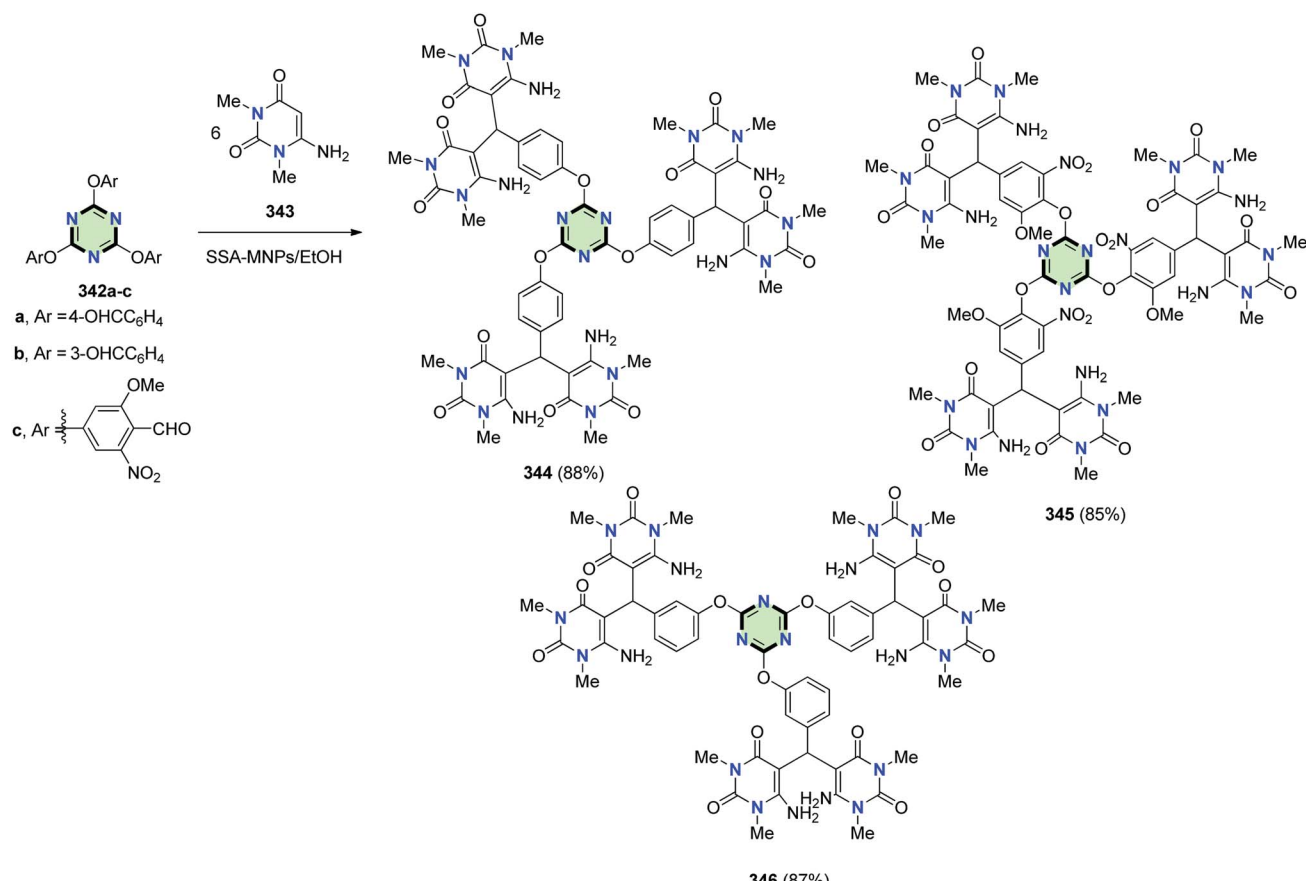




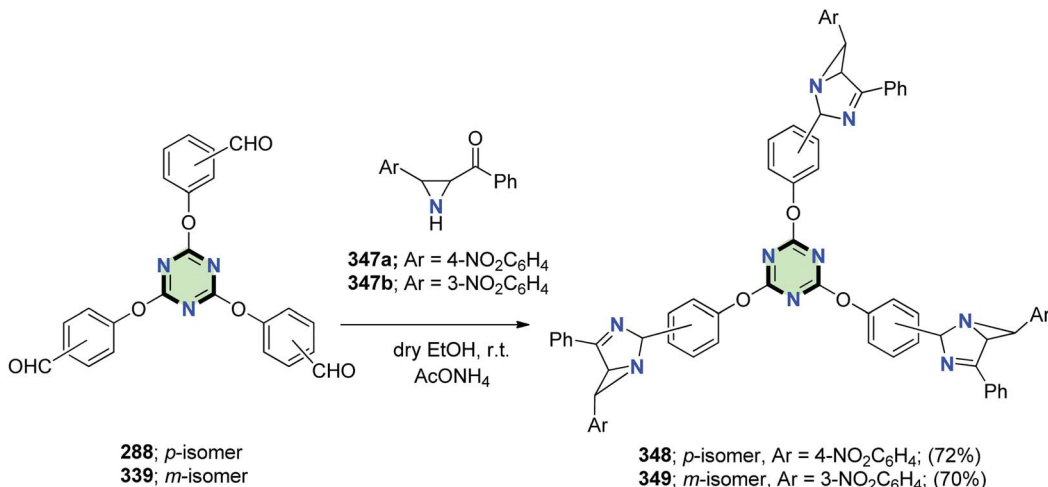
Scheme 90 Synthesis of tripodal 1,4-dihydropyridines 341a–d.

strength of the peripheral group or introduction of an ethynyl spacer, but on the position of the same electron-donating substituent as well (as in case of 307b and 307d). The electrochemical data of these compounds displayed a reversible or

a quasi-reversible redox behavior due to their donor–acceptor properties. In addition, these compounds indicated large two-photon absorption cross-sections at 720–880 nm, greatly



Scheme 91 Synthesis of tri[bis(6-aminopyrimidinyl)methanes] 344–346.



Scheme 92 Synthesis of SSMs with 1,3-diazabicyclo[3.1.0]hex-3-enes side arms 348 and 349.

affected by the intramolecular charge transfer and the extent of π -conjugation.¹²⁴

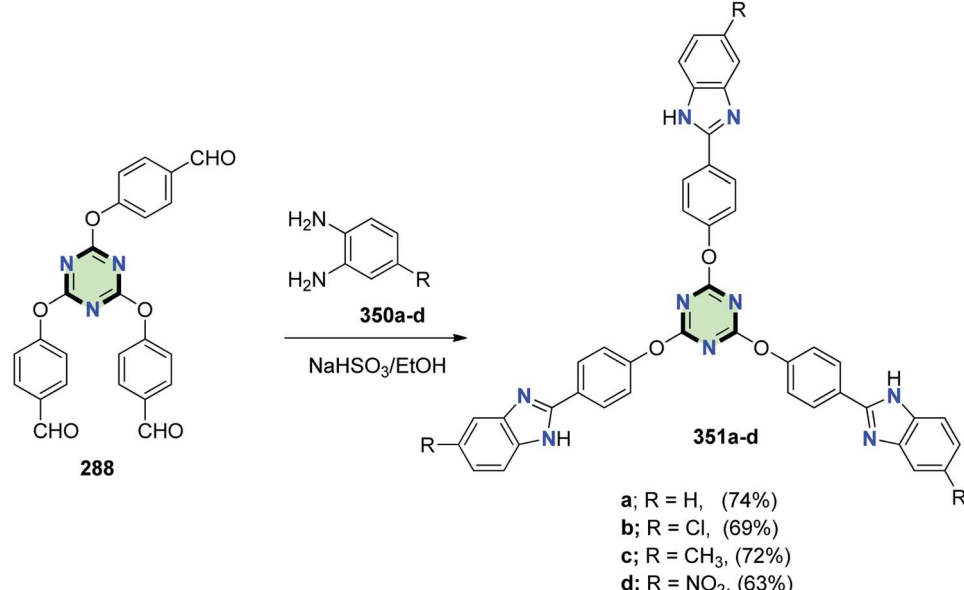
Leriche *et al.*¹²³ reported the synthesis of star-shaped 1,3,5-triazine molecules **310a,b** with thiophene or bithiophene tails in 80 and 60% yields, respectively, by the reaction of cyanuryl chloride **260** with tributylstannylarenes **7a** or by the reaction of 2,4,6-tris(5-bromothiophen-2-yl)-1,3,5-triazine **303** with 2-tributylstannylthiophene **7b** in the presence of $\text{Pd}(\text{PPh}_3)_4$ (Scheme 82). It was shown that enlargement of thiophene tail resulted in a bathochromic shift in their UV-vis absorption spectra and a reduction in their oxidation potential as shown from their cyclic voltammograms.

4.3.3.5. Imidazolidine. Condensation of trisaldehyde **288** with 2,3-dihydroxyamino-2,3-dimethylbutane **311** in

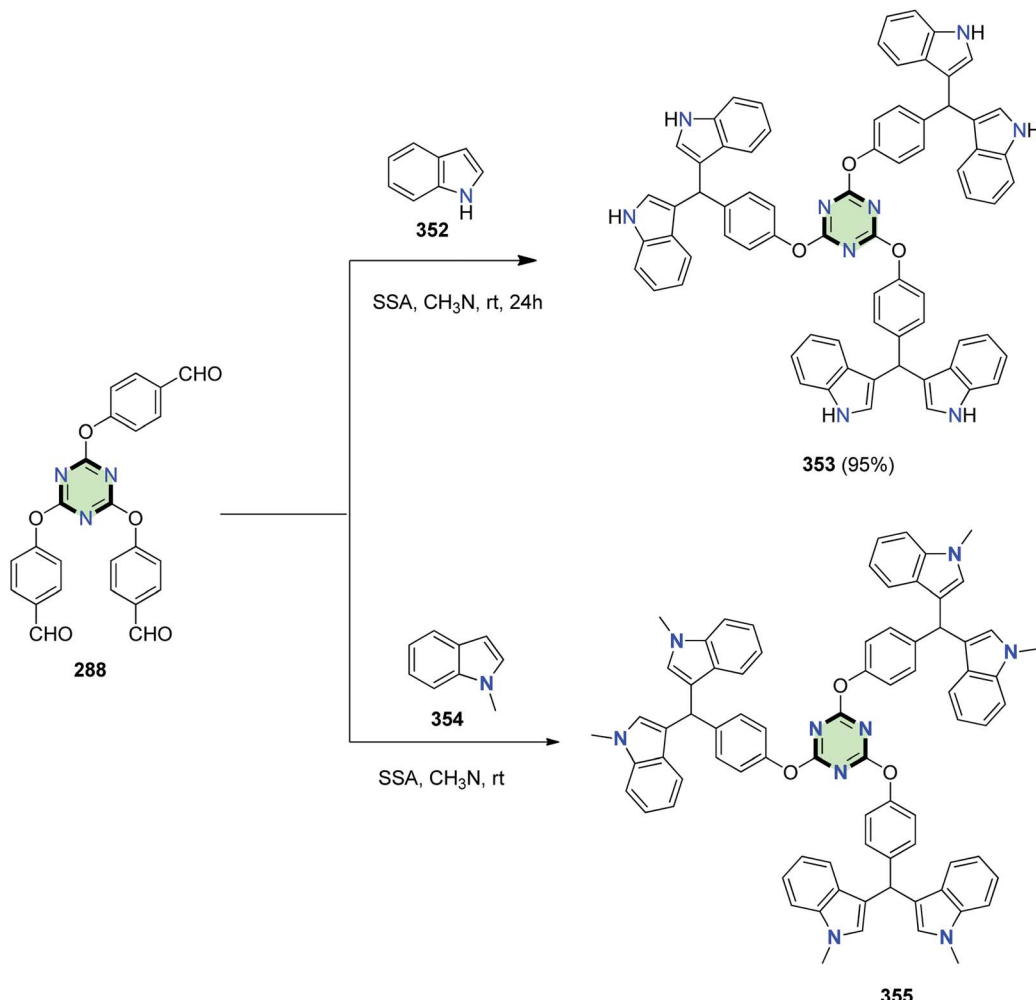
acetonitrile afforded a star-shaped molecule with triazine core and 4,4,5,5-tetramethyl-2-phenylimidazolidine-1,3-diol side arms **312** in 45% yield (Scheme 83).

4.3.3.6. 4,5-Dihydro-1H-pyrazole. A series of tris-pyrazoline **317a-f** were synthesized in good yields by tris-cyclization of tris-chalcones **315** with thiosemicarbazide **316** under basic conditions in DMF. The chalcones **315** were prepared by condensation of tris-acetophenone **313** with the appropriate aldehydes **314** in MeOH in the presence of NaOH (Scheme 84).¹²⁵

4.3.3.7. 1,2,4-Triazole. Star-shaped Schiff bases **319a-c** with triazine core and 1,2,4-triazole side arms were synthesized in good yields through condensation of 2,4,6-tris(*p*-formylphenoxy)-1,3,5-triazine **288** with the appropriate amino-triazole **318** in glacial acetic acid at reflux (Scheme 85).¹²⁶



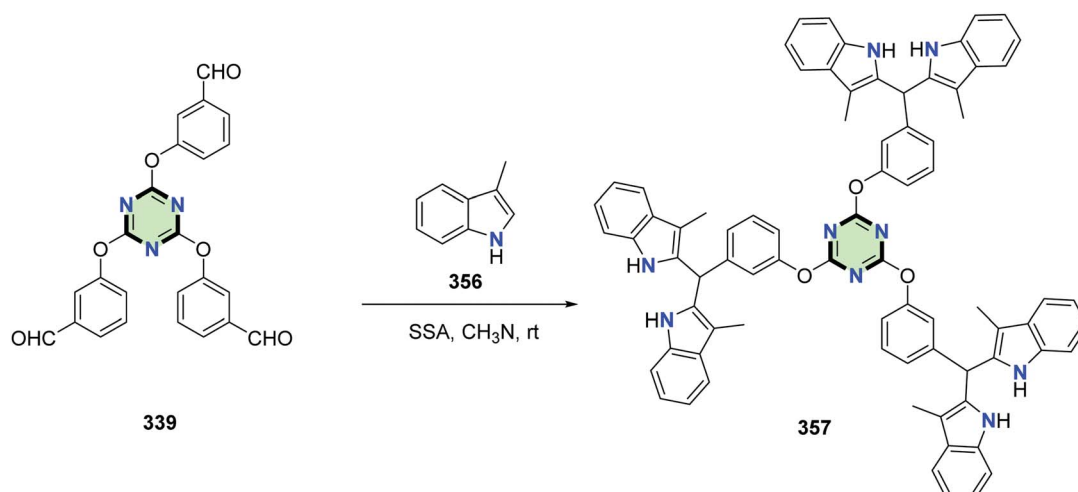
Scheme 93 Synthesis of tripodal-benzimidazole derivatives 351a-d.



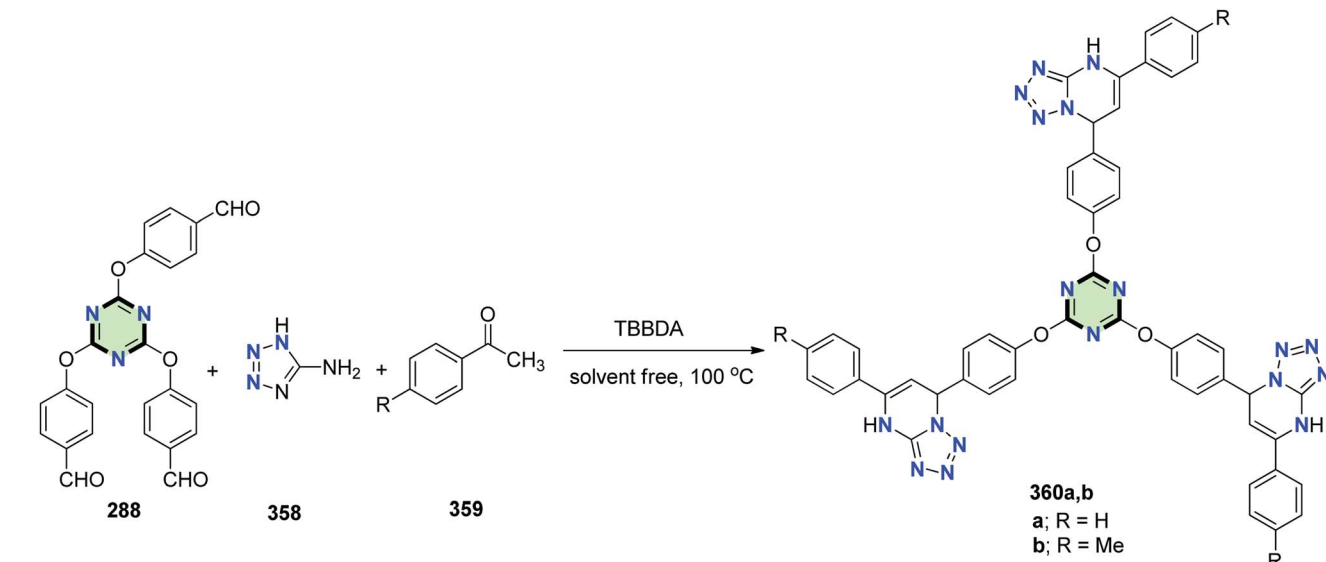
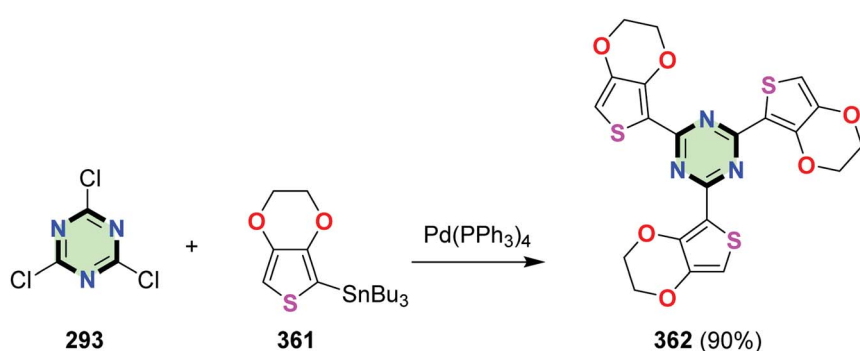
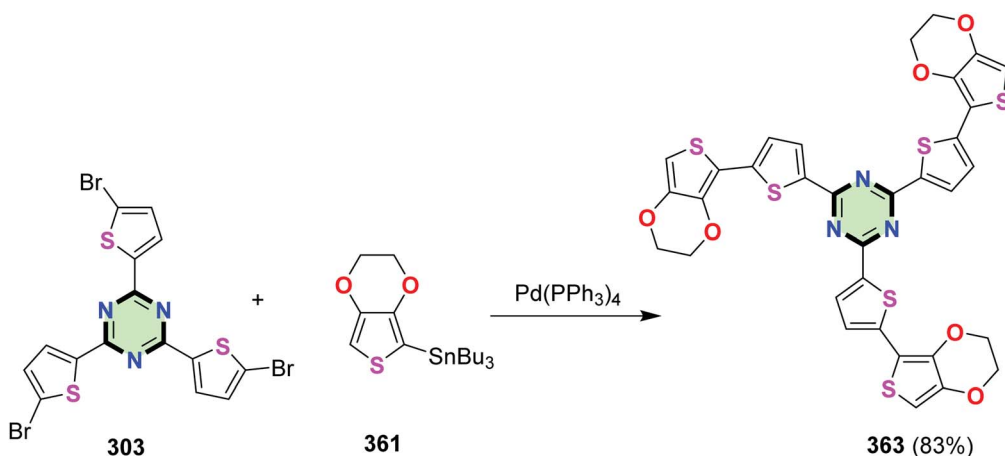
Scheme 94 Synthesis of tris(bis(indolyl)methanes) compounds 353 and 355.

4.3.3.8. *1,2,3-Triazole*. The synthesis of tripodal 322 with 1,2,3-triazole side arms were performed using a copper catalyzed Huisgen's reaction. Thus, reaction of a mixture of alkyne

321 and benzylazide 320 in DMF afforded tris[(1-benzyl-1*H*-1,2,3-triazole-4-yl)methyl]-1,3,5-triazinane-2,4,6-trione 322 in 60% yield (Scheme 86).¹²⁷

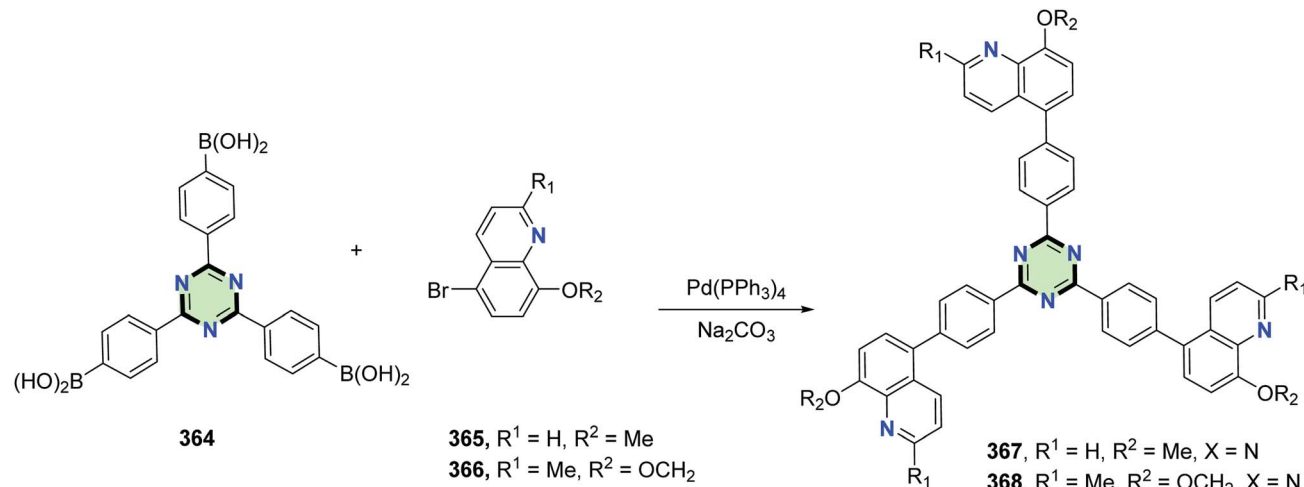


Scheme 95 Synthesis of 2,4,6-tris((bis(indol-2-yl)methyl)phenoxy)-1,3,5-triazine 357.

Scheme 96 Synthesis of tris-dihydrotetrazolo[1,5-a]pyrimidines **360a** and **360b**.Scheme 97 Synthesis of 2,4,6-tris(2,3-dihydrothieno[3,4-b][1,4]dioxin-5-yl)-1,3,5-triazine **362**.

Scheme 98 Synthesis of SSM with triazine core linked to thieno[3,4-b][1,4]dioxine.





Scheme 99 Synthesis of SSMs with quinolone side arms 367 and 368.

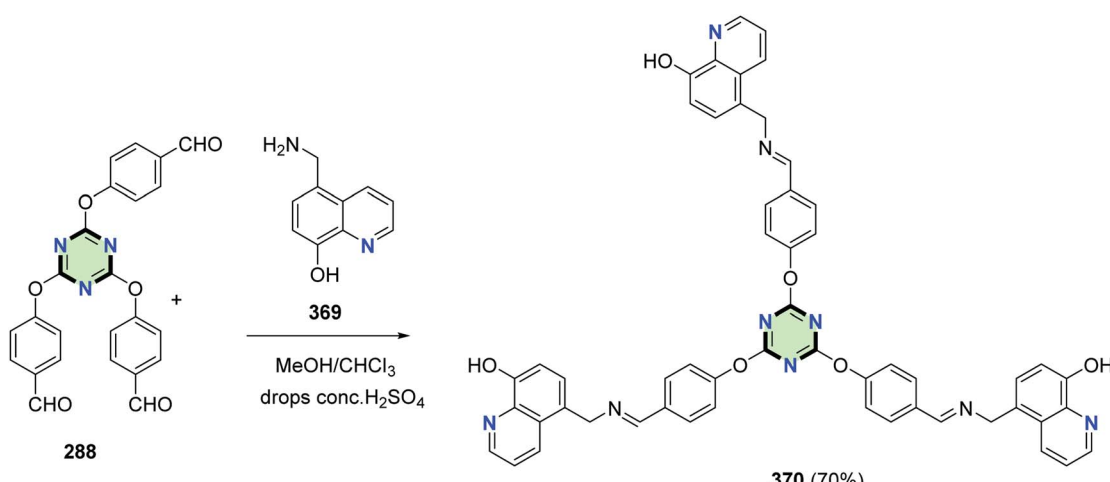
The same method was applied to synthesize the triazole derivative 325 in 67% yield, using the tris azide 323 and phenylacetylene 324 (Scheme 87).¹²⁷

The click copper-catalyzed cycloaddition reaction of tris [(trimethylsilyl)ethynyl]-1,3,5-triazine 326 with azide derivatives 327 afforded SSMs 328 with triazine core and phenyl-triazole side arms containing mono-, di-, and trialkoxy groups (Scheme 88). The star-shaped materials 328 showed ordered columnar mesophases. They displayed luminescence from the blue to green light depending on the peripheral substitution. Electrochemical behavior of these compounds was good correlated to their electron-deficient nature and their potential for electron transport.¹²⁸

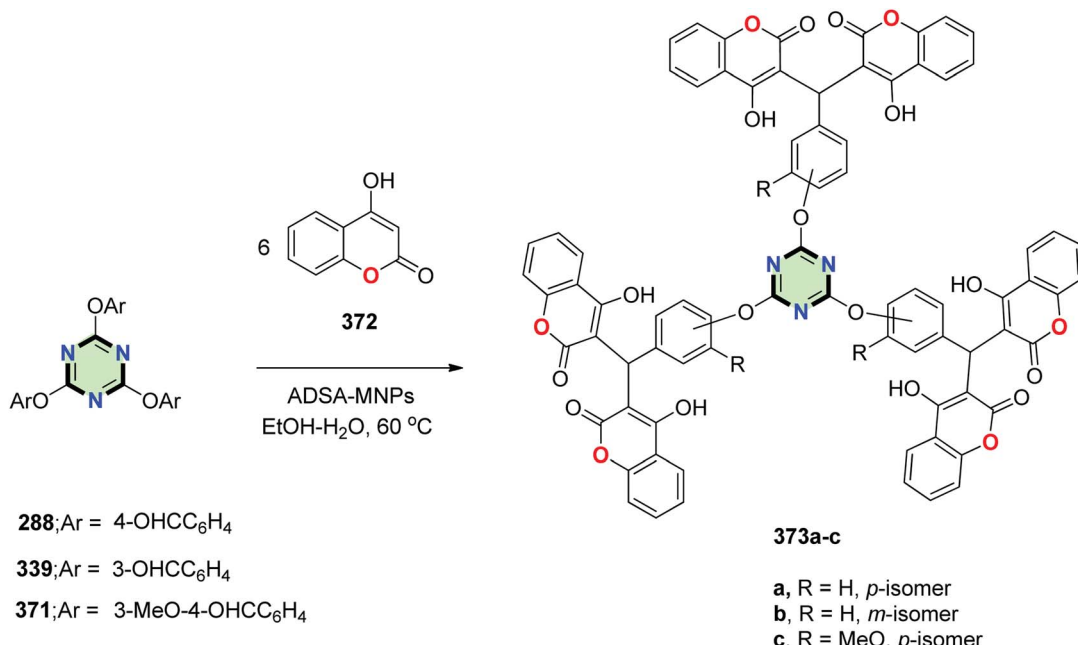
In a similar fashion, SSMs 330a–e with triazine core and arms containing triazole moieties and aroyloxy groups could be synthesized in moderate yields (28–51%) starting from the appropriate 4-azidophenyl benzoate 329 (Fig. 7). It has been

found that inclusion of long alkoxy chains in compounds 330 decreases both solvatofluorochromism and electron-accepting properties.¹²⁹

4.3.3.9. Oxadiazole. Pradhan *et al.*¹³⁰ reported the synthesis of star-shaped molecules with a central triazine core appended with three 1,3,4-oxadiazole arms 338a–h through multi-step reactions including, firstly the transformation of alkoxy esters 331a–h into their respective hydrazides 332a–h upon treatment with hydrazine hydrate in ethanol. Reaction of the hydrazides with 4,4',4''-(1,3,5-triazine-2,4,6-triyl)tribenzoyl chloride 336 (obtained upon treatment of 4,4',4''-(1,3,5-triazine-2,4,6-triyl) tribenzoic acid 335 with POCl₃) in THF in the presence of triethylamine yielded tri-N-benzoylbenzohydrazides 337a–h. These compounds were heated with POCl₃ to give the target molecules 338a–h. The key intermediate 4,4',4''-(1,3,5-triazine-2,4,6-triyl) tribenzoic acid 335 was prepared in good yield from *p*-tolunitrile 333 by firstly triflic acid catalyzed trimerization to give



Scheme 100 Synthesis of tripodal Schiff base with triazine core and quinoline side arms 370.

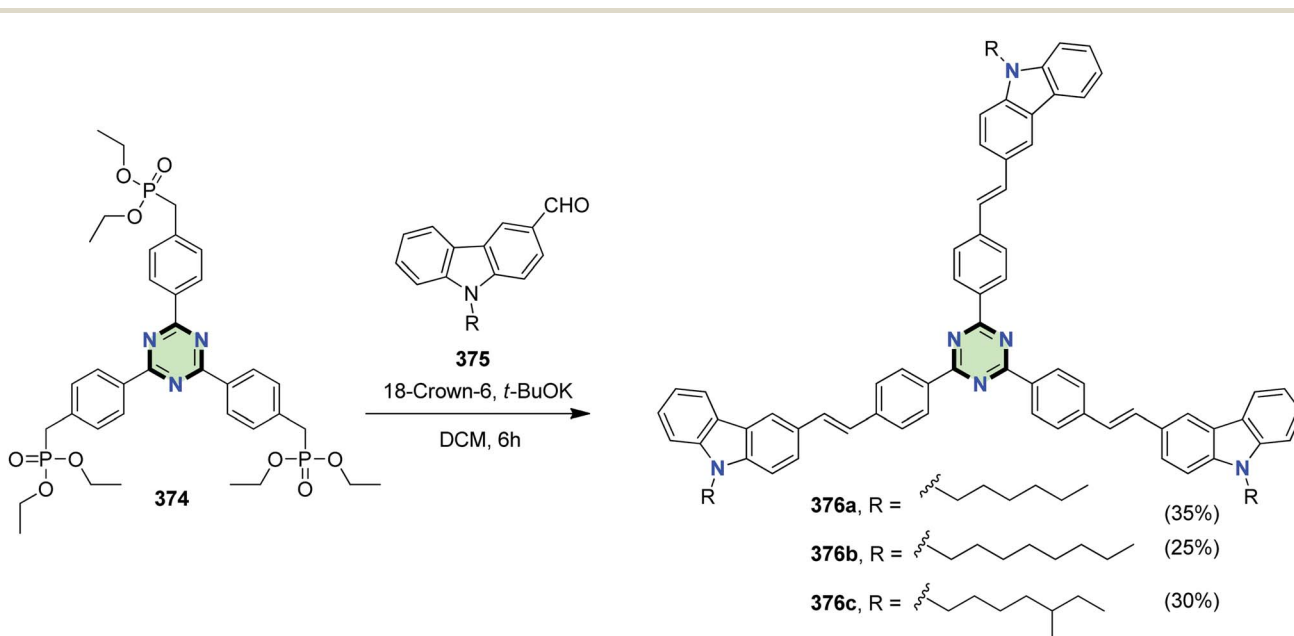


Scheme 101 Synthesis of tris[bis(4-hydroxycoumarinyl)methanes] 373a–c.

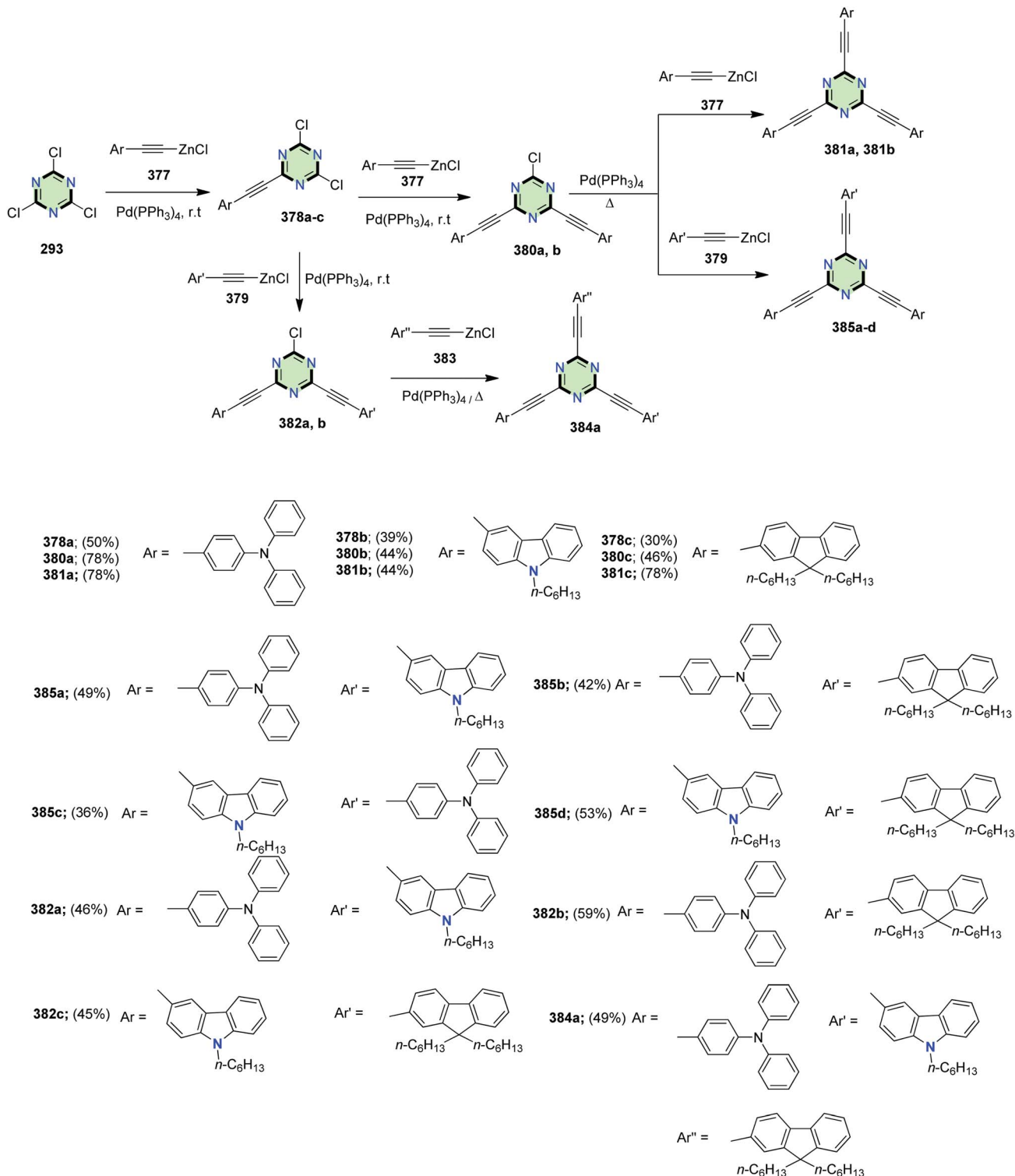
2,4,6-tri-*p*-tolyl-1,3,5-triazine 334 and subsequent chromic oxide mediated oxidation (Scheme 89). In general, a decrease of the chain length of the alkoxy groups led to enhancement of core–core interaction and subsequently, stabilizing both Col_r and Col_h phases and improving the thermal range. The SSMs 338 fluoresced blue-green light either in solution or in the solid state according to the type of peripheral chains. The persistence of fluorescene in the solid state was attributed to the columnar

assembly of the star molecules. Cyclic voltammograms of 338 implied that these molecules have lower LUMO and band gaps making them potential electron-transporting candidates for OLEDs.

4.3.3.10. 1,4-Dihydropyridine. Tripodal 1,4-dihydropyridines 341a–d were synthesized in good yields through Hantzsch reaction of tris-aldehydes 288 and 339 with β -keto esters 340 in the presence of NH₄F (Scheme 90).¹³¹



Scheme 102 Synthesis of SSMs 376a–c with 1,3,5-triazine core linked to three carbazole units.

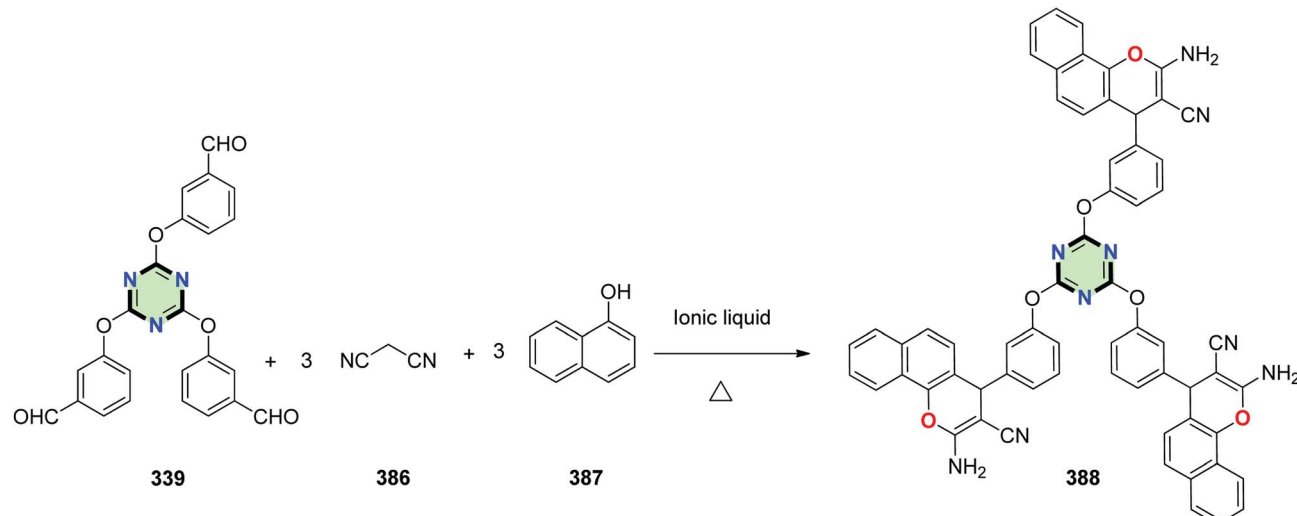


Scheme 103 Synthesis of symmetrical and asymmetrical 2,4,6-tris(arylethynyl)-1,3,5-triazines.

4.3.3.11. Pyrimidine. Karimi *et al.*¹³² reported the synthesis of tri[bis(6-aminopyrimidinyl)methanes] 344–346 in good yields by reaction of the appropriate trisaldehydes 342a–c with 6-amino-1,3-dimethyluracil 343 using sulfuric acid functionalized

silica-coated magnetic nanoparticles (SSA-MNPs) as a catalyst (Scheme 91).

4.3.3.12. 1,3-Diazabicyclo[3.1.0]hex-3-ene. Mahmoodi *et al.*¹³³ reported the synthesis of star shaped molecules with 1,3-diazabicyclo[3.1.0]hex-3-enes side arms 348 and 349 in 72% and



Scheme 104 Synthesis of tris(2-amino-4H-chromene) 388.

70% yields, respectively, through reaction of tris-aldehydes **288** and **339** with aziridinyl ketones **347a** and **347b**, respectively, in dry EtOH in the presence of AcONH_4 (Scheme 92).

4.3.3.13. Benzimidazole. A series of tripododal-benzimidazole derivatives **351a–d** were synthesized in 63–74% yields by Schiff base reaction between 2,4,6-tris(*p*-formylphenoxy)-1,3,5-triazine and *o*-phenylenediamine derivatives **350a–d** in the presence of NaHSO_3 (Scheme 93).¹³⁴

2,4,6-Tris(4-(di(indol-3-yl)methyl)phenoxy)-1,3,5-triazines **353** and **355** were prepared in good yields by the Friedel–Crafts reaction of tris-aldehyde **288** with each of 1*H*-indole **352** and 1-methyl-1*H*-indole **354**, respectively, in acetonitrile in the presence of silica sulfuric acid (Scheme 94).^{7,10}

On the other hand, Shiri *et al.*¹³⁵ reported the synthesis of 2,4,6-tris(3-(bis(3-methyl-1*H*-indol-2-yl)methyl)phenoxy)-1,3,5-triazine **357** in good yields by Friedel–Crafts reaction of 3-methyl-1*H*-indole **356** with tris-aldehyde **339** catalyzed by silica sulfuric acid in acetonitrile (Scheme 95).

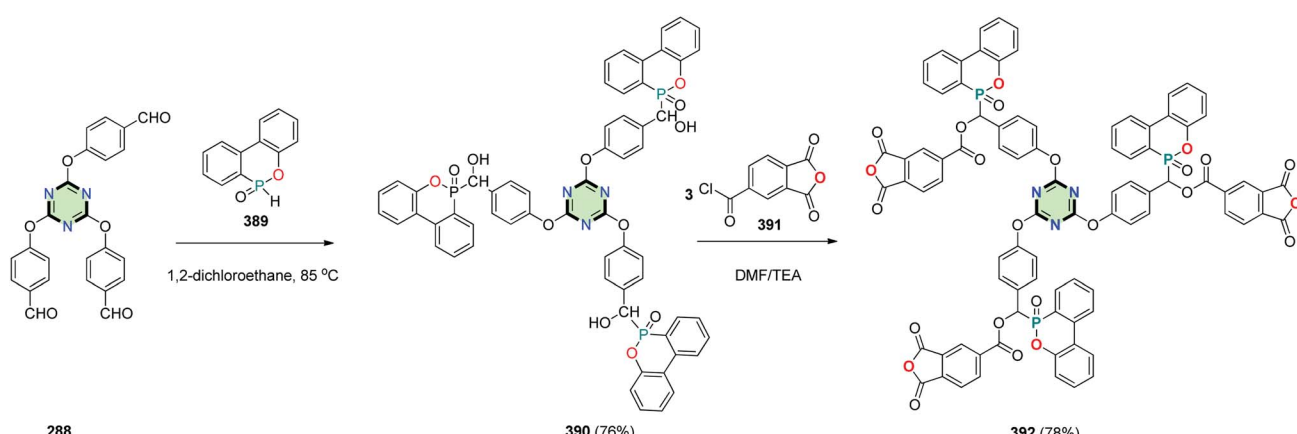
4.3.3.14. Dihydropyrazolo[1,5-*a*]pyrimidine. Vaghei *et al.*¹³⁶ reported the synthesis of tris-dihydropyrazolo[1,5-*a*]pyrimidines **360a** and **360b** in 85% and 92% yield, respectively,

through a multi-component reaction between tris-aldehyde **288**, acetophenone derivatives **359** and 5-aminotetrazole **358** under solvent free conditions (Scheme 96).

4.3.3.15. 2,3-Dihydrothieno[3,4-*b*][1,4]dioxine. 2,4,6-Tris(2,3-dihydrothieno[3,4-*b*][1,4]dioxin-5-yl)-1,3,5-triazine **362** was synthesized in 90% yield by Stile coupling reaction between cyanuric chloride **293** and tributyl(2,3-dihydrothieno[3,4-*b*][1,4]dioxin-5-yl)stannane **361** in the presence of $\text{Pd}(\text{PPh}_3)_4$ (Scheme 97).¹²³

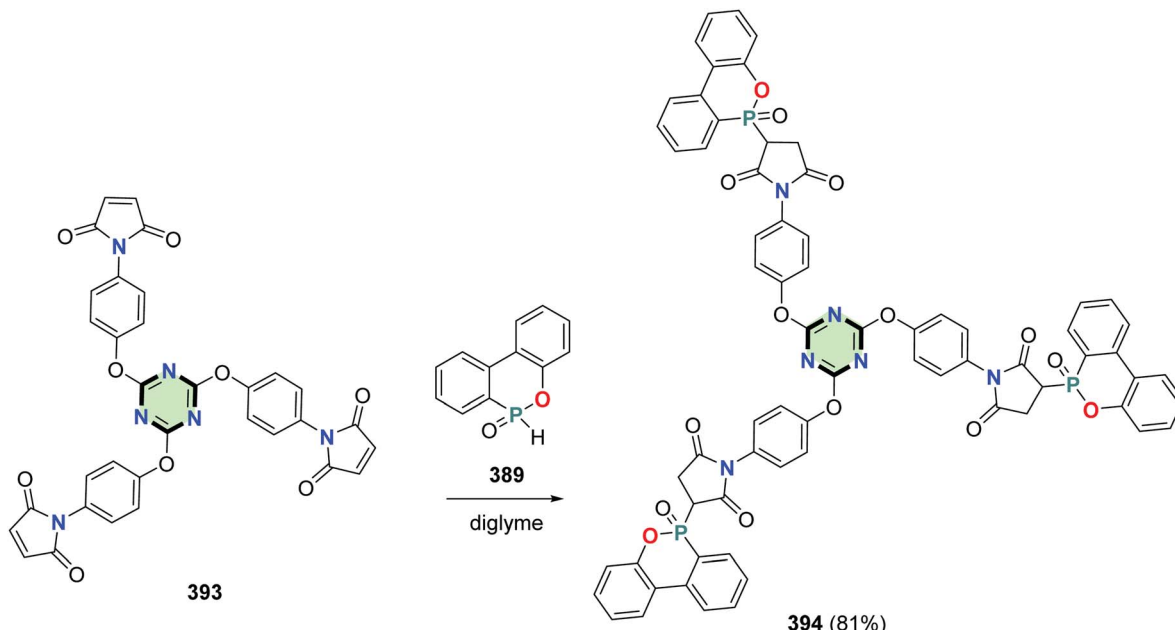
A star-shaped molecule with triazine core linked to thieno[3,4-*b*][1,4]dioxine via thiophene moiety **363** was synthesized in 83% yield by the reaction of 2,4,6-tris(5-bromothiophen-2-yl)-1,3,5-triazine **303** with tributyl(2,3-dihydrothieno[3,4-*b*][1,4]dioxin-5-yl)stannane **361** under similar conditions (Scheme 98).¹²³ The effect of conjugation persisted in compounds **362** and **363**. It was shown that increasing the number of thiophene moieties led to a remarkable red shift in their UV-vis absorption spectra and a decrease in their oxidation potential as evident from cyclic voltammetry.

4.3.3.16. Quinoline. Star-shaped conjugated molecules with quinolone side arms **367** and **368** were synthesized in good



Scheme 105 Synthesis of tri(phosphaphenanthrenemethyl(phenoxy))-1,3,5-triazine 390 and 392.





Scheme 106 Synthesis of tris(3-(6-oxido-6H-dibenzo[c,e][1,2]oxaphosphinin-6-yl)pyrrolidine-2,5-dione) 394.

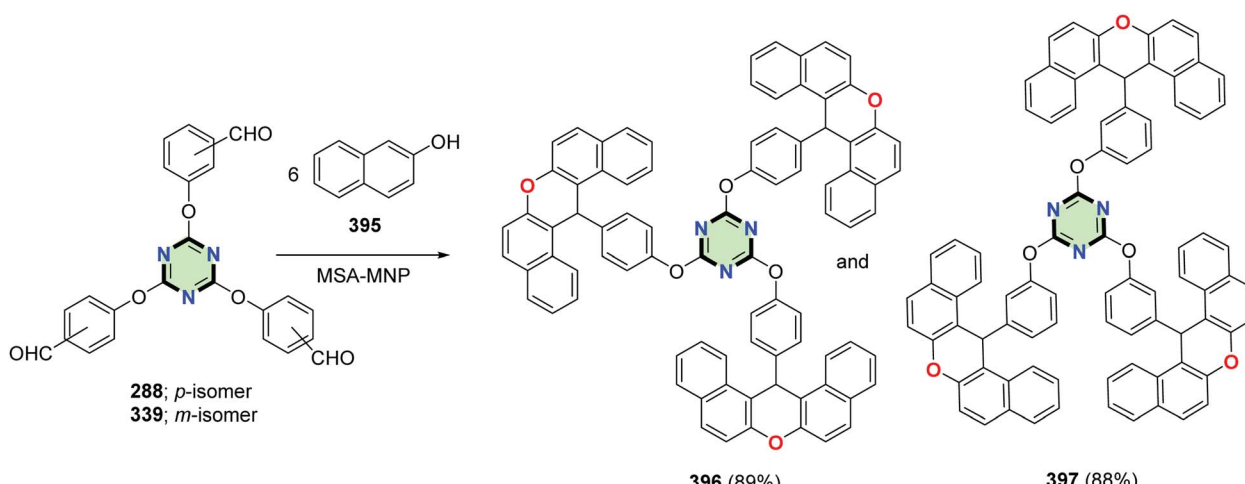
yields, using Suzuki coupling reaction of the appropriate boronic acid **364** with 5-bromo-8-methoxyquinoline **365** or 5-bromo-8-methoxy-2-methylquinoline **366** in the presence of Na_2CO_3 and $\text{Pd}(\text{PPh}_3)_4$ (Scheme 99).¹¹²

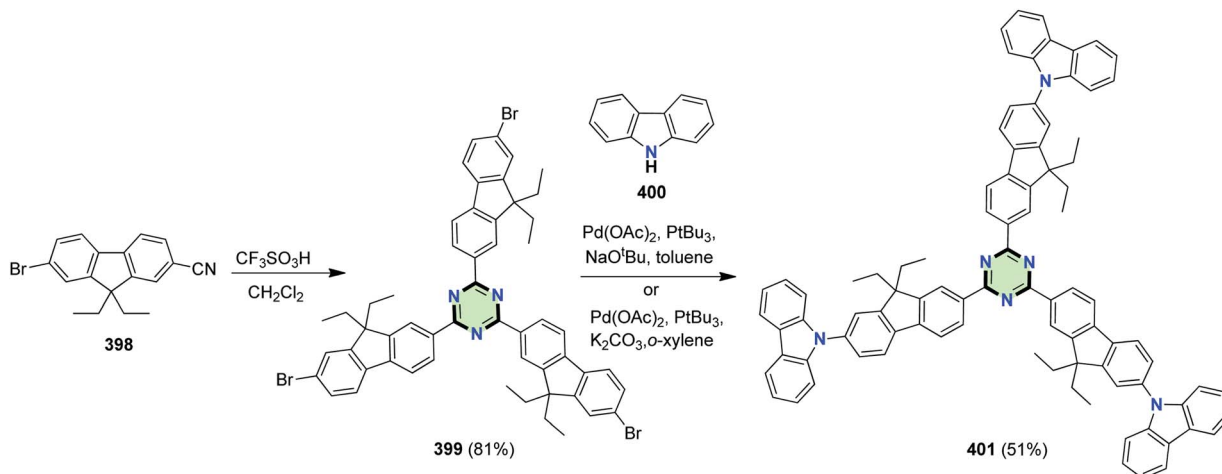
Karatas and Ucan reported a synthesis of a tripodal Schiff base molecule with triazine core and quinoline side arms **370** in 70% yield through reaction of 5-aminomethyl-8-hydroxylquinoline **369** with 2,4,6-tris(*p*-formylphenoxy)-1,3,5-triazine **288** in the presence of acidic catalyst (Scheme 100).¹³⁷

4.3.3.17. Coumarin. Tris[bis(4-hydroxycoumarinyl) methanes] **373a–c** were synthesized by condensation of 4-hydroxy-2*H*-coumarin-2-one **372** with the appropriate tris-aldehydes **288**, **339** or **371**. The reaction proceeded using alkane-disulfamic acid-functionalized silica-coated magnetic nanoparticles (ADSA-MNPs) as a catalyst (Scheme 101).¹³⁸

4.3.3.18. Carbazole. Star-shaped molecules with 1,3,5-triazine core linked to three carbazole units *via* ethenyl linkage **376a–c** were synthesized in 35, 25 and 30% yields *via* Wittig–Horner coupling reaction between the appropriate carbazole-3-carbaldehydes **375** and 2,4,6-tris[4-(diethylphosphonomethyl) phenyl]-1,3,5-triazine **374** in the presence of *t*-BuOK (Scheme 102). The star-shaped molecules showed high optical properties, efficient fluorescence, AIE properties and also provide useful information for the further design of OLEDs and solar cell materials.¹³⁹

Symmetrical and asymmetrical star-shaped 2,4,6-tris(arylethynyl)-1,3,5-triazine **378a–c**, **380a,b**, **381a,b**, **282a,b**, **384a** and **385a–d** containing triphenylamine, fluorene, and/or carbazole moieties were synthesized in moderate yields (36–53%) *via* step-by-step Negishi reactions of 2,4,6-trichloro-1,3,5-

Scheme 107 Synthesis of tris-14*H*-dibenzo[a,j]xanthen-14-ylarenes **396** and **397**.



Scheme 108 Synthesis of SSM 401 containing triazine core and fluorine–carbazole arms.

triazine 293 with the appropriate arylethynylzinc chloride 377, 379 or 383 in the presence of $\text{Pd}(\text{PPh}_3)_4$ (Scheme 103).¹⁴⁰

4.3.3.19. 4H-Benzo[*h*]chromene. Tris(2-amino-4*H*-chromene) 388 has been developed using the reaction between tris(aldehyde) 339, malononitrile 386 and α -naphthol 387 in the presence of 3,3'-(pentane-1,5-diyl)bis(1,2-dimethyl-1*H*-imidazol-3-ium)bromide. The present methodology offers several advantages such as solvent-free conditions, excellent yields, simple procedure, mild conditions and reuse of the recovered ionic liquid (Scheme 104).¹⁴¹

4.3.3.20. 6*H*-Dibenzo[*c,e*][1,2]oxaphosphorinine 6-oxide. Tri(phosphaphenanthrenehydroxymethylphenoxy)-1,3,5-triazine 390 was synthesized in 76% yield by the reaction of 2,4,6-tris(*p*-formylphenoxy)-1,3,5-triazine 288 with 6*H*-dibenzo[*c,e*][1,2]oxaphosphorinine 6-oxide 389.^{142,143} Reaction of 390 with 4-chloroformylphthalic anhydride 391 in DMF in the presence of TEA afforded SSM with triazine core and (6-oxido-6*H*-dibenzo[*c,e*][1,2]oxaphosphorin-6-yl)methyl 1,3-dioxo-1,3-dihydroisobenzofuran-5-carboxylate side arm 392 in 78% yield (Scheme 105).⁶

Tris(3-(6-oxido-6*H*-dibenzo[*c,e*][1,2]oxaphosphorin-6-yl)pyrrolidine-2,5-dione) linked to 1,3,5-triazine core 394 was prepared in 81% yield by the reaction of tris(1*H*-pyrrole-2,5-dione) 393 with 6*H*-dibenzo[*c,e*][1,2]oxaphosphorin-6-oxide 389 in diglyme (Scheme 106).¹⁴⁴

4.3.3.21. 14*H*-Dibenzo[*a,j*]xanthen. Tris-14*H*-dibenzo[*a,j*]xanthen-14-ylarenes 396 and 397 were synthesized in 89% and 88% yields, respectively, by reacting 2-naphthol 395 with tris-aldehydes 288 and 339, respectively, under solvent free conditions using magnetite-sulfuric acid ($\text{Fe}_3\text{O}_4 \cdot \text{SO}_3\text{H}$) nanoparticles as a catalyst (Scheme 107).¹⁴⁵

4.3.3.22. Miscellaneous arms

4.3.3.22.1. Fluorene linked to carbazole, phenoxazine or phenothiazine. Omer *et al.*¹⁴⁶ reported the synthesis of C3-symmetrical SSM 401 in a two-step procedure. The reaction starts with trifluoromethanesulfonic acid-catalyzed trimerization of 7-bromo-9,9-diethylfluorene-2-carbonitrile 398 to form triazine derivative 399 in 81% yield, followed by C–N cross-coupling reaction with 9*H*-carbazole 400 to give 401 in

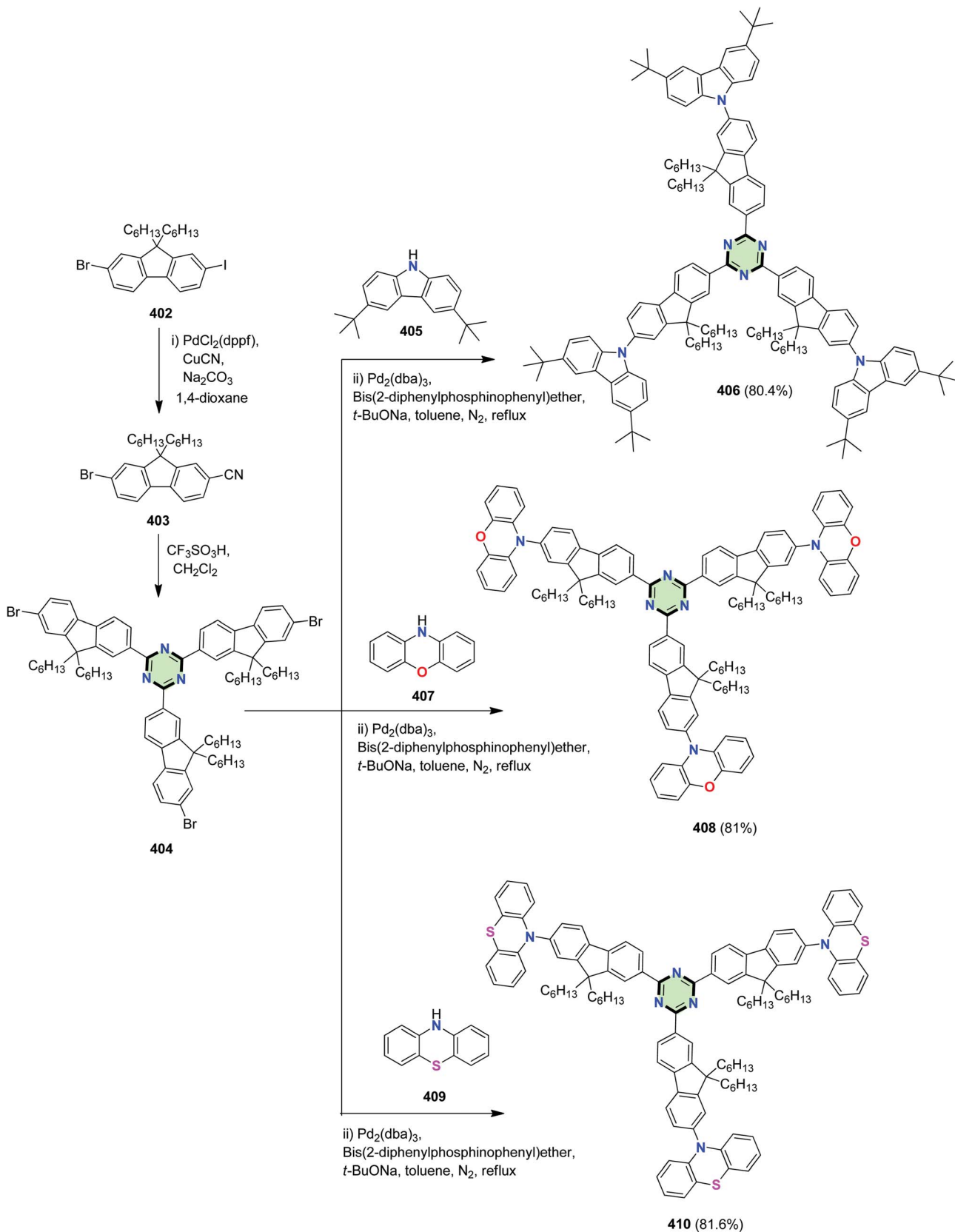
51% yield (Scheme 108). Compound 401 with electron-accepting triazine core bridged by fluorene linked to electron-donating carbazolyl groups showed a high fluorescent activity. The carbazole moiety undergoes dimerization during the electrochemical oxidation producing a polymer film on the electrode surface which exhibits electrochromic behavior.¹⁴⁶

By analogy, a series of 1,3,5-triazine derivatives peripherally decorated with fluorene ring linked to carbazole 406, phenoxazine 408 or phenothiazine 410 moieties were designed and synthesized by Liu *et al.*¹⁴⁷

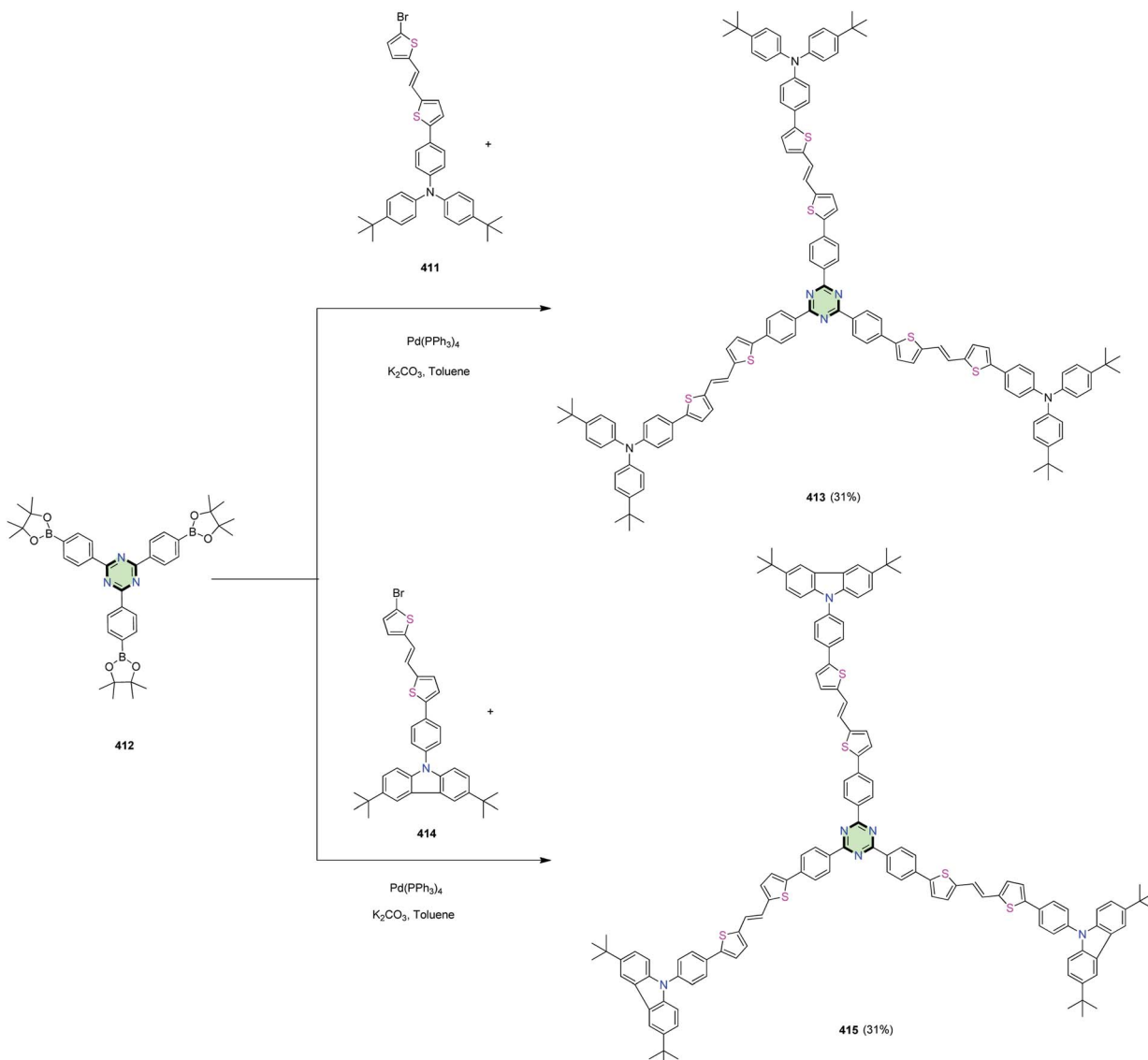
The reactions proceeded *via* initial cyanation of 2-bromo-9,9-dihexyl-7-iodo-9*H*-fluorene 402 upon treatment with CuCN in the presence of Pd catalyst to give 7-bromo-9,9-dihexyl-9*H*-fluorene-2-carbonitrile 403. Trifluoromethanesulfonic acid-catalyzed trimerization of 403 led to the formation of triazine derivative 404. Subsequent C–N cross-coupling reaction with the appropriate N-heterocyclic compounds 405, 407 and 409 yielding SSMs 406, 408 and 410, respectively, in good yields (Scheme 109).

The carbazolyl-, phenoxazinyl- and phenothiazinyl-groups were selected as electron-donating substituents, which would not only extend the π -conjugation, but also build the donor– π –acceptor (D– π –A) architectures in the target molecules. Fluorenyl units are commonly used as building blocks in two-photon absorption (TPA) molecules, on which alkyl chains were introduced to reduce the intermolecular aggregation and consequently improve the solubility. In addition, termination by the N-heterocyclic aromatic chromophores, which can rotate around the triazine–fluorene core, may cause aggregation-induced emission (AIE) feature based on the mechanism of restriction of intramolecular rotation (RIR). These compounds exhibit intense fluorescence, AIE and TPA features.

4.3.3.22.2. Di(thiophen-2-yl)ethene linked to triphenylamine or carbazole. 1,3,5-Triazine centered star-shaped molecules with thiénylvinylene arms 413 and 415 connected to structurally similar triphenylamine or carbazole end group were



Scheme 109 Synthesis of SSMs with 1,3,5-triazine core with fluorene ring linked to carbazole **406**, phenoxazine **408** and phenothiazine **410**.



Scheme 110 Synthesis of SSMs with thienylvinylene arms connected to triphenylamine **413** or carbazole **415**.

synthesized by Huang *et al.*¹⁴⁸ via Suzuki coupling reaction of 2,4,6-tris-boronic acid ester **412** with the appropriate bromo compounds **411** and **414**, respectively, in the presence of $\text{Pd}(\text{PPh}_3)_4$ (Scheme 110).¹⁴⁸

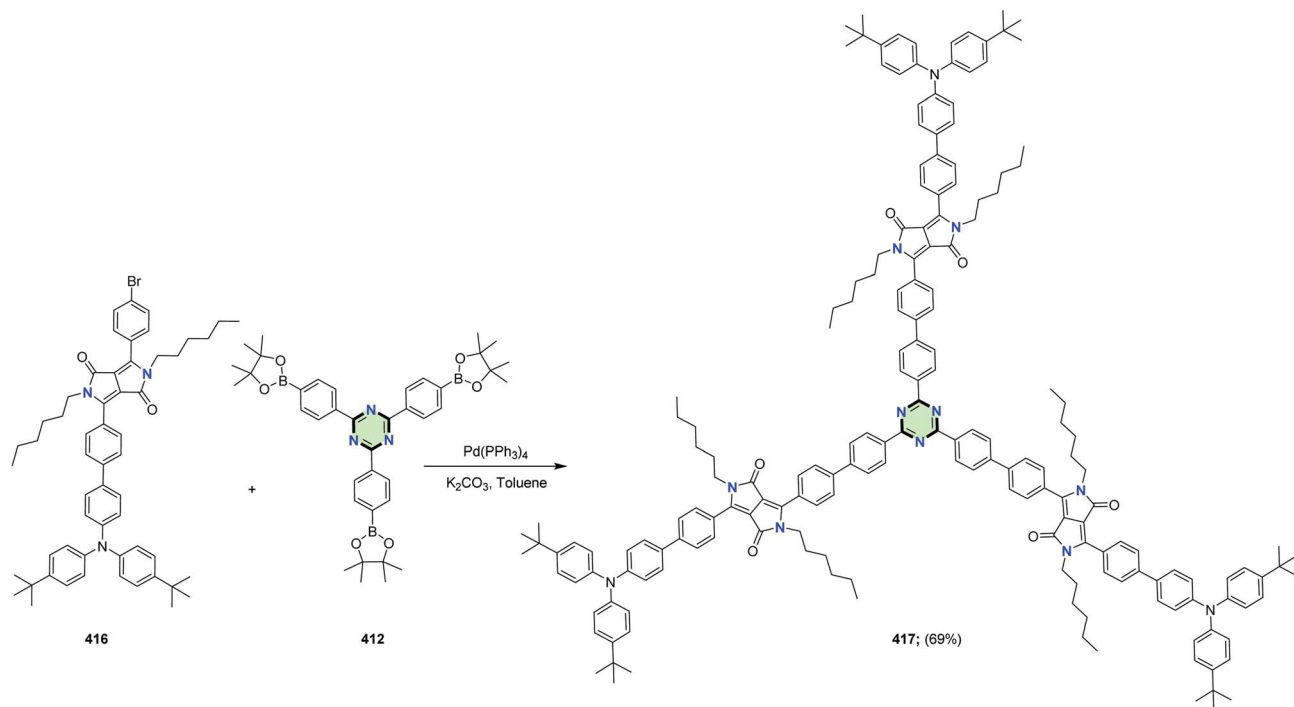
4.3.3.22.3. Diketopyrrolo[3,4-*c*]pyrrole linked to triphenylamine, thiophene and/or carbazole. Shiau *et al.*¹⁴⁹ reported the synthesis of a series of star-shaped molecules with triazine-core **417**, **419** and **421** in 69, 70 and 68% yields, as a donor materials for organic solar cells, through Suzuki coupling reaction of tris(4-(4,4,5,5-tetramethyl-1,3,2-dioxaborolan-2-yl)phenyl)-1,3,5-triazine **412** with the appropriate bromo derivatives **416**, **418** and **420**, respectively, in the presence of $\text{Pd}(\text{PPh}_3)_4$ in refluxing toluene (Schemes 111–113).

4.3.4. Miscellaneous heterocyclic-cored SSMs with different arms

4.3.4.1. Thieno[3,2-*b*]thiophene. Magnan *et al.*¹¹³ reported the synthesis of star shaped molecules **424** and **427** in 63 and

62% yields, respectively, by fourfold Negishi coupling between tetrabromothieno[3,2-*b*]thiophene **422** with each of 2-hexylthiophene **423** and 2-hexylthieno[3,2-*b*]thiophene **426**. Subsequent oxidative cyclodehydrogenation of the latter compounds using anhydrous ferric chloride gave tetra(5-hexylthieno)benzothieno[3,2-*b*]benzothiophene **425** and tetra(5-hexylthieno[3,2-*b*]thieno)benzo thieno[3,2-*b*]benzothiophene **428** in 30 and 53% yield, respectively (Scheme 114).

4.3.4.2. Benzo[1,2-*b*:4,5-*b'*]dithiophene. Sheng *et al.*¹⁵⁰ reported the synthesis of a star shaped molecule with benzo[1,2-*b*:4,5-*b'*]dithiophene core and terthiophene side arm **431** in good yield, by Stille coupling reaction between tributyl(5,5'-didodecyl-[2,2':3',2"-terthiophen]-5'-yl)stannane **430** with the dibromo compound **429** in the presence of $\text{Pd}(\text{PPh}_3)_4$ (Scheme 115). Compound **431** showed high thermal stability with decomposition temperature (447 °C), low-lying HOMO level

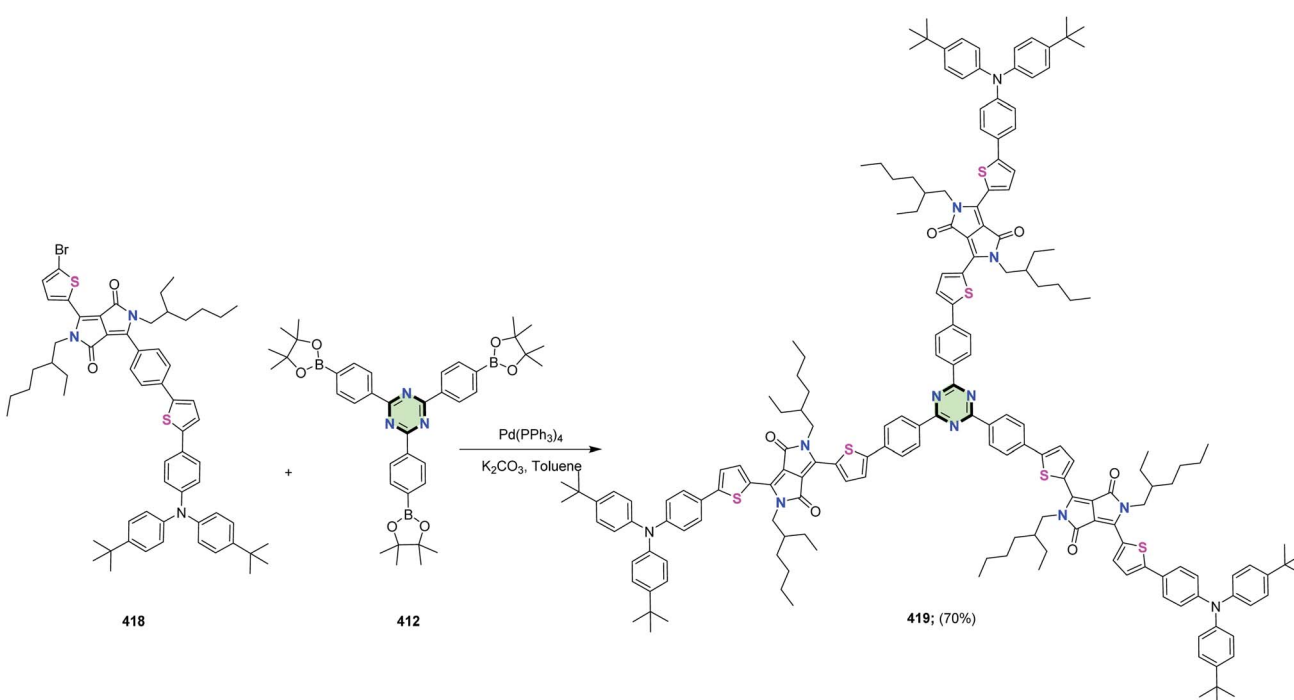


Scheme 111 Synthesis of SSM with triazine-core linked to diketopyrrolo[3,4-c]pyrrole and triphenylamine 417.

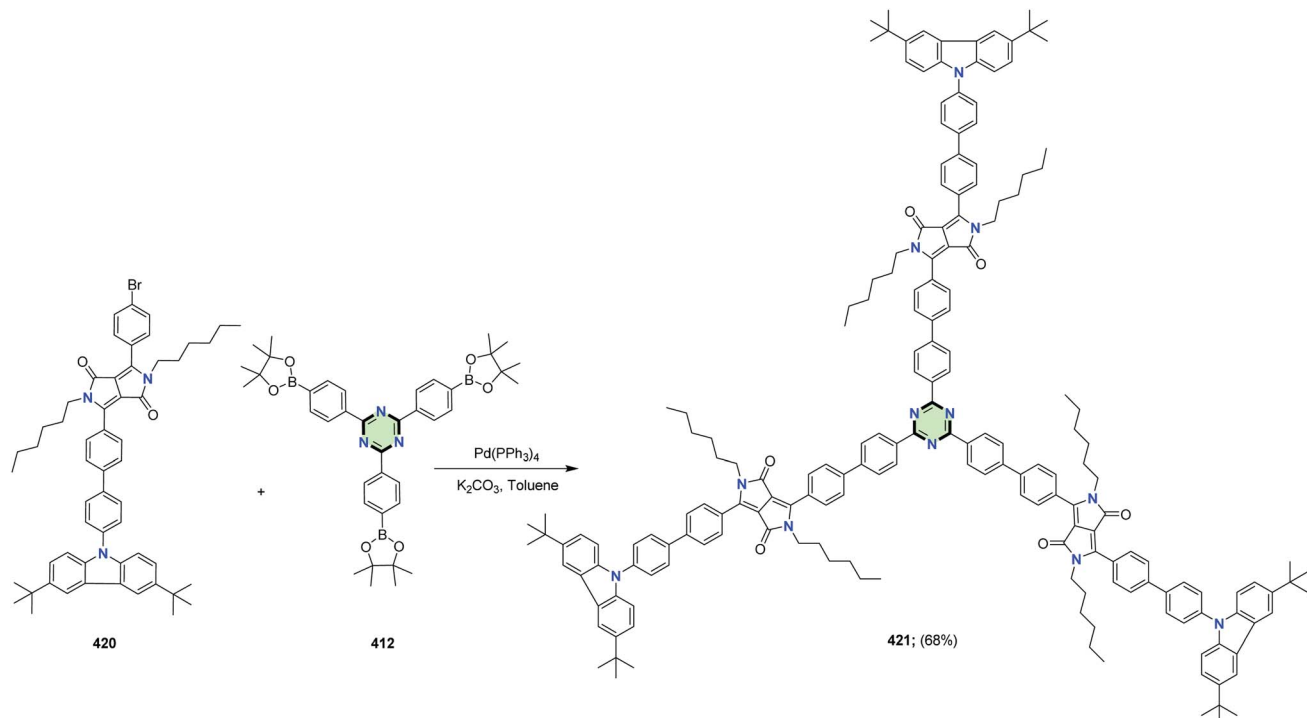
(-5.52 eV), and wide UV-vis absorption between 300 and 530 nm ($E_g = 2.36$ eV).

4.3.4.3. Benzo[1,2-*b*:4,5-*b*']difuran. The Suzuki cross-coupling reaction of 2,3,6-tris(4-bromophenyl)-4,8-didecyl-7-

phenylbenzo[1,2-*b*:4,5-*b*']difuran 432 with 1,3,6,2-dioxazaborocane-4,8-diones 433 afforded different SSMs with benzo[1,2-*b*:4,5-*b*']difuran core 434a-c in 37-99% yields (Scheme 116).¹⁵¹



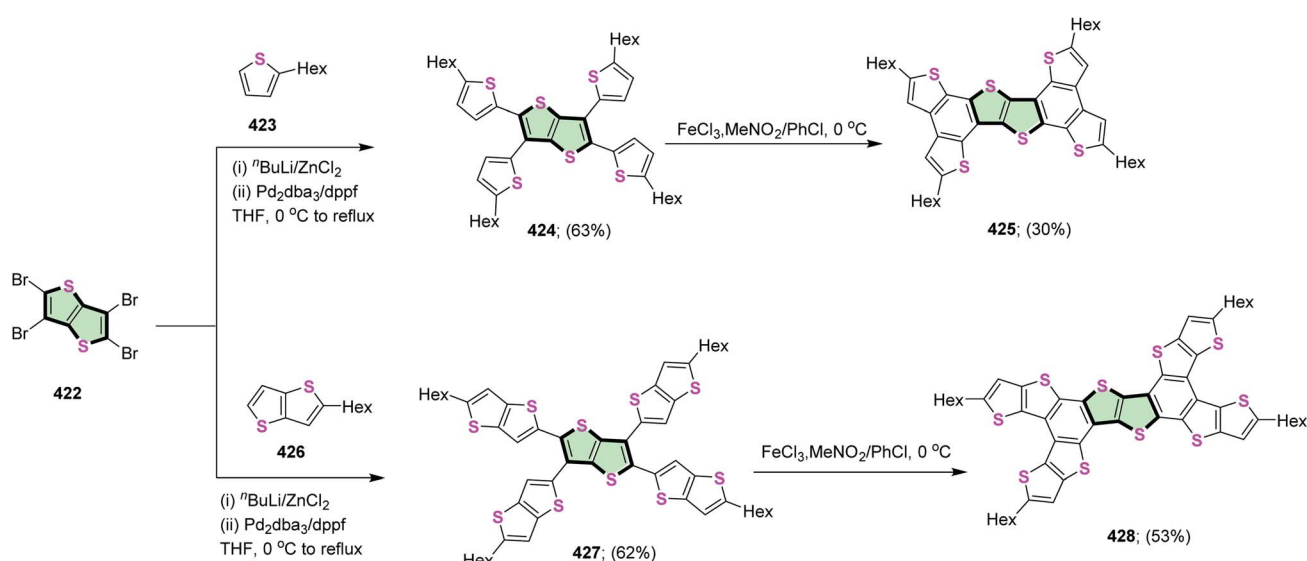
Scheme 112 Synthesis of SSM with triazine-core linked to diketopyrrolo[3,4-c]pyrrole and thiophene 419.

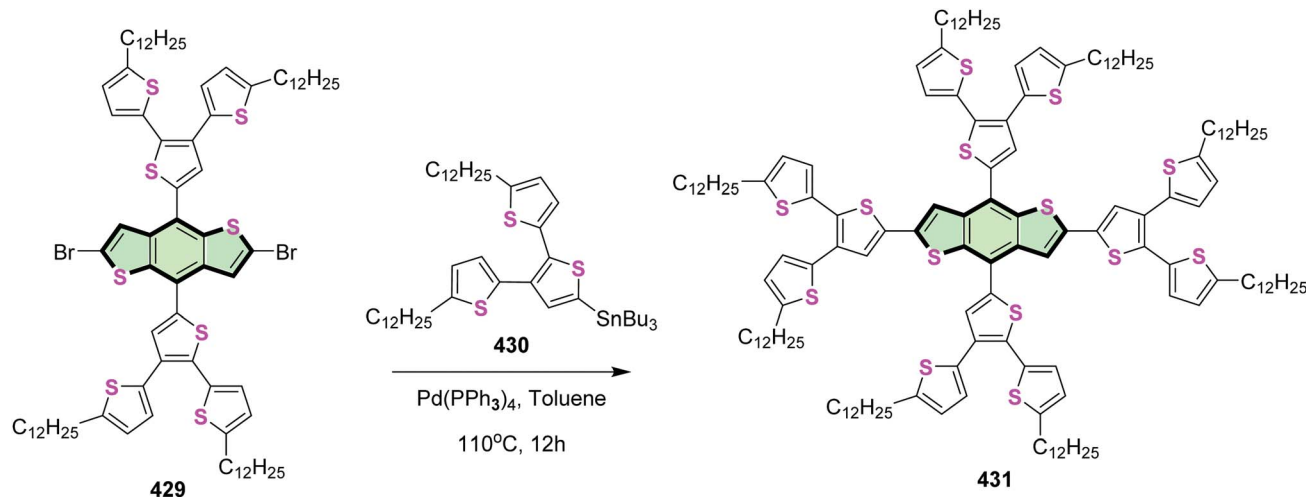


Scheme 113 Synthesis of SSM with triazine-core linked to diketopyrrolo[3,4-c]pyrrole and carbazole 421.

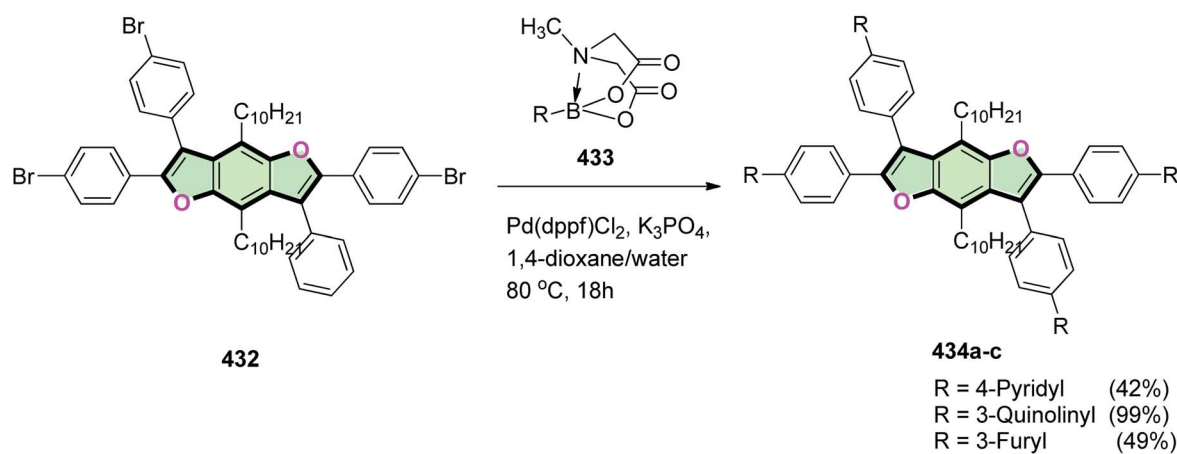
4.3.4.4. 9H-Carbazole. Tribromo compound 436 was obtained *via* the bromination of 9-(4-bromophenyl)-9H-carbazole 435 with *n*-bromosuccinimide. Lithiation of 436 followed by treatment with fluorodimesitylborane yielded SSM with carbazole core 437 (Scheme 117). The latter compound showed excellent thermal stability ($T_d = 234$ °C), electrochemical stability and high Φ (0.95) as well as high triplet energy (2.83 eV).¹⁵²

4.3.4.5. Naphthothiophene. Tan *et al.*¹⁵³ reported the synthesis of two molecules 440 and 442 having 4,9-di(thiophen-2-yl)naphtho[2,3-*b*]thiophene core and diketopyrrolopyrrole arms 440 and 442 in 62% and 73% yields, respectively. The formation of the latter compounds proceeded through Stille coupling reaction of (5,5'-(6,7-dimethoxy-2-(trimethylstannyl)naphtha[2,3-*b*]thiophene-4,9-diy)bis(thiophene-5,2-diyl))bis(trimethylstannane) 438 with each

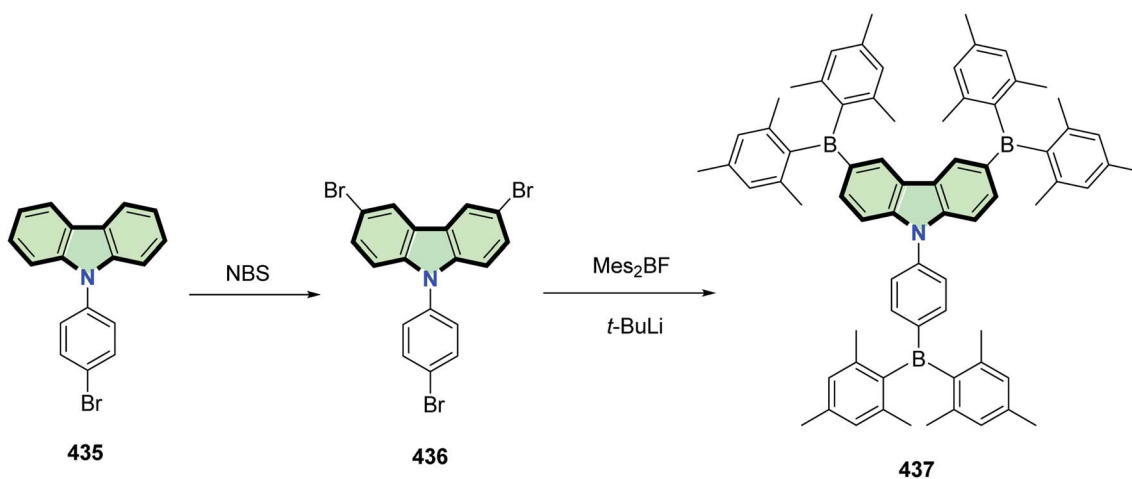
Scheme 114 Synthesis of SSMs 425 and 428 with thieno[3,2-*b*]thiophene core and their oxidized derivatives 425 and 428.



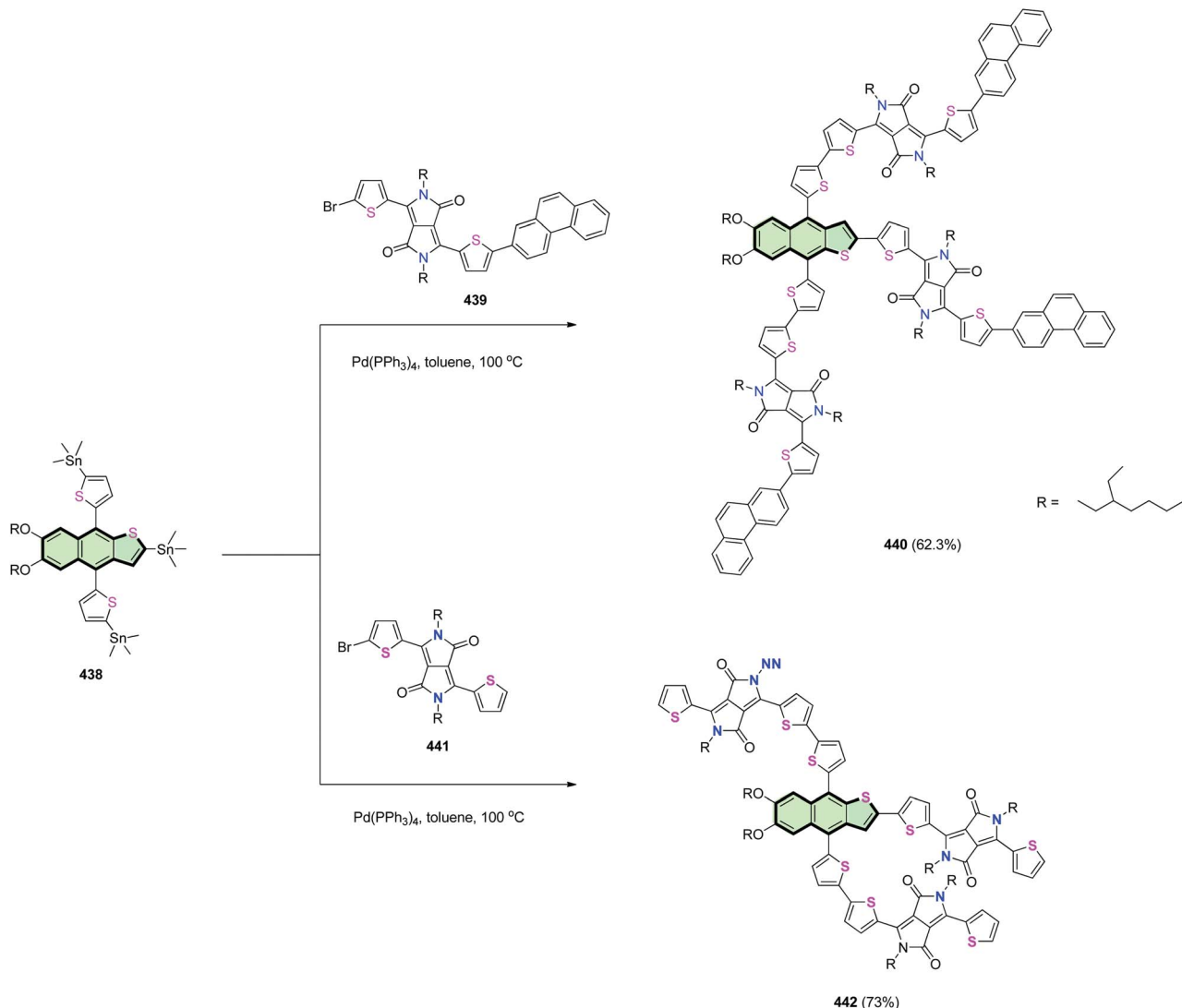
Scheme 115 Synthesis of SSMs with benzo[1,2-b:4,5-b']dithiophene core 431.



Scheme 116 Synthesis of SSMs with benzo[1,2-b:4,5-b']difuran core 434a-c.



Scheme 117 Synthesis of SSM with carbazole core 437.



Scheme 118 Synthesis of SSMs with naphtho[2,3-b]thiophene core 440 and 442.

of 3-(5-bromothiophen-2-yl)-6-(5-(phenanthren-2-yl)thiophen-2-yl)pyrrolo[3,4-c]pyrrole-1,4(2H,5H)-dione **439** and 3-(5-bromothiophen-2-yl)-2,5-dimethyl-6-(thiophen-2-yl)pyrrolo[3,4-c]pyrrole-1,4(2H,5H)-dione **441**, respectively (Scheme 118).¹⁵³

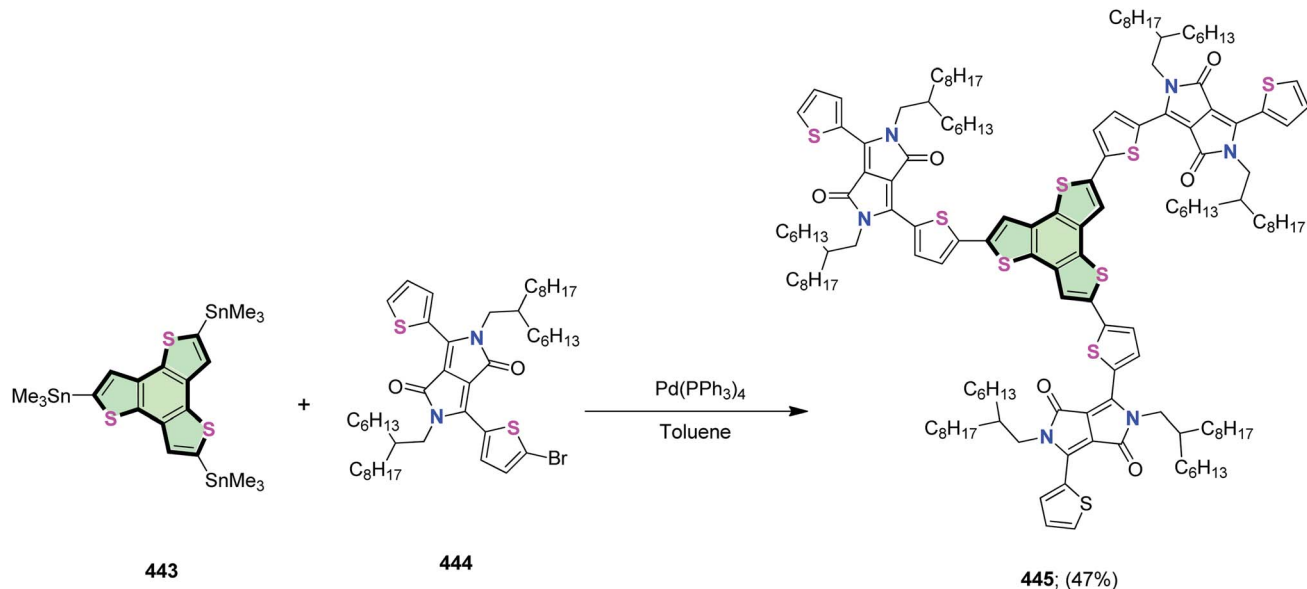
4.3.4.6. Benzo[1,2-b:3,4-b':4,6-b'']trithiophene. Star-shaped molecule with benzotri thiophene core and diketopyrrolo[3,4-c]pyrrole unit arms **445** was synthesized in 47% yield *via* Stille coupling of 2,5,8-tris(trimethylstannyl)benzo[1,2-b:3,4-b':5,6-b'']trithiophene **443** with bromo(thiophen-2-yl)pyrrolo[3,4-c]pyrrole derivative **444** in the presence of $\text{Pd}(\text{PPh}_3)_4$ (Scheme 119).^{20,154}

Similarly, Stille coupling of **443** with bromo derivatives **446a-c** afforded SSMs with benzotri thiophene core and (oligo)thiophene-benzo[c][1,2,5]thiadiazole-thiophene side arms **447a-c** in good yields (44–70%) (Scheme 120). The star-shaped molecule **447c** with enlarged π -can be delocalization used in photovoltaic applications as increasing the number

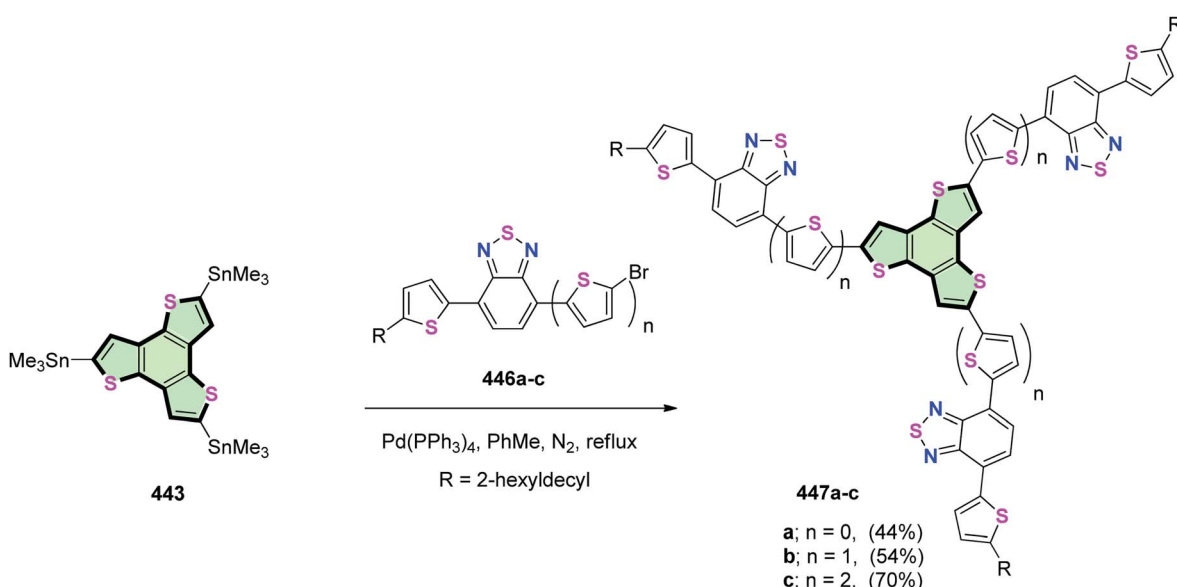
of thiophene connecting units elevates the HOMO energy level of the based molecule.¹⁵⁵

4.3.4.7. Benzo[9,1]quinolizino[3,4,5,6,7-defg]acridine. Paek *et al.*¹⁵⁶ managed to synthesize SSM **450** with benzo[9,1]quinolizino[3,4,5,6,7-defg]acridine core and trithiophene as a side arm *via* Suzuki coupling of the trithiophene boronic acid **448** with tribromo compound **449** in the presence of $\text{Pd}(\text{PPh}_3)_4$ (Scheme 121). Compound **450** with π -conjugated bridge undergoes photovoltaic performances in solution-processed organic solar cells OSCs.

Lim *et al.*¹⁵⁷ reported the synthesis of SSM **453** which contain benzo[9,1]quinolizino[3,4,5,6,7-defg]acridine core and 4-(silylene-2,2'-bithiophen-5-yl)-7-(2,2',2''-terthiophen-5-yl)-[1,2,5]thiadiazolo[3,4-c]pyridine as a side arm *via* Stille coupling reaction of bromo compound **451** with 4,4,8,8,12,12-hexamethyl-2,6,10-tris(trimethylstannyl)-8,12-dihydro-4H-benzo[1,9]quinolizino[3,4,5,6,7-defg]acridine **452** (Scheme 122). This star-shaped molecule has optical and



Scheme 119 Synthesis of SSM with benzotri thiophene core 445.



Scheme 120 Synthesis of SSMs with benzotri thiophene core 447.

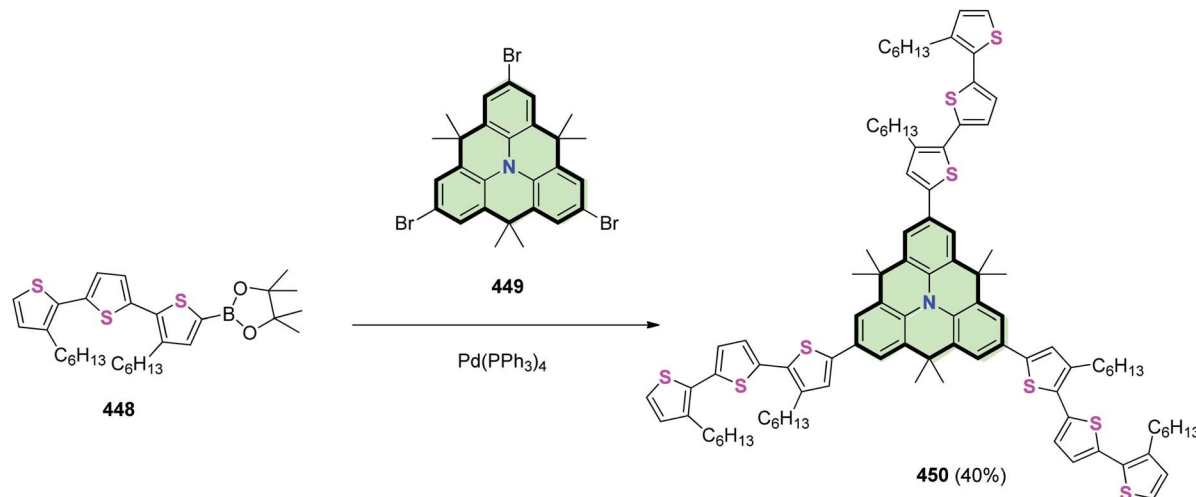
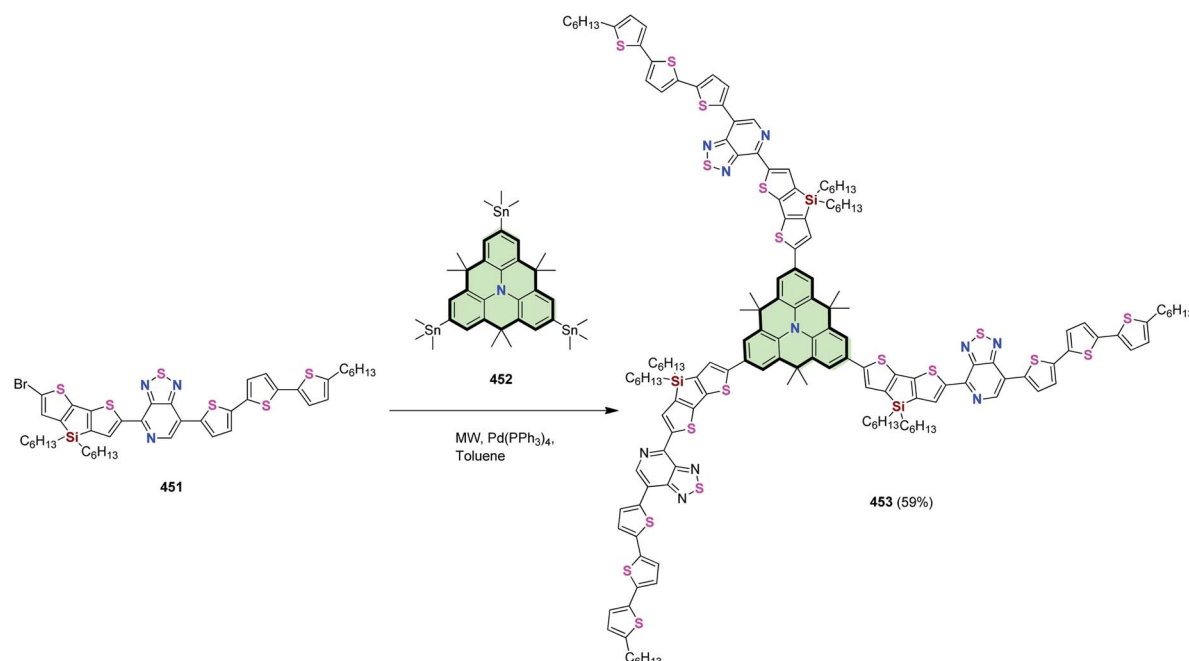
electrochemical properties and can be used as donor components in solution-processed organic solar cells.

4.3.4.8. Diindolo[3,2-*a*:3',2'-*c*]carbazole. SSMs 456 and 458 with diindolo[3,2-*a*:3',2'-*c*]carbazole core were synthesized in 85% and 84% yields by Shao *et al.*¹⁵⁸ *via* the Horner-Wadsworth-Emmons reaction of the trialdehyde 454 with phosphonate esters 455 and 457, respectively (Scheme 123).

2,2',2''-((5,5',5''-((5,10,15-Tridodecyl-10,15-dihydro-5H-diindolo[3,2-*a*:3',2'-*c*]carbazole-3,8,13-triyl)tris(ethene-2,1-diyl))tris(thiophene-5,2-diyl))tris(ethene-2,1-diyl))tris(benzo[*d*]thiazole) 462 was synthesized in 82% yield by Shao *et al.*¹⁵⁸ *via* the Horner-

Wadsworth-Emmons reaction of the tris(thiophene-2-carbaldehyde) 460 with diethyl (benzo[*d*]thiazol-2-ylmethyl) phosphonate 461. The trialdehyde 460 was obtained in 93% yield by formylation of tris-(2-(thiophen-2-yl)vinyl)-10,15-dihydro-5H-diindolo[3,2-*a*:3',2'-*c*]carbazole 459 upon treatment with POCl₃ in DMF (Scheme 124). Compound 462 showed good thermal and photo stabilities. It can be used as chromophore with significant bathochromic shift of the emission spectra together with a larger Stokes shift in polar solvents due to intramolecular charge transfer.

Lu *et al.*¹⁵⁹ reported the synthesis of triindole-cored star-shaped molecules 465 in 70% yield by heating a mixture of

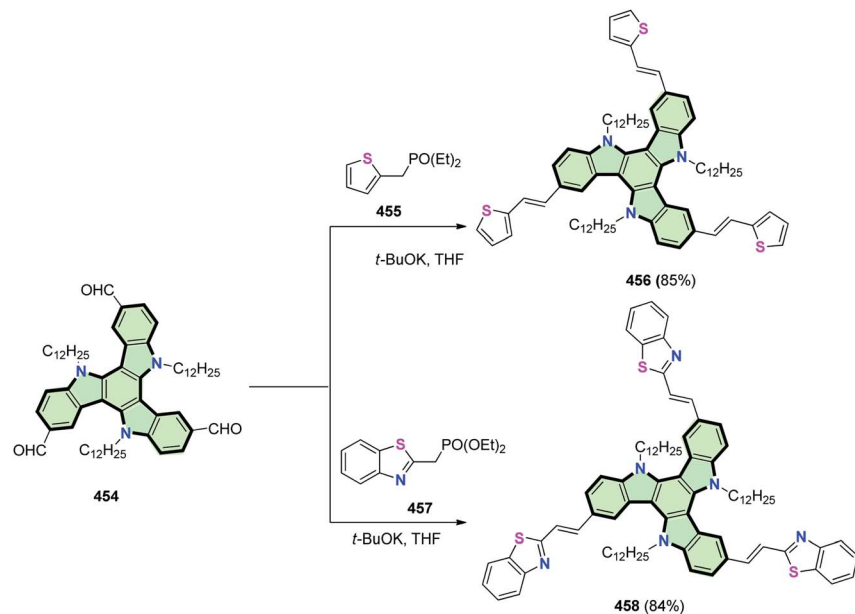
Scheme 121 Synthesis of SSM 450 with benzo[9,1]quinolizino[3,4,5,6,7-*defg*]acridine core.Scheme 122 Synthesis of SSM 453 with benzo[9,1]quinolizino[3,4,5,6,7-*defg*]acridine core.

5,10,15-trihexyltriindole-2,7,12-triboronic ester **463** and 5-(5-bromothiophen-2-yl)thiophene-2-carbaldehyde **464** in the presence of K₂CO₃ and Pd(PPh₃). On the other hand, heating compound **463** with 4-(5-(4-(5-bromothiophen-2-yl)benzo[c][1,2,5]thiadiazol-7-yl)-thiophen-2-yl)-N,N-diphenylbenzylamine **466** in the presence of Bu₄NBr and Pd(PPh₃)₄ at reflux afforded triindole-cored star-shaped compound **467** in 75% yield. The two star-shaped molecules **465** and **467** showed good thermal stability, intensive absorption in a broad region, relatively high hole mobility and high efficiency as organic solar cells (Scheme 125).

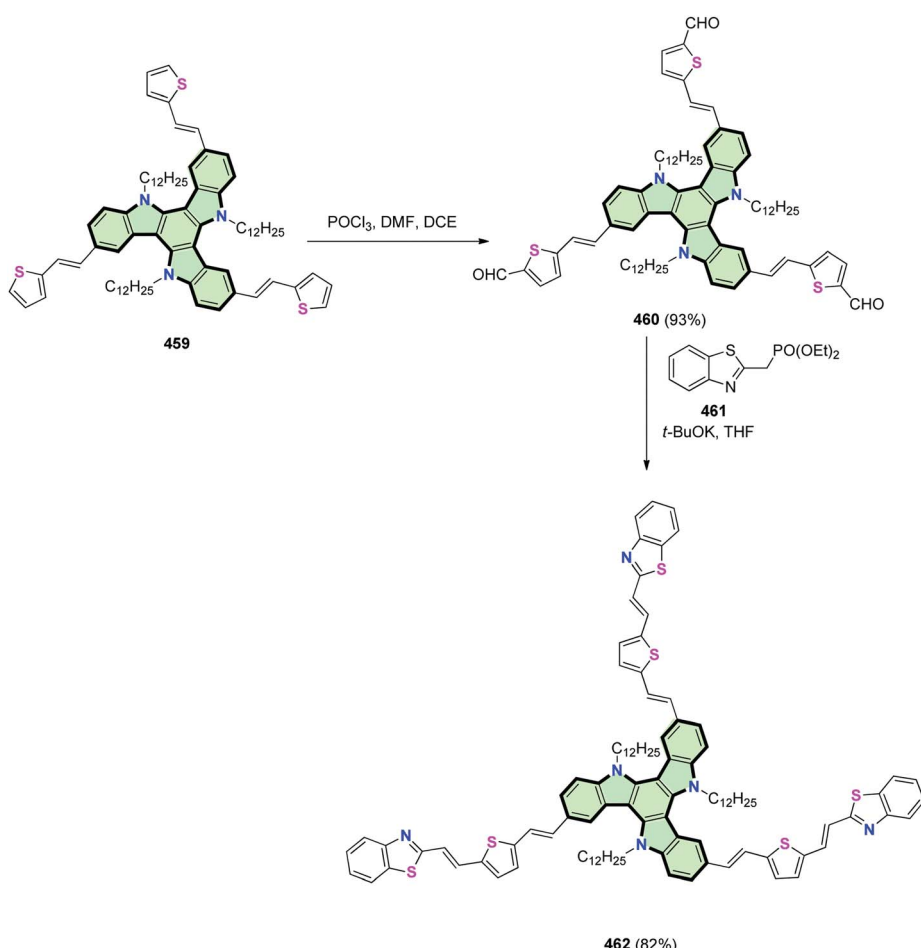
4.3.4.9. Anthra[1,2-*b*:4,3-*b*':5,6-*b*":8,7-*b*"]tetrathiophene.

Komiyama *et al.*¹⁶⁰ reported the synthesis of a star shaped molecule **470** in 44% yield by the reaction of 2,5,9,12-tetrabromoanthra[1,2-*b*:4,3-*b*':5,6-*b*":8,7-*b*"]tetrathiophene **468** with stannyli(thiophen-2-yl)pyrrolo[3,4-*c*]pyrrole derivative **469** in dry DMF and in the presence of Pd(PPh₃)₄ (Scheme 126).

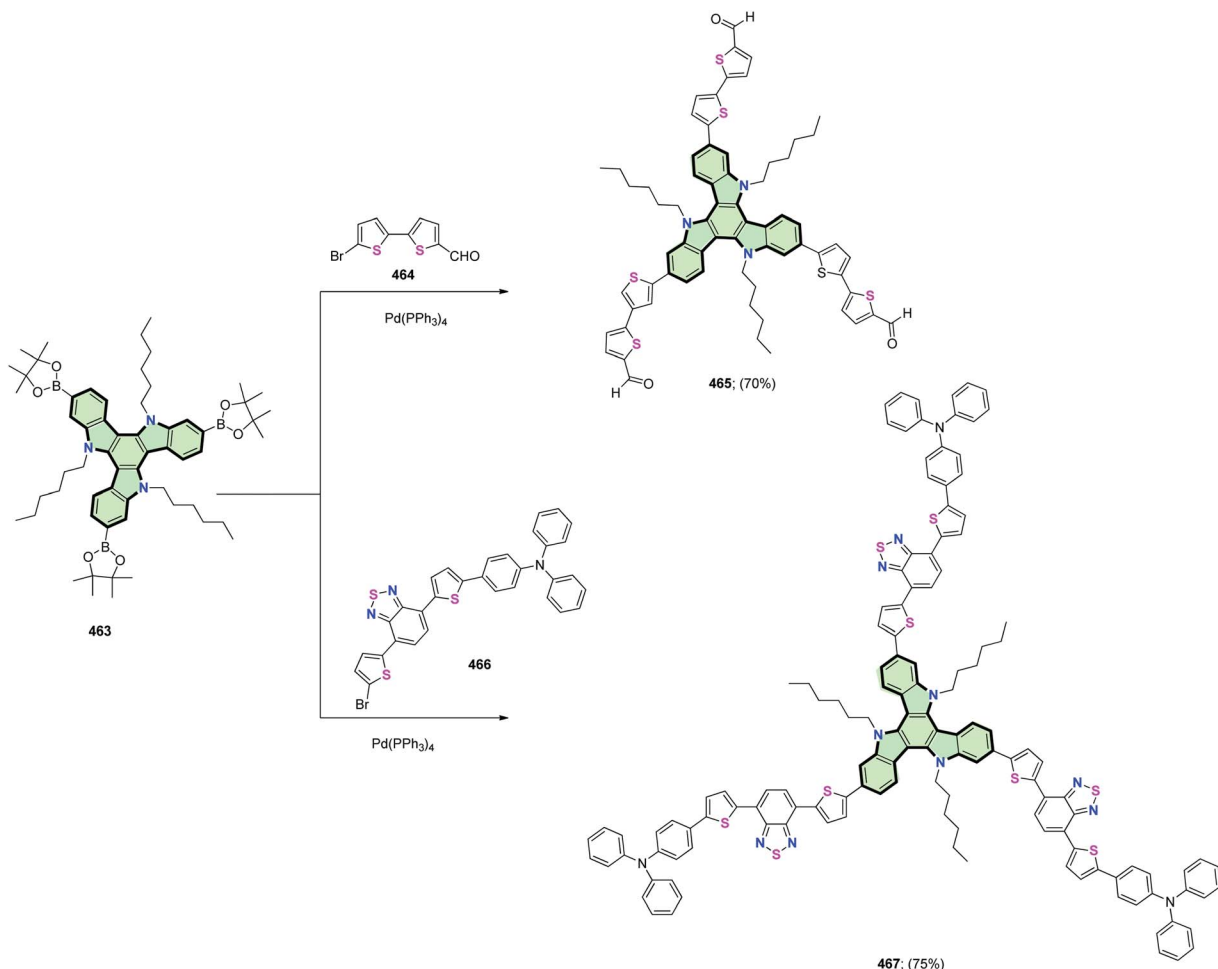
4.3.4.10. Diquinoxalino[2,3-*a*:2',3'-*c*]phenazine. Zhao *et al.*¹⁶¹ reported the synthesis of SSM **473** containing hexaazatriphenylene cored fused with perylene-3,4,9,10-tetracarboxylic acid bisimides, as conjugated n-type semi-



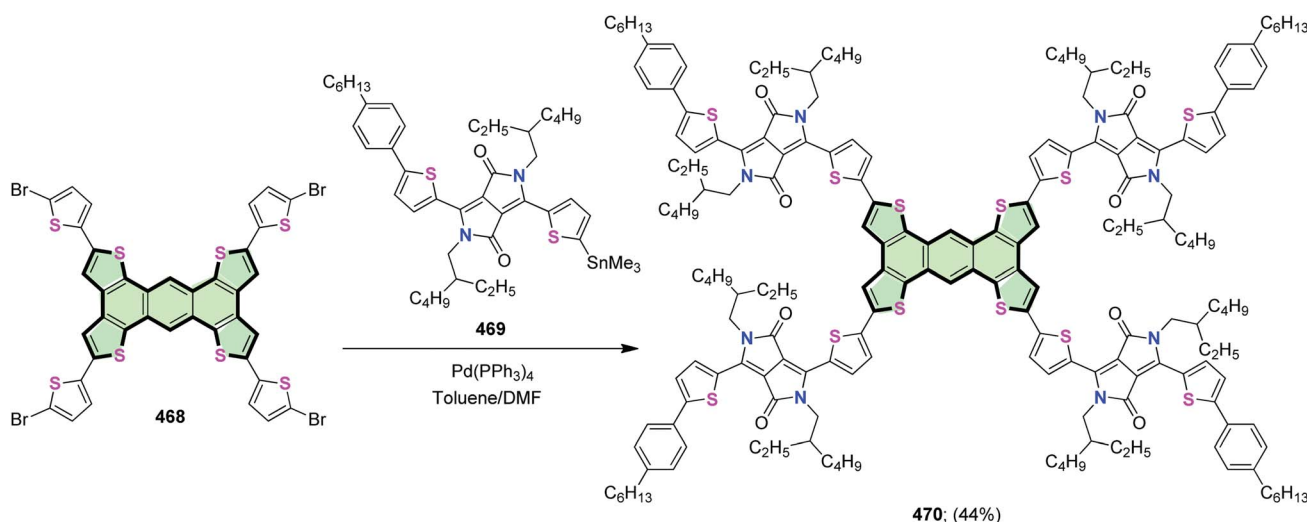
Scheme 123 Synthesis of SSMs 456 and 458 with diindolo[3,2-a:3',2'-c]carbazole core.



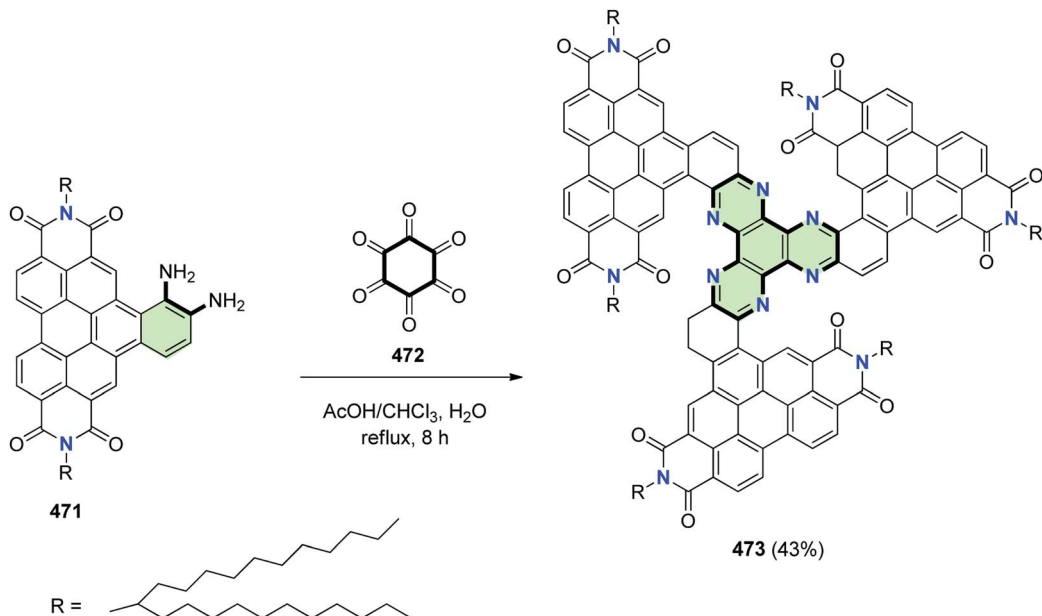
Scheme 124 Synthesis of SSM 462 with diindolo[3,2-a:3',2'-c]carbazole core.



Scheme 125 Synthesis of triindole-cored star-shaped molecules 465 and 467.



Scheme 126 Synthesis of SSM 470 with anthra[1,2-b:4,3-b':5,6-b'':8,7-b'']tetrathiophene core.



Scheme 127 Synthesis of SSM 473 with hexaazatriphenylene core.

conductor in 43% yield by fusion of 9,10-diaminonaphtho[1,2,3,4-*ghi*]perylene **471** with cyclohexane-1,2,3,4,5,6-hexaone **472** (Scheme 127).

5. Conclusions

This review gives an overview of the new developments over the last decades in the synthesis of star-shaped molecules especially those containing heterocyclic core and/or heterocyclic arms. The physical properties of these compounds are markedly different to their linear analogues. These molecules are considered as versatile building blocks for the formation of liquid crystals, dendrimers as well supramolecular host-guest compounds. Their applications in organic solar cells OSCs and as promising candidates for organic semiconducting materials are recently studied. The star-shaped molecules mentioned in this review are arranged in an organized manner with respect to the type of the core as well as the side arms.

The methods described for the synthesis of such compounds includes a variety of synthetic methodologies, among which the *O*-, *S*- and *N*-alkylation, condensation and cyclocondensation, cyclo-trimerization reactions, and palladium-catalyzed C-C and C-N bond formation *via* Heck, Negishi, Sonogashira, Stille and Suzuki cross-coupling reactions seem to be the most interesting strategies.

From a synthetic chemist's perspective, it is extremely challenging to develop new strategies to synthesize novel structures of these molecules.

We hope that this review will be useful not only for organic synthetic chemists, but also for Physicists as well as for those who are interested in the field of industrial applications.

Conflicts of interest

There are no conflicts to declare.

Notes and references

- 1 J. R. Schaeffgen and P. J. Flory, *J. Am. Chem. Soc.*, 1948, **70**, 2709–2718.
- 2 M. Morton, T. E. Helminiak, S. D. Gadkary and F. Bueche, *J. Polym. Sci.*, 1962, **57**, 471–482.
- 3 B. Walker, C. Kim and T.-Q. Nguyen, *Chem. Mater.*, 2011, **23**, 470–482.
- 4 J. Roncali, *Acc. Chem. Res.*, 2009, **42**, 1719–1730.
- 5 Y. Lin, Y. Li and X. Zhan, *Chem. Soc. Rev.*, 2012, **41**, 4245.
- 6 H. Muraoka, M. Mori and S. Ogawa, *Phosphorus, Sulfur and Silicon Relat. Elem.*, 2015, **190**, 1382–1391.
- 7 J. Cremer and C. A. Briehn, *Chem. Mater.*, 2007, **19**, 4155–4165.
- 8 Z. Luo, W. Xiong, T. Liu, W. Cheng, K. Wu, Y. Sun and C. Yang, *Org. Electron.*, 2016, **41**, 1–7.
- 9 J. X. Qiu, Y. X. Li, J. L. Miao, Z. W. Zhang and Z. H. Chen, *Synth. Met.*, 2015, **199**, 353–359.
- 10 X. Cheng, J. Zhao, C. Cui, Y. Fu and X. Zhang, *J. Electroanal. Chem.*, 2012, **677–680**, 24–30.
- 11 W. Li, Q. Li, C. Duan, S. Liu, L. Ying, F. Huang and Y. Cao, *Dyes Pigm.*, 2015, **113**, 1–7.
- 12 R. Misra, R. Maragani, C. P. Singh and R. Chari, *Dyes Pigm.*, 2016, **126**, 110–117.
- 13 K. Karon, M. Lapkowski, A. Dabuliene, A. Tomkeviciene, N. Kostiv and J. V. Grazulevicius, *Electrochim. Acta*, 2015, **154**, 119–127.
- 14 Z. Hao, Y. Liu, Y. Huang, F. Meng, Y. Wang, H. Tan, S. Su and W. Zhu, *J. Organomet. Chem.*, 2017, **835**, 52–59.
- 15 W. Li, L. Chen, Y. Pan, S. Yan, Y. Dai, J. Liu, Y. Yu, X. Qu, Q. Song, M. Ouyang and C. Zhang, *J. Electrochem. Soc.*, 2017, **164**, 84–89.
- 16 A. Irfan, S. Muhammad, A. R. Chaudhry, A. G. Al-Sehemi and R. Jin, *Optik*, 2017, **149**, 321–331.

17 Y. N. Luponosov, J. Min, A. N. Solodukhin, O. V. Kozlov, M. A. Obrezkova, S. M. Peregudova, T. Ameri, S. N. Chvalun, M. S. Pshenichnikov, C. J. Brabec and S. A. Ponomarenko, *Org. Electron.*, 2016, **32**, 157–168.

18 F. A. Olate, M. L. Parra, J. M. Vergara, J. Barberá and M. Dahrouch, *Liq. Cryst.*, 2017, **44**, 1173–1184.

19 S. K. Pathak, S. Nath, J. De, S. K. Pal and A. S. Achalkumar, *New J. Chem.*, 2017, **41**, 4680–4688.

20 X. Wu, Z. Zhang, H. Hang, Y. Chen, Y. Xu, H. Tong and L. Wang, *Macromol. Rapid Commun.*, 2017, **38**, 1–8.

21 N. V. Usol, O. B. Akopova, A. I. Smirnova, I. Maria, N. V. Bumbina, N. V. Zharnikova, N. V. Usol, O. B. Akopova, A. I. Smirnova, I. Maria, N. V. Bumbina and N. V. Zharnikova, *Phase Transitions*, 2017, **90**, 800–807.

22 R. Sharma, R. Maragani and R. Misra, *New J. Chem.*, 2018, **42**, 882–890.

23 A. Rananaware, R. S. Bhosale, K. Ohkubo, H. Patil, L. A. Jones, S. L. Jackson, S. Fukuzumi, S. V. Bhosale and S. V. Bhosale, *J. Org. Chem.*, 2015, **80**, 3832–3840.

24 A. L. Kanibolotsky, I. F. Perepichka and P. J. Skabara, *Chem. Soc. Rev.*, 2010, **39**, 2695–2728.

25 S. K. Pathak, B. Pradhan, R. K. Gupta, M. Gupta, S. K. Pal and A. S. Achalkumar, *J. Mater. Chem. C*, 2016, **4**, 6546–6561.

26 A. S. Achalkumar, U. S. Hiremath, D. S. S. Rao, S. K. Prasad and C. V. Yelamaggad, *J. Org. Chem.*, 2013, **78**, 527–544.

27 E. Westphal, M. Prehm, I. H. Bechtold, C. Tschierske and H. Gallardo, *J. Mater. Chem. C*, 2013, **1**, 8011–8022.

28 P. J. Stackhouse, A. Wilson, D. Lacey and M. Hird, *Liq. Cryst.*, 2010, **37**, 1191–1203.

29 P. V. Dmitryakov, M. A. Shcherbina, S. M. Peregudova, G. V. Cherkaev, S. N. Chvalun, J. Brabec and S. A. Ponomarenko, *J. Mater. Chem. C*, 2016, **4**, 7061–7076.

30 S. K. Pathak, S. Nath and J. De, *New J. Chem.*, 2017, **41**, 9908–9917.

31 S. K. Pathak, R. K. Gupta, S. Nath, D. S. S. Rao, S. K. Prasad and A. S. Achalkumar, *J. Mater. Chem. C*, 2015, **3**, 2940–2952.

32 D. Astruc, E. Boisselier and C. Ornelas, *Chem. Rev.*, 2010, **110**, 1857–1959.

33 P. Rajakumar and S. Raja, *Tetrahedron Lett.*, 2008, **49**, 6539–6542.

34 D. L. Reger, R. F. Semeniuc and M. D. Smith, *Inorg. Chem.*, 2003, **42**, 8137–8139.

35 W. Zhang and Y. Jin, *Dynamic covalent chemistry: principles, reactions, and applications*, John Wiley & Sons, New York City, USA, 2017.

36 M. Grillaud and A. Bianco, *J. Pept. Sci.*, 2015, **21**, 330–345.

37 S. Roquet, A. Cravino, P. Leriche, O. Ale, P. Fre, J. Roncali, B. La and V. F. Angers, *J. Am. Chem. Soc.*, 2006, **128**, 3459–3466.

38 C. He, Q. He, Y. Yi, G. Wu, F. Bai, Z. Shuai and Y. Li, *J. Mater. Chem.*, 2008, **18**, 4085–4090.

39 K. Rundel, S. Maniam, K. Deshmukh, E. Gann and C. R. McNeill, *J. Mater. Chem. A*, 2017, **5**, 12266–12277.

40 C. Lu, I. T. Choi, J. Kim and H. K. Kim, *J. Mater. Chem. A*, 2017, **5**, 20263–20276.

41 T. Aytun, P. J. Santos, C. J. Bruns, D. Huang, A. R. Koltonow, M. Olvera De La Cruz and S. I. Stupp, *J. Phys. Chem. C*, 2016, **120**, 3602–3611.

42 K. Lin, B. Xie, Z. Wang, R. Xie, Y. Huang and C. Duan, *Org. Electron.*, 2018, **52**, 42–50.

43 V. A. Online, L. Chen and Y. Xiao, *RSC Adv.*, 2015, **5**, 32283–32289.

44 Y. Zhou, W. Chen, Z. Du, D. Zhu, D. Ouyang, L. Han and R. Yang, *Sci. China: Chem.*, 2015, **58**, 357–363.

45 Y. C. Chao, C. H. Chuang, H. L. Hsu, H. J. Wang, Y. C. Hsu, C. P. Chen and R. J. Jeng, *Sol. Energy Mater. Sol. Cells*, 2016, **157**, 666–675.

46 P. Zhou, D. Dang, Q. Wang, X. Duan, M. Xiao, Q. Tao, H. Tan, R. Yang and W. Zhua, *J. Mater. Chem. A*, 2015, **3**, 13568–13576.

47 J. Zhang, L. Xu, J. Chen, P. Shen, M. Ye, N. Y. Yuan and J. N. Ding, *Thin Solid Films*, 2018, **645**, 129–133.

48 C. He, Q. He, X. Yang, G. Wu, C. Yang, F. Bai, Z. Shuai, L. Wang and Y. Li, *J. Phys. Chem. C*, 2007, **111**, 8661–8666.

49 C. He, Q. He, G. Wu, F. Bai and Y. Li, *Proc. SPIE*, 2007, **6656**, 66560Z.

50 G. Wu, G. Zhao, C. He, J. Zhang, Q. He, X. Chen and Y. Li, *Sol. Energy Mater. Sol. Cells*, 2009, **93**, 108–113.

51 C. He, Q. He, Y. He, Y. Li, F. Bai, C. Yang, Y. Ding, L. Wang and J. Ye, *Sol. Energy Mater. Sol. Cells*, 2006, **90**, 1815–1827.

52 J. Roncali, P. Leriche and A. Cravino, *Adv. Mater.*, 2007, **19**, 2045–2060.

53 D. Wang and Z. GENG, *Can. J. Chem.*, 2015, **93**, 1181–1190.

54 R. Jin, *C. R. Chim.*, 2015, **18**, 1–6.

55 R. Jin, *J. Mol. Model.*, 2015, **21**, 1–9.

56 F. Goubard and F. Dumur, *RSC Adv.*, 2015, **5**, 3521–3551.

57 K. H. Park, W. Kim, J. Yang and D. Kim, *Chem. Soc. Rev.*, 2018, **47**, 4279–4294.

58 N. O. Mahmoodi and M. Mohammadi, *J. Iran. Chem. Soc.*, 2018, **15**, 311–336.

59 M. Lehmann, *Chem.-Eur. J.*, 2009, **15**, 3638–3651.

60 C. Viñas, F. Teixidor and R. Núñez, *Inorg. Chim. Acta*, 2014, **409**, 12–25.

61 H. Zhang, D. Wu, H. Liu and J. Yin, *Curr. Org. Chem.*, 2012, **16**, 2124–2158.

62 P. Gale, *Chem. Soc. Rev.*, 2009, **38**, 1551–1561.

63 E. De Jesu and J. C. Flores, *New J. Chem.*, 2007, **31**, 1161–1191.

64 M. Thelakkat, *Macromol. Mater. Eng.*, 2002, **287**, 442–461.

65 C. Tschierske, *Annu. Rep. Prog. Chem., Sect. C: Phys. Chem.*, 2001, **97**, 191–267.

66 P. Agarwala and D. Kabra, *J. Mater. Chem. A*, 2017, **5**, 1348–1373.

67 A. S. Santra, A. F. Khasanov, A. Mukherjee, M. Rahman, I. S. Kovalev, D. S. Kopchuk, V. Zyryanov, A. Majee, O. N. Chupakhin and N. Charushin, *Eur. J. Org. Chem.*, 2018, **2018**, 4351–4375.

68 M. Ishikawa, H. Teramura, K. K. Lee, W. Schneider, A. Naka, H. Kobayashi, Y. Yamaguchi, M. Kikugawa, J. Ohshita, A. Kunai, H. Tang, Y. Harima, T. Yamabe and T. Takeuchi, *Organometallics*, 2001, **20**, 5331–5341.



69 Y. N. Luponosov, S. A. Ponomarenko, N. M. Surin and A. M. Muzaferov, *Org. Lett.*, 2008, **10**, 2753–2756.

70 Y. N. Luponosov, S. A. Ponomarenko, N. M. Surin, O. V. Borshchev, E. A. Shumilkina and A. M. Muzaferov, *Chem. Mater.*, 2009, **21**, 447–455.

71 M. Halik, H. Klauk, U. Zschieschang, G. Schmid, W. Radlik, S. Ponomarenko, S. Kirchmeyer and W. Weber, *J. Appl. Phys.*, 2009, **93**, 2977–2981.

72 N. P. Yevlampieva, A. P. Khurchak, Y. N. Luponosov and E. A. Kleimyuk, *Russ. J. Appl. Chem.*, 2013, **86**, 747–755.

73 Z. Lin, J. Bjorgaard, A. G. Yavuz and E. K. Muhammet, *J. Phys. Chem. C*, 2011, **115**, 15097–15108.

74 H. F. T. Klare and M. Oestreich, *Dalton Trans.*, 2010, **39**, 9176–9184.

75 J. Ohshita, Y. Hatanaka, S. Matsui, Y. Ooyama, Y. Harima and Y. Kunugi, *Appl. Organomet. Chem.*, 2010, **24**, 540–544.

76 M. F. Mohamed, A. F. Darweesh, A. H. M. Elwahy and I. A. Abdelhamid, *RSC Adv.*, 2016, **6**, 40900–40910.

77 F. Cheng, N. Tang, J. Chen, F. Wang and L. Chen, *Inorg. Chem. Commun.*, 2011, **14**, 852–855.

78 J. Lellouche, Z. Pomerantz, R. Persky, H. E. Gottlieb and S. Ghosh, *Synth. Met.*, 2011, **161**, 2378–2383.

79 Z. Xu, T. Yu, Y. Zhao, H. Zhang, G. Zhao, J. Li and L. Chai, *J. Fluoresc.*, 2016, **26**, 149–154.

80 S. Kotha, D. Kashinath, K. Lahiri and R. B. Sunoj, *Eur. J. Org. Chem.*, 2004, **2004**, 4003–4013.

81 S. Kotha, S. Todeti, M. B. Gopal and A. Datta, *ACS Omega*, 2017, **2**, 629–6297.

82 J. Luo, Z. Xie, J. W. Y. Lam, L. Cheng, H. Chen, C. Qiu, H. S. Kwok, X. Zhan, Y. Liu, D. Zhu and B. Z. Tang, *Chem. Commun.*, 2001, 1740–1741.

83 Q. Niu, Y. Lu, H. Sun and X. Li, *Spectrochim. Acta, Part A*, 2013, **107**, 377–385.

84 D. Suresh, C. S. B. Gomes, P. S. Lopes, C. A. Figueira, B. Ferreira, P. T. Gomes, E. Di Paolo, A. L. Maåanita, M. T. Duarte, A. Charas, J. Morgado, D. Vila-Viåosa and M. Joso, *Chem.-Eur. J.*, 2015, **21**, 1–18.

85 P. Rajakumar, S. Raja and A. Thirunarayanan, *Synlett*, 2010, 1669–1673.

86 M. E. Salem, A. F. Darweesh, A. M. Farag and A. H. M. Elwahy, *J. Heterocycl. Chem.*, 2017, **54**, 586–595.

87 M. Al-Smadi and S. Mohammad, *J. Heterocycl. Chem.*, 2009, **46**, 201–206.

88 X. He, L. Chen, Y. Zhao, S. C. Ng, X. Wang, X. Sun and X. M. Hu, *RSC Adv.*, 2015, **5**, 15399–15406.

89 S. Nath, S. K. Pathak, J. De, S. K. Pal and A. S. Achalkumar, *Mol. Syst. Des. Eng.*, 2017, **2**, 478–489.

90 C. Yang, X. Chen, X. Lu, Q. Zhou and Y. Yang, *Chem. Commun.*, 1997, 2041–2042.

91 M. Al-Smadi and S. Ratrout, *J. Heterocycl. Chem.*, 2004, **41**, 887–891.

92 A. H. M. Elwahy, R. M. Sarhan and M. A. Badawy, *Curr. Org. Synth.*, 2013, **10**, 786–790.

93 K. Rajesh, B. P. Reddy and V. Vijayakumar, *Can. J. Chem.*, 2011, **89**, 1236–1244.

94 I. A. Abdelhamid, A. F. Darweesh and A. H. M. Elwahy, *Tetrahedron Lett.*, 2015, **56**, 7085–7088.

95 X. Yin and M. Tan, *Synth. Commun.*, 2003, **33**, 1113–1119.

96 D. A. McMorran and P. J. Steel, *Tetrahedron*, 2003, **59**, 3701–3707.

97 N. A. Abd El-Fatah, A. F. Darweesh, A. A. Mohamed, I. A. Abdelhamid and A. H. M. Elwahy, *Tetrahedron*, 2017, **73**, 1436–1450.

98 X. Yin, J. Miao, Y. Xiang, H. Wu and Y. Cao, *Macromol. Rapid Commun.*, 2015, **36**, 1658–1663.

99 D. Shi, Y. Wang, Y. Liu, Z. Zhang, J. Luo, J. He, Q. Chen, G. Lei and W. Zhu, *Chem.-Asian J.*, 2012, **7**, 2096–2101.

100 C. Aubert, C. Dallaire, G. Pêpe, E. Levillain, G. Félix and M. Gingras, *Eur. J. Org. Chem.*, 2012, **2012**, 6145–6154.

101 J. Pang, E. J. P. Marcotte, C. Seward, R. S. Brown and S. Wang, *Angew. Chem.*, 2001, 4166–4169.

102 Y. Xiang, Q. Wang, G. Wang, X. Li and D. Zhang, *Tetrahedron*, 2016, **72**, 2574–2580.

103 J. X. Qiu, Y. X. Li, X. F. Yang, Y. Nie, Z. W. Zhang, Z. H. Chen and G. X. Sun, *J. Mater. Chem. C*, 2014, **2**, 5954–5962.

104 J. Qiu, Y. Li, J. Miao, Z. Zhang and Z. Chen, *Synth. Met.*, 2015, **199**, 353–359.

105 K. Jiang, Y. C. Wu, H. Q. Wu, S. L. Li, S. H. Luo and Z. Y. Wang, *J. Photochem. Photobiol. A*, 2018, **350**, 52–58.

106 Y. Wu, J. Huo, L. Cao, S. Ding, L. Wang, D. Cao and Z. Wang, *Sens. Actuators, B*, 2016, **237**, 865–875.

107 W. White, Z. M. Hudson, X. Feng, S. Han, Z. H. Lu and S. Wang, *Dalton Trans.*, 2010, **39**, 892–899.

108 F. Wei and G. X. Yu, *J. Lumin.*, 2013, **134**, 710–717.

109 M. R. A. Al-Mandhary, C. M. Fitchett and P. J. Steel, *Aust. J. Chem.*, 2006, **59**, 307–314.

110 P. Singh and S. Kumar, *Tetrahedron Lett.*, 2006, **47**, 109–112.

111 P. Taylor, S. Kumar, S. Kaur and G. Singh, *Supramol. Chem.*, 2010, **200**, 37–40.

112 Y. Cui and S. Wang, *J. Org. Chem.*, 2006, **71**, 6485–6496.

113 F. Magnan and J. L. Brusso, *RSC Adv.*, 2016, **6**, 97420–97429.

114 M. H. Hoang, M. J. Cho, D. C. Kim, K. H. Kim, J. W. Shin, M. Y. Cho, J. soo Joo and D. H. Choi, *Org. Electron.*, 2009, **10**, 607–617.

115 K. Kotwica, A. S. Kostyuchenko, P. Data, T. Marszalek, L. Skorka, T. Jaroch, S. Kacka, M. Zagorska and A. Pron, *Chem.-Eur. J.*, 2016, **22**, 1–13.

116 K. Madasamy and M. Kathiresan, *ChemistrySelect*, 2016, **1**, 354–359.

117 A. Brzeczek, P. Ledwon, P. Data, P. Zassowski, S. Golba, K. Walczak and M. Lapkowski, *Dyes Pigm.*, 2015, **113**, 640–648.

118 W. Jiang, Z. Ge, P. Cai, B. Huang, Y. Dai, Y. Sun, J. Qiao, L. Wang, L. Duan and Y. Qiu, *J. Mater. Chem.*, 2012, **22**, 12016–12022.

119 L. Hu, J. Li, J. Huang and J. Yin, *Chin. J. Chem.*, 2017, **35**, 93–97.

120 W. Hung, P. Chiang, S. Lin, W. Tang, S. Liu, P. Chou, Y. Hung and K. Wong, *ACS Appl. Mater. Interfaces*, 2016, **8**, 4811–4818.

121 L. Peng, C. Chen, C. R. Gonzalez and V. Balogh-Nair, *Int. J. Mol. Sci.*, 2002, **3**, 1145–1161.

122 M. Ak, M. S. Ak and L. Toppore, *Macromol. Chem. Phys.*, 2006, **207**, 1351–1358.



123 P. Leriche, F. Piron, E. Ripaud, P. Frère, M. Allain and J. Roncali, *Tetrahedron Lett.*, 2009, **50**, 5673–5676.

124 L. Zou, Z. Liu, X. Yan, Y. Liu, Y. Fu, J. Liu, Z. Huang, X. Chen and J. Qin, *Eur. J. Org. Chem.*, 2009, **2009**, 5587–5593.

125 N. O. Mahmoodi and M. Mohammadi, *Res. Chem. Intermed.*, 2017, **43**, 2641–2651.

126 H. Duan, L. Wang, D. Qin, X. Li, S. Wang and Y. Zhang, *Synth. Commun.*, 2011, **41**, 380–384.

127 J. A. Seijas, M. Carracedo-Taboada, X. Feás and M. P. Vázquez-Tato, *Int. Electron. Conf. Synth. Org. Chem.*, 15th, 2011, **15**, 1–30.

128 E. Beltra, L. Serrano, T. Sierra and R. Gime, *Org. Lett.*, 2010, **12**, 2649–2652.

129 E. Beltrán, J. L. Serrano, T. Sierra and R. Giménez, *J. Mater. Chem.*, 2012, **22**, 7797–7805.

130 B. Pradhan, S. K. Pathak, R. K. Gupta, M. Gupta, S. K. Pal and A. S. Achalkumar, *J. Mater. Chem. C*, 2016, **4**, 6117–6130.

131 M. Ali, Z. Eskandar, A. Abdoli and M. Shiri, *Mol. Diversity*, 2010, **14**, 809–813.

132 A. R. Karimi, Z. Dalirnasab, M. Karimi and F. Bagherian, *Synthesis*, 2013, **45**, 3300–3304.

133 N. Mahmoodi, K. Tabatabaeian and H. Kiyani, *Helv. Chim. Acta*, 2012, **95**, 536–542.

134 Z. Erdem, H. Bingol, A. O. Saf, E. Torlak and A. Coskun, *J. Hazard. Mater.*, 2010, **183**, 251–255.

135 M. Shiri, A. Zol and A. Shamsian, *J. Heterocycl. Chem.*, 2012, **49**, 1429–1433.

136 R. Ghorbani-Vaghei, Z. Toghraei-Semiroomi, M. Amiri and R. Karimi-Nami, *Mol. Diversity*, 2013, **17**, 307–318.

137 E. Karatas and H. I. Ucan, *J. Heterocycl. Chem.*, 2016, **54**, 692–698.

138 A. R. Karimi, Z. Eftekhari, M. Karimi and Z. Dalirnasab, *Synthesis*, 2014, **46**, 3180–3184.

139 G. Sathiyan and P. Sakthivel, *Dyes Pigm.*, 2017, **143**, 444–454.

140 L. Zhang, L. Zou, J. Xiao, P. Zhou, C. Zhong, X. Chen, J. Qin, I. F. A. Mariz and E. Maçôas, *J. Mater. Chem.*, 2012, **22**, 16781–16790.

141 M. Nikpassand, L. Zare Fekri, H. Badri and L. Asadpour, *Synthesis and Antimicrobial Activity of Mono, Bis and Tris 2-Amino-4H Chromenes*, 2015, vol. 12.

142 L. Qian, Y. Qiu, J. Liu, F. Xin and Y. Chen, *J. Appl. Polym. Sci.*, 2014, **131**, 1–8.

143 Z. Bai, L. Song, Y. Hu, X. Gong and R. K. K. Yuen, *J. Anal. Appl. Pyrolysis*, 2014, **105**, 317–326.

144 S. Yang, J. Wang, S. Huo, M. Wang and L. Cheng, *Synthesis of a Phosphorus/Nitrogen-Containing Additive with Multifunctional Groups and Its Flame-Retardant Effect in Epoxy Resin*, 2015, vol. 54.

145 A. R. Karimi, Z. Dalirnasab and M. Karimi, *Synthesis*, 2014, **46**, 917–922.

146 K. M. Omer, S. Ku, Y. Chen, K. Wong and A. J. Bard, *J. Am. Chem. Soc.*, 2010, 10944–10952.

147 R. Liu, M. Shu, J. Hu, S. Zhu, H. Shi and H. Zhu, *Dyes Pigm.*, 2017, **137**, 174–181.

148 C. Y. Huang, W. H. Lee and R. H. Lee, *RSC Adv.*, 2014, **4**, 48150–48162.

149 S. Shiau, C. Chang, W. Chen, H. Wang, R. Jeng and R. Lee, *Dyes Pigm.*, 2015, **115**, 35–49.

150 R. Sheng, Q. Liu, M. Qiu, C. Gu, Y. Zhou, J. Ren, M. Sun and R. Yang, *Chem. Lett.*, 2015, **44**, 291–293.

151 M. J. Bosiak, P. Trzaska, D. Kędziera and J. Adams, *Dyes Pigm.*, 2016, **129**, 199–208.

152 H. Shi, D. Xin, X. Dong, J. X. Dai, X. Wu, Y. Miao, L. Fang, H. Wang and M. M. F. Choi, *J. Mater. Chem. C*, 2014, **2**, 2160–2168.

153 H. Tan, W. Peng, H. Liu, Y. Luo, Y. Chen and L. Duan, *Eur. J. Org. Chem.*, 2016, **2016**, 5127–5135.

154 A. Riaço, I. Arrechea-Marcos, M. J. Mancheço, M. Burrezo, A. De Peça, S. Loser, A. Timalsina and A. Facchetti, *Chem.-Eur. J.*, 2016, **22**, 6374–6381.

155 Y. Jiang, D. Yu, L. Lu, C. Zhan, D. Wu, W. You, Z. Xie and S. Xiao, *J. Mater. Chem. A*, 2013, **1**, 8270–8279.

156 S. Paek, H. Choi, J. Sim, K. Song, J. K. Lee and J. Ko, *J. Phys. Chem. C*, 2014, **118**, 27193–27200.

157 K. Lim, S. Y. Lee, K. Song, G. D. Sharma and J. Ko, *J. Mater. Chem. C*, 2014, **2**, 8412–8422.

158 J. Shao, Z. Guan, Y. Yan, C. Jiao, Q. Xu and C. Chi, *J. Org. Chem.*, 2011, **76**, 780–790.

159 Z. Lu, C. Li, T. Fang, G. Li and Z. Bo, *J. Mater. Chem. A*, 2013, **1**, 7657–7665.

160 H. Komiyama, C. Adachi and T. Yasuda, *Beilstein J. Org. Chem.*, 2016, **12**, 1459–1466.

161 H. W. Zhenbo Zhao and Y. Xiao, *RSC Adv.*, 2013, **3**, 21373–21376.

